UNIVERSIDADE DE LISBOA
FACULDADE DE FARMÁCIA

MEDICINAL CHEMISTRY APPROACHES FOR NOVEL DNA LIGANDS

Ana Rita Português Duarte

Orientadores: Doutora Ana Sofia Ressurreição;
Professor Doutor Rui Moreira.

Tese especialmente elaborada para obtenção do grau de Doutor em Farmácia, especialidade Química Farmacêutica e Terapêutica

2018

UNIVERSIDADE DE LISBOA
FACULDADE DE FARMÁCIA

MEDICINAL CHEMISTRY APPROACHES FOR NOVEL DNA LIGANDS

Ana Rita Português Duarte

Orientadores: Doutora Ana Sofia Ressurreição;
Professor Doutor Rui Moreira.

Tese especialmente elaborada para obtenção do grau de Doutor em Farmácia, especialidade Química Farmacêutica e Terapêutica

Júri:
- Doutora Matilde da Luz dos Santos Duque da Fonseca e Castro, Professora Catedrática
  Faculdade de Farmácia da Universidade de Lisboa, Presidente do Júri;
- Doutora Marta Piñeiro Gómez, Professora Auxiliar
  Faculdade de Ciências e Tecnologia da Universidade de Coimbra;
- Doutor Carlos Manuel Magalhães Afonso, Professor Auxiliar com Agregação
  Faculdade de Farmácia da universidade do Porto;
- Doutor João Paulo Martins Ferreira Lavrado, Químico
  Hovione FarmaCiência, SA., na qualidade de especialista de reconhecido mérito e competência;
- Doutora Maria Matilde Soares Duarte Marques, Professora Catedrática
  Instituto Superior Técnico da Universidade de Lisboa;
- Doutora Maria Alexandra da Silva Paulo, Professora Auxiliar com Agregação
  Faculdade de Farmácia da Universidade de Lisboa;
- Doutora Ana Sofia Marques da Ressurreição
  Faculdade de Farmácia da Universidade Lisboa, Orientadora.

Trabalho financiado pela Fundação para a Ciência e Tecnologia através da bolsa de doutoramento SFRH/BD/70491/2010

2018

O presente trabalho foi desenvolvido sob orientação da Doutora Ana Sofia Ressurreição e co-orientação do Professor Doutor Rui Moreira, ambos do iMed.ULisboa (Instituto de Investigação do Medicamento) da Faculdade de Farmácia da Universidade de Lisboa. Este trabalho foi financiado pela Fundação para a Ciência e Tecnologia através da bolsa de doutoramento SFRH/BD/70491/2010.

This work was developed under scientific supervision of Dr. Ana Sofia Ressurreição and co-supervision of Professor Rui Moreira, from iMed.ULisboa (Instituto de Investigação do Medicamento), Faculty of Pharmacy, University of Lisbon. The work was financially supported by Fundação para a Ciência e Tecnologia, through the doctoral grant SFRH/BD/70491/2010.

List of publications

Papers in international scientific periodicals with referees

Ana R. Duarte, João Lavrado, Raquel F. M. Frade, Joana D. Amaral, Alexandra Paulo, Cecília M. P. Rodrigues, Ana S. Ressurreição, Rui Moreira, *Design, synthesis and biological evaluation of bifunctionalized naphtalenes as potencial anticancer agents*, in preparation

Ana R. Duarte, Enrico Cadoni, Ana S. Ressurreição, Rui Moreira and Alexandra Paulo. Design of modular G-quadruplex ligands. ChemMedChem (*invited review*), accepted

Book chapter

Ana R. Duarte, Marta P. Carrasco, and Ana S. Ressurreição, Synthesis of Aurone Derrivatives Through Acid-Catalysed Aldol Condensation. In *Comprehensive Organic Chemistry Experiments for the Laboratory Classroom*, Carlos A. M. Afonso, Nuno R. Candeias, Dulce Pereira Simão, Alexandre F. Trindade, Jaime A. S. Coelho, Bin Tan, Robert Franzén Ed. The Royal Society of Chemistry: Cambridge, 2016; pp 352-354.

Oral communications in conferences

A. R. P. Duarte, R. F. M. Frade, J. Lavrado, R. Moreira, A. S. Ressurreição. *Synthesis and Biological Evaluation Of Putative G-Quadruplex Ligands.* **2014**, 6th iMed.ULisboa Post-Graduate Students Meeting, Lisbon (Portugal), OC13.

Posters in conferences

A. R. P. Duarte, A. Ressurreição, R. Moreira. *Synthesis of cysteine-based building blocks of alpha-Peptide Nucleic Acids via thiol-ene reactions*. **2011**, 3rd iMed.UL Post-Graduate Students Meeting, Lisbon (Portugal), PC36.

A. R. P. Duarte, R. Moreira, A. Ressurreição*. Synthesis of New Cysteine-based Building Blocks of alpha-Peptide Nucleic Acids (Alpha-PNAs) Via Thiol-ene Reactions*. **2012**, EFMC – XXII International Symposium on Medicinal Chemistry, Berlin (Germany), P019.

A. R. P. Duarte, R. Moreira, A. Ressurreição. *Thiol-ene Chemistry: A Click to alpha-Peptide Nucleic acid (Alpha-PNA) Building Blocks*. **2012**, 3rd Portuguese Meeting on Medicinal Chemistry, Aveiro (Portugal), P4.

A. R. P. Duarte, R. Moreira, A. Ressurreição. *Synthesis of Cysteine-based Building Blocks of α-Peptide Nucleic Acids (α-PNAs) Via Thiol-ene Reactions*. **2012**, 4th iMed.UL Post-Graduate Students Meeting, Lisbon (Portugal), PC34.

A. R. P. Duarte, A. Ressurreição, R. Moreira. *Synthesis of New Nucleobase-Funtionalized Cysteines to be used as Building Blocks of Alpha-Peptide Nucleic Acids (Alpha-PNAS)*. **2013**, III SEQT Summer School, Tres Cantos (Spain), P34.

A. R. P. Duarte, R. Moreira, A. S. Ressurreição. *New Nucleobase-Funtionalized Cysteines: Building Blocks of Alpha-Peptide Nucleic Acids (Alpha-PNAS).* **2013**, 5th iMed.UL Post-Graduate Students Meeting, Lisbon (Portugal), PC45.

A. R. P. Duarte, R. Moreira, A. S. Ressurreição. *Synthesis of Naphtalene Derivatives as New Class of Putative G-Quadruplex Ligands*. **2013**, 10º Encontro Nacional de Química Orgânica, Lisbon (Portugal), PC178.

A. S. Ressurreição, A. R. P. Duarte, J. Iley, R. Moreira. *Thiol-ene reactions: a "click" to α-Peptide Nucleic Acid Building Blocks*. **2013**, 10º Encontro Nacional de Química Orgânica, Lisbon (Portugal), PC115.

A. R. Duarte, R. F. M. Frade, J. Lavrado, R. Moreira, A. S. Ressurreição. *Synthesis and Biological Evaluation of Putative G-quadruplex Ligands.* **2014**, EFMC – XXIII International Symposium on Medicinal Chemistry, Lisbon (Portugal), V010.

A. R. Duarte, R. F. M. Frade, J. Lavrado, R. Moreira, A. S. Ressurreição. Synthesis and Biological Evaluation of Putative G-quadruplex Ligands. **2014**, EFMC – 1st Young Medicinal Chemist Symposium, Lisbon (Portugal), P17.

Table of contents

List of Figures

List of Schemes

List of Tables

List of abbreviations

A	Adenine
Ac	Acetyl
AIBN	2,2'-Azobis(2-methylpropionitrile)
ALT	Alternative lengthening of telomeres
An	Methoxybenzoyl
Arom	Aromatic
Ben.	Benzene
Bhoc	Benzhydryloxycarbonyl
Boc	*Tert*-butyloxycarbonyl
Boc_2O	Di-*tert*-butyl dicarbonate
C	Cytosine
Cbz	Benzyloxycarbonyl
CD	Circular dichroism
CPPs	Cell-penetrating peptides
D	Diaminopurine
DABCO	1,4-diazabicyclo-[2.2.2]octane
DCE	Dichloroethane
DCM	Dichloromethane
Dde	1-(4,4-dimethyl-2,6-dioxocyclohexylidene)ethyl
DIAD	Diisopropyl azodicarboxylate
DIBAL	Diisobutylaluminium hydride
DIPEA	*N,N*-diisopropylethylamine
DMAP	4-dimethylaminopyridine
DME	Dimethoxyethane
DMF	*N*,*N*-Dimethylformamide
DMP	Dess–Martin periodinane
DMSO	Dimethyl sulfoxide
DNA	Deoxyribonucleic acid
DPAP	2,2-dimethoxy-2-phenylacetophenone

Dppf	1,1'-Ferrocenediyl-bis(diphenylphosphine)
dsDNA	Double-stranded DNA
Equiv.	Equivalent
ESI	Electrospray Ionization
Et	Ethyl
Et_2O	Diethyl ether
EtOH	Ethanol
EtOAc	Ethyl acetate
Exo	Exocyclic
FAM	5'-carboxyfluorescein
Fmoc	9-Fluorenylmethylcarbonyl
FRET	Fluorescence (or Förster) resonance energy transfer spectroscopy
G	Guanine
G4	G-quadruplex
G-quartets	Guanine quartets
H	Hours
HOBt	1-hydroxybenzotriazole
hPOT1	Human protection of telomeres 1
HRMS	High-resolution Mass Spectrometry
hTERT	Human telomerase reverse transcriptase
HWE	Horner-Wadsworth-Emmons
IBX	*o*-iodooxybenzoic acid
IC_{50}	Half maximal inhibitory concentration
LNA	Locked nucleic acid
Me	Methyl
MeOH	Methanol
min	Minutes
miRNA	MicroRNA
Mmt	Monomethoxytrityl
Mor	Morpholine
mRNA	Messenger RNA

MS	Mass Spectrometry
mtDNA	Mitochondrial DNA
MW	Molecular weight
M.p.	Melting point
NA	Nucleic acid
ND	Not determined
NMR	Nuclear magnetic resonance
Naph.	Naphthalene
NVOC	*Ortho*-nitroveratryloxycarbonyl
OA	Oligonucleotides analogues
o/n	Overnight
PCR	Polymerase chain reaction
pcPNA	Pseudocomplementary PNA
Ph	Phenyl
Ph_2O	Diphenyl ether
Pip	Piperidino
PMO	Phosphorodiamidate morpholino oligomer
PNA	Peptide nucleic acid
Ppz	Piperazino
PS	Phosphorothiolate oligonucleotides
Pyr	Pyrrolidino
QFS	Quadruplex forming sequences
RNA	Ribonucleic acid
rRNA	Ribosomal RNA
Rt	Room temperature
SAR	Structure-activity relationship
S_N2	Substitution nucleophilic bimolecular
SPPS	Solid-phase peptide synthesis
SPR	Surface plasmon resonance
ssDNA	Single-stranded DNA
TLC	Thin-layer chromatography

T_m	Melting temperature
ΔT_m	Melting temperature variations
TAMRA	3'-carboxytetramethylrhodamine
TEA	Triethylamine
TES	Triethylsilane
TFA	Trifluoroacetic acid
TBTU	*O*-(Benzotriazol-1-yl)-*N*,*N*,*N'*,*N'*-tetramethyluronium tetrafluoroborate
THF	Tetrahydrofuran
TMG	1,1,3,3-Tetramethylguanidine
tRNA	Transfer RNA
Trt	Trityl
U	Uracil
^{s}U	Thiouracil

Acknowledgements

First of all, I would like to express my gratitude to my supervisors Dr. Ana Sofia Ressurreição and Professor Rui Moreira for all the advices and the dedication expressed during these years and for the review of this thesis.

I would like to thank to Dr. João Lavrado for helping me during my work on G-quadruplexes ligands, Dr. Joana Amaral for the apoptose assays and João Ferreira for the mass spectrometry and element analysis of my compounds. I can not forget Professora Alexandra Paulo for invite me for write the review about G4s. I also would like to thank Professor Carlos Afonso for accepting me in his lab during some months.

I would like to thank Fundação para a Ciência e Tecnologia for the financial support to this PhD program.

This journey would have been harder without my labmates! I will never forget the evenings in the lab with Carlos Ribeiro, Marta Carrasco and Catarina Charneira working and listening ABBA songs. I also want to acknowledge André Dias, who was such an amazing friend, always trying to make me laugh. Ana Raquel Sitoe, the first person that I met in the lab, was another important friend who encoraging me all the time. I cannot forget Marta Figueiras who transform the lab in a funnier place with her good mood. During the period that I worked in Professor Carlos Afonso lab I was also surprised by incredible people especially Raquel Frade (who also fundamental in this thesis as she performed the antiproliferative and toxicity assays), Andreia Rosatella and Carlos Monteiro who became my friends. I also want to express my gratitude to Ângelo Monteiro, Mariana Reis, Joana Magalhães, Paulo Madeira, Rudi Oliveira, Susana Lucas and all the people who worked in the lab while I was there.

I also express my gratitude to my friends who helped me to relax during these stressful years.

Finally, I want to aknowledge to my family especially to my godparents, for their very important role in my life while I was growing, and Rui, who help me to overcome some of my fears and doubts during this journey and encouraged me in the more difficult moments. This thesis is dedicated to two most special human beings that I met who always give me their inconditional love and support and never let me give up on anything: my beloved parents!

Abstract

As nucleic acid lesions are involved in most of the diseases, deoxyribonucleic acid (DNA) and ribonucleic acid are attractive targets for drug design. Due to the high homogeneity of B-DNA, the main drawback of DNA binding drugs is their random distribution thereby affecting genome functions in an uncontrolled manner.

To overcome this situation, secondary structures such as G-quadruplexes (G4), which can be found in genome regions involved in cell proliferation and genome stability, can be target. This thesis opened new perspectives and reinforced previously existing perceptions over the structural feactures that G4 ligand should have. With regards to non-fused aromatic ligands, this work confirmed that the presence of more than one aromatic core (such as benzene or naphtalene) seems to be essential to: (a) have an aromatic surface big enough to selectively interact with the G-quartet; (b) give some rigidity to the structure. Respecting the polyaromatic fused compounds, a new scaffold (benzo[*h*][1,6]naphthyridin-2(1*H*)-one) was tested as G4 ligand aromatic core and the FRET melting data give information that can be used in the design of new derivatives. Besides that, it is also essential to highlight the very good antiproliferative results obtained with some of the compounds synthesised. Alternativelly, peptide nucleic acids (PNAs) also have nucleic acids as drug target. Attempts to understand the structure-activity relationship and improve solubility, cell permeability, bioavailability, and binding orientation with nucleic acids of PNA have resulted in several structural modifications, such as α-PNA. α-PNA has a backbone consisting of α-amino acids, some of them carrying a nucleobase in their side chain. This thesis also described their synthesis of new α-PNA monomers containing sulfur. From a chemical point of view, this work is also interesting for the variety of reactions that were employed where the click thiol-ene reactions stood out.

KEYWORDS: G-quadruplexes ligands; Naphthalene; Benzo[*h*][1,6]naphthyridin-2(1*H*)-one ; α-Peptide Nucleic Acids; Chimeric cysteine.

Resumo

Tendo em conta que as lesões ou mutações nas moléculas de ácidos nucleicos contribuem para a etiopatogenia da maioria das doenças (como por exemplo as neoplasias malignas) os ácidos desoxirribonucleico e ribonucleico têm sido encarados como importantes alvos terapêuticos. No entanto, a sua elevada homogeneidade estrutural torna difícil a acção dos fármacos em regiões específicas do genoma. Esta ligação não específica às moléculas de ácidos nucleicos resulta, muitas vezes, em reacções adversas. Para evitar estas reacções adversas é importante desenvolver fármacos que actuem em regiões específicas do genoma. Ao longo dos tempos, diferentes abordagens têm sido adoptadas com esse objectivo entre elas a síntese de moléculas que tenham como alvo estruturas secundárias específicas, como os G-quadruplexes (G4), ou mesmo sequências de nucleótidos específicas.

Os G4 são estruturas secundárias de sequências de ácidos nucleicos ricos em guanina que são capazes de se organizar num arranjo em quadrado de guaninas (tétradas) estabilizado por ligações de hidrogénio e pela existência de catiões monovalentes no centro das tétradas. Os G4 podem ser intramoleculares, bimoleculares ou tetramoleculares e dependendo da direcção das cadeias ou partes da cadeia que formam as tétradas, as estruturas podem ser descritas como paralelas ou antiparalelas. Deste modo, os G4 têm algumas características estruturais que os permitem diferenciar da dupla hélice de ácido desoxirribonucleico como (a) uma maior superfície aromática das tétradas de guanina disponível para interacções com os fármacos, (b) os quatro sulcos que se diferenciam dos sulcos da dupla hélice de ácido desoxirribonucleico no que diz respeito à profundidade, largura, potencial electrostático e distribuição dos átomos que participam nas ligações de hidrogénio e (c) a presença do ião metálico. Estas sequências ricas em guaninas são um interessante alvo terapêutico não só pelas suas características estruturais mas sobretudo por se localizarem geralmente em regiões do genoma envolvidas na divisão celular (como por exemplo nos promotores dos oncogenes) ou nas extremidades dos cromossomas (telómeros). O objectivo dos ligandos de G4 é estabilizar estas estruturas secundárias dos ácidos nucleicos de modo a evitar a divisão e proliferação celular (no caso dos G4 presentes nos promotores dos oncogenes) ou evitar a conservação do tamanho dos telómeros (associada à imortalidade das células característica das células neoplásicas). Apesar das diferenças estruturais supracitadas, um dos maiores desafios para o desenvolvimento de moléculas que estabilizem os G4 é a sua pouca selectividade relativamente à dupla hélice de ácido desoxirribonucleico. Com o objectivo de aumentar esta selectividade, os ligandos de G4 apresentam geralmente as seguintes características estruturais: (a) uma extensa superfície aromática com tamanho e forma similar à das tétradas de guanina de modo

a estabelecerem interacções de empilhamento π-π, (b) cadeias laterais com grupos carregados positivamente capazes de interagir com os grupos fosfato presentes nos sulcos e assegurar a solubilidade das moléculas e (c) um centro catiónico no núcleo aromático que geralmente interage com o centro electrostático negativo do G4. Os ligandos de G4 descritos na literatura dividem-se em 3 grupos: compostos macrocíclicos, poliaromáticos fundidos e aromáticos não fundidos. Esta tese apresenta a síntese de duas novas famílias de moléculas (desenhadas com base nas características previamente referidas para os ligandos de G4) e que foram testadas como potenciais ligandos de G4 recorrendo à transferência ressonante de energia por fluorescência (FRET). No Capítulo II são descritos compostos simétricos cujo núcleo aromático é o benzeno, o naftaleno ou o 2,7-bifenilnaftaleno e que contêm heteroatomos (enxofre na maioria dos compostos) nas suas cadeias laterais. Estes compostos pertencentes à família dos compostos aromáticos não fundidos, revelaram não aumentar significativamente a estabilidade das sequências oligonucleotídicas testadas. Estes resultados realçam a importância de existir mais de um anel aromático na estrutura dos ligandos aromáticos não fundidos de modo a que: (a) a superfície aromática dos compostos seja suficientemente grande para estabelecer interacções de empilhamento π-π com as tétradas de guanina; e (b) para conferirem rigidez à estrutura. Alguns destes compostos apresentaram actividade antiproliferativa interessante em três linhas tumorais e aumentaram significativamente os níveis de apoptose quando as células foram expostas à concentração da molécula que induziu metade do efeito máximo. Com base nestes resultados, a indução da apoptose parece ser importante para o mecanismo de acção destes compostos ao passo que a estabilização dos G4 não parece ter um papel relevante. Com o objectivo de melhorar a capacidade de estabilização de G4, um grupo de compostos pertencentes à família de compostos poliaromáticos fundidos foi sintetizado, conforme descrito no Capítulo III. Estes compostos derivados de benzo[*h*][1,6]naftiridin-2(1*H*)-ona não são simétrico (contrariamente aos compostos descritos no Capítulo II) e possuem uma maior superfície aromática. Estas moléculas apresentaram uma melhor capacidade de estabilização do G4 quando comparados com os compostos descritos no Capítulo II. Além disso, os resultados obtidos com os ensaios de FRET forneceram informações que poderão ser úteis futuramente na síntese de compostos derivados deste núcleo aromático.

Alternativamente aos compostos que têm como objectivo a estabilização de G4, foram sintetizadas moléculas cujo alvo são sequências nucleotídicas específicas. Os oligonucleótidos naturais possuem limitações importantes à sua acção como o facto de (a) poderem ser degradados por nucleases, tanto *in vivo* como *in vitro*, e por isso serem clivados antes de atingirem o alvo, (b) terem dificuldade em penetrar na célula atravessando a membrana, e (c) a sua síntese ser pouco rentável. Por este motivo, foram

desenvolvidos análogos dos oligonucleótidos com capacidade de estabelecer interações específicas com bases azotadas dos ácidos nucleicos, mas com uma maior estabilidade em meio biológico, maior capacidade de atravessar membranas e mais facilmente sintetizáveis. Dentro dos vários análogos de oligonucleótidos sintetizados encontram-se os ácidos nucleicos peptídicos. Nestes análogos o esqueleto ribose-fosfato foi substituído por um pseudopéptido com bases azotadas nas cadeias laterais. Os ácidos nucleicos peptídicos apresentam algumas vantagens quando comparados com os ácidos nucleicos naturais nomeadamente o facto de (a) não serem degradados nem por nucleases nem por proteases; (b) terem pouca afinidade para as proteínas plasmáticas; (c) terem uma maior afinidade e especificidade para cadeias de ácidos nucleicos que as duas cadeias de ácido desoxirribonucleico que constituem a dupla hélice, e (d) a sua síntese ser menos complexa uma vez que se baseia na formação de ligações peptídicas entre os diferentes monómeros. Os ácidos nucleicos peptídicos podem ter várias aplicações nomeadamente na terapêutica, no diagnóstico e como sondas. Com o objectivo de melhorar algumas das características dos ácidos nucleicos peptídicos como a sua solubilidade, permeabilidade celular ou biodisponibilidade foram feitas algumas alterações estruturais. Um dos exemplos desta modificação são os α-ácidos nucleicos peptídicos em que o esqueleto do análogo é composto por α-aminoácidos, alguns dos quais com uma base azotada na cadeia lateral. Para a síntese deste análogo de oligonucleótidos são necessários aminoácidos quiméricos. Na literatura, já foram descritos, por exemplo, derivados da alanina, homoalanina, serina tirosina, lisina e prolina. O Capítulo IV desta tese foca-se na síntese de aminoácidos quiméricos derivados da cisteína que poderão vir a ser utilizados como monómeros na síntese de α-ácidos nucleicos peptídicos. A escolha da cisteína teve como objectivo aumentar a variabilidade estrutural dos α-ácidos nucleicos peptídicos. Futuramente, poder-se-á verificar qual o impacto da presença destes aminoácidos quiméricos com um átomo de enxofre na afinidade dos α-ácidos nucleicos peptídicos que os incorporem para as sequências-alvo de oligonucleótidos. De um ponto de vista sintético também é importante realçar a grande diversidade de reações que foram utilizadas durante a elaboração deste trabalho. A reações tiol-eno merece ser destacada não só por ter sido essencial na síntese dos monómeros α-ácidos nucleicos peptídicos mas também por ter sido usada na síntese dos ligandos descritos no Capítulo II.

PALAVRAS-CHAVE: Ligandos de G-quadruplexes; Naftaleno; benzo[*h*][1,6]naftiridin-2(1*H*)-ona; α-Ácidos Nucleicos Peptídicos; Cisteína quimérica.

CHAPTER 1

I. STATE OF THE ART

1. Nucleic acids

Nucleic acids (NA) – deoxyribonucleic acid (DNA) and ribonucleic acid (RNA) – are biological macromolecules that exist in every living cells. DNA is the storage of genetic information to encode other components of cells, such as proteins and RNA molecules.[1] RNA may: (a) act as a messenger between DNA and ribosomes – the protein synthesis machinery (messenger RNA, mRNA); (b) form vital portions of ribosomes (ribosomal RNA, rRNA); (c) serve as the carrier of amino acids used in protein synthesis (transfer RNA, tRNA); (d) play critical roles in biological reactions as catalyst.[2]

Structurally, DNA and RNA differ in their nucleotide composition, namely in the nitrogenous bases (also referred as nucleobase) and in the five-carbon sugar.[3] These polynucleotide chains can twist and fold into three-dimensional conformations stabilized by hydrogen bonding between specific pairs of nitrogenous bases. Besides the differences in nucleotide composition, DNA and RNA conformations are also quite different.

DNA conformation. In 1953 Watson and Crick first described the DNA as a right-handed double helix (double strand, dsDNA) based on X-ray crystallography obtained by Rosalind Franklin.[4] Their description refers to B-DNA (Figure I.1), the most common conformation in living cells, but there are two other dsDNA conformations: A-DNA and Z-DNA. The former is a shorter and wider form that has been found in dehydrated samples of DNA and rarely under normal physiological circumstances. Z-DNA, a left-handed conformation, is a transient form of dsDNA which exists only in response to certain types of biological activity and seems to be important in the protection against viral disease.[1] Besides that, it has been found that under certain conditions, DNA has the potential to fold into various other secondary structures. As exemplified in Figure I.1, these unusual secondary structures can involve one to four strands of NAs including triplexes, tetraplexes (G-quadruplexes, G4, and complementar i-motifs), and other non-B forms. Common features in these peculiar NA architectures include sequence dependency, base stacking and base pairing through H-bond interactions, although a wide variety of pairing motifs are found. Interestingly, these DNA secondary structures can be formed by sequences that are widely distributed throughout the human genome, typically in regions associated with critical biological processes. Moreover, all these structures are hypothesized, or even known, to play crucial roles in a range of biological functions *in vivo*, including replication, gene expression regulation, and DNA

recombination. There is also increasing evidence that non-canonical DNA structures might be involved in a number of human diseases.[5]

RNA conformation. Unlike DNA, RNA is usually a single-stranded molecule which can form secondary structures, such as hairpin loops, stabilized by intramolecular hydrogen bonds between complementary bases. Such base-pairing of RNA is critical for many RNA functions, for example the ability of tRNA to bind to the correct sequence of mRNA during translation. Furthermore, it can also form double-stranded structures (RNA/RNA, DNA/RNA).[6]

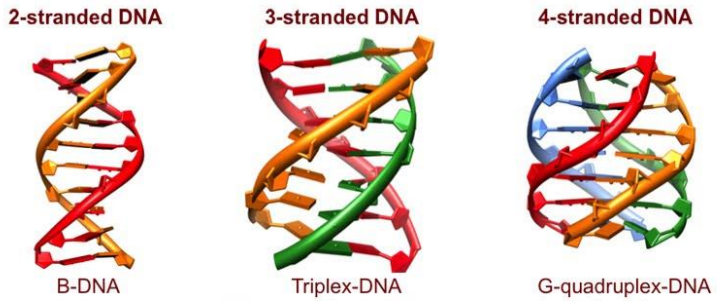

Figure I.1. Different NA conformations (adapted from [7]).

As NA play a significant role in gene mutation, defects in repair mechanism and uncontrolled proliferation of cells, they are very interesting molecular targets. Actually, there are several small molecules which act on proliferating cells by causing DNA damages that lead to inhibition of critical processes like replication and transcription and ultimately to blockage of cell proliferation. Due to the high homogeneity of B-DNA, the main drawback of DNA binding drugs is their random interaction on the polymeric DNA scaffold thereby affecting genome functions in an unspecific manner. To overcome this situation, an approach currently explored is the targeting of secondary structures, such as G4. Alternatively, oligonucleotide analogues (OAs), such peptide nucleic acids (PNAs), have been synthesised.

2. G-quadruplexes (G4s)

Guanine-rich sequences of NAs have a high propensity to self-associate into planar guanine quartets – G-quartets or G-tetrads (Figure I.2). These G-quartets, which were first reported by Gellert and co-workers[8] over 50 years ago, arise from the association of four guanines into a cyclic Hoogsteen hydrogen bonding motif in which each guanine is both the donor and acceptor of two hydrogen bonds with its neighbours (from N^1–O^6 and N^2–N^7). As G-quartet contains eight hydrogen bonds in comparison to the two or

three present in Watson–Crick base pairs, they are often more stable than dsDNA.[9] Due to their large π-surfaces, the G-quartets tend to stack on each other adopting a secondary NA structure, G-quadruplexes. G4s are then further stabilized by association of metal ions that coordinate to carbonyl *O*[6] atoms (with strong negative electrostatic potential).[10] The metal ion stabilizing influence is linked to the increasing radii ($Li^+ < Na^+ < K^+$) with K^+ being optimal, and dramatically increasing G4 stability.[11]

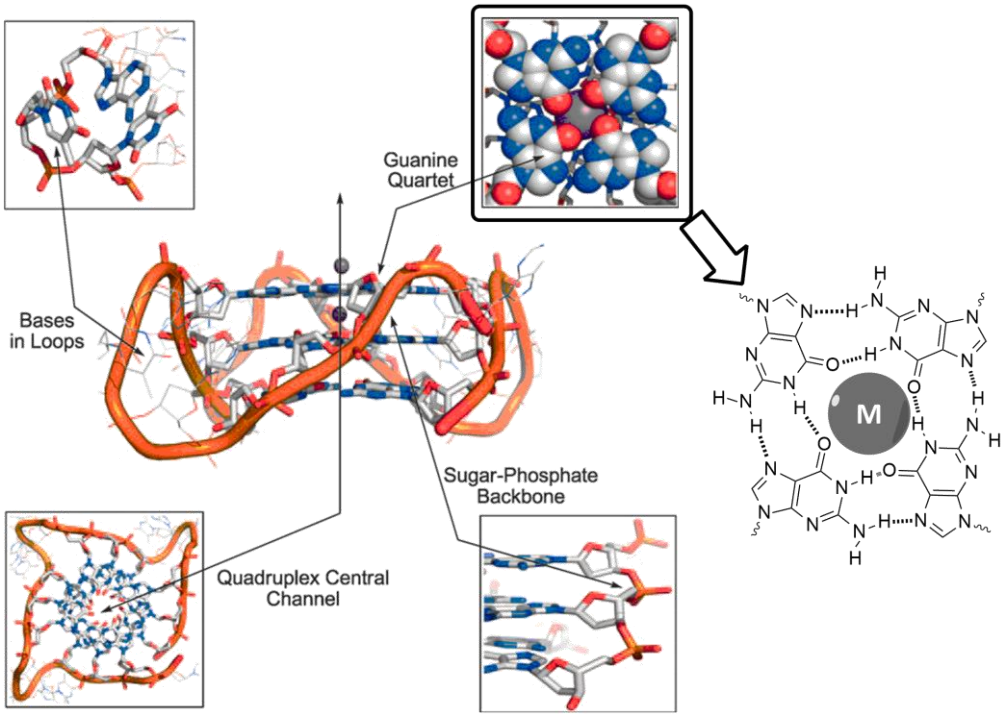

Figure I.2. Structural features of G4s (M: metal ion; adapted from [12]).

2.1. G-Quadruplex strutural polymorphism

From the earliest days of studying G4s *in vitro*, extensive structural polymorphism was noted contrasting with the highly predictable B-form dsDNA. G4s are formed for one (monomer), two (dimer) or four (tetramer) NA strands which may be oriented in anti-parallel, parallel, or mixed configuration (Figure I.3).

The structural diversity also depends on the number of G-quartets comprising a quadruplex, variations in size and composition of linkers connecting G-strands (loop), conformation of glycosidic bonds of guanine bases in quartets and sometimes on the nature of the metal ion.[13]

Loop length plays a major role in defining the final topology and stability of G4s and is more important in therapeutic selectivity to target a G4 than its topology. In addition,

loop residues can themselves form stacking and hydrogen bonding interactions, further stabilizing (or destabilizing) the G4.[11]

Conformational state of the glycosidic bond (C^4-N^9-C^1) refers to the angle between the guanine base (N^9) and the sugar in the G-tetrad and can be either syn (0 to 90°) or anti (-120 to 180°) and is dependent on the backbone strand orientation. The relationship between backbone strand orientation, glycosidic torsion angles and groove width is based on simple geometric relationships and structural constraints imposed by the guanines held in stacked G-quartets. The combinations of syn and anti base orientations around the tetrads changes significantly the access to hydrogen bond donors and acceptors within the grooves, altering hydration networks, accessibility and a variety of surfaces for protein, DNA and ligand interaction.[14]

Although some general trends are apparent, it is difficult to predict the propensity of a sequence to fold into a particular structure. In addition to that, as many G4-forming sequences (QFS) adopt multiple folding topologies in solution, depending on the presence of metal ions, ligands, or molecular crowding conditions, it is possible that different conformations are present *in vivo* in different conditions. The *in vivo* equilibrium may be affected by temperature, ionic conditions, and the binding of particular proteins.[13] Therefore, each sequence needs to be structurally characterized empirically under different folding conditions and checked for conformational heterogeneity between two or more topologies in solution. There has been some developing computational methods for predicting G4s stabilities,[15-17] which will likely improve further as in increasing amounts of empirical data are incorporated.

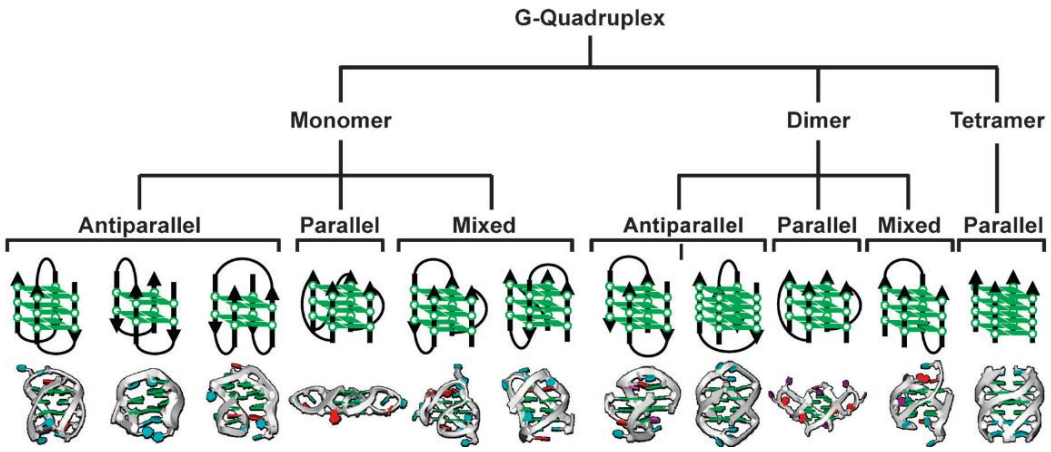

Figure I.3. Some of the G4s topologies (reproduced from [18])

2.2. Important G-quadruplexes in human genome

The unique structural characteristics of G4s and their polymorphism may contribute to their varied biological roles. Bioinformatic analysis has identified approximately 376 000 QFS within the human genome.[19] These sequences are found, for instance, in the promoter regions of proto-oncogenes (*c-MYC*, *BCL-2*, *c-KIT*, *k-RAS*) and other important genes (*HIF-1α*, *VEGF*, *PDGF-A*, *PDGFR-β*, *hTERT*, *RB1*) and telomeric 3'-overhang.[20] Unlike telomeric regions that contain a well-defined repetitive sequence (TTAGGG in vertebrates) and where G4 can be formed from the single-stranded DNA (ssDNA) template at the 3' end of human telomeres, QFS within promoter regions of genomic DNA are diverse in G-run length, loop sequences and the G4s formation is constrained by the duplex nature of genomic DNA. The formation of G4 within promoters may occur during cellular mechanisms that involve unwinding of the dsDNA. The driving forces for the duplex to the G4 DNA transition are the transcription induced negative superhelicity, molecular crowding conditions, and stabilization of the resultant G4s by proteins and ligands.[20] The major role of the DNA G4s may be its ability to "turn-on" or "turn-off" some physiological events by the transcriptional regulation of genes or telomere length.[11]

While much attention in the G4s field has been focused on DNA, in the 1990s, there were early reports of G4s formation from biologically relevant RNA molecules.[21] An example of the potential importance of G4s RNA emerged from the discovery of G-rich telomeric repeat-containing RNA, a non-coding RNA molecule which arise from RNA polymerase II transcription of the C-rich strand human DNA telomeres.[22] Another example is the presence of quadruplex forming sequences in the 3'- and 5'-untranslated regions of mRNAs, which has been shown to play important roles in the post-transcriptional regulation of gene expression.[23]

Moreover, G4s have been found to play roles in epigenetics and evolution process. Observation has indicated close relations between G4 motif and CpG methylation in the genome of cancer samples. Also, G4s DNA were found to relate to DNA damages, such as genomic instability and chromosomal rearrangements.[24]

2.3. G-quadruplex as drug target

The recent demonstration of the presence of G4s DNA and RNA in human cells[25-27] has added support to the concept that these structures can be targets for therapeutic intervention, at the single gene or polygene levels.

The concept of targeting G4s as a therapeutic strategy was first developed for telomeric DNA. The G4 formation and stabilization in the telomeric 3'-overhang by the binding of small molecules can: (a) inhibit the end-capping[28] and catalytic functions[29] of the telomerase enzyme (the reverse transcriptase which is responsible for maintaining the telomere length, Figure I.4a) and (b) binding of other telomere-binding proteins (hPOT1).[30] These telomerase inhibitors can be a very specific cancer therapeutic tools because (a) this enzyme is upregulated in most cancer cells, and (b) there is a marked difference in telomere length between telomerase-positive adult stem cells or germ cells (average telomere length ~15 kb) and cancer cells (~5 kb).[31]

More recently this strategy has been extended to the stabilization of other G4s DNA structures which can lead to a range of biological effects: (a) G4 formation and stabilization in promoters can result in inhibition of the transcription of a targeted gene (Figure I.4b);[32] and (b) binding to G4 ribossomal DNA selectively disrupt interaction of with the nucleolin protein thereby inhibiting RNA Polymerase I complex activity.[33]

The G4s RNA structures can also be a target for small molecules resulting in the modulation the mRNA translation. It can happen either by stabilization of G4s RNA structures (and thus impairing the assembly and/or the scanning process of the 43S ribosomal complex) or by destabilizing the G4s RNA structures (and thus stimulating translation).[21]

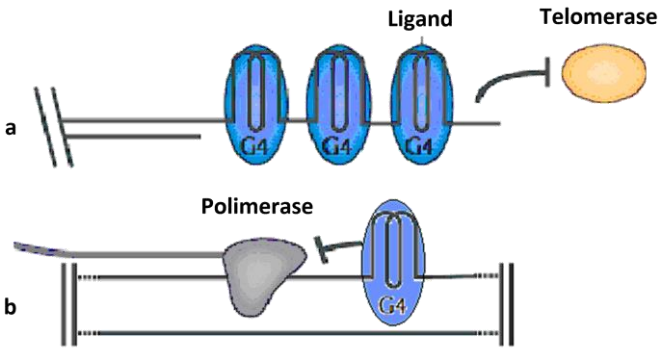

Figure I.4. Inhibition of (a) telomerase (yellow) activity or (b) gene transcription by ligands (blue) (adapted from [34]).

2.4. G-quadruplex ligands

There are some structural features that differentiate dsDNA and G4s: (a) a guanine quartet has a greater surface available for stacking contacts; (b) the four G4 grooves are diverse and differ from the duplex grooves in width, depth, electrostatic potential and distribution of hydrogen bond donor/acceptor atoms; (c) loops present in G4 are

variously arranged around the quartets and grooves; and (d) there are metal ions in the central channel.[30] Despite these differences, one of the main challenges for the development of G4-interacting molecules is the selectivity. In fact, excepting few cases, the selectivity for G4 over dsDNA of most ligands is in the range of 10-100 folds.[24] Besides that, with the increasing number of G4 reported in genomic studies, drug design must be directed not only to differentiating between secondary DNA species but also to recognizing different G4s.

Ligands may bind to G4 through different binding modes: (a) inner intercalation between G-quartets, (b) stacking from top or bottom surface of G4, (c) loops or grooves binding, or (d) a combination of more than one of these binding modes. As inner intercalation between G-quartet planes is disadvantageous in terms of energy (because it alters the π-π quartet stacking and weakens the coordination bonds between the guanines and metal ions), stacking with the terminal G-quartets is thereby the main mode of interactions with G4s.[30] In order to bind to G4, ligands usually present some of the following features: (a) an extended planar aromatic system (fused or flexible) similar to G-quartet in size and shape to establish interactions through π-π stacking; (b) side chains that are able to interact with the loops and grooves (positively charged substituents usually enhance the binding affinities with the anionic phosphate backbone and ensure sufficient solubility of a molecule with a large hydrophobic aromatic core); (c) a cationic center of the aromatic core which usually interacts with the negative electrostatic center of the G4 by electrostatic interaction; and (d) hydrogen bonding patterns generated by specific molecular shape that offer recognition to the groove regions of G4. This bonding network can be built on either aromatic or nonaromatic core.[24] Other important requirements are that a ligand should be stable in physiological conditions (without degradation or aggregation), be simple to synthesize, and have acceptable pharmacological parameters.[30]

A database known as G4LDB (http://www.g4ldb.org), which has a collection of G4-interactive ligands, provide a platform for the study of these ligand and their discovery.[35] Usually, they are divided in three G4 ligand families: the macrocyclic family, the polyaromatic fused family and a family of aromatic non-fused system.

2.4.1. Macrocyclic compounds

The macrocyclic systems (Figure I.5) described up to now as G4 ligands can be divided in three different categories: (a) telomestatin like (i.e., neutral and rigid macrocycles), (b) porphyrin (TMPyP4) like (i.e., cationic and rigid macrocycles), and the less studied (c) family of flexible cyclophane-macrocycles (i.e., cationic and non planar).

Telomestatin like. Telomestatin (**I.1**), a secondary metabolite isolated from *Streptomyces anulatus*,[36] is one of the most active known G4 ligands. It has a characteristic planar macrocyclic structure consisting of seven oxazoles and a thiazoline moiety and presents high affinity for G4 and no affinity for dsDNA.[37] Its exceptional effectiveness in binding G4 can be probably explained by the hydrophobic character of the molecule, which contributes to stacking interactions, and the similarity between the macrocycle and the G-quartet size. In addition, it exhibited an antiproliferative activity against a wide variety of cancer cell lines with half maximal inhibitory concentration (IC_{50}) values between 0.1 and 5 µM and with no effect observed at 5 µM on fibroblast MRC-5 cells. This observation has been substantiated by the finding that telomestatin does not interfere with telomere replication in normal cells. In contrast, one major disadvantages of telomestatin is its synthesis.[38] Various modifications were performed on this molecular structure by changing the number and/or type of heterocycles used[39-57] or by dimerization of the macrocyclic scaffolds.[58,59] But a real breakthrough was achieved with the aminoquinoline-based cyclic oligoamide (**I.2**)[60,61] which retained a high selectivity for G4 DNA and it is also able to discriminate different G4 DNA (human telomeric vs. oncogenic *c-KIT*). The very attractive *in vitro* biophysical results were also complemented by the low general cytotoxicity of the cyclic oligopeptides. Despite the real viability of the neutral macrocyclic scaffold for G4 recognition, the equilibrium between hydrosolubility and activity is difficult to achieve. One improvement has been the introduction of amino side chains that increase water-solubility and electrostatic attraction with the DNA target without altering the G4 selectivity of the ligand, which relies on the shape and rigidity of the polyhetroaryl cyclic scaffold itself.[38]

Porphyrins like. TMPyP4 (**I.3**) is the pivotal example of this family of ligands. This tetracationic porphyrin has been widely used, essentially due to its great affinity for several G4 targets, as well as its commercial availability.[38] However, the interest in employing TMPyP4 is somewhat counterbalanced by its lack of G4 selectivity.[37,62,63] The porphyrin core has been extensively explored as a macrocyclic scaffold not only by changing the nature and number of the surrounding side arms[64-70] but also employing ring-size analogues of the 16-membered porphyrins for the construction of G4 ligands.[18,71-78] However, worth noting that the equilibrium between affinity and selectivity is difficult to achieve maybe due to the highly cationic nature of this scaffold.[38] *N*-methyl mesoporphyrin IX (**I.4**) is interesting as the unique representative of the negatively charged macrocyclic G4 ligands, since the two carboxylic groups deprotonated at physiological pH.[63,79] Whilst this molecule became rapidly known as highly G4 selective, it is regarded as a weak G4 binder because its negative charge prevents favorable electrostatic interactions with DNA.[80] With an inner cavity particularly suited to coordination of a metal, porphyrins and their analogues have been

also widely exploited to form metal complexes.[74,81-95] Among them, a Mn(III) complex (**I.5**) deserves particular attention since it was able to interact with G4 10,000 times faster than with dsDNA.[96] More recently, metal-porphyrin conjugates with Re(I)[70] and Pt(II)[97] in periphery were found to effectively stabilize various kinds of G4s.

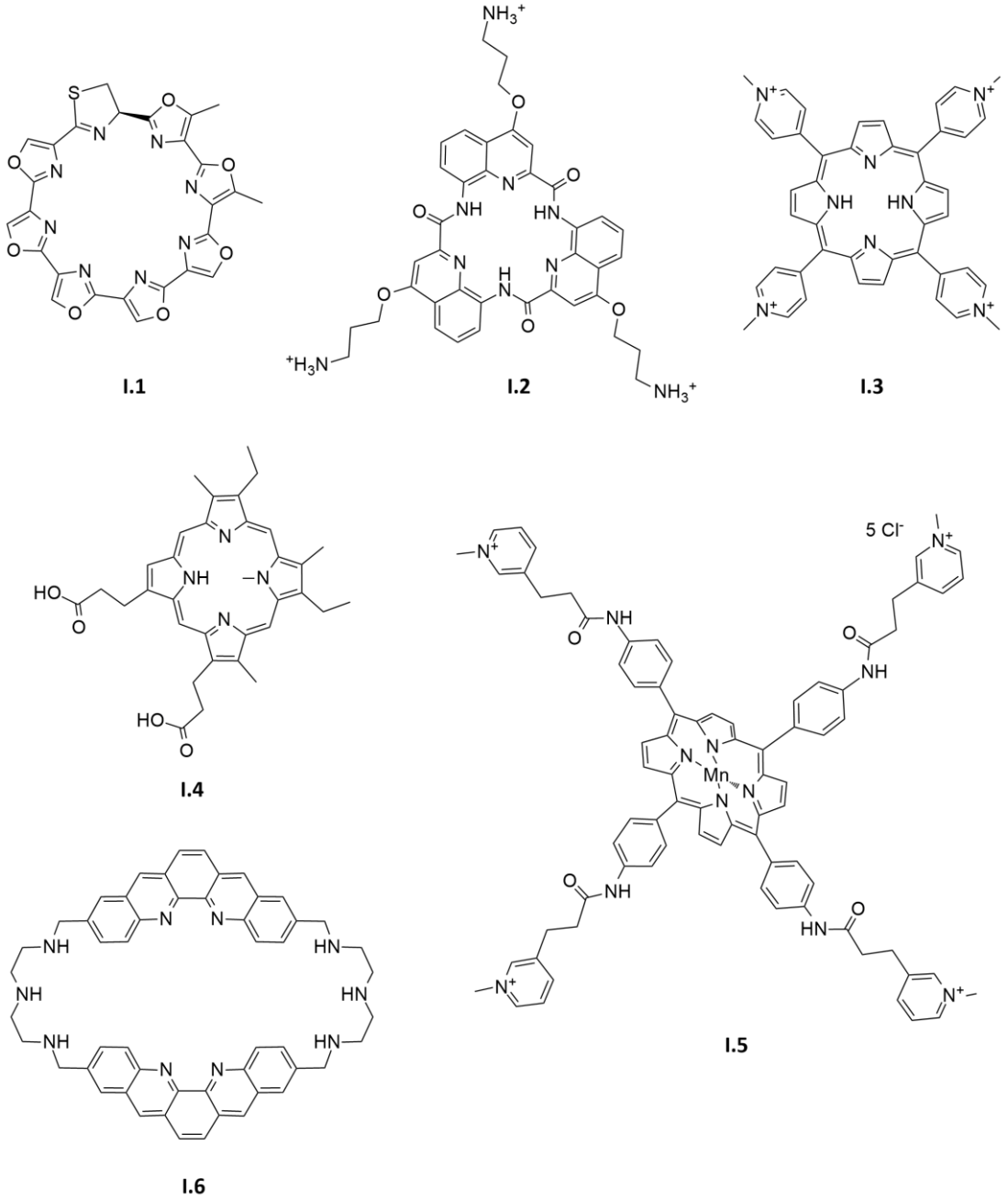

Figure I.5. Examples of macrocyclic G4 ligands.

Cyclophane-Type Macrocycles. Mainly two types of cyclophane-like macrocycles have been studied for their interaction with G4s: (a) the cyclo-bis-intercalator and cyclo-tris-intercalator family and (b) the neomycin-capped aromatic platforms. The cyclo-bis-

intercalator and cyclo-tris-intercalator macrocycles contain two or three flat aromatic units, respectively, usually derived from simple intercalators linked together by different chains.[98-100] Bis-ortho-quinacridine (**I.6**)[101] and bis-acridine,[102] two well-known examples of this family, formed non-planar cage like structures and showed a better binding affinity than their monomeric analogues. Some molecules containing only one flat aromatic unit and a macrocyclic framework were also synthesised as G4 ligands.[99,103,104] The second category of cyclophane-type macrocycles combine an aromatic platforms able to stack on a G-quartet with a well-known loop-binding motif, that is, the aminoglycoside neomycin.[105,106] The most active prototype of this series is the quinacridine derivative[105] that is a potent binder of the telomeric G4 DNA whereas it elicits a poor affinity for dsDNA.

2.4.2. Polyaromatic fused compounds

The overwhelming majority of ligands belongs to this group. Here, only some of the more important families will be mentioned.

Acridine and acridone derivatives. Some acridine derivatives (e.g., the 3,6-disubstituted acridine,[107-109] 3,6,9-trisubstituted acridine)[110,111] are among the most important ligands while others (such as 3,9- and 4,9-disubstituted acridine derivatives) present more modest results.[112] BRACO-19 (**I.7**, Figure I.6) stands out among the members of this family. This ligand showed strong binding affinity for G4s structures, high telomerase inhibitory activity which resulted in telomere uncapping and removal of telomere-binding protein from telomere, resulting in telomere aberration, DNA damage response and cell growth cessation in cancer cell lines. Moreover, this molecule can cause translocation of telomerase from nuclear to cytoplasm. Additionally, **I.7** did not induce the growth inhibition of normal human primary astrocytes, as well as the DNA damage response, telomere abnormality and T-loop disassembly.[113] **I.7** also showed significant *in vivo* anticancer activity in tumor xenografts, with tumor shrinking up to 96% and curative responses in some animals.[114] A series of BRACO-19 dimer ligands showed to bind to human telomeric G4 DNA and exhibited potent inhibition of human telomerase with IC_{50} values similar to or lower than those of BRACO-19. Furthermore, these ligands displayed greater potency in the inhibition of hPOT1 and increased selectivity for G4 DNA when compared to BRACO-19.[115]

The tricyclic system of acridines was subsequently modified to tetracyclic[116,117] and pentacyclic system,[116,118-121] to enlarge the plane size for π-π stacking. One example of the pentacyclic system, RHPS4 (**I.8**, Figure I.6) have shown a potent telomerase inhibition at submicromolar concentrations, causing irreversible proliferation arrest and exhibiting antitumoral activity *in vivo* and *ex-vivo*.[122]

Several series of disubstituted acridone compounds have also been studied as G4 ligands.[123] Particularly, a series of 4,5-disubstituted acridone derivatives (**I.9**, Figure I.6) were found to have high affinity for human telomeric G4 DNA, with improved selectivity compared with trisubstituted acridine compounds.[124] Most of the compounds have distinguishing cytotoxicity between cancer cells and normal cell lines. Interestingly, the properties of these 4,5-acridones are in striking contrast with a series of 4,5-disubstituted acridines that show low G4 stabilizing ability.[125]

In xanthene and xanthone derivatives, the nitrogen of the acridine and acridone scaffold is replaced by an oxygen. Two and three-side chain xanthone and xanthene derivatives, as well as a dimeric "bridged" were synthesised. A trisubstuted compound (**I.10**, Figure I.6) showed the highest binding affinity to the human telomeric G4 DNA.[126] Based on the dimeric xanthone derivative (**I.11**, Figure I.6), the new 7-ring compound HELIXA4C (**I.12**, Figure I.6) was tested and the experimental results clearly indicated that the drug induces a certain amount of telomere-localized damage.[127]

Anthraquinones and derivatives. Anthraquinones are well-known pharmacophores with DNA-interacting properties. Doxorubicin is example of an anthraquinone derivative widely used as antitumor drug in clinical practice which bind to the human telomeric sequence without selectivity over dsDNA.[128] Mitoxantrone is another anthraquinone used clinically that stabilized G4 very efficiently.[129]

Several types of disubstituted amido anthraquinones with amine terminal side chains were evaluated as G4s ligands.[130,131] They represent an example of how the pattern of disubstitution modulates dsDNA vs. G4s selectivity. In fact, the presence of 1,4-substituents shifts the binding preference to the dsDNA structure, whereas 2,6- or 2,7-congeners incremented G4 recognition.[132] Nevertheless, the modification of side-chain terminal groups from amine to amino acid can enhance the interactions between the ligand and the G4s groove regions, therefore improving selectivity toward G4s structures.[132,133] More recently, researchers found that peptidyl-anthraquinones were excellent selective ligands for G4s. In this molecules, shifting side chains from position 2,6- or 2,7- to 1,5- or, to a lesser extent, to 1,8- helps increasing G4 stabilization but it also promotes effective binding to dsDNA.[134] Alternatively, conjugation of the anthraquinone core with neomycin resulted in ligand **I.13** (Figure I.6) which exhibits a nanomolar affinity for human telomeric G4 DNA, 1000-fold higher when compared to its constituent units.[135] This higher affinity is ascribed to the dual binding mode of the conjugate which can interact with the guanines of the G4 (anthraquinone) via π-stacking interactions and with the grooves (since neomicyn is a loop-binding agent as previously stated). Ethynyl-anthraquinones derivatives were also synthesised as G4 bi-modal ligands, acting on a selective reversible recognition and subsequent alkylation upon

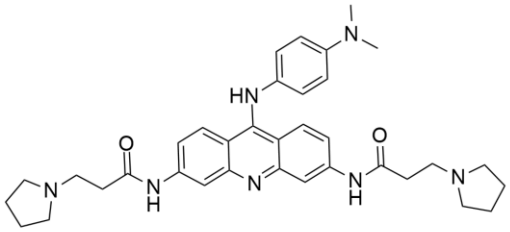

I.7

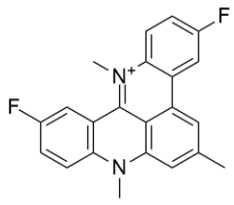

I.8

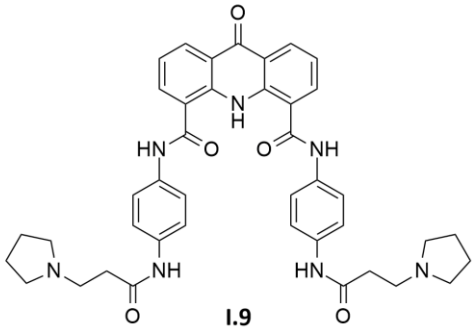

I.9

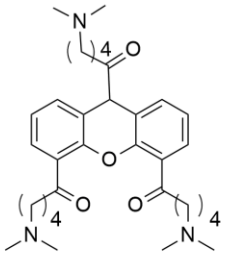

I.10

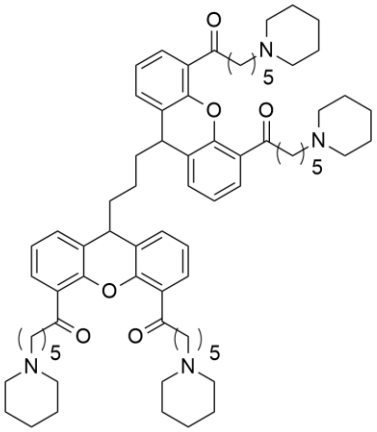

I.11

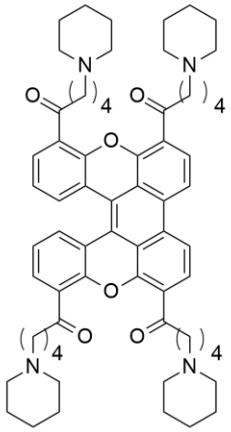

I.12

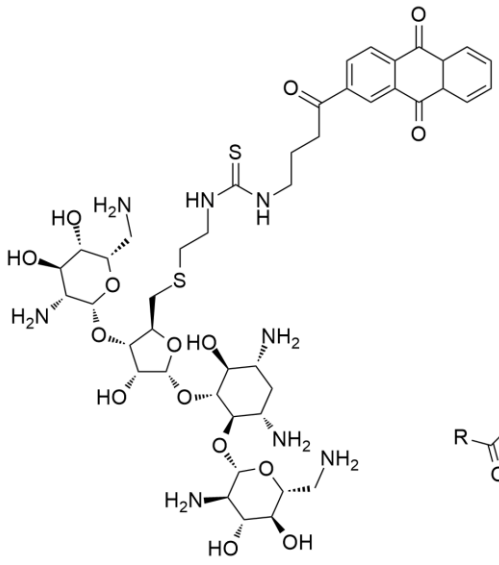

I.13

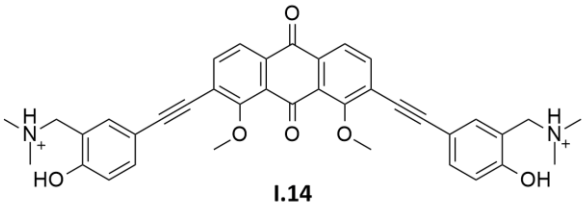

I.14

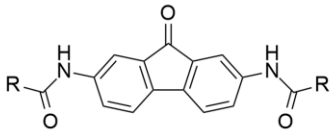

I.15, R = alkylamine

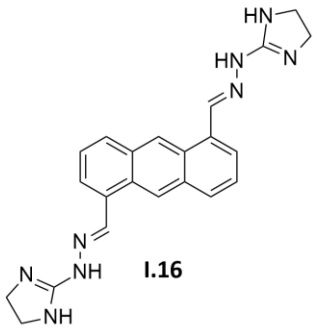

I.16

Figure I.6. Examples of acridine, anthraquinone and anthracene derivatives G4 ligands.

reductive activation. The best compound of this series (**I.14**, Figure I.6) presented good binding affinity and it lacked significant intercalation into the dsDNA.[136] Other examples of anthraquinone derivatives includes molecules that present a fourth aromatic ring.[137,138] Fluorenones and derivatives can also be included among the anthraquinone derivatives, e.g. **I.15** (Figure I.6).[139-142]

Anthracene derivatives. In contrast with acridines or anthraquinones, anthracene is not characterized by the presence of a localized charge density on the aromatic system what should grant high flexibility of location over the G-quartet. As in anthraquinones, different regioisomers showed distinct binding affinities for human telomeric G4 DNA: the most effectives were the 1,5- (**I.16**, Figure I.6) and 1,7-bis-substituted analogues while the 1,8-regioisomer was poorly effective. Besides that, the 1,5-regioisomer presented a better selectivity (difference in affinity by one order of magnitude) for G4 vs. dsDNA binding when compared with bis-substituted anthraquinone and acridine congeners. Additionally, G4 binding was clearly related to telomerase inhibition in this class of compounds.[143] Based on this data, constrained analogues of the 1,5-regiosiomer have been synthesised.[144]

Phenanthrolines derivatives. Several structures containing 1,10-phenanthrolines have been investigated as G4 ligands (Figure I.7). Some of the compounds belonging to this class present the 2,9-substitutional pattern including highly potent and selective bisquinolinium amides (**I.17**),[145] bistriazoles carrying tethered positive end groups,[146] analogues with cationic amino side chains[147,148] and metal complexes.[149,150] Besides that, other 1,10-phenantroline substitution patterns have also been studied,[120,148,151-153] including conjugation with carbohydrates.[154] Additionally, a series of 4,7-diamino-1,10-phenanthroline derivatives (**I.18**) carrying positively charged side chains showed appreciable G4-stabilizing properties but poor selectivity over dsDNA.[153] Tetrasubstituted phenanthrolines carrying both 4,7-diamino substituents and 2,9-carboxamide-linked quinolines (**I.19**) were also studied. They showed improvements over both parent structures exhibiting a strong affinity, a high degree stabilization and selectivity for the G4 structure. *N*-Methylation of the quinolines and positive charges on the terminal 4,7-substituents were found to be essential for the G4 interaction of compounds of this series.[155] Bis-phenanthroline ligands, containing two phenanthroline moieties covalently linked through an amine or thioether bond, and its metal complexes were also tested. In particular, Ni(II) and Cu(II) complexes showed dramatic increase ligand-stabilising effects on G4, promote the G4 folding and inhibit the activity of telomerase.[156] Phenanthroimidazole derivatives[157,158] and its metal complexes[159-164] were also studied. Overall Pt(II) complexes (**I.20**) displayed a significantly greater binding affinity and selectivity for G4 than dsDNA, inhibited telomerase activity *in vitro*, caused a significant dose- and time- dependent decrease in average telomere length and

presented antiproliferative activity on A549 lung cancer cells and to a lesser extent on primary MRC5 fibroblast cells.[159,165,166] More recently, several cyclometalated Ir(III) phenanthroimidazole complexes showed to bind with low micromolar affinity to G4 DNA sequences and exhibited enhanced luminescence upon binding to these sequences. Due to the this luminescence enhancement, the complexes are able to be used as selective G4 indicators.[167]

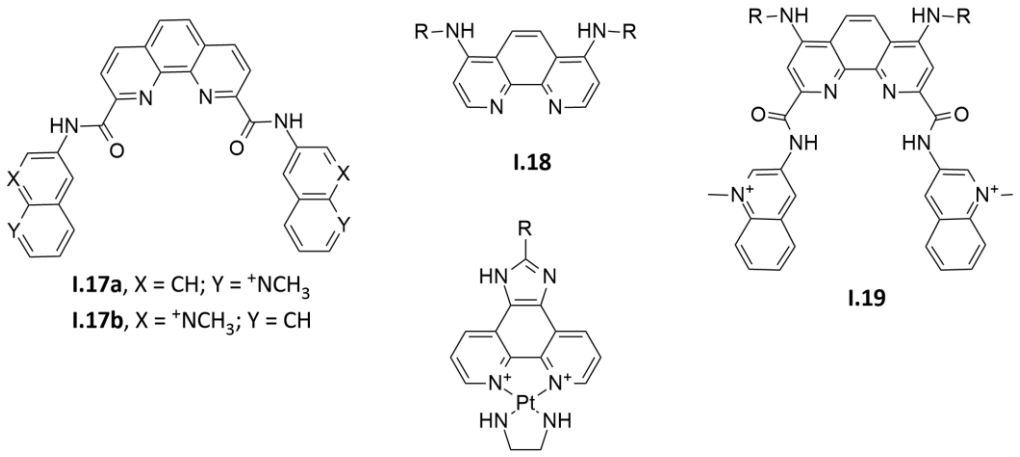

Figure I.7. Examples of phenanthrolines derivatives G4 ligands (R: alkylamine).

Carbazole derivatives. One of the most studied G4 ligands of carbazole skeleton is BMVC (**I.21a**, Figure I.8) which recognizes and stabilizes specific G4 structures, particularly human telomeric sequence. Besides that, it also exhibits excellent ability to inhibit telomerase activity and have proved to repress tumor progression. This molecule have also been used as fluorescent probe for G4 DNA recognition.[168] *Ortho*-isomer of BMVC (**I.21b**, Figure I.8) is also a good G4 stabilizer but a better G4 fluorescent probe with greater ability to distinguish G4 DNA from dsDNA. In addition, 3,6-bis(1-methyl-4-vinylpyrazinium)carbazole diiodide (**I.21c**, Figure I.8) is likely a better core molecule than BMVC for G4 stabilizers.[169] Several other carbazole derivatives with different substituents present on the tricyclic ring system have been synthesised in order to study their activity as G4 ligand and/or G4 probe.[168-172] Results suggested that the tri-cations of 9-substituted BMVC derivatives are better G4 stabilizers than the bi-cations.[169] Recently, benzimidazole−carbazole (**I.22**, Figure I.8) conjugates and their dimers demonstrated high binding affinity and stabilization of G4 DNA and also induce significant apoptotic response and antiproliferative activity toward cancer cells selectively when compared to the normal cells.[170,171]

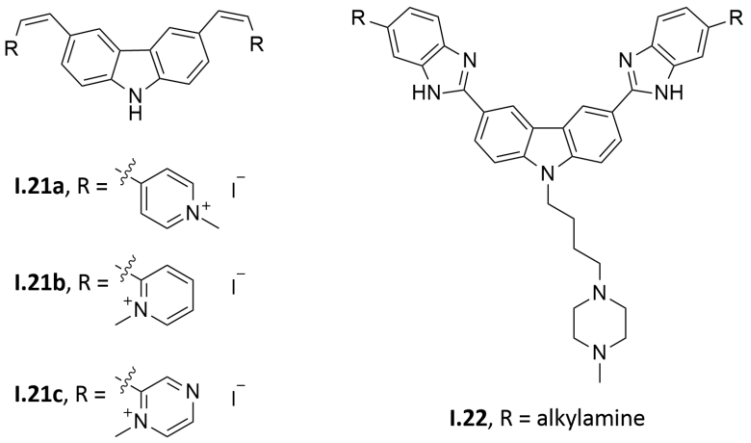

Figure I.8. Examples of carbazole derivatives G4 ligands.

Indoloquinoline derivatives. One of the first series of indoloquinolines tested for G4 binding were the pentacyclic benzoindoloquinoline derivatives (**I.23**, Figure I.9).[173] However, the majority of indoloquinoline ligands developed for G4 recognition are derived from quindoline (10*H*-indolo[3,2-*b*]quinolone) or its *N*-methyl derivative (cryptolepine). The disubstituted quindoline derivatives (with two alkyl amino groups at the 2,7-,[174,175] 2,10-[176] or at the 10,11-[177]) presented modest to good G4 stabilization and telomerase inhibition activity. Analogues with an electron-donating group at the 11-position significantly improved their ability to stabilize a G4. This fact is due to the significant increase in the electron density at the quinoline nitrogen (N^5) atom resulting in easy protonation under physiological pH that is an important feature to improve binding to external G-quartets of G4s.[178-180] The most active derivative, SYUIQ-05 (**I.24**, Figure I.9), interacts with human telomere or *c-MYC* oncogene G4s (with relatively stronger affinity) and has effects on the biological functions of these two genes, resulting in telomere shortening, autophagy, inhibition of cell proliferation, cell senescence, and apoptosis.[179,181] Besides the introduction of the positive charge via *in situ* protonation, an alternative pathway was *N*-methylation at 5-position. Cryptolepine-11-amine derivatives were also studied and exhibited a significant improvement in the ligand mediated stabilization of the G4 structure.[180,182-184] In particular, trisubstituted quindoline derivatives presented an increased and more selective G4 stabilisation over dsDNA relative to the correspondent disubstituted derivatives and also some inter-G4 selectivity.[184,185] Recently, a small library of mono- and di-substituted alkyldiamine isocryptolepine (11*H*-indolo[3,2-*c*]quinolone) derivatives showed very potent thermal stabilization of the telomeric sequence.[186] Among these ligands, disubstituted compounds (**I.25**, Figure I.9) are potent and selective G4 stabilizers vs. dsDNA.[187] Other indoloquinolines, such as neocryptolepine (5-methylindolo[2,3-*b*]quinoline), are weak telomerase inhibitors and exhibit a significant preference for triplexes over G4 or

dsDNA.[188] Besides that, a series of peptidylbenzofuroquinoline conjugates was synthesized to improve the selectivity of cryptolepine analogues. The most active compound (**I.26**, Figure I.9) presented potent inhibitory effect and 50-fold higher selectivity for human telomeric G4 DNA against the dsDNA. Additionally, cellular experiments also showed a promising anticancer effect.[189] Recently, metal complexes containing indoloquinoline moiety have been synthesised,[190-192] higlightning a Ru(II) complex containing which presented a significant selectivity to human telomeric over *c-MYC* G4s DNA.[192]

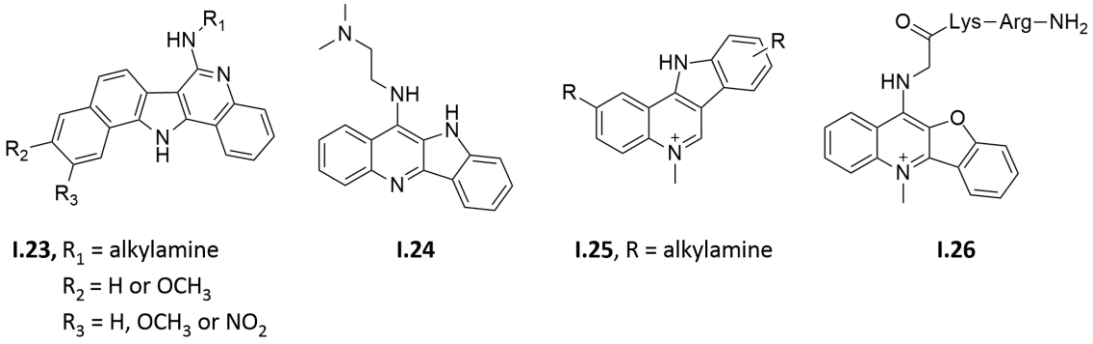

I.23, R_1 = alkylamine
R_2 = H or OCH_3
R_3 = H, OCH_3 or NO_2

I.24

I.25, R = alkylamine

I.26

Figure I.9. Examples of indoloquinoline derivatives G4 ligands.

Isoquinoline derivatives. Berberine, palmatine, chelerythrine, coralyne, and sanguinarine are isoquinolines whose nucleic acid binding abilities have been studied. The more planar compounds (coralyne, **I.27** and sanguinarine, **I.28**, Figure I.10) are better G4 ligands than the others.[193-197] However, all these isoquinolines showed a strong binding ability to dsDNA.[198] Structural modifications of these isoquinoline alkaloids, mainly in berberine, have greatly improved the G4 selectivity. These modifications include side chain introduction (positions 9[198-200] and 13[201,202]), dimerization[203,204] and scaffold revisions, such as quinolino-benzo-[5,6]-dihydroisoquindolium compounds (**I.29**, Figure I.10), which exhibited better binding affinity for *c-MYC* G4 and excellent inhibition of its transcription and expression in cancer cells but not in normal cells).[205]

Quinobenzoxazine derivatives. A series of quinobenzoxazines derivatives were patented by Whitten *et al.* in 2006, including over 1800 compounds. Among them, quarfloxin (**I.30**, Figure I.10) showed good selectivity toward *c-MYC* G4. It displayed antitumor activities to a broad range of tumor types, IC_{50} from sub-micromole to micromole range. Later, it was found to interact with rDNA G4 and disrupt nucleolin binding, which would lead to cancer cell apoptosis.[24] The drug completed phase I in patients with advanced solid tumors and lymphoma in 2009 but it did not proceed beyond phase II clinical trials, due to its limited bioavailability.[206]

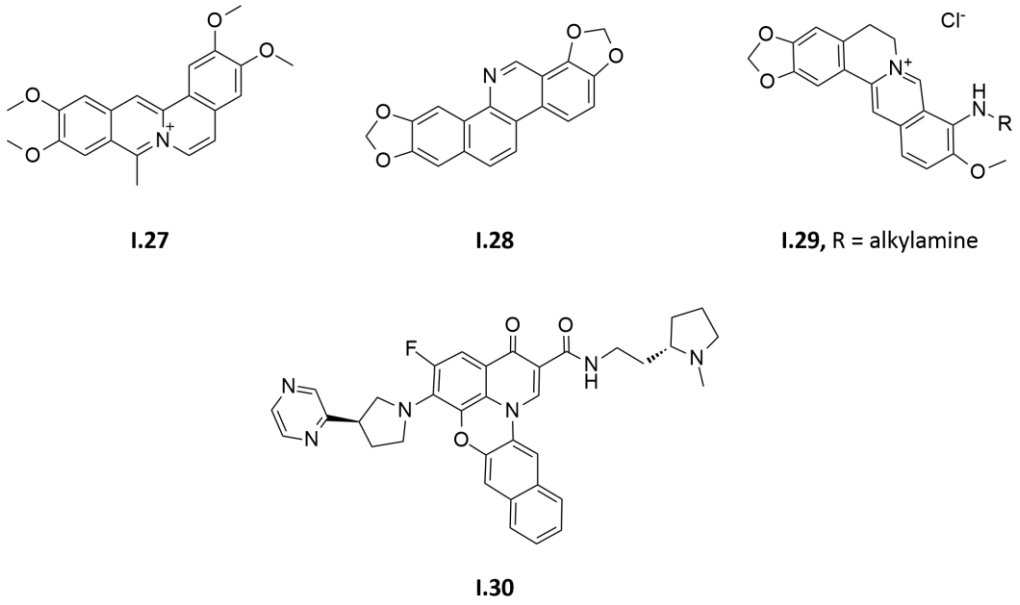

I.27 **I.28** **I.29,** R = alkylamine

I.30

Figure I.10. Examples of isoquinoline derivatives G4 ligands and quarfloxin.

Diimides derivatives. Perylene diimide[207-211] and corenene diimide[207,212] derivatives exhibiting different side chains were studied as G4 ligands. Based on these two scaffolds, some authors modified the number of condensed aromatic rings and introduced different side chains obtaining several series of mono-[208] and tri-substituted[213] naphthalimides and di-,[208,214,215] tri-[214] and tetra-substituted[214,216-220] naphthalene diimides. Disubstituted naphthalene diimide analogues showed low selectivity for G4, while tri- and tetra-substituted analogues exhibited high G4 affinity. Concerning the tetrasubstituted naphthalene diimide analogues, the binding affinity of naphthalene-based ligands depends on structural constituents of the ligand as well as the arrangement of the phosphate and other polar groups in DNA structure, since the four substituents interact through hydrogen bonds, water bridges and electrostatic contact with each G4 groove. Usually bulky terminal groups improve stability of G4 structure by positioning itself in the G4 grooves.[221] Remarkably, in spite of their size and high net cationic charge, these compounds are rapidly transported into MCF7 breast cancer cell nuclei, possibly by active transport mechanisms.[222] BMSG-SH-3 (**I.31**, Figure I.11) is a potent G4 DNA stabilizing ligand with sub-micromolar cell growth inhibitory activity in a range of pancreatic (and other) cancer cell lines, and also inhibits telomerase in these cells.[223] As previously observed in other derivatives, the presence of metal ions seems to be advantageous.[224,225] An example of this is a disubstituted naphthalene diimide derivative incorporating Zn(II) ions into its dipicolylamine groups (**I.32**, Figure I.11) which revealed higher affinity to investigate oligonucleotides, comparing to the compound without the metal.[224] A series of naphthalene diimides capable of reversibly binding human telomeric G4 DNA and alkylate it through an electrophilic quinone methide

moiety (**I.33**, Figure I.11) showed a marked stabilization and selectivity towards telomeric G4 DNA.[226,227] Recently, carbohydrate naphthalene diimide conjugates have shown certain selectivity for G4 structures against dsDNA. Interestingly, a correlation between the more efficient cell uptake (through glucose transporters) of these molecules and their higher toxicity in cancerous cell lines has been observed.[228]

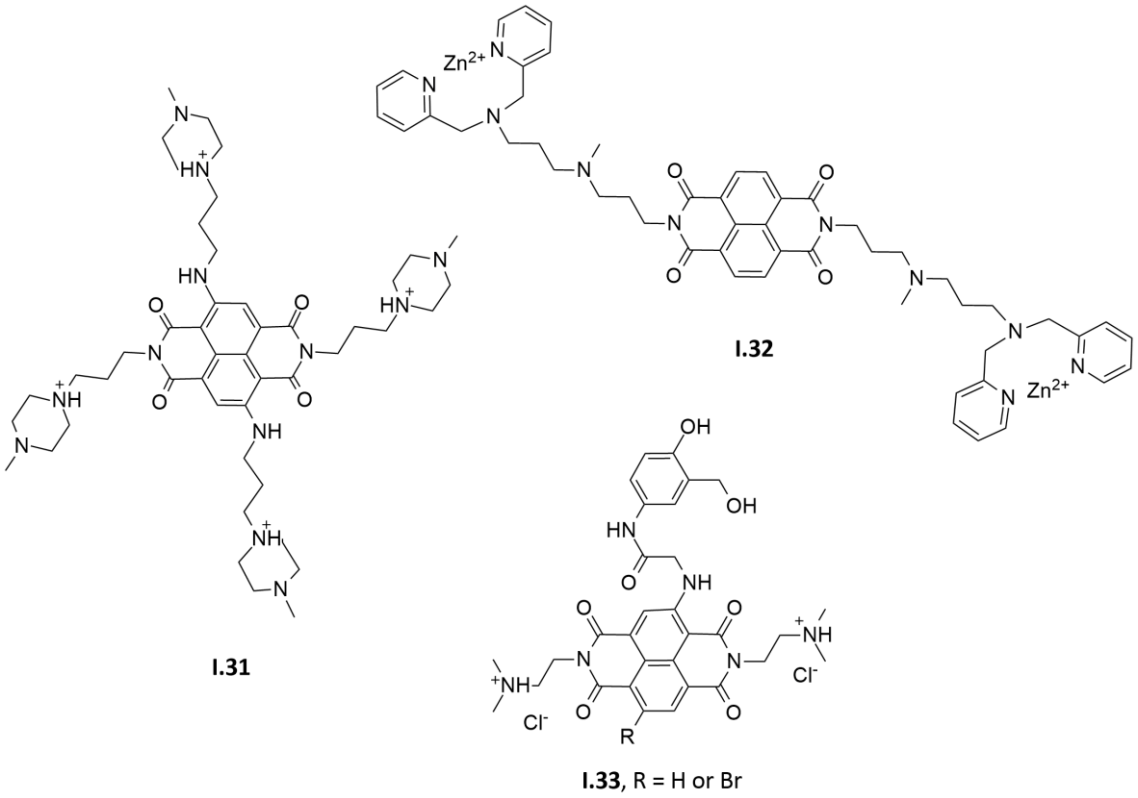

Figure I.11. Examples of naphthalene diimides derivatives G4 ligands.

2.4.3. Non-fused aromatic compounds

The acyclic compounds tend to be characterised by a crescent shape. These molecules were designed with the main objectives of potentially enhance the drug-like features when compared with the other families.[229] Here, only some of the more relevant families will be described.

Bis-quinoline derivatives. Several ligands where the two quinolinium moieties are connected through different aromatic or more flexible linkers were synthesised. Examples of aromatic linkers were 2,6-pyridine,[230,231] 2,6-pyridodicarboxamide,[232-235] triazine,[236,237] 2,2'-bipyridinecarboxamide,[238] bis(vinylquinolinium)benzene[239] and 1,8-naphthyridinecarboxamide.[240]

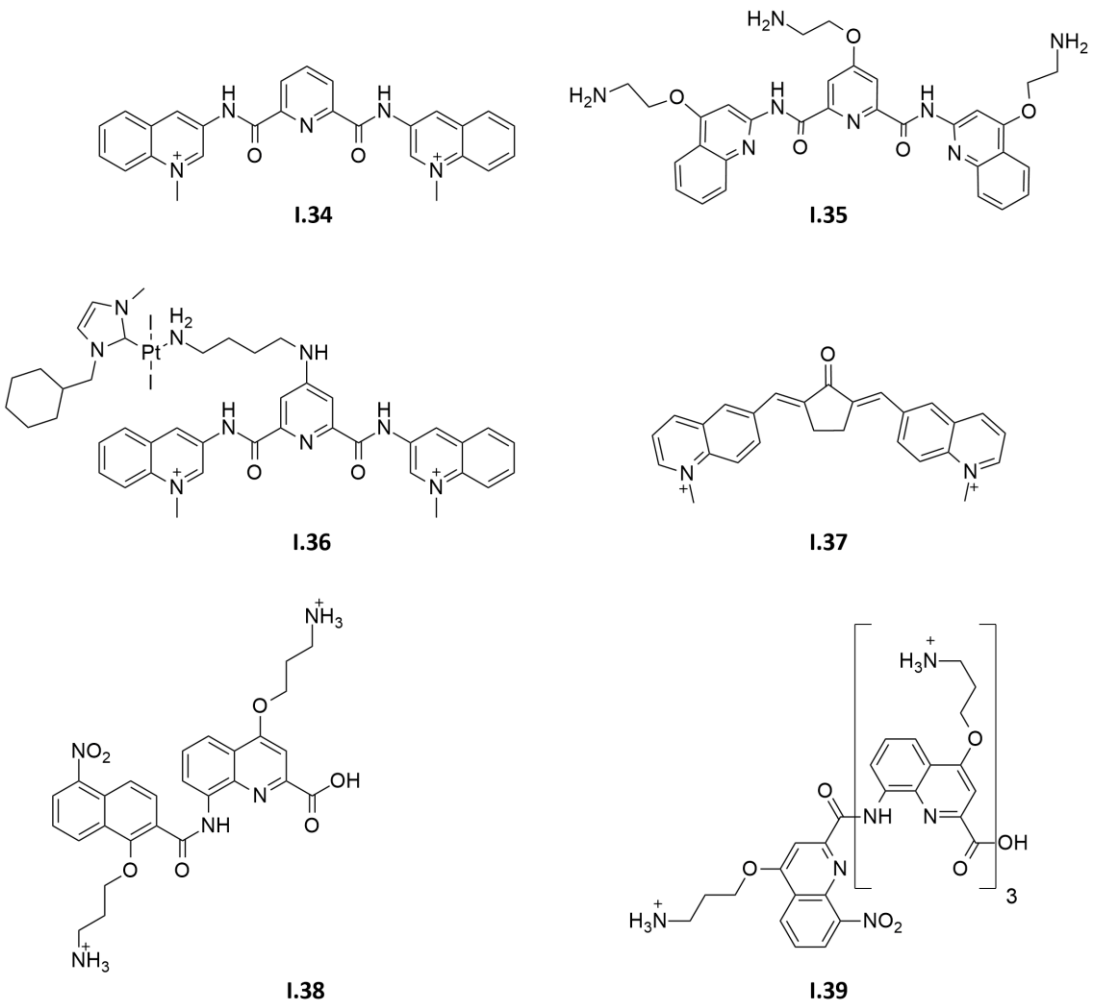

Figure I.12. Examples of bis-quinoline derivatives G4 ligands.

Among them, the compounds linked through 2,6-pyridodicarboxamide are the most studied, especially compounds **I.34** (Figure I.12) and pyridostatin **I.35** (Figure I.12). Generally, these compounds displayed strong specificity and selectivity for G4 structures and strong inhibition of telomerase *in vitro*. They also inhibited proliferation and induced apoptosis of telomerase-positive glioma cell lines with short telomeres and were also effective on ALT cell lines.[232,234,235] Pyridostatin interacts with telomeres and alters the integrity of shelterin in cells through POT1 uncapping (resulting in a DNA-damage response)[235] and alters transcription and replication of particular human genomic loci containing high G4 clustering within the coding region.[234] The successful design of pyridostatin prompted the synthesis of analogues with different substituents.[234,241,242] It was described that the nature of the substitution at the pyridine moiety has a great influence on the stabilization potential of the molecules for human telomeric G4 DNA while the nature of the amine on the side chain was found to have a small influence on the stabilization potential of the analogues.[241] Recently, a conjugate

of **I.34** with an already identified antitumor *N*-heterocyclic carbene-platinum complex (**I.36,** Figure I.12) showed a strong stabilization of G4 structures *in vitro* binding preferentially and irreversibly the with the human telomeric sequence.[243]

Molecules having the bisquinolinium moiety linked through more flexible central linkers such as vinyl bridge,[244] diene spacer,[244] heptamethylene and decamethylene linkers[245] and a series of bisaryldiketene derivatives[246] were also tested. Among this compounds, one of the bisaryldiketene derivatives (**I.37**, Figure I.12) stood out since it was 200 times more selective for *c-MYC* over telomeric G4 DNA.[244,246]

Dimer **I.38** (Figure I.12) and tetramer **I.39** (Figure I.12) presented different FRET results. While the compound **I.38** is a poor G4 ligand the helical trimer **I.39** is a moderately strong G4 stabilizing ligand with apparent selectivity relative to dsDNA.[247]

Bis- and tris-triazoles derivatives. Bis-triazole ligands linked by a benzene[248,249] or a naphthalene[250,251] scaffold are described in Chapter II. A series of symmetric phenyl derivatives containing three triazole moieties (**I.40**, Figure I.13) did not stabilize neither G4 DNA nor dsDNA.[252]

Bis-indole derivatives. Bis-indole carboxamides exhibiting a pyridine (**I.41**, Figure I.13) as planar central core and *N,N*-dimethylpropylamine side chains were evaluated. Pyridine bis-indoles exhibited moderate stabilization potential for four different G4 forming oligonucleotides studied and showed better selectivity for promoter G4 (*c-KIT2* and *c-MYC*) over human telomeric G4 DNA. In addition, a diminished dsDNA stabilization was observed for the ligand **I.41**.[253,254] Analogues of these ligand with variations in amine side chains (different substitution position, length and stereochemistry) also exhibit significant selectivity for G4 DNA over dsDNA. Besides that, the substitution of pyridine by a fluorobenzene ring on the bis-indole scaffold was found to enhance the stabilisation potential for human telomeric and *c-KIT2* G4s.[254]

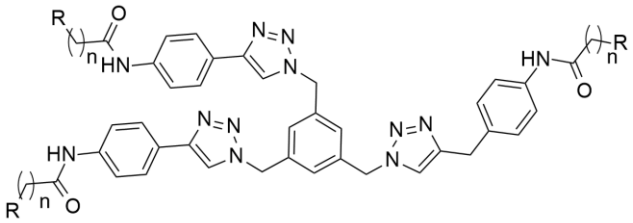

I.40

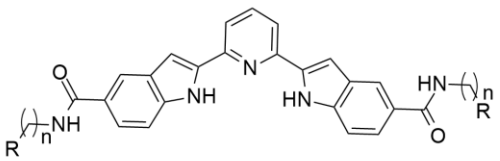

I.41

Figure I.13. Examples of bis-triazoles and bis-indole derivatives G4 ligands (R: amine).

Bis-benzimidazole derivatives. Bis-imidazole ligand **I.42** (Figure I.14), one of the first ligands of these class tested, only stabilized the human telomere G4 DNA at high concentrations.[255] Conjugation of **I.42** with neomycin enhances its binding to G4 DNA.[256]

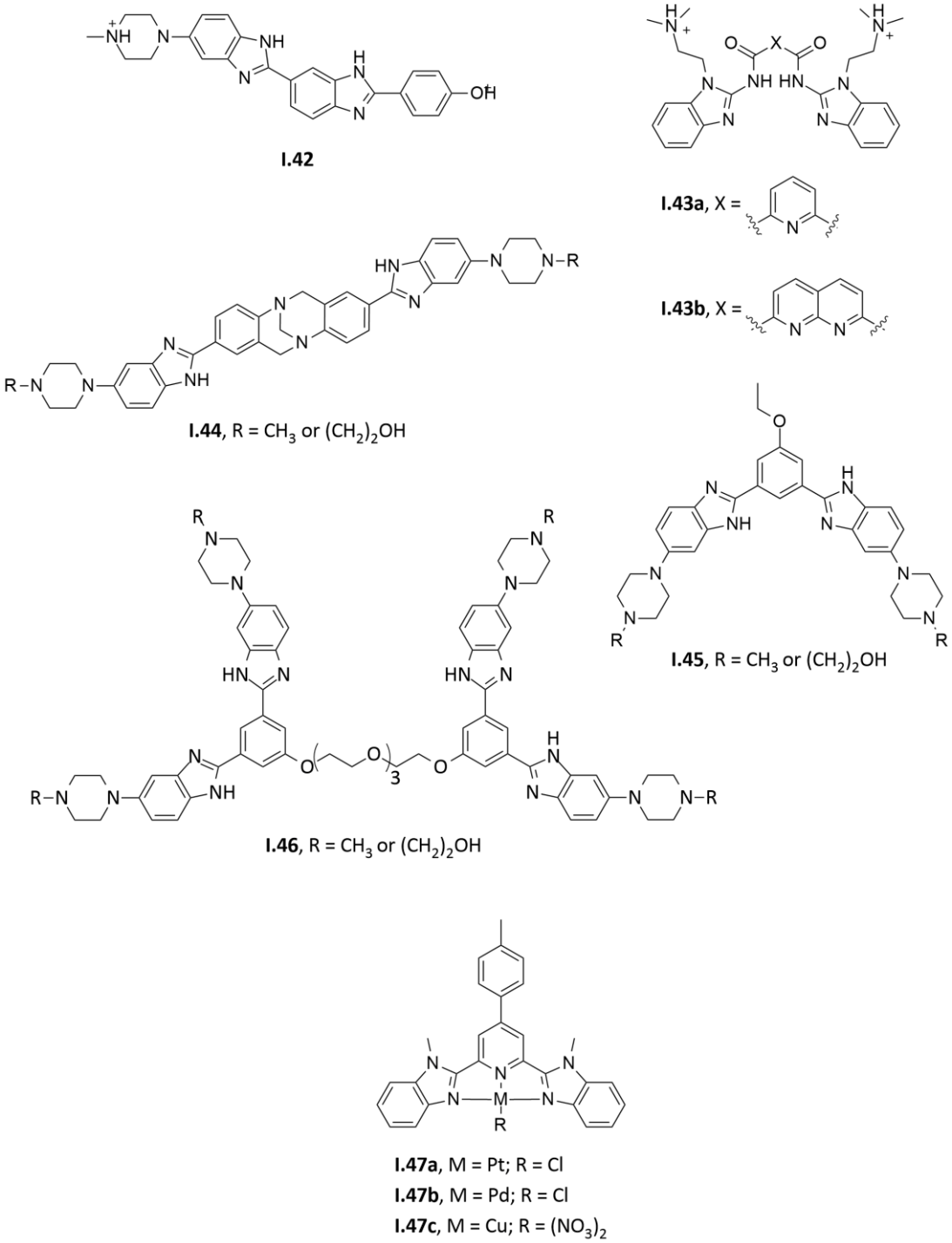

Figure I.14. Examples of bis-benzimidazole derivatives G4 ligands.

Different bis-benzimidazole derivatives linked through an aromatic cores were also developed.[257,258] Among them, compounds presenting pyridine (**I.43a**) and 1,8-naphthyridine (**I.43b**) as a central core specifically bind to and stabilize promoter G4 DNA having parallel topology over any of the human telomeric G4 DNA topologies and dsDNAs.[257] Substituted benzenes[245,259] and Tröger's base (**I.44**, Figure I.14)[260] are other examples of core group that were used to link the two benzimidazoles.

A series of monomeric and dimeric *m*-phenylene-bis(piperazinylbenzimidazole) derivatives (respectively **I.45** and **I.46**, Figure I.14) were also studied. Monomeric ligands presented a significant stabilization and selectivity for G4 DNA while the dimeric ones induced less stabilization. *In vitro* studies showed that both ligands have concentration-dependent cytotoxicity toward cancer cells and selectively toward cancer cells over normal cells.[245]

Some tolyl derivatives and metal complexes (**I.47**, Figure I.14) were also synthesised. The crucial effect of the metallic cation was once again confirmed since the free organic ligand present little or no stabilizing effect.[230]

Bis-oxazoles derivatives. The pentacyclic BOxaPy (**I.48**, Figure I.15) and heptacyclic TOxaPy (**I.49**, Figure I.15) were the first examples of bis-oxazole derivatives studied as G4 ligands. The heptacyclic derivative **I.49** was found to be totally devoided of affinity for dsDNA while exhibiting a binding preference for certain G4 topologies over others. In contrast, the pentacyclic oligomer **I.48** appears to be unable to stabilize human telomeric G4 DNA. Consistent with the previously stated, compound **I.49** was found to inhibit strongly the proliferation of the cell lines with IC_{50} values lying down to the nanomolar range. Conversely, the pentacyclic analogue **I.48** was poorly efficient even at high concentration.[261]

A series of triazole-centred ligands flanked by phenyloxazoles (**I.50**, Figure I.15) were also synthesised but demonstrated to be quite poor binding to G4 DNA.[262]

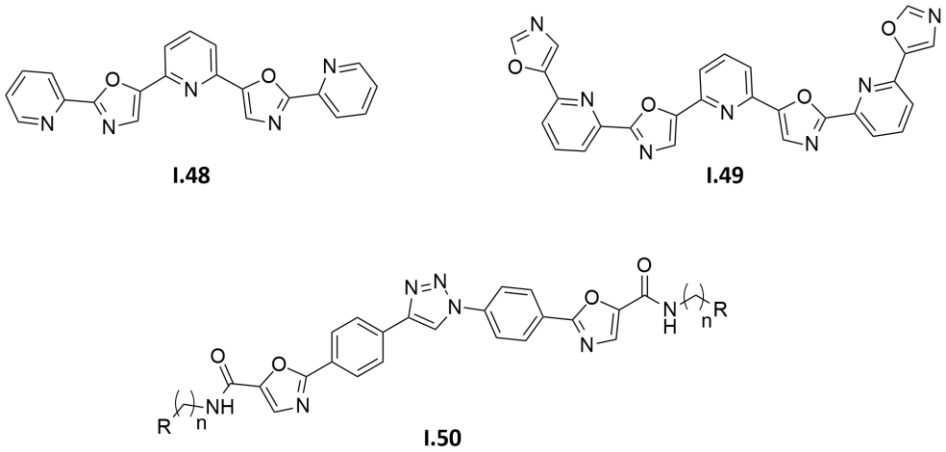

Figure I.15. Examples of bis-oxazole derivatives G4 ligands (R: amine).

Diarylureas derivatives. G4 stabilizing ability of diarylurea ligands depends on different structural features of these ligands, namely the urea bond substitution pattern, the length of alkylamino side chain and the terminal amine (Figure I.16). For example, in a series of diarylurea ligands with a triazole linker, *ortho*- and *meta*-analogues have significantly enhanced stabilising affinity to telomeric and non-telomeric G4 DNA over

the more extended *para*-analogues, suggesting that the 'square-planar' conformation of the ligand core is critical for efficient G4 interaction. In this series and in another without triazole, the *meta*-substituted analogue with pyrrolidino side chains presented the best results as G4 ligands (respectively **I.51** and **I.52**).[263,264]

Smaller diarylurea compounds **I.53** and **I.54** were identified by high-throughput screenings.[244,265] Other urea-based G4 targeting ligand (**I.55**) presenting significant selective stabilisation of telomeric G4 was also identified.[244]

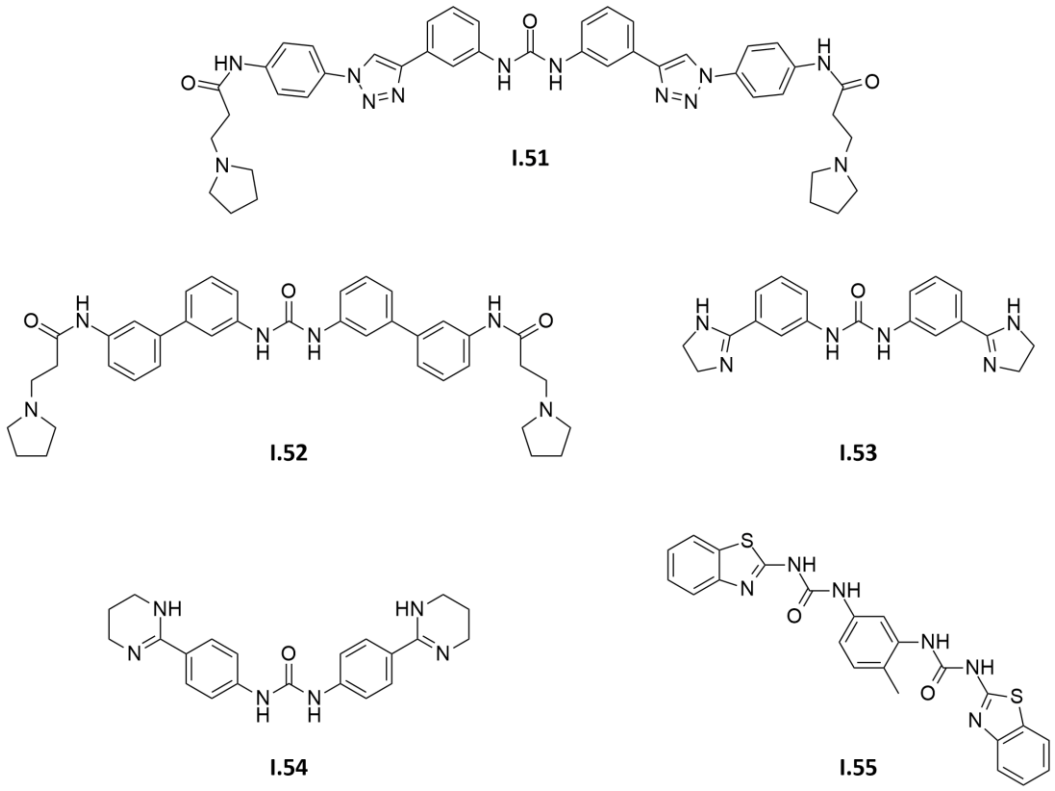

Figure I.16. Examples of diarylureas derivatives G4 ligands.

Diethynylamides derivatives. Bis-phenylethynyl amide derivative linked through a pyridine ring and containing *N,N*-dimethylpropylamine side chains (**I.56**, Figure I.17) showed moderate stabilization for three promoter G4 DNA with no detectable stabilization of dsDNA.[266] In order to achieve enhanced binding ability and differential recognition towards diverse G4 sequences, substituted analogues were synthesised. These analogues significantly increased the stabilisation potential and selectivity for a

particular G4 target compared to the parent ligand **I.56**, being **I.57** the best G4 DNA stabilising ligand in this series.[267]

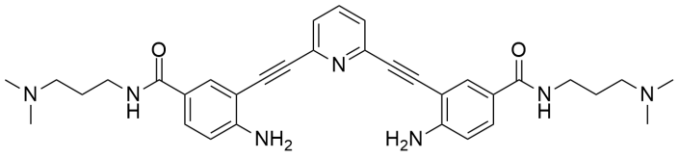

I.56

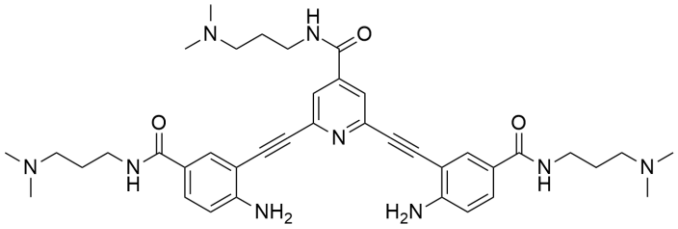

I.57

Figure I.17. Examples of diethynylamides derivatives G4 ligands.

Terpyridine derivatives. Terpyridine derivatives were studied as G4 ligands.[230,268-274] Some of them showed a high G4 stabilization and a good selectivity profile over dsDNA, especially compounds with tetraalkylammonium pendants in the central pyridine ring (**I.58**, Figure I.18).[269]

A series of metal–terpyridine complexes using transition metals[230,269,270,272] were also synthesised. A striking difference between the binding ability of different metal complexes was observed. This indicates that the nature of the metal and consequently the different geometries of the complexes are strong determinants for target recognition. For example, Pd(II), Cu(II) and Pt(II) complexes are more potent G4 binders than the corresponding free terpyridines derivatives. In contrast, Zn(II) and Ru(II) complexes are poor G4 stabilizers. Complex **I.59** also strongly inhibited the proliferation of the three tested cancer cell lines with IC_{50} values in the nanomolar range.[230]

A series of terpyridine-based dimetallic complexes (**I.60**, Figure I.18) were also evaluated. Once again, the free ligand showed poor G4 DNA binding affinity while the dinuclear Cu(II) (**I.60a**) and Pt(II) (**I.60b**) complexes display higher affinity toward G4 DNA, highlighting the importance of the metal centers in defining ligands binding ability.[275] Recently, another terpyridine-based metallic complexes with different cyclic amine substituents in different positions showed to stabilize G4 DNA and displayed cytotoxicity similar of cisplatin. Among them, dimetallic complexes **I.61** showed higher affinity towards G4 DNA compared to their monometallic counterparts.[273]

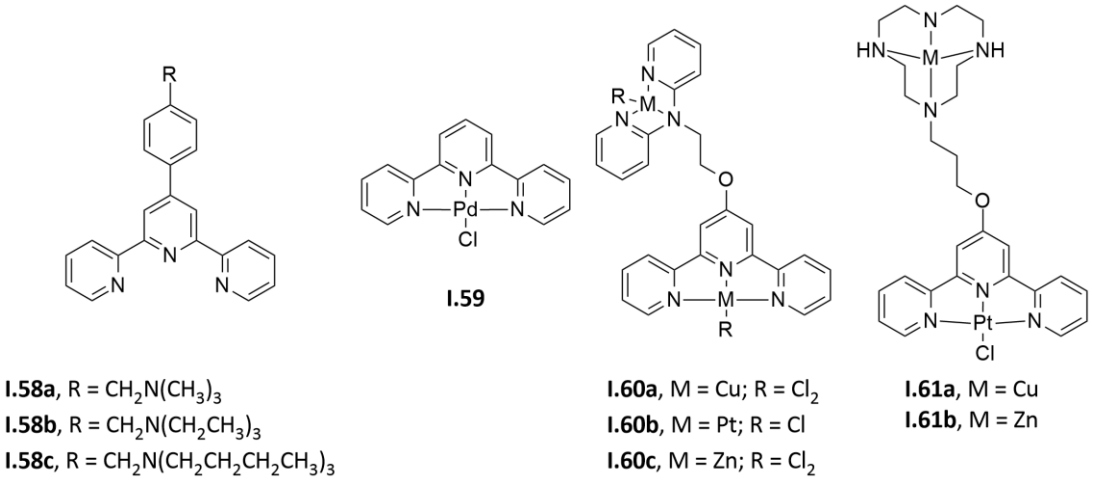

I.58a, R = $CH_2N(CH_3)_3$
I.58b, R = $CH_2N(CH_2CH_3)_3$
I.58c, R = $CH_2N(CH_2CH_2CH_2CH_3)_3$

I.60a, M = Cu; R = Cl_2
I.60b, M = Pt; R = Cl
I.60c, M = Zn; R = Cl_2

I.61a, M = Cu
I.61b, M = Zn

Figure I.18. Examples of terpyridine derivatives G4 ligands.

Triphenylpyridine derivatives. Triphenylpyridines derivatives presented a wide variation in G4 binding affinity. The nature of the 4-aryl substituents along with side chain governs the G4 DNA stabilizing ability of these compounds. For example, the absence of 4-aryl substituent (**I.62**, Figure I.19) had a negative effect stabilization of G4. Compounds with a *para*-bromophenyl or *para*-thiomethylphenyl substituent on the central pyridine ring (**I.63a** and **I.63b**, respectively) exhibited the highest stabilizations for all G4 DNA sequences studied. However, these compounds presented a medium specificity for G4 over dsDNA. On the other hand, compounds containing 5-membered aromatic substituents (**I.64**, Figure I.19) or piperonal substituent (**I.65**, Figure I.19) on the central pyridine ring exhibited mid-range stabilizations for G4 DNA and have high specificity for G4 over dsDNA. Cytotoxicity studies of these compounds in HeLa adenocarcinoma cells showed that the majority of compounds which display high to mid-range stabilization of G4 DNA exhibit significant cytotoxicity.[268,276,277]

Polyamides. This family of compounds were designed having distamycin A (**I.66**, Figure I.20) as lead molecule. The majority of 2,4-pyrrole polyamides and its 2,5-pyrrole counterparts (**I.67** and **I.68**, respectively) tested displayed 2 to 4-fold selectivity for dsDNA over G4 DNA.[278] In contrast, analogues with biaryl building blocks showed significant selectivity towards G4 compared to dsDNA and the best molecule of the series (**I.69**, Figure I.20) has no significant action on dsDNA.[279] Polyamides **I.70** and **I.71** were also identified as G4 binding ligands.[244]

Isaindigotone derivatives. Isaindigotone derivatives with different cationic amino side chains attached to the unfused aromatic chromophore, different aliphatic ring sizes and different substitution patterns in the aromatic fused ring were developed and evaluated as G4 ligands. Compounds with two side chains (**I.72**, Figure I.21) proved to

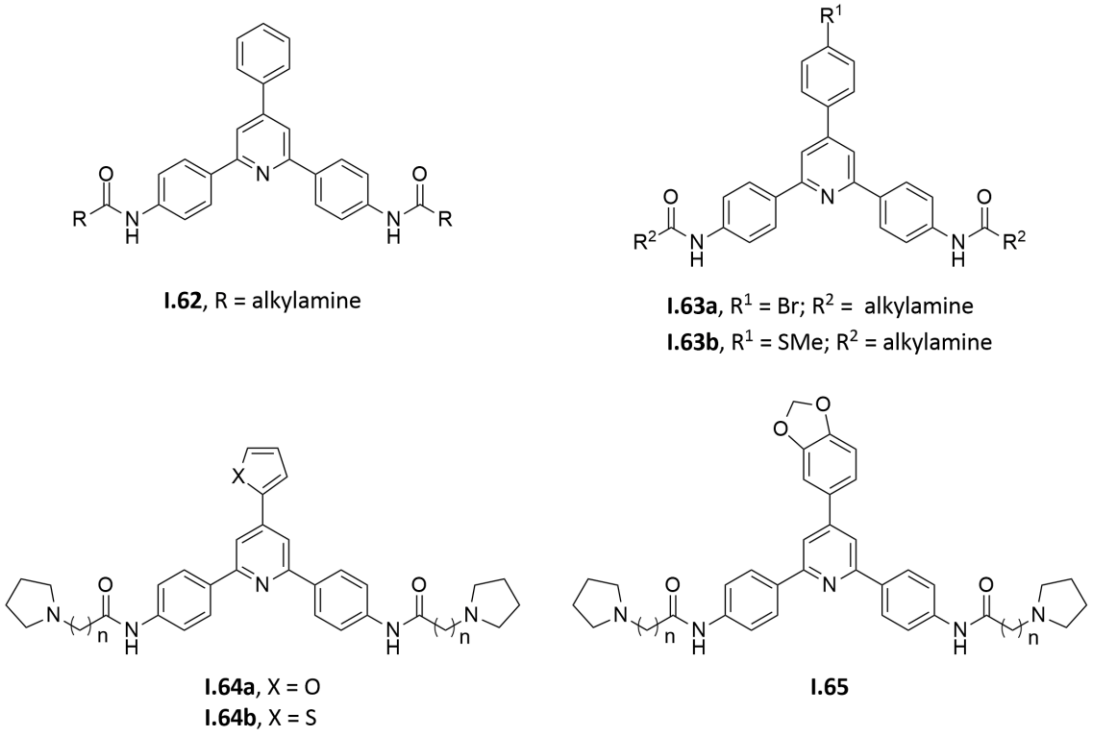

Figure I.19. Examples of triphenylpyridine derivatives G4 ligands.

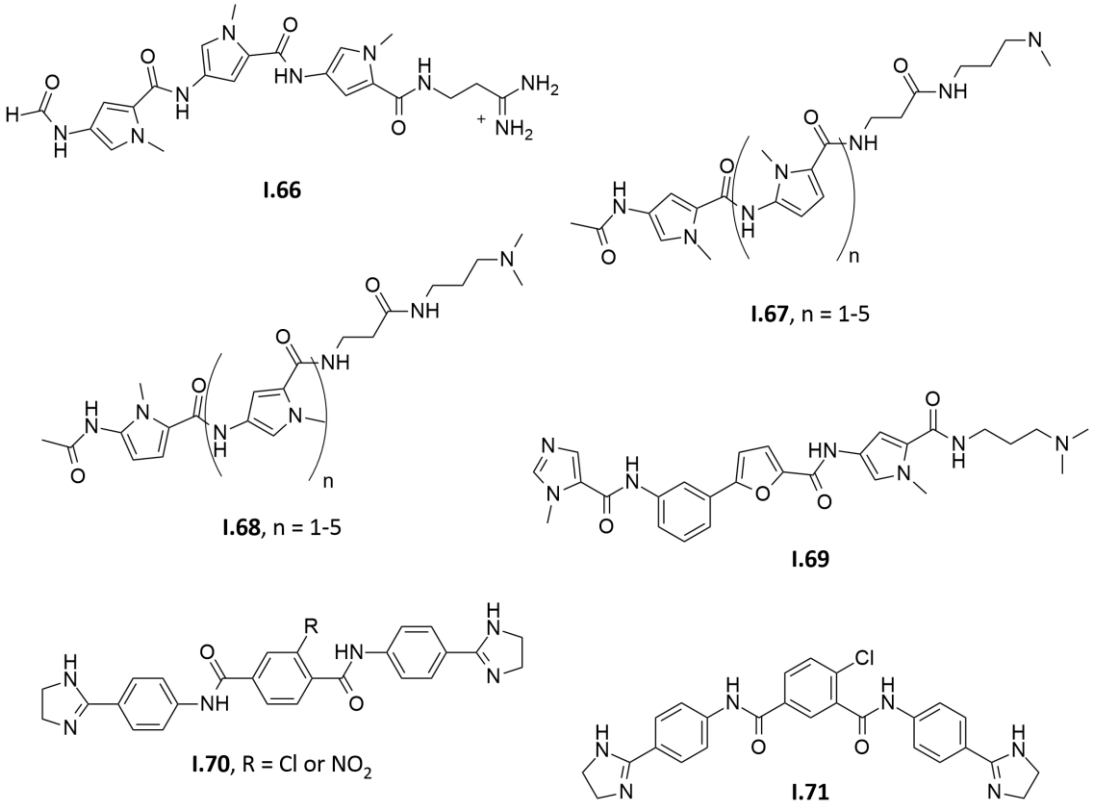

Figure I.20. Examples of polyamides G4 ligands.

be better G4 ligands than compounds with a single side chain (**I.73**, Figure I.21). Among ligands with two side chains, it was apparent that increasing size chains resulted in a weaker G4 stabilizing effect being. It was also apparent that all 4',6-disubstituted isomers had generally an enhanced G4 DNA stabilization compared to those with 4',7-disubstituted isomers. The selectivity of these compounds for G4 over dsDNA was also confirmed. [280,281] A molecule based on thiazole orange and isaindigotone skeleton (**I.74**, Figure I.21) showed to stabilize G4 DNA without affecting dsDNA, suggesting its excellent selectivity to G4.[282]

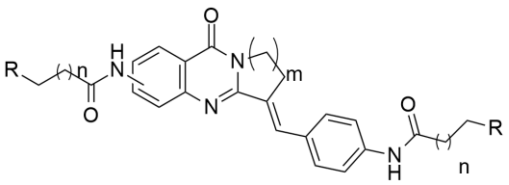

I.72, side chain: 6- or 7-; n= 1 or 2; p = 1, 2 or 3

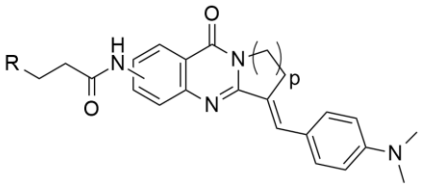

I.73, side chain: 6- or 7- ; p =1 or 2

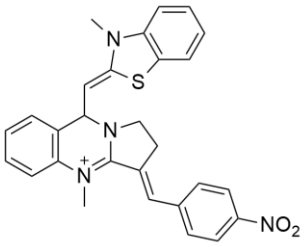

I.74

Figure I.21. Examples of isaindigotone G4 ligands (R: amine).

Quinazoline and Quinazolone derivatives. A series of 2,4-disubstituted quinazoline derivatives were very selective to G4 over dsDNA but had varying effects in stabilizing the telomeric G4 DNA. For example, the existence and the length of the amide side chain at the *ortho*- position of the aromatic group had a significant effect on its stabilizing ability: while ligand **I.75** without the amide side chain did not show any effect on G4 stability, compounds **I.76** with side chains increased telomeric G4 DNA stabilization. On the other hand, alterations of the basic terminus of the amide side chains showed that the *N*-methyl piperazino analogues had strongly enhanced affinity for G4 DNA while the less basic morpholino analogues had the weakest effect. The existence of an additional benzene ring (**I.77**) or the presence of the chlorine substituent (**I.76b**) greatly increase the telomeric G4 DNA stabilizing ability of these compounds Moreover, the disubstituted quinazoline derivatives were found to be strong telomerase inhibitors, and cellular experiments demonstrated a remarkable decrease in the population of cells with a shortening of the telomere length.[283,284]

Another class of quinazolone derivatives (**I.78** and **I.79**, Figure I.22) targeting *c-KIT* G4 DNA were synthesised. The stabilizing ability of these compounds also increased with the length of the side chains. These derivatives demonstrated an excellent selectivity between G4 DNA and dsDNA and inhibited the transcription and expression of *c-KIT* gene.[285]

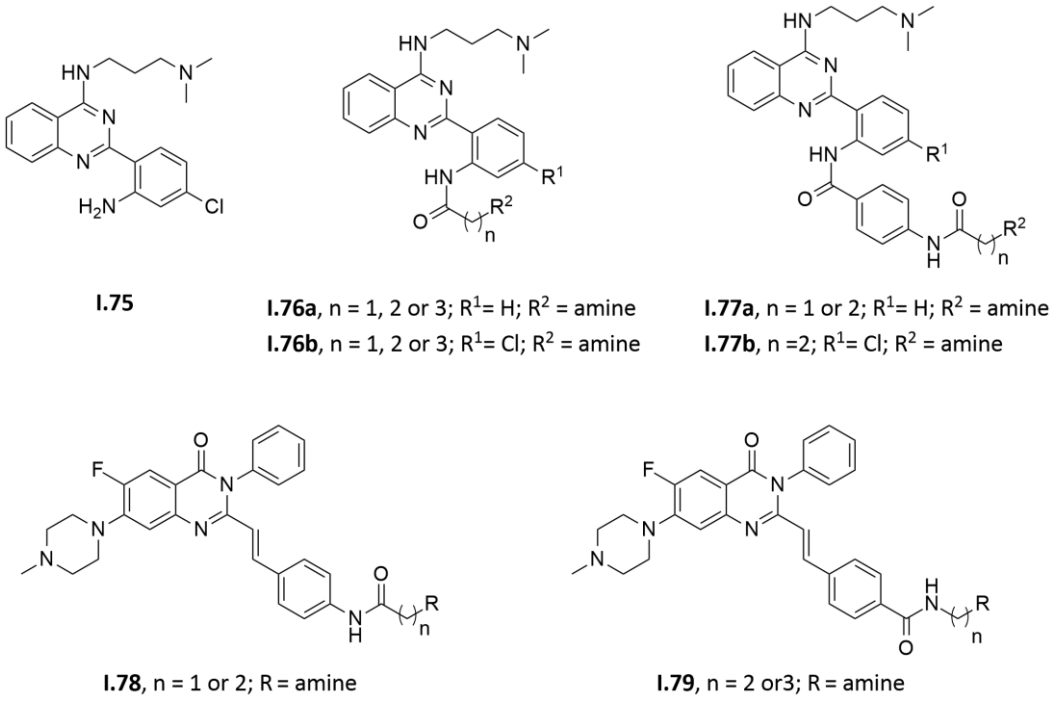

Figure I.22. Examples of quinazoline and quinazolone derivatives G4 ligands.

2.5. Methodologies for structural analysis of G-quadruplex/ligand interactions

A number of experimental methods are able to study the G4-ligand interactions. Optical spectroscopic methods (Ultraviolet-visible, circular dichroism, fluorescence), competition dialysis, electrospray ionisation mass spectrometry, isothermal titration calorimetry and surface plasmon resonance (SPR) are among the more common used ones. These methods provide a wealth of information about stabilization potency, selectivity and stoichiometry of the complexes formed by G4s and small organic molecules. However, in order to determine structural parameters for these interactions, high-resolution techniques such as nuclear magnetic resonance (NMR) spectroscopy and X-ray crystallography are required. Such information could be of immense value for improving the properties of existing ligands or designing new ones. However, it should

be mentioned that the structural parameters obtained using both methods might differ even for the same molecule, which again emphasizes the versatility of G4 topology.[286]

2.5.1. Optical spectroscopy

These methods are rapid, require small amounts of material and are non-destructive. In addition, the spectrometers used for optical studies are routinely available in laboratories.[286]

Ultraviolet-visible absorption spectroscopy is the simplest instrumental technique. The study of G4-ligand interactions is carried out by monitoring the changes in the absorption properties of the G4 (which depends on base stacking and temperature) at 295 nm, a wavelength that maximizes the hypochromic shift between the folded and unfolded states.[11] In addition to this qualitative information, experiments involving titration of the DNA with the ligand (or vice versa) provide quantitative information such as stoichiometry and binding constants. A different strategy for detecting interactions between G4 and drugs is to study the thermodynamic parameters calculated from UV-monitored melting experiments. The melting temperature (T_m), i.e. the point at which half of the bases in the G4 have unstacked, and thermodynamic parameters are determined from the changes in the absorbance as a function of temperature. Comparing the T_m values in the absence and presence of a ligand is a tool for establishing the existence and type of interaction (stabilization or destabilization) between the ligand and the G4.[287]

Circular dichroism has been extensively used as a G4 analysis tool, namely to detect the presence of a G4 structure in an oligonucleotide sequence. It is commonly accepted that the conformation of a G4 structure can be roughly assigned from the position and magnitude of the CD bands. Hence, a positive band at 260 nm is commonly assigned to a parallel conformation, whereas a positive band at 295 nm and a negative band at 260 are indicative of an antiparallel conformation. CD is also used to study interactions between G4 and ligands by measuring the T_m. This is usually performed by plotting the measured ellipticity at the wavelength corresponding to the maximum of a positive band versus temperature. Besides that, this method has been used extensively as a G4 analysis tool being its primary use to detect the presence of a G4 structure for a given NA sequence [287]

Molecular fluorescence is probably one of the techniques most commonly used to study interactions between ligands and G4 structures. The advantages of molecular fluorescence over other techniques are: its high sensitivity, large linear concentration range and selectivity.[287] When studying G4-ligand interactions, there are several different approaches to molecular fluorescence spectroscopy. One requires the use of a

chemically modified fluorescent base, such as 2-aminopurine (an adenine analogue) –, in the NA sequence of interest. This purine can be incorporated in any G4 NA without changing its conformation and only slightly affecting its stability. The overall fluorescence of a G4 changes if a small molecule interacts in the proximity of 2-aminopurine.[11] An alternative fluorescence method that evaluate the affinity of a compound for G4 and its selectivity towards dsDNA is called G4 fluorescent intercalator displacement. This assay is based on the loss of fluorescence of thiazole orange upon competitive displacement from NA by a putative ligand under steady-state.[62,287,288] Another technique for studying ligand-G4 interactions, which has become very popular, is fluorescence (or Förster) resonance energy transfer (FRET) spectroscopy. In this method, oligonucleotides are labelled at 3'- and 5'-ends using a two dyes (e.g., 5'-carboxyfluorescein, FAM, and 3'-carboxytetramethylrhodamine, TAMRA). When G4 is formed, the two dyes are close and energy is transferred from the excited dye to the other dye, which then re-emits at a longer wavelength (Figure I.23a). However, as the G4 undergoes thermal denaturation, the two dyes move apart and direct emission is restored (Figure I.23b). The amount of direct emission versus FRET emission indicates how close the dyes are. This variation in fluorescence is measured to obtain melting curves. FRET systems are very used due to a large difference between the fluorescence properties of the folded and unfolded forms and therefore this method provides well-resolved melting curves. However, it should be noted that melting temperature studies do not allow precise measurements of affinity constants.[286]

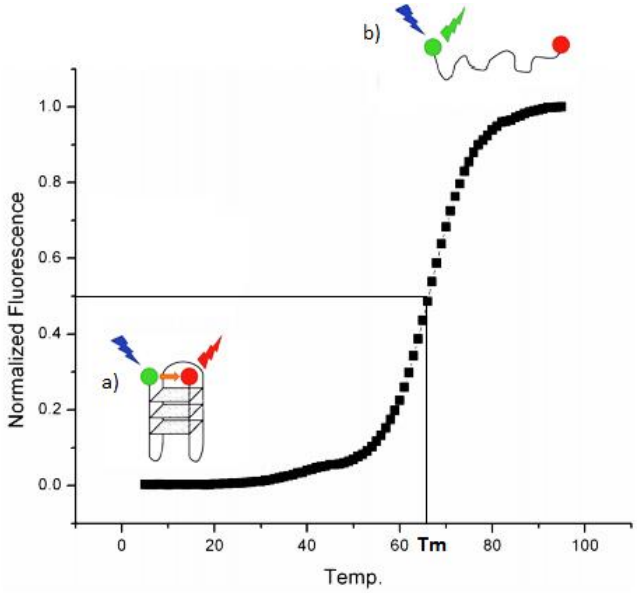

Figure I.23. FRET melting spectroscopy: a) Quenching occurs when the two probes are close; b) Direct emission occurs when the two probes are apart (adapted from [289]).

2.5.2. Other methods

Competition dialysis is used to determine the preferential conformation of nucleic acids for small molecule recognition. The method is fast and allow the determination of the apparent affinity constant of a ligand.[32,79]

Electrospray ionisation mass spectrometry is another useful tool to determine the properties and the structures of G4s, and to study ligand-G4 interactions in the gas phase. The relatively soft ionisation conditions of this system ensures that non-covalent interactions are preserved, allowing G4 structure, stability, kinetics, strand stoichiometry and ligand binding strengths to be determined using a small amount of compound. The determination of ligand binding dissociation constants is a particularly useful capability of this method, as this allows rapid, cheap and accurate screening of potential G4 ligands. Additionally, it is possible to measure ligand binding constants in the presence of multiple targets (e.g. G4 and dsDNA) in order to give a measure of ligand-binding specificity.[11]

Isothermal titration calorimetry is used to measure thermodynamic parameters – like change in enthalpy and entropy during a binding interaction –, along with the affinity constant and stoichiometry of interaction. [287]

Surface plasmon resonance is used to characterize the G4 structure and study interactions between G4 and ligands using surface-immobilized oligonucleotides. It provides a quantitative analysis of the binding parameters, that is, thermodynamic (equilibrium constant, Gibbs energy of binding, and stoichiometry) and kinetic parameters of the interaction of small molecules. The current instrumentation allows the interaction of a certain ligand to be studied with several oligonucleotides simultaneously. This makes it possible to compare the binding of a number of different ligands with different G4 quickly and easily.[287]

X-Ray diffraction is an important technique in the structural elucidation of complex formed between the small molecule and G4, as it provides details of strand orientation and G-tetrad arrangement, determines the hydrogen bonds involved in stabilization of the complex, and allows the structural arrangement to be studied at the atomic level. As the acquisition is made in the solid state, using a crystal of the complex, it reflects the state of matter in a condensed state. In consequence, the crystal structures may or may not fairly represent the solution.[11] X-ray crystallography also showed that it is theoretically possible to design molecules that can discriminate between RNA and DNA quadruplexes: the hydroxyl group at the C2' position of a sugar moiety in the RNA modifies interaction by preventing the formation of hydrogen bonds.[290]

NMR spectroscopy is a powerful experimental technique that allows a rapid qualitative analysis, confirming G-tetrad formation and the folded topology of the DNA

or RNA in solution. Interaction between the G4 and ligands is confirmed from the comparison of the experimental NMR spectra from samples with different ratio of concentrations of G4 and the ligand. Depending on the changes observed in the NMR signals, the binding mode and the strength of the binding between the ligand and G4 can be proposed. NMR main advantage over crystallography is the fact that the structure is studied in solution and not in a crystal lattice.[287]

Molecular modelling and molecular dynamics have been used to understand and improve the recognition of G4 by small organic molecules. Models have been used as starting point for structure-based design of selective and potent G4 binders. Molecular dynamics simulations have been also applied to the study of complexes between G4 and small organic molecules, in order to complement experimental data lacking atomic resolution.[286]

3. Peptide Nucleic Acids (PNAs)

The possibility to control the expression of specific genes at the level of NA has attracted great interest since Stephenson and Zamecnik reported that the replication of Rous sarcoma virus was inhibited by a synthetic 13-mer oligodeoxynucleotide complementary to a specific mRNA.[291] Following this discovery, NAs became the bases for the development of synthetic compounds (oligonucleotide analogues, OAs) with the potential to maintain complementary interactions between nucleobases with higher affinity than the natural NAs while displaying sufficient specificity to distinguish single base mismatches. In addition, OAs should overcome the drawbacks inherent to natural NAs, which mean increasing the stability in biological media and in cells and furnishing the ability to cross cell membranes. From a chemical point of view, it would be also important to develop efficient preparative methods for the synthesis of OA in sufficient amount for their practical use. With these purpose a huge variety of new oligonucleotide derivatives with modifications in the phosphodiester backbone, the sugar ring, and/or the nucleobase have been synthesized and analysed.[292]

OAs have been classified into three generations based upon variation of these modifications (Figure I.24):

First generation: based on backbone modification of natural NAs (such as replacement of an oxygen atom of the phosphate linkage by sulphur (phosphorothiolate oligonucleotides, PS, **I.80**) or methylation of an oxygen (methylphosphonate oligonucleotides). PS are the major representative of this generation. Their main advantages: (a) are resistance to nucleases, (b) ease of synthesis, and (c) their attractive pharmacokinetic properties. However, their lower binding affinities and nonspecific interactions lead to undesirable side effects *in vivo*, such as immune stimulation and

cellular toxicity.[293] Despite these limitations – partly overcome by further modifications[294-296] – Vitravene™ was an approved drug belonging to this group.

Second generation: presents an electronegative substituent at the 2'-position of the ribose ring (2'-OMethyl (**I.81**) and 2'-O-methoxyethyl (**I.82**) RNAs are the major representatives). These building blocks conferred an RNA-like C-3'-endo conformation to the oligonucleotide that greatly increases its binding affinity. They also show increased nuclease resistance and reduced toxicity. Mixed backbone oligonucleotides (known as 'gapmer' chimeras) were developed by surrounding a phosphorothioate-modified core (gap) with nuclease resistant arms such as 2'-OMe ribonucleosides. Kynamro™, a FDA- approved drug, and a vast number of OAs undergoing multiple clinical trials are exploring this 'gapmer' chimera to achieve improved therapeutic properties.[293]

Third generation: mainly contains modified phosphate linkages and modified ribose rings or different chemical moiety replacing the ribose ring. This group is mainly represented by locked nucleic acids (LNAs, **I.83**), phosphorodiamidate morpholino oligomers (PMOs, **I.84**) and peptide nucleic acids (PNAs, **I.85**). LNAs possess a methylene bridge that connects the 2'-oxygen of the ribose moiety with the 4'-carbon. PMOs are noncharged OA in which the ribose sugar is replaced by a six-membered morpholino ring and the phosphodiester bond is replaced by a phosphorodiamidate-linkage.[293]

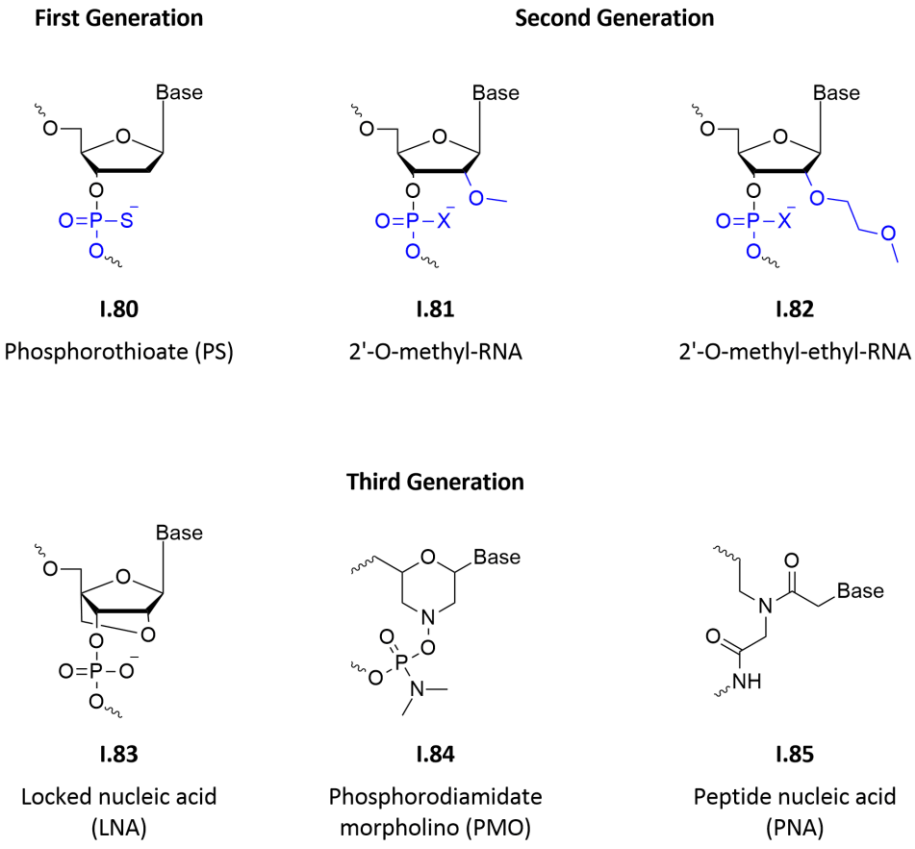

Figure I.24. Monomers of OAs from different generations.

PNAs were originally designed and developed as a ligand for the recognition of dsDNA by Nielsen and collaborators.[297] The goal was that PNAs binded as a third strand to a dsDNA major groove *via* Hoogsteen base pairing and thereby modify its properties in transcription or translation. In order to obtain this OA, the Danish group detached the negatively charged sugar-phosphate backbone in a computer model and replaced it with a pseudopeptide composed of *N*-(2-aminoethyl)glycine units in which the four nucleobases are anchored to the glycine nitrogen by means of a methylene carbonyl linker. Although formally is neither a peptide nor a NA, PNAs embody structural features from each of these classes of biomolecules. Unlike NAs, PNAs have uncharged peptide backbones that is achiral and contain the same number of backbone bonds between the bases (i.e. 6) and the same number of bonds from the backbone to the base (i.e. 3) as in DNA (Figure I.25).[297-299]

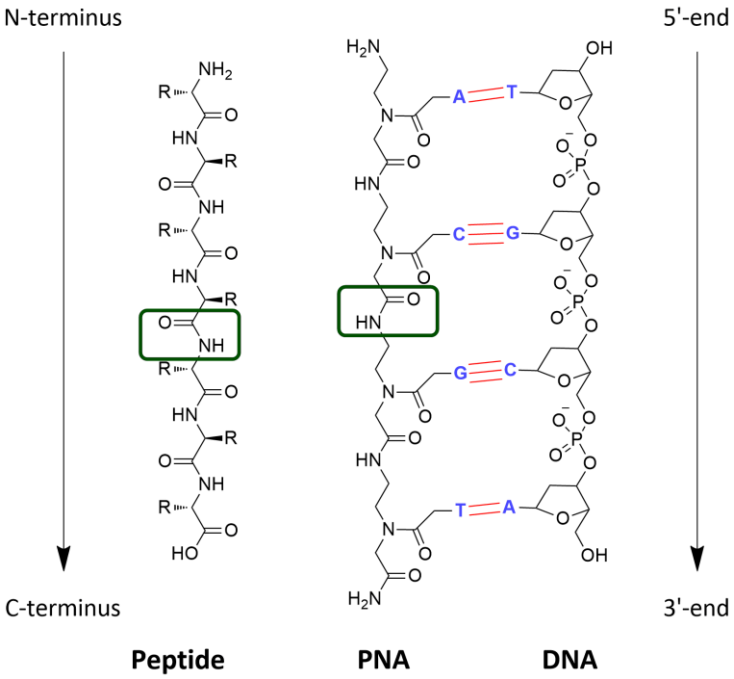

Figure I.25. Chemical structure of DNA, PNA and a peptide (R: amino acid side chain; green: amide bond characteristic of peptides; blue: nucleobases; red: Watson-Crick bonds.).

3.1. PNAs stability

In contrast to DNA, which depurinates on treatment with strong acids, PNAs are completely acid stable and are also sufficiently stable to weak bases. It is thus possible to synthesise these molecules using standard protecting groups from peptide chemistry (that require acid-cleavage) and base-cleavable nucleobase protecting groups. However,

when PNA has the nucleophilic amino functionality free at the *N*-terminus, a slow *N*-acyl migration of the nucleobase acetic acid, or detachment of the *N*-terminal PNA monomer by ring closure can occur, predominantly under basic conditions. Such migration would result in a free secondary amine which could continue the chain upon coupling of the next monomer. This side-reaction can be suppressed by capping the final *N*-terminal amino function, for example with an acetyl group.[300]

In terms of biologic stability, while unmodified oligonucleotides are digested relatively rapidly by nucleases in serum, PNAs have a remarkably high stability in both human serum and in cell extracts[301] and exhibits little or no binding to serum proteins.[302] This high stability was confirmed after intravenous injections in rat where approximately 90% of the PNA was recovered as intact molecules in the urine within 24 hours after administration.[303]

3.2. PNAs solubility and cellular uptake

Although the results with PNAs in cell-free systems are very encouraging, their poor cellular uptake is, at present, the main obstacle to their effective use.

One of the contributors for this poor uptake is PNAs solubility. As PNAs are neutral and relatively hydrophobic molecules, single-stranded PNAs have poor water solubility compared to DNA and tend to aggregate in aqueous solution. PNA solubility is dependent on the length and sequence of the oligomer, dropping when length and purine:pyrimidine ratio increases. Surprisingly, however, it was found that a homoadenine PNA polymer to be highly water soluble. The introduction of charged amino acid residues such as lysines,[304] and negative charges such as in the PNA-DNA chimeras, showed to increase water solubility.[300]

In addition, the lack of charges in the backbone make the passive diffusion of PNA over anionic surface of the cell membrane extremely slow. In bacteria the diffusion is even worse because they have thick cell barriers that are composed of a low-permeability cell wall. Furthermore, many pathogens occupy host vesicles or form biofilms that provide added protection.[302] This problem has prompted a variety of strategies to improve uptake. One strategy is transiently disrupt the cellular membrane, e.g. by electroporation,[305-309] pore forming agents (such as streptolysin-O,[310] lysolecitin[311] or detergents like Tween 20[312]), or physical scrape loading.[313] These methods have proven useful for unmodified PNA delivery in several systems, but are limited to cells in culture and also exert a significant stress on the cells.[314] Otherwise, liposome vehicles were exploited. Although cationic liposomes are very efficient in delivering anionic oligonucleotides to eukaryotic cells, the uncharged nature of the PNA difficult the creation of stable complexes needed to its transport into cells using

traditional transfection protocols.[302] The use of liposomes has, however, been successful when PNA was partly hybridized with a complementary "carrier" DNA,[315-317] conjugated with the DNA intercalating dye 9-aminoacridine[316] or with a lipophilic moiety (adamantly acetic acid).[318] In addition, PNAs were also conjugated with small cationic peptides, so called cell-penetrating peptides (CPPs) or cell-specific receptors ligands. CPPs have been reported to display capacity to transport a cargo over the cell membrane in an energy and receptor independent manner. The efficiency of the CPP strategy seems to depend on the nature and size of the CPP and on the target cell line. Despite intense studies the mechanisms of translocation are not completely understood.[319] Natural peptides derived from viral (such as the trans-acting activator of transcription of the human immunodeficiency virus-1),[320] insect (such as penetratin)[321] and synthetic peptides (such as transportan,[320,322] R6-penetrin[320,322] and $(R/W)^9$ nonapeptide[319]) have been used for this purpose. Also, synthesizing the PNA as a chimera with a highly basic peptide, the classic SV40 large T antigen nuclear localization signal,[323,324] polylysine[313] or polyarginine[325] tails, seems to be enough to promote increased cellular uptake *in vitro*. Finally, other groups have chosen the strategy of coupling PNA to cell-specific receptors ligands. The targeting approach has the advantage of directing PNA delivery to specific cell types avoiding the risk of adverse side-effects in non-targeted cells. Examples of targeted receptors are the transferrin receptor,[326] the insulin-like growth factor 1 receptor,[327] and the liver-specific ascialoglycoprotein receptor.[328]

Another problem can occur in delivery strategies that uses endocytosis as a route of cellular entry. In these cases, PNA confinement to endosomes can occur resulting in very weak biological effects. This problem can be solved via peptide linkers containing specific amino-acid sequences that will be cleaved by cellular proteases in the endosome. After being released from the PNA, these peptides will induce endosomal rupture and release PNA into the cytoplasm.[329] Alternatively, photochemical internalization can also be used. This approach is based on irradiation of a photosensitizing compound (photosensitizer) that localizes preferably in endosomal and lysosomal membranes. Irradiation initiates an oxidative process of the photosensitizer, resulting in formation of reactive oxygen species that destroy the endosomal membranes. As endosomal escape is induced only in the presence of a light-trigger, the delivery process can be temporally and spatially modulated and controlled.[330,331]

3.3. PNA–Nucleic acids complexes

3.3.1. Binding affinity

The PNA molecule is capable of recognizing its complementary sequence in DNA and RNA as well as in PNA, according to the Watson-Crick base-pairing rules.[332,333] Depending on sequence and experimental conditions, PNA-NA duplexes or $(PNA)_2$-NA triplexes can be formed. In order to measure their binding affinity, one of the most common methods is to observe the T_m. In this case, T_m is defined as the temperature at which half of the oligonucleotide strands are in the helical state and half are in the random coil states and is from it that the thermodynamic parameters are derived.[334]

3.3.2. Triple helix formation with complementary DNA and RNA

As PNAs are uncharged, they appear to be predestined to form triple helical structures with dsDNA (PNA/$(DNA)_2$, Figure I.26a). However, PNA/$(DNA)_2$ is only observed in the case of C-rich PNAs and GC-rich dsDNA while $(PNA)_2$/DNA triple helix (Figure I.26c) formation is observed for homopyrimidine PNAs with a minimum of 10-mers, as well as PNAs containing a high proportion of pyrimidine.[300] The $(PNA)_2$/DNA complex is comprised of a PNA–DNA double helix formed by Watson–Crick hydrogen bonds with a second PNA strand lying in the major groove of the duplex formed by Hoogsteen hydrogen bonds (Figure I.26d). The formation of $(PNA)_2$/DNA triplexes require the opening of the dsDNA with a DNA strand displacement highly sequence specific – via a so-called “strand invasion” mechanism – leading to the formation of a single-stranded loop structure (P-loop).[335] The binding rate is increased by permanent or transient opening of the dsDNA at or near the PNA binding site in actively transcribed genes caused by: passing RNA polymerase,[336] negative DNA supercoiling,[337] or adjacent strand displacement complex[338] that facilitated binding of PNA not only to the sense but also to the template strand. The explanation for the DNA/$(PNA)_2$ triplexes formation can be found on its extraordinarily stability which depends on the length of the oligomers in a regular manner.[300] The T_m of triplexes containing cytosine in their sequences is pH-dependent, being more stable at pH 5, since the N^3 of cytosine must be protonated for the Hoogsten pairing (triad CG^*C^+ in Figure I.26d). To ensure pH independence of binding of the Hoogsteen strand, cytosines in the “Hoogsteen-pairing” strand are exchanged to pseudo-isocytosines (also called J bases), which mimics N^3-protonated cytosine (triad CG*J in Figure I.26d).[302] In contrast to DNA, PNAs lack 3’ to 5’ polarity and can bind in either parallel (N/5’) or antiparallel orientation (N/3’). Nevertheless, if only

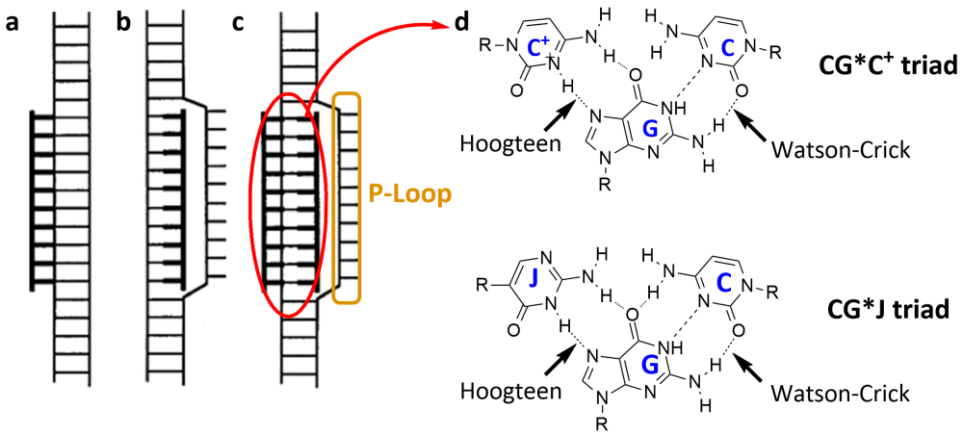

Figure I.26. Examples of binding modes of PNA when targeting dsDNA: (a) triplex formed with cytosine-rich PNAs binding to complementary homopurine DNA targets, (b) duplex invasion complex formed with some homopurine PNAs and, (c) triplex invasion complex, leading to the displacement of the second DNA strand into a P-loop; (d) chemical structures of CG*C$^+$ and CG*J triads with Hoogsteen – represented by *– and Watson-Crick bonds present in the triplex invasion complex; adapted from [339]).

one PNA sequence is used to form a $(PNA)_2$/DNA triple helix, then both strands are necessarily either antiparallel (more stable) or parallel to the DNA strand. When two different homopyrimidine PNA sequences are used, the most stable complex is formed when the Watson-Crick PNA strand is oriented antiparallel and the Hoogsteen strand is parallel to the purine strand of the DNA.[300]

The construction of bis-PNA increased the possibility for PNA strand invasion under physiological conditions. Bis-PNA or "PNA clamp" is a palindrome sequence with a flexible linker in the middle designed such that one strand is antiparallel ("Watson–Crick-pairing" strand) and the other strand is parallel ("Hoogsten-pairing" strand) to the DNA target. This leads to a small increase in the T_m, which presumably arises from a slight reduction in the entropy loss on triple helix formation. The high local concentration of the third strand presumably leads to much more rapid triple helix formation. Sequence discrimination in bis-PNAs is extremely high due to the double recognition process (by both PNA strands).[300,302] Alternatively, the rate of binding can be increased several orders of magnitude by using cationic PNAs or by conjugating the DNA intercalator 9-aminoacridine to a PNA.[302]

In the case of duplex invasion (Figure I.26b), PNAs form very stable complexes via Watson–Crick base pairing of the homopyrimidine target DNA and the homopurine PNA sequence.[339]

Otherwise, pseudocomplementary PNAs (pcPNAs, Figure I.27a) exhibit a distinct binding mode, double-duplex invasion, which is based on the Watson-Crick recognition

principle supplemented by the notion of pseudocomplementarity. Pseudocomplementarity means that the base pairing between two mutually pcPNA oligomers is not possible but pcPNAs are capable of a stable Watson-Crick-type pairing with the natural nucleobase counterparts. 2,6-diaminopurine (D, Figure I.27b) and 2-thiouracil (^{S}U, Figure I.27b) were used instead of adenine and thymine, respectively, because they satisfied both criteria. PcPNAs have been found to be capable of targeting the designated dsDNA sites with mixed sequence of purines and pyrimidines, with the exception of very GC-rich (A+T content <40%) sites.[340]

Likewise, homopyrimidine PNAs also form stable $(PNA)_2$/RNA triple helices with RNA with T_m values that appear to be similar to those of $(PNA)_2$/DNA triple helices.[339]

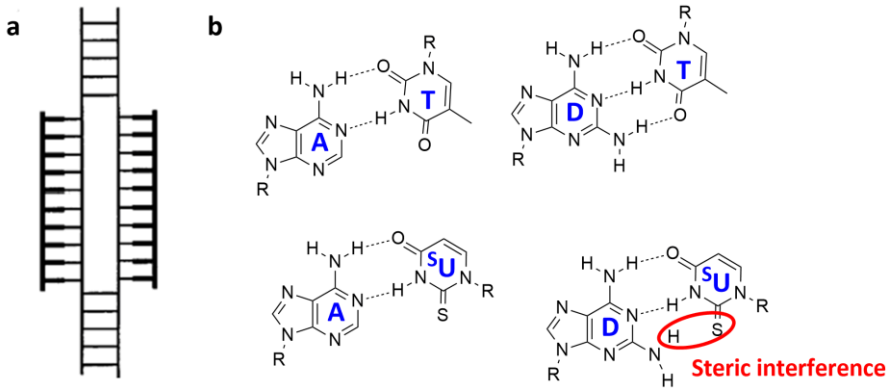

Figure I.27. (a) Double-duplex invasion of dsDNA by pcPNA and (b) schematic drawing of nucleobase pairing: adenine-thymine (A-T), diaminopurine-thymine (D-T), adenine-thiouracil (A-^{S}U), diaminopurine-thiouracil(D-^{S}U), and how diaminopurine can form an extra hydrogen bond with thymine, whereas a steric clash occurs between diaminopurine and thiouracil) (adapted from [339]).

3.3.3. Duplex Formation with Complementary DNA and RNA

PNA-NA duplexes are generally more stable than the corresponding NA complexes due to the uncharged nature of PNA that prevents any electrostatic repulsion during the complexation of the target. The antiparallel orientation of the PNA is more stable[332] and is also kinetically favoured, the antiparallel complex is formed immediately (<30 s), whereas the formation of the parallel complex require several hours. An interesting aspect of PNA/DNA duplexes is its independence on ionic strength. In contrast with dsDNA, these complexes are stable under low salt conditions because no cations are needed to counteract the interstrand repulsion typical of the duplex formation between the two negatively charged strands of natural oligonucleotides. However, at high salt concentration (>1 M), where electrostatic contributions saturate, similar trends in the

decrease in T_m were observed for the DNA/DNA and DNA/PNA duplexes. PNAs show also a remarkable specificity in binding to complementary natural oligonucleotides; indeed, sequence discrimination is generally higher for a PNA/DNA duplex than for a DNA/DNA mismatch.[300] The restriction of the flexibility of the PNA molecule can improve selectivity with respect both to binding and to the preferred formation of complementary complexes with DNA or RNA. The replacement of the glycine unit in PNA building blocks by other amino acids has various effects on duplex stability that depend upon the amino acid side-chain. Small, uncharged side chains, such as those of alanine[341] and serine,[304] do not influence duplex stability. Positively charged side-chains, such as in lysine[304,342] and arginine,[343] have a stabilizing effect, whereas negatively charged side-chains, such as in glutamic acid,[304] have a destabilizing effect.

3.3.4. PNA homoduplexes

PNAs form extremely stable duplexes with complementary PNA sequences when compared with the corresponding DNA/PNA or DNA/DNA duplexes. Also in this case, the antiparallel strand orientation is characteristically more stable.[300]

3.4. Other PNA monomers

Attempts to understand the structure-activity relationship (SAR) of PNA and improving its solubility, cell permeability, bioavailability, and binding orientation with RNA and DNA have resulted in several structural modifications of *N*-(2-aminoethyl)glycine (Figure I.28). Polyamide backbone suffer several modifications such as: (a) extension by one methylene group using monomers such *N*-(2-aminoethyl)-β-alanine or a *N*-(3-aminopropyl)glycine (**I.86a** and **I.86b**, respectively);[344] (b) replacement of the amide linkage to the nucleobase by a tertiary amine (**I.87**);[345] (c) introduction of other aminoacids in the glycine place, e.g. arginine (**I.88**)[346] or phenylalanine (**I.89**);[347] and (d) introduction of cyclic structures (**I.90** and **I.91**).[348,349] The majority of the modifications had as goal to restrict the PNA conformational flexibility in order to obtain derivatives with better binding orientation and that bind even tighter to the NAs. As a drawback, the introduction of stereocenters into the PNA oligomer, makes the synthesis more complex since enantiomeric purity of both the monomers and oligomers needs to be assured.

According to Falkiewicz,[350] the PNA analogues can be divided in two types depending on the manner of attachment of nucleobase to polyamide backbone. The first category is a polyamide with alternating peptide–pseudopeptide bonds as backbone, consisting

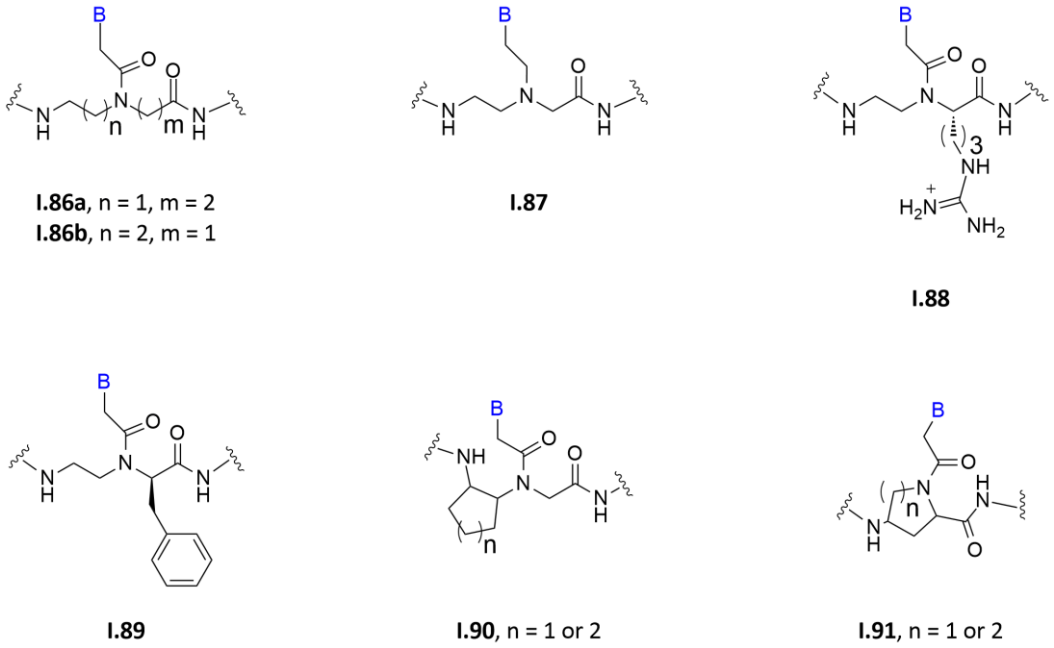

Figure I.28. Chemical structures of some monomers of PNA analogues (B: nucleobase).

of *N*-(aminoalkyl)amino acid units to which secondary nitrogen nucleobases are attached with the linker. PNA analogues of the second category contain a backbone consisting of amino acid residues carrying the nucleobase in their side chains, named nucleoamino acids or chimeric amino acids. In this second group is included the alpha-PNA (α-PNA).

3.4.1. Alpha-PNA

α-PNA has a backbone consisting of α-amino acids, some of them carrying a nucleobase in their side chain (Figure I.29).

Although the nomenclature of α-PNA is recent, the concept of nucleoamino acids is not new. Some authors described the synthesis of nucleobase-bearing α-amino acids (such as alanines[351,352] and homoalanines[353,354]) some decades ago. In order to obtain peptides in which the nucleobases are correctly spaced for interaction with NAs, various spacer amino acids have been used.

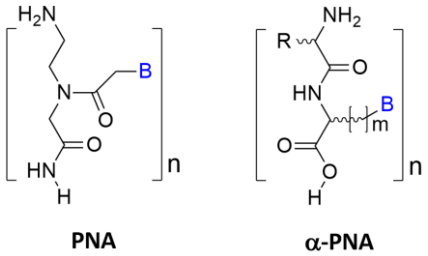

Figure I.29. Chemical structures of PNA and α-PNA (B: nucleobase; R: amino acid side chain).

In alanine-based building blocks (Figure I.30), nucleobases are covalently linked to alanyl side chains in the β-position (**I.92a**). Dipeptides and/or polypeptides composed of nucleobase-bearing alanine with glycine,[355] serine[356] and proline[357] as spacers (**I.93a**, **I.93b** and **I.94**, respectively) were reported. The experimental attempts to obtain complementary complexes of oligonucleotides with some of these α-PNAs presented different results and in some cases were not successful.[358] Interestingly, the synthesis of dipeptides composed of adenine- and uracil-containing alanines and glycines by multi-component reaction (U-4CR) was described.[359] Not less important, new α-PNA, made of L-β-(thymin-1-yl)alanine at (*i, i+3*) positions separated by α-amino acids such as alanine (**I.95a**) and aminoisobutyric acid (**I.95b**), were presented recently.[360,361] Some of these compounds were able to penetrate the cells and reach the nucleus without cytotoxic effects.[361] In alanyl-PNAs (**I.96**), the backbone is composed of nucleobase-bearing alanine units with alternating configuration. These oligomers are able to form linear double strands, with collinear strands, based on hydrogen bond recognition and stacking of the nucleobases. The distance of two base pairs (3.6 Å) results from the distance of consecutive side chains in peptides with β-strand conformation and is close to stacking in DNA (3.4 Å).[362] Alanyl-PNA/DNA chimera that can serve as a tool for very sensitive DNA detection following the molecular beacon concept was also synthesised.[363] Proteins containing some alanyl residues with nucleobase side chains were also synthesied.[364]

Homoalanines containing nucleobases covalently bounded at ɣ position were also synthesized (**I.92b**, Figure I.30). Monomers with different chiralities were synthesised from different aminoacids: D-monomers derived from D-glutamic acid;[365] methionine was used as starting material in L-, D- and DL-monomers synthesis;[365] L-homoserine was used to synthesise L-monomers.[367] α-PNAs with D-monomers in which the glycine residue was used as spacer (**I.93c**) showed a defined T_m suggesting the possibility of a DNA-like self-aggregation in solution.[365,368] α-PNAs of opposite chirality were also described.[367] The L-monomers containing adenine were alternated with several α-amino acids: glycine (**I.93c**), serine (**I.93d**), threonine (**I.93e**) and tyrosine (**I.93f**) to give different tetrapeptides. The tetrapeptides interacted base-specifically with

polynucleotides – poly (dT) or poly (U) – to form 1:2 complexes, in the same manner as adenylyladenosine, but more potently. The tetrapeptides that do not present the glycine unit as spacer showed higher potencies, so further modification at this position may be feasible to increase the stability of the complexes or to modulate the DNA recognition ability.[369] Three decapeptides adenine-bearing homoalanines were synthesised: one made up of DL-monomers, the second one composed of homoalanyl units with alternating configuration, and the third resulting from the oligomerization of the L-monomers. The preliminary T_m data obtained by hybridization experiments demonstrated that these α-PNAs annealed to their complementary NA strand and the peptide composed of both enantiomers with alterning configuration had stronger affinity to the complementary dT10 strand than the peptide made of L-monomer.[334] Different α-PNAs made of nucleobase-bearing homoalanines alterned with glycine were also synthesised in order to study the impact of Cu(II) and Ni(II) on their structures.[370,371] The synthesis of α-PNAs, with seven-residue periodicity, through a self-replication reaction where the nucleobase-functionalized homoalanine separated by six amino acids were also reported.[372,373]

Furthermore, an α-PNA based on adeninyl D-homoalanine alternated with thyminyl L-alanine residues showed to be a self-pairing in a stable double strand and there might be an excellent potential for specific binding of a third strand.[374] Additionally, a series of α-PNAs based on nucleobase-containing norvalyl (**I.92c**, Figure I.30) monomers without other aminoacids as spacers were also synthesised.[362]

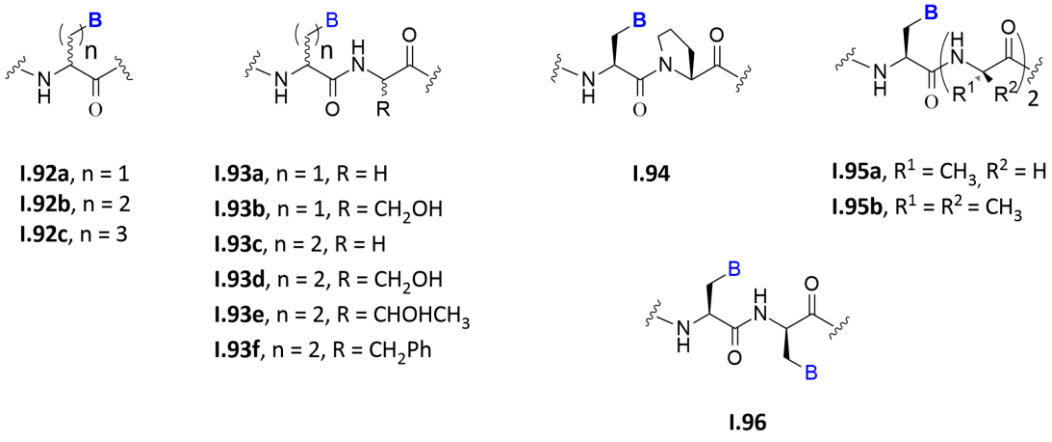

Figure I.30. Chemical structures of alanine-, homoalanine- and norvalyl-based building blocks of α-PNA (B: nucleobase).

Serine-based building blocks where the nucleobase is attached to a L-serine residue via a hemiaminal linkage (**I.97**, Figure I.31) were also prepared. These building blocks were used in the synthesis of PNA, made of serine-based amino acids at (*i, i+4*) positions

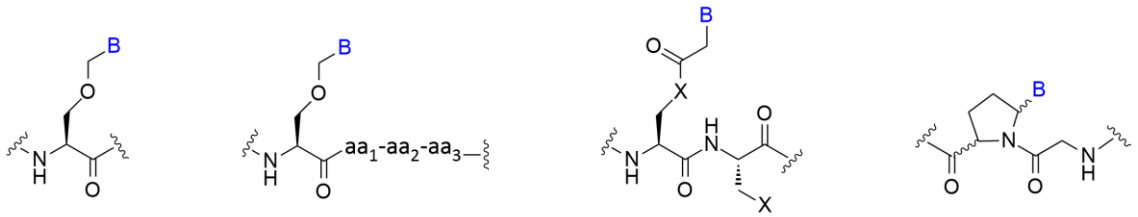

Figure I.31. Chemical structures of serine-, tyrosine-, lysine- and proline-based building blocks of α-PNA (B: nucleobase).

separated by other α-amino acids (**I.98**, Figure I.31) to favor α-helix formation.[375-377] These α-PNAs exhibited excellent water solubility with no evidence of self-aggregation. In this media, helical nature of α-PNAs was confirmed. It was also found that these α-PNAs form complexes with complementary DNA targets with higher T_m than the corresponding dsDNA but with the parallel orientation being favoured both thermodynamically and kinetically over the antiparallel.[376-378] Dithymine tetrapeptide made of both thymine-containing and unfunctionalized L-serine units alternated in the sequence were also synthesised. In this case, the nucleobases were anchored to the hydroxyl groups of the L-serine units by means of ester bonds (**I.99a**). This analogue showed a good solubility in water and it was more resistant in plasma than standard tetrapeptides (and oligopeptides) but the interaction with complementary DNA was weak.[379]

A short tetrapeptide based on both thymine-containing and underivatized L-tyrosine moieties alternated in the sequence (**I.99b**) was also synthesised.[380]

An hexathymine nucleopeptide, obtained by alternating thyminyl lysine monomers and unfunctionalized L-lysine units in the sequence (**I.99c**) was also reported.[381] This basic nucleopeptide proved to be well soluble in water and able to interact with both DNA and RNA.[382]

In another approach, D- and L-proline with nucleobases incorporated at the 4-position with *cis*- and *trans*-stereochemistry were synthesized and interspaced with glycine residue in an α-PNA (**I.100**, Figure I.31). The α-PNA with *cis*-stereochemistry in the L- and D-series bound strongly to poly(dA) but *trans* series failed to hybridized. Using a mixed sequence decamer of the four nucleobases it was found that the thermal stability of the α-PNA/oligonucleotide complex was comparable to that formed by *N*-(2-aminoethylglycine).[383] Two 8-mer (one using the L-proline with nucleobases incorporated at the 4-position with *cis*-stechiometry and the other using a similar chimeric amino acid but in *trans*-stereochemistry) both with glycine as spacer were

synthesised and no hybridization was observed with the complementary oligodeoxynucleotides.[384]

3.5. PNA Synthesis

Different protocols for the assembly of PNA monomers to oligomers have been reported. PNAs incorporate repetitive elements which are readily amenable to assembly via solid-phase peptide synthesis (SPPS), pioneered by Robert Bruce Merrifield.[385] Specifically, protecting group strategies, SPPS protocols, deprotection methods and purification procedures developed for peptide synthesis may be directly applicable to the synthesis of PNAs and their analogues. This is one of the strengths of PNA technology because it allows the automation of the process using commercial peptide synthesizers, under controlled and standardized conditions.

3.5.1. Protecting Group Strategies

In the PNA synthesis, the protection of the primary amino group of the backbone and of the exocyclic amino groups of the nucleobases with orthogonal protecting groups is necessary. Protection at these sites not only blocks undesired side reactions in the oligomerization, but also increases the solubility of the monomers, especially the purines.[386] Different protection schemes have been tested as exemplified in Table I.1.

3.5.2. Solid-Phase Synthesis and Characterization of the Oligomer

The general principle of solid-phase synthesis is based on the repetition cycles of elongation, capping of unreacted free amines, and deprotection of the primary amino group of the backbone (Scheme I.1).

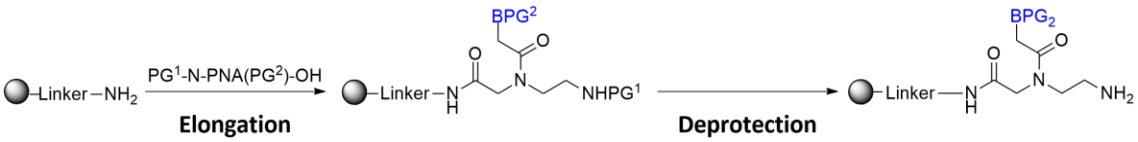

Scheme I.1. A SPPS cycle of *N*-(2-aminoethylglycine)PNA synthesis (B: Nucleobase; PG^1: Terminal *N*-protecting group; PG^2: Exocyclic nucleobase *N*-protecting group).

The solid-phase synthesis starts with the attachment of the first monomer of the chain to a solid polymer by a covalent bond. The elongation of the PNA oligomer takes place through condensation of the carboxy function of the building block with the deprotected amino function of the growing chain, aided by a condensing agent. The succeeding monomers are added until the desired sequence is assembled. Then, the PNA oligomers are deprotected, removed from the solid support and purified by reverse-phase high-performance liquid chromatography.[387] While sequencing is not yet a routine option, the oligomers are conveniently characterized by MALDI-TOF mass spectrometry.[388]

Table I.1. Protecting groups used in PNA monomer synthesis and orthogonal strategies employed. [298,386,389-397]

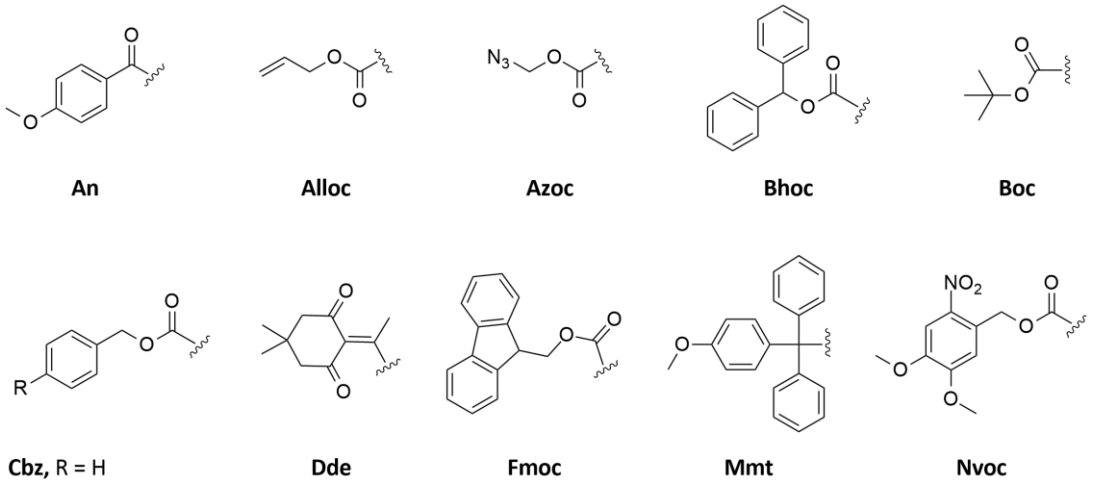

Terminal *N*-protecting group	Exocyclic nucleobase *N*-protecting group
Boc	Acyl
Fmoc	Acyl
Nvoc	An
Mmt	An
Azoc	Boc
4-OTBSCbz	Boc
Fmoc	Boc

Terminal *N*-protecting group	Exocyclic nucleobase *N*-protecting group
Alloc	Bhoc
Azoc	Bhoc
4-N_3Cbz	Bhoc
Boc	Cbz
Fmoc	Cbz
Fmoc	Dde
Fmoc	Mmt

3.6. Potential Applications

3.6.1. Therapeutic Applications

3.6.1.1. Effects on DNA

The capacity of PNA to invade into dsDNA has opened the possibility of interfering directly with gene regulation, either as a transcription activator or inhibitor (antigene). In addition, PNA may also interfere with gene expression by acting as a decoy molecule binding different transcription factors or targeting DNA G4 Structures.

PNA as Transcriptional Activator Agent. P-loop structures, formed via strand displacement, have been found able to initiate transcription of genes downstream of the PNA-binding site *in vitro*[309,398,399] and *in vivo,*[309,400] either with bacterial or eukaryote RNA polymerases. In fact, the $(PNA)_2$/DNA complex is recognized by RNA polymerases, and RNA transcription is initiated. Thus PNA oligomers may function as artificial transcription factors using the PNA target as a promotor.[309] The optimal length of a PNA, to act as artificial promoter, is 16-18 bases in a HeLa nuclear extract *in vitro* and in GFP-reporter plasmid in cell culture.[400] This principle should be therapeutically applicable in place of a protein substitution therapy, provided that the appropriate gene (which is not or only weakly expressed) is not defective in the coding region.

PNA as Antigene agent. In an antigene approach, PNAs are designed to hybridize to complementary DNA sequences in a particular gene in order to inhibit transcription either at the level of transcriptional initiation and/or RNA polymerase elongation (Figure I.32a).[401] In PNA designed to target transcriptional initiation site, the structural hindrance may effectively suppress overall expression of the gene due to the blockage of DNA recognition by proteins, such as transcription factor and RNA polymerase.[402] It should be mentioned that although the antigene PNA was targeted against the sense strand of the DNA, it inhibited transcription from both strands of the DNA template equally well. This contradicts the results of studies in cell-free systems, and may result, for example, from the RNA polymerase II elongation complex *in vivo* being much larger than the polymerase II complex in reconstituted systems, or to the additional influence exerted by the nucleosomal structures of the chromatin template used.[300]

Antigene effects of PNA have been reported from *in vitro* transcription experiments,[403] as well as in cell cultures[311,404,405] and in live animal studies.[406,407] One interesting application of the antigene therapy would be the treatment of patients with diseases caused by heteroplasmy of the mitochondrial DNA (mtDNA) – where the mutated and wild-type DNA are both present in the same cells. It has been shown that

the use of PNAs under physiological conditions can inhibit the replication of the mutated mtDNA without affecting the wild-type mtDNA.[300,408] The main obstacle appears to be the access of the PNA to the DNA under physiological conditions which include the presence of cations that stabilize the dsDNA and therefore dramatically reduces the rate of helix invasion by the PNA. Furthermore, the effect of chromatin structure on PNA binding would be expected to decrease the access to the DNA binding sites.[409]

PNA containing "decoy" Transcription Factor Responsive Elements. Transcription factors recognize double-stranded consensus sequences within gene promoter regions (Figure I.32b). Decoy molecules are short double-stranded NAs designed to mimic genomic transcription factor-binding sites and sequester factors that may be overactive in disease. This approach could be very useful to alter the gene expression. As double-stranded PNA/PNA and PNA/DNA hybrids exhibit structural features significantly different from those of dsDNA, they are not suitable for transcription factor decoy. On the contrary, PNA-DNA chimeras are active as TFD decoy reagents.[410,411]

Targeting DNA G4 Structures with PNAs. PNA probes can provide a powerful instrument to target guanine-rich regulatory DNA sequences. These sequences can be target in different ways: (a) guanine-rich PNA can invade a DNA G4 and simultaneously bind to the complementary cytosine-rich strand, thus facilitating G4 formation; (b) PNA can bind exclusively to the complementary cytosine-strand, thus providing additional stabilization of the G4-PNA complex and (c) short PNA oligomers can be designed to bind to the ssDNA in the exposed loops of G4 structures. The goal of using PNA probes is to: (a) interfere with G4 recognition by protein factors; (b) lead to stabilization of native G4 structures and promote binding of G4 specific protein factors which can switch on or off gene transcription, depending on that particular protein function.

Until now, targeting G4 structures with PNA has been demonstrated only *in vitro*, and in many cases only models containing single-stranded guanine rich DNA were used.[412]

3.6.1.2. Effects on RNA

All cellular RNAs are potential targets for recognition and inhibition with PNAs. PNAs can affect gene expression and RNA processing (antisense), ribonucleoprotein activities and inhibit microRNA (miRNA). Also, PNA binding can potentially alter RNA abundance by triggering nonspecific degradation of unused or structurally altered RNAs.[302]

PNA as Antisense agent. Antisense mechanisms have attracted great interest as selective mRNA inhibitors by inducing a blockade or alteration in the transfer of genetic information from DNA to protein.[413] As PNAs duplexes are not substrates for RNAse H (an ubiquitous enzyme that hydrolyzes the RNA strand of an RNA/DNA duplex) or other RNAses, the primary mechanism of action for PNA on RNA is almost certainly steric

hindrance (Figure I.32c).[401,414] However, RNase H-mediated degradation can occur in the case of DNA-PNA chimeras (Figure I.32d).[415] The antisense agents can inhibit mRNA splice site selection or block translation.

Following transcription, splicing of pre-mRNA into their mature can be inhibited by PNA/mRNA duplex formation at the entron-exon junction.[413] In consequence, down regulation of a mature protein[416,417] or the correction of aberrant splicing and the restoration of a functional protein[306,418] can occur.

In steric blockage of translation, both duplex and triplex-forming PNA molecules can inhibit the translation initiation (around or upstream the start codon of the mRNA), where ribosomal components and translation factors assemble prior to elongation.[419] However, only triplex-forming PNAs, can be used to cause the translation elongation arrest. When working with this antisense oligonucleotides, it is advisable to perform an mRNA scanning (gene-walk) by testing a series of PNAs targeting different regions of the mRNA.[302]

Antisense oligonucleotides can attenuate aberrant gene expression, such as occurs in many cancers, but can also be applied against infectious diseases caused by viruses, bacteria and parasites. Growth inhibition has been well demonstrated in several bacterial species using PNAs targeting mRNAs of growth essential genes.[420-422] In addition, PNAs are not effectively exported from the bacteria by the efflux pumps that normally eliminate antibiotics such as penicillins.[423] On the other hand, viral RNA also presents susceptible targets for recognition and steric hindrance, such as genes essential for viral growth (in RNA viruses) or internal ribosomal entry sites (in DNA viruses).[302]

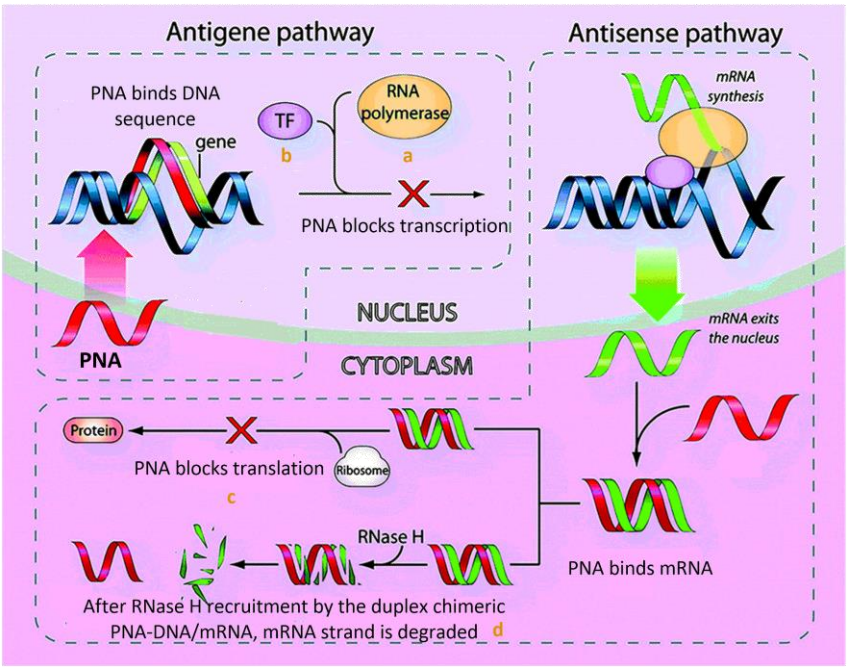

Figure I.32. Possible therapeutic effects of PNA or PNA-DNA chimera (adapted from [293]).

Besides that it was reported that PNAs can inhibit elongation of viral reverse transcriptases on RNA templates.[401] Over time, several laboratories have shown that PNAs can inhibit viral replication in infected cells.[424,425] Moreover, PNAs were found to be very efficient tools in correction of aberrant splicing and the restoration of a functional protein. One of the examples is the restoration of dystrophin expression in Duchenne muscular.[418]

Inhibition of ribonucleoprotein interactions by PNA. Ribonucleoproteins are nucleoprotein that contains RNA, like ribosomes and telomerase.

rRNA, which makes up approximately 40% of total mass of ribosome, plays an active role in translation. While most rRNAs are inaccessible to sequence recognition, the active regions are often exposed. As many useful antibiotics target rRNA, this can be one of the main applications of this approach since these sequences are accessible to hybridization. In fact, some PNA targeting bacterial rRNA functional domains have already been tested.[426,427]

In telomerase, the internal RNA moiety, which serves as a template for the synthesis of repeating sequences of telomeres, is an accessible target for PNA. Several studies show that PNAs can inhibit telomere extension *in vitro*[428-430] and in human cells[307] with low-nanomolar IC_{50} values. However, anti-telomerase PNAs were only effective if present before assembly of the full RNA–protein complex.[302] Nevertheless, inhibition of telomerase interactions may have impact in cancer treatment, as seen before.

miRNA Inhibitors. miRNAs are a family of small (ca. 21 nucleotides) noncoding RNAs implicated in post-transcriptional gene expression regulation by sequence-selective targeting of mRNAs. At least 30% of protein-coding genes are estimated to be regulated by miRNAs[430]establishing them as one of the largest classes of regulatory molecules. These miRNAs/mRNAs interactions lead to the regulation of very important biological processes, including cell metabolism, inflammation, pathogen infection, and cancer. The reports available demonstrate that PNAs targeting specific miRNAs lead to de-repression of the major endogenous mRNA targets of miRNAs. This might have important therapeutic applications, in consideration of the involvement of miRNAs in important human diseases.[410] The potential of PNA as miRNA antagonists in cell cultures has been illustrated for some miRNA, such as miRNA-210[431] (associated with hypoxia that is modulated during erythroid differentiation), miRNA-122[432] (a liver-specific miRNA that has direct control over cholesterol biosynthesis and which is required for hepatitis C infection) or miRNA-155[433] (expressed in the haematopoietic system).

3.6.2. Molecular diagnosis and imaging

PNAs have been widely proposed in protocols aimed at performing highly sensitive hybridization with NA due to the higher stability of the PNA/DNA complex and the higher specificity of PNA binding to DNA. Techniques, such as polymerase chain reaction (PCR) clamping, and hybridization probes have benefited from the unique properties of PNA

PNA-mediated PCR clamping. This method is based on the inefficiency of PNA as a primer for DNA polymerases. As a consequence, PNAs are very specific blockers of PCR amplification, as they compete with DNA primers for binding to the template strand, and can prevent the amplification of the mutated fragment or specific amplify the mutated and not the wild-type sequence (Figure I.33a). Due to extremely high-sequence discrimination of mismatches in PNA–DNA hybridization, it is possible to obtain a specific signal from a single-base mismatch, as occurs in single nucleotide polymorphisms, in the presence of a 1,000-10,000 fold excess of the non-mutated wild type normal gene. PNA clamping has the advantages of higher sensitivity, speed, simplicity and lower cost compared with the standard direct sequencing, although it cannot be used to detect new mutations.[434,435] This method can be used to detect mutations affecting the BRAF, epidermal growth factor receptor, *k-RAS*, and *BCR-ABL* quickly and accurately and consequently diagnose tumors in the early stages to enable effective treatment.[410]

Hybridization Probes. In diagnostics and in research, hybridization probe molecules are required for the detection of target bioanalytes. The most important strategies are the unimolecular probes, e.g. molecular beacon, forced intercalation probes and binary probes.

Molecular beacons are probes with a fluorophore with intrinsically strong fluorescence (e.g. fluorescein and rhodamine derivatives) at one terminus and a quencher group at the other. If a beacon remains unhybridized the fluorophore and quencher lie next to each other and the molecule does not emit a signal because the energy emitted by the fluorophore is absorbed by the quencher. On hybridization the molecule stretches out, separating the quencher and the fluorophore, leading the fluorescent dye to emit a signal, reporting the occurrence of hybridization.[436] The first reported use of PNA to detect PCR products used a chimeric DNA–PNA probe,[437] but the method was rapidly improved to involve pure PNA probes.[438] In contrast with DNA beacons, PNA beacons do not require the hairpin structure since the hydrophobic structure and lack of charge repulsions in the PNA is sufficient to favour a condensed structure with quenched signals from the free PNA probe. Besides that, PNA probes are also less dependent on salt concentrations, and less sensitive to the presence of proteins that bind to ssDNA.[439] This enables the usage of PNA beacons to immobilize on both flat

surfaces and optical fibres,[440] as well as, detection of NAs directly in different buffers and protein-containing solutions.[441]

Fluorogenic PNA-based forced intercalation probes lack a stem-loop structure and contain a hybridization responsive fluorophore. On hybridization with a target, a duplex structure is formed; the fluorophore intercalates in this structure and the probe becomes brightly fluorescent.[436] So far, thiazole orange containing PNA have been used as fluorophore, for example, to detect viral mRNA in H1N1 influenza A infected live cells,[442,443] to localize miRNA-122 in live Huh7 cells,[432] in detection of *k-RAS* mRNA within living cells[444] and cancer associated transcript in living cells and human adenocarcinoma of colon tissues.[445]

Binary probes use two single-labelled PNAs complementary to the target oligonucleotide. Typically, one oligonucleotide is labelled with a donor fluorophore and the other is labelled with an acceptor molecule. After hybridization to complementary oligonucleotide at the adjacent locations, the labels were close enough to enable strong fluorescence quenching. This probes have been used as mRNA imaging agents to know its expression levels in living cells.[446]

Fluorescence *in situ* hybridization using PNA probes. PNA probes are highly effective in fluorescence *in situ* hybridization applications because their neutral backbone provides a high specificity *in situ*, requires less concentration and hybridizes quickly. Additional advantages of using PNA probes *in situ* are reduced background binding, i.e. excellent signal-to-noise ratio, low photobleaching and a mild washing procedure resulting in morphologically better samples.[447,448] Thus, this technique has been developed for telomere analyses,[449] multiple gene abnormalities identification[450] and viral,[451] yeast[452-454] and bacterial[455-462] diagnostics both in medical as well as environmental samples. Recently, peptide nucleic acid-colorimetric *in situ* hybridization has been proposed. Chromogenic visualization (colorimetric method) is typically based on enzyme-conjugated antibodies that recognize the targeted probe. Then, the addition of the correct substrate to the enzyme used leads to chromogenic precipitates. The colorimetric method have some advantages over the fluorescent one: only requires a standard light microscope, the stability of the probes allows slide storage at room temperature for extended periods of time, and the cellular morphology of the specimen is maintained, markedly aiding in the interpretation of result. Nonetheless, in this colorimetric technique, future improvements are necessary in order to solve the permeabilization issues in bacteria and improve the detection limit of the procedure.[455,463]

Surface plasmon resonance (SPR). PNA-based molecules have also been used in combination with SPR. This procedure is a nonradioactive methodology, rapid, informative, and does not require gel electrophoresis and/or dot-spot analysis. The

combined employment of SPR-based instruments and PNA probes has been used to detect point mutations, for example, *k-RAS* gene mutations[464] or in diagnosis of a cystic fibrosis mutation.[465] Alternatively, SPR imaging couples the sensitivity of spectral SPR measurements with spatially-controlled imaging capabilities. A nanoparticle-enhanced SPR imaging sensing strategy in non-amplified genomic DNA proved to be ultrasensitive (attomolar concentrations of target genomic DNA are detected), specific and the sensitive to detect point mutations[466] and identification of bacteria (Figure I.33b).[467] The direct detection of genomic DNAs with no need for PCR amplification represents an important step toward the development of simpler, cheaper and more reliable detection methods.[468]

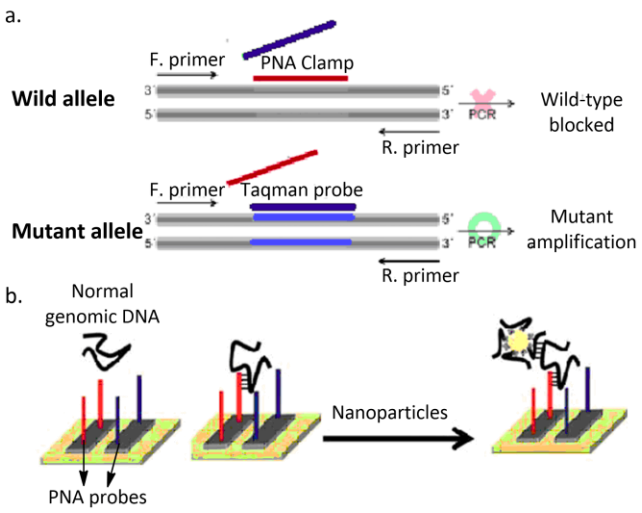

Figure I.33. (a) PCR clamping technique (blue - taqman probe; red – PNA clamp); (b) SPR imaging method using a nanoparticle conjugated to an oligonucleotide complementary to a tract of the target DNA not involved in the hybridization with the PNA probe (adapted from [469,470]).

3.6.3. Tools for molecular biology and functional genomics

PNAs can be used in combination with a nuclease for the modulation of enzymatic cleavage. Indeed, PNAs can be designed and prepared to hybridize a complementary target on a dsDNA and locally unwind this NA by strand displacement rendering the displaced strand sensitive to S1 nuclease.[471] This dsDNA cleavage is especially efficient when two adjacent PNA sites are targeted yielding quantitative double-strand breaks. Therefore PNA can be used as a cutting tool in combination with single-strand-specific S1 nuclease to make an “artificial restriction enzyme” system whose recognition sequence is determined by the PNA sequences employed. Otherwise, dsDNA can be

cleaved by PNA-assisted protection against enzymatic methylation. Providing that methylation would defend from dsDNA from enzymatic digestion, only those DNA sites previously bound to PNA remained susceptible for the restriction enzyme activity. Notably, protection against methylation was less complete when the methylation site was placed at the end of the PNA-binding site. Thus, PNAs used in combination with methylases and other restriction endonucleases can act as "rare genome cutters". This method is called the PNA-assisted rare cleavage technique.[340,472] More recently, a completely chemistry-based DNA cutter selectively cuts dsDNA at designated site with desired specificity. There, Ce(IV)/EDTA complex is used as molecular scissors for hydrolytic scission of DNA, whereas the target sequence is recognized by two strands pcPNA. One of the most important characteristics of this cutter is that it do the hydrolysis of targeted phosphodiester linkages exactly as naturally occurring nucleases do. Thus, the DNA fragments obtained by the completely chemistry-based DNA can be connected with other DNA fragments by using the DNA ligase, exactly as it is done in conventional molecular biology. A possibility to create artificial restriction enzymes has long been highly desired in order to facilitate manipulation of large genomic DNA molecules.[473] In contrast, PNA can reduce the number of naturally occurring enzyme cleavage sites in a stretch of genomic DNA since short PNA sequences, preferably bis-PNAs, can efficiently block restriction enzymes.[474]

Southern hybridization is a routine technique used daily in most molecular biology laboratories for predicting size and sequence information on DNA and information regarding the genetic context. As PNA binding, in contrast to DNA binding, is largely independent of the ionic strength, it is possible to dissociate dsDNA at low salt concentrations and hybridize it with fluorescent-labelled PNA before gel electrophoresis. The neutral backbone of PNA renders higher mobility to the complex PNA/DNA compared with the excess unbound PNA. Pre-gel hybridization using PNA provides a solution to reduce the number of steps in the process of southern hybridization, as the cumbersome post separation, probing and washing steps are eliminated. Consequently, the analysis is much faster than with the conventional southern hybridization technique.[475]

Because of their unique high binding affinity, PNAs are also useful for the sequence-specific purification of NAs and for the isolation of active genes. For instance, methodologies to perform sequence-specific separations of oligonucleotides using PNA linked to alkane chains – discriminated by hydrophobic interaction chromatography[475] – and PNA probes with biotin label at 5' end attached to strepavidin coated superparamagnetic iron oxide beads were developed.[476]

4. Scope and general objectives of this thesis

The dream of modern drug research is to discover biologically active molecules that are absolutely specific and able to act efficiently only on the molecular targets responsible for the disease progression.

As NA lesions or mutations are involved in most of the diseases, these essential cell molecules are attractive targets for drug design. Over the years different approaches were used to target DNA and RNA. However, due to the high homogeneity of B-DNA, it is rather difficult to achieve a selective effect on particular DNA region.

In order to overcome that situation, non-canonical DNA structures, such G4, were chosen as new targets in drug research. Despite several molecules have already been tested as G4 ligands but there is room for improvements. In order to increase the structural diversity among the G4 ligands, this thesis describes the design, synthesis and biological evaluation of two libraries of novel compounds based in distinct aromatic core scaffolds. Chapter II describes a library of novel symmetric derivatives belonging to non-fused aromatic family (**I.101**) in which it was explored the: (a) benzene, naphthalene and 2,7-biphenylnaphthtlene scaffolds as aromatic core structures and (b) side-chains containing sulphur and oxygen in order to obtain chemical diversity. To accomplish this purpose, one of the methodologies explored to construct the side-chains was the thiol-ene click chemistry. Chapter III is focus on a more rigid family of compounds based on benzo[*h*][1,6]naphthyridin-2(1*H*)-one scaffold (**I.102**). As far as we know, this aromatic core structure was not yet explored as G4 ligand.

Alternatively to the non-canonical DNA structures, different OAs (including α-PNAs) were synthesised to target specific sequences on NAs. Chapter IV described the synthesis of new chimeric cysteines with nucleobase side chains that can be used as building blocks of α-PNAs (**I.103**) also using thiol-ene click chemistry.

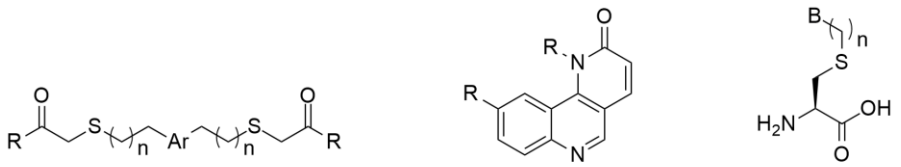

I.101 **I.102** **I.103**

Figure I.34. General structures of the compounds described in this thesis (Ar: non-fused aromatic core; B: Nucleobase; R: side chains).

CHAPTER II

II. SYNTHESIS AND BIOLOGICAL EVALUATION OF NON-FUSED AROMATIC COMPOUNDS AS G4 LIGANDS

1. Introduction

As described in chapter I, different non-fused aromatic compounds have been synthesised and tested as G4 ligands. Some members of these family share chemical features, namely a symmetric structure comprising:

i. An aromatic core to establish interactions through π-π stacking;

ii. Two side chains with amine end-groups to interact with the loops and grooves and ensure sufficient solubility of the molecules.

The aromatic core is composed, in the majority of the compounds, by one-ring aromatic nucleus (benzene or pyridine) substituted in positions 1 and 3 by two other aromatic groups. A series of disubstituted bis(vinylquinolinium)benzene derivatives (**II.1** and **II.2**, Figure II.1) were synthesised.[239] The FRET-melting data indicated that derivatives presenting a "bent" shape (**II.1**) had higher stabilizing ability to G4 DNA than linear compounds (**II.2**) and compounds with more rigid cyclic amine (**II.1c-d**, **II.1g** and **II.2g**) displayed stronger stabilizing ability for G4 than those with flexible acyclic amine (**II.1e-f** and **II.2e-f**). Interestingly, **II.1e-f** could destabilize c-1 G4 DNA structures. Moreover, these derivatives had good selectivity on G4 DNA over dsDNA.[239] Bis-triazole ligands (**II.3**, Figure II.1) linked by a benzene were selective for G4 DNA vs. dsDNA over the given concentration range and also showed high activity telomerase inhibition.[248,249] Phenylene bis-indoles (**II.4,** Figure II.1) exhibited stabilization potential for four different G4 forming oligonucleotides studied and showed better selectivity for promoter G4 (*c-KIT2* and *c-MYC*) over human telomeric G4 DNA.[253] Ligands incorporating carboxamide side chains at the *meta* position relative to the indole NH (**II.4g-h**) were found to show very weak stabilisation of G4 compared to the *para* substituted analogues (**II.4a-b**). Although ligands **II.4e** and **II.4f** (prepared from (R)- and (S)-quinuclidin-3-amines) showed comparable stabilisation of telomeric G4 DNA, ligand **II.4e** showed slightly better stabilisation of *c-KIT2* G4 and a reduced stabilisation of dsDNA when compared with its isomer. Comparing the length of the side chains, aminopropyl-substituted ligands (**II.4b** and **II.4h**) demonstrated improved stabilisation over the corresponding aminoethyl derivatives (**II.4a** and **II.4g**). UV/Vis titration studies revealed that bis-indole ligands binded tightly to G4 and showed a three- to fivefold preference for *c-KIT2* over telomeric G4 DNA. These ligands also had good selectivity on G4 DNA over dsDNA.[254] Comparing two bis-benzimidazoles (**II.5** and **II.6,** Figure II.1), the compound **II.5** with a

"bent" shape showed higher affinity toward the G4 than compound **II.6** with a linear shape.[259] Phenyl bis-oxazoles compounds without side chains (**II.7** and **II.8,** Figure II.1) were synthesised but none of the compounds stabilised either the G4 nor the dsDNA.[477] In contrast, a library of phenyl bis-oxazoles with terminal tertiary amines in the *para* position (**II.9,** Figure II.1) showed significant stabilization of the two HSP90 G4, yet no stabilization of a human telomeric G4 DNA sequence or dsDNA.[478] Surprisingly, the weakly basic di-morpholine derivative (**II.9d**) presented a significant activity, in contrast with the majority of other G4 ligands with the same amine. The selectivity of the most efficient ligand, **II.9f**, was examined further and showed modest stabilisation of the *k-RAS* G4 DNA but none with the *c-KIT2* G4 DNA. Compound **II.9f** also shows low-micromolar cell growth inhibitory activity in cancer cells, yet only modest selectivity compared to its effect on normal fibroblast cells. In addition, **II.9f** only changed modestly HSP90 expression in these cell lines and was not an inhibitor of human telomerase activity.[478] Analogue compounds having phenyl bis-oxazoles with side chains in the *meta* position **II.10** did not stabilize G4 sequence tested or only stabilize at high concentrations. The cellular evaluation of these compounds showed IC_{50} values in low micromolar range in four cancer cell lines and one fibroblast cell line.[251] The regioisomeric compound **II.11** showed no significant increase in melting temperature using five G4 sequences.[478] Two diethynyl amide derivatives containing *N,N*-dimethylpropylamine side chains and presenting benzene as aromatic nucleus (**II.12,** Figure II.1) showed moderate stabilization for three promoter G4 DNA with no detectable stabilization of dsDNA. This compound also showed discrimination capacity between intramolecular promoter G4, showing *c-KIT1* the higher ΔT_m values. [266]

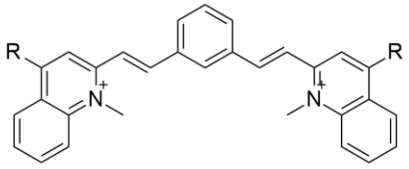

	G4 DNA		ds
	hTelo	c-kit1	
II.1a, R = H	6	6	0
II.1b, R = *N*-Pyr	8	8	0
II.1c, R = *N*-MePpz	20	19	1
II.1d, R = *N*-Mor	19	16	1
II.1e, R = $NH(CH_2)_2N(Me)_2$	9	- 5	1
II.1f, R = $NH(CH_2)_2(Et)_2$	9	- 9	1
II.1g, R = 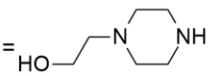	17	20	1

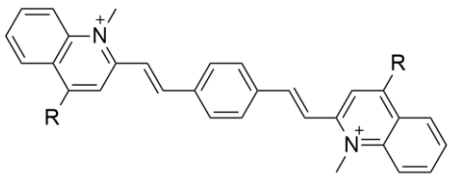

	G4 DNA		ds
	hTelo	c-kit1	
II.2a, R = H	2	3	1
II.2b, R = *N*-Pyr	4	8	0
II.2c, N= MePpz	3	5	1
II.2d, R = *N*-Mor	5	3	1
II.2e, R = $NH(CH_2)_2N(Me)_2$	3	3	1
II.2f, R = $NH(CH_2)_2(Et)_2$	2	3	1
II.2g, R = 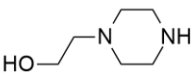	9	5	1

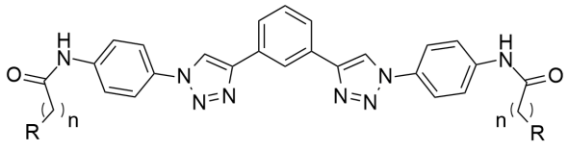

	hTelo	ds
II.3a, n = 1; R = *N*-(Me)$_2$	9	0
II.3b, n = 1; R = *N*-(Et)$_2$	4	0
II.3c, n = 1; R = *N*-Pyr	14	0
II.3d, n = 1; R = *N*-Pip	2	0
II.3e, n = 1; R = *N*-Mor	0	0
II.3f, n = 2; R = *N*-(Me)$_2$	19	0
II.3g, n = 2; R = *N*-Pyr	18	0
II.3h, n = 2; R = *N*-Pip	14	0

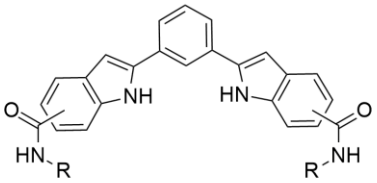

	G4 DNA				ds
	hTelo	c-kit1	c-kit2	c-myc	
II.4a, side chain: 5-; R = (CH$_2$)$_2$N(Me)$_2$	17	n.d.	17	n.d.	3
II.4b, side chain: 5-; R = (CH$_2$)$_3$N(Me)$_2$	22	28	22	17	4
II.4c, side chain: 5-; R = (CH$_2$)$_3$*N*-Pyr	18	n.d.	20	n.d.	3
II.4d, side chain: 5-; R = 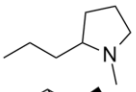	10	n.d.	10	n.d.	3
II.4e, side chain: 5-; R = 	14	n.d.	20	n.d.	2
II.4f, side chain: 5-; R = 	15	n.d.	17	n.d.	3
II.4g, side chain: 6-; R = (CH$_2$)$_2$N(Me)$_2$	4	n.d.	4	n.d.	0
II.4h, side chain: 6-; R = (CH$_2$)$_3$N(Me)$_2$	10	n.d.	10	n.d.	1

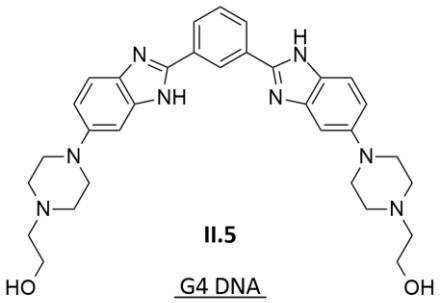

II.5

G4 DNA
12[a]

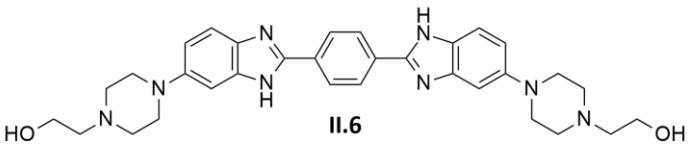

II.6

G4 DNA
4[a,b]

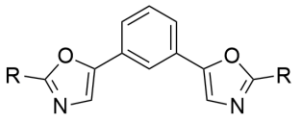

	G4 DNA		ds
	hTelo	c-myc	
II.7a, R = H	0	1	0
II.7b, R = 2-Pyridine	0	1	1

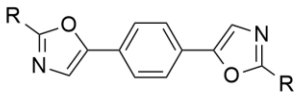

	G4 DNA		ds
	hTelo	c-myc	
II.8a, R = H	0	1	0
II.8b, R = 2-Pyridine	0	1	1

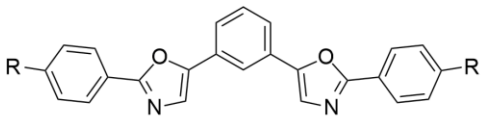

	G4 DNA					ds
	h-Telo	HSP90A	HSP90B	c-kit2	k-ras	
II.9a, R = $CH_2N(i\text{-}Pr)_2$	< 2	8	8	n.d.	n.d.	1
II.9b, R = CH_2*N*-Pyr	2	7	2	n.d.	n.d.	0
II.9c, R = CH_2*N*-MePpz	< 2	7	3	n.d.	n.d.	0
II.9d, R = CH_2*N*-Mor	< 2	6	5	n.d.	n.d.	0
II.9e, R = CH_2*N*-Azep	3	8	9	n.d.	n.d.	1
II.9f, R = $(CH_2)_2$*N*-MePpz	< 2	14	2	< 2	7	0
II.9g, R = $O(CH_2)_2$*N*-Pyr	< 2	7	2	n.d.	n.d.	0
II.9h, R = $O(CH_2)_3$*N*-Pyr	< 2	7	2	n.d.	n.d.	0
II.9i, R = $O(CH_2)_4$*N*-Pyr	2	5	2	n.d.	n.d.	0

	IC_{50}					
	MCF-7	786-O	RCC4	A549	Mia-Pa-Ca2	W138
II.9f	1.3	1.3	0.9	1.0	1.3	2.6

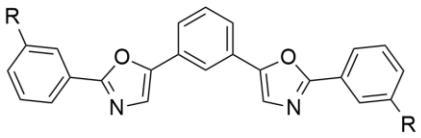

	G4 DNA			ds	IC_{50}				
	hTelo	HSP90A	c-kit2		MCF-7	786-O	RCC4	A549	W138
II.10a, R = CH_2*N*-Pip	< 2	5	< 2	2	1.4	2.3	1.9	1.2	4.4
II.10b, R = $O(CH_2)_2$*N*-Pyr	< 2	28	< 2	0	1.2	0.7	1.3	1.0	1.0
II.10c, R = $NH(CH_2)_2N(Et)_2$	< 2	< 2	< 2	0	3.1	1.3	1.1	2.5	2.8
II.10d, R = $NH(CH_2)_2$*N*-Pyr	< 2	< 2	< 2	0	2.1	1.1	1.1	0.6	1.0
II.10e, R = $NH(CH_2)_3$*N*-MePpz	< 2	< 2	< 2	0	1.0	0.9	1.2	1.2	1.1

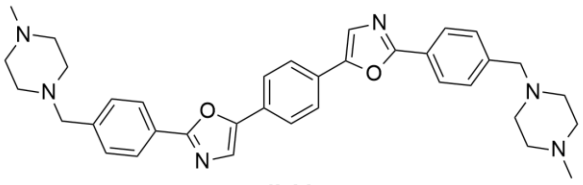

II.11

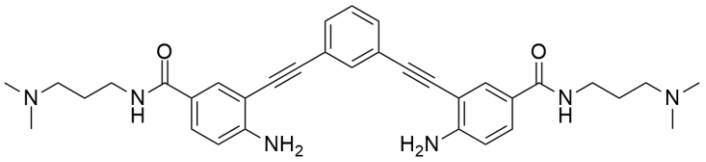

II.12

G4 DNA				ds
c-kit1	c-kit2	k-ras	c-myc	
9	6	n.d.	3	0

Figure II.1. Structures of non-fused aromatic compounds with benzene aromatic core, ΔT_m values (^{0} C) for FRET melting analysis with a series of G4 forming DNA sequences [human telomeric (*hTelo*), a set of promoters (*HSP90A*, *HSP90B*, *c-KIT1*, *c-KIT2*, *k-RAS* and *c-MYC*)] and dsDNA (ds) ([ligand]/[oligonucleotide] = 5) and short-term antiproliferative activity (IC_{50} in μM) in a cancer cell line panel [MCF7 (breast), 786-O/RCC4 (renal), A549 (lung) and Mia-Pa-Ca2 (pancreas)] and WI38 (fibroblast) cell line. a: ΔT_m obtained by CD with the G4 forming sequence 5'-(TTGGGG)4-3'; b: [ligand]/[oligonucleotide] = 4.

Few molecules has a naphthalene ring as central nucleus. However, these could be a good alternative to one-ring aromatic nucleus as it is sufficiently small to overcome some of the druggability problems associated with large polycyclic groups, yet of sufficient surface area to interact with G-quartet. Among the compounds tested as G4 ligands with naphthalene in its structure are a series of derivatives with disubstituted triazole side-arms.[250] One of these compounds (**II.13**, Figure II.2) shows a high level of selectivity for renal, osteo- and Ewing's sarcomas that express the HIF-1a transcription factor. Furthermore, it also interacts selectively with the G4 DNA located in the promoter of the HIF genes (according to the SPR data) what suggests that the mechanism of action involves inhibition of transcription by drug-mediated G4 stabilization in these regions.[250] In order to further develop a SAR study on **II.13**, other bis-triazoles and bis-oxazole derivatives (respectively **II.14** and **II.15**, Figure II.2) were synthesised.[251] Compound **II.14a,** presenting the terminal tertiary amines in the *para* position, did not stabilized any of the G4 DNA sequences tested and showed IC_{50} values above 25 μM for all lines in a small panel of cancer cell lines. Modifying the substitution pattern on the terminal phenyl ring system from *para* to *meta* resulted in a slightly better performance on G4 stabilization and in a significant decrease in IC_{50} value for the two renal cancer cell lines. This is in accord with previous findings for compound **II.13** which has highly selective activity in renal compared to a number of other carcinoma cell lines and suggests that the *meta* substitution may be a critical factor in this selectivity. When the linking heterocyclic moiety was changed from a triazole to an oxazole ring (**II.15**, Figure II.2) a significant improvement in antiproliferative activity was observed. However, this

compound did not stabilize the G4 sequences tested.[251] Comparing ΔT_m **II.10e** with **II.15,** it is possible to conclude that variation in the aromatic core does not have a huge effect neither in the G4 stabilization nor in the antiproliferative effect of the compounds.

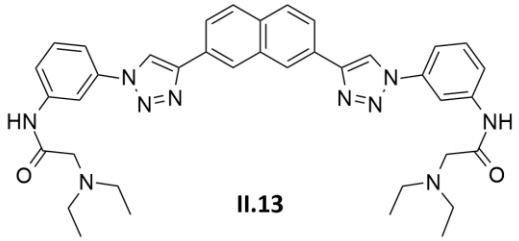

II.13

IC$_{50}$													
MCF-7	HOS	MG63	MNNG	U20S	SaOS2	OST	TC135	TC71	TC32	786-O	A498	RCC4	RCC4$_{VHL}$
63	2.4	7.9	3.2	5.3	2.6	2.4	2.4	7.8	0.9	2.3	2.5	1.4	2.6

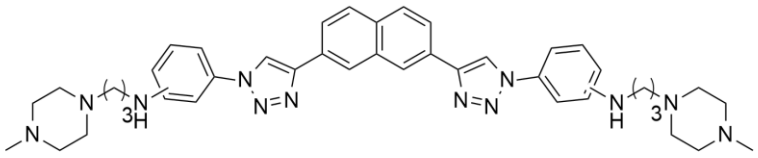

	G4			ds	IC$_{50}$				
	hTelo	HSP90A	c-kit2		MCF-7	786-O	RCC4	A549	WI38
II.14a, side chain: 3-	3	6	2	0	> 25	8.7	8.4	> 25	15.3
II.14b, side chain: 4-	< 2	< 2	< 2	0	> 25	> 25	> 25	> 25	> 25

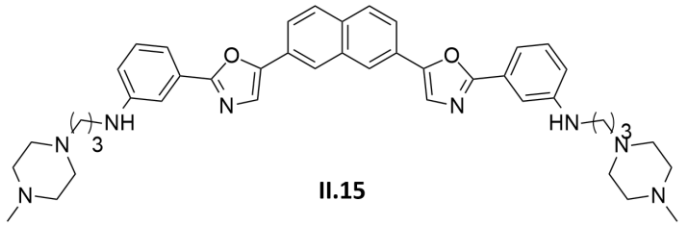

II.15

G4 DNA			ds	IC$_{50}$				
hTelo	HSP90A	c-kit2		MCF-7	786-O	RCC4	A549	WI38
< 2	3	< 2	0	1.9	1.2	2.1	1.6	3.1

Figure II.2. Structures of non-fused aromatic compounds with naphthalene aromatic core, ΔT_m values (^{0} C) for FRET melting analysis with a series of G4 forming DNA sequences [human telomeric (*hTelo*), a set of promoters (*HSP90A* and *c-KIT2*)] and dsDNA (ds) ([ligand]/[oligonucleotide] = 5) and short-term antiproliferative activity (IC_{50} in μM) in a cancer cell line panel [MCF7 (breast), HOS/MG63/MNNG/U2OS/SaOS/OST (osteosarcoma), TC135/TC71/TC32 (Ewing's sarcoma), 786-O/A498/RCC4/RCC4$_{VHL}$ (renal), A549 (lung)] and WI38 (fibroblast) cell line.

In order to further explore the importance of the above mentioned aromatic cores in new G4 ligands, this chapter will focus on the synthesis and biological evaluation of a group of compounds (Figure II.3) with a symmetrical structure comprising:

(a) An aromatic core with benzene (**II.16**), naphthalene (**II.17, II.18**) or 2,7-biphenyl naphthalene core (**II.19, II.20**) to establish interactions through π-π stacking;

(b) A side chain containing a terminal tertiary amine group to interact with the loops and grooves and ensure sufficient solubility of the molecules (with exception of **II.20**);

(c) Different side chain lengths to observe their influence on G4 stabilizing ability of the ligands;

(d) Sulphur (**II.16**-**II.19**) or oxygen (**II.19**) atoms in the side chains conferring chemical diversity to the structures.

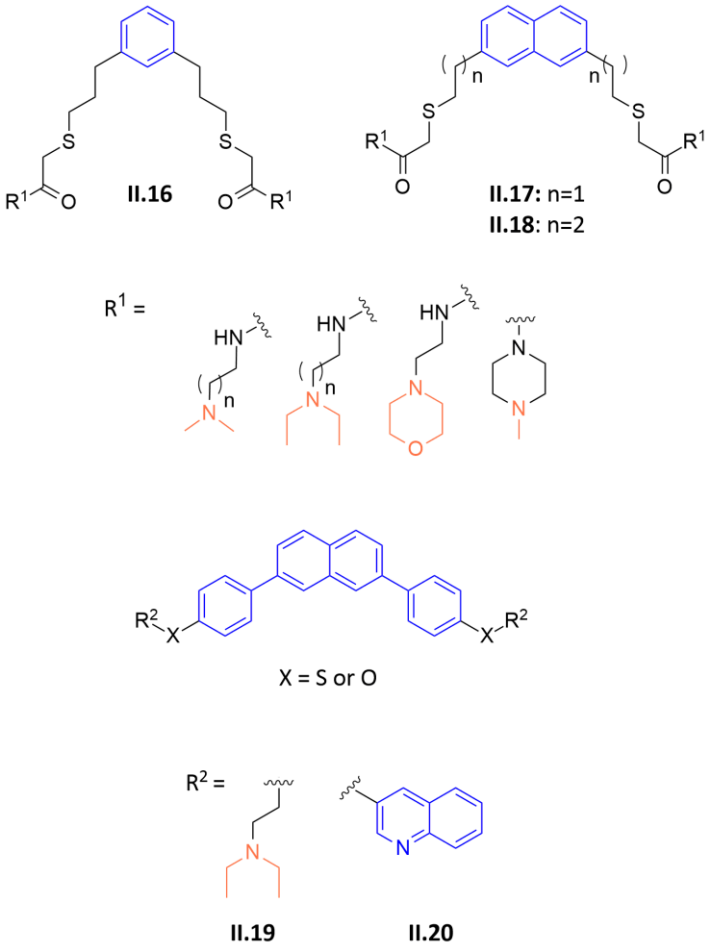

Figure II.3. Structure of the compounds synthesised to be tested as G4 ligands (in blue the aromatic core; in orange the basic group of side chains).

2. Methods, Results and Discussion

2.1. Synthesis of ligands based on benzene and naphthalene core

2.1.1. Retrosynthetic analysis

Compounds **II.16**, **II.17** and **II.18** were obtained according to the proposed synthetic pathway illustrated in Scheme II.1, in which benzene derivatives were substituted in position 1 and 3 and naphthalene derivatives were substituted in position 2 and 7.

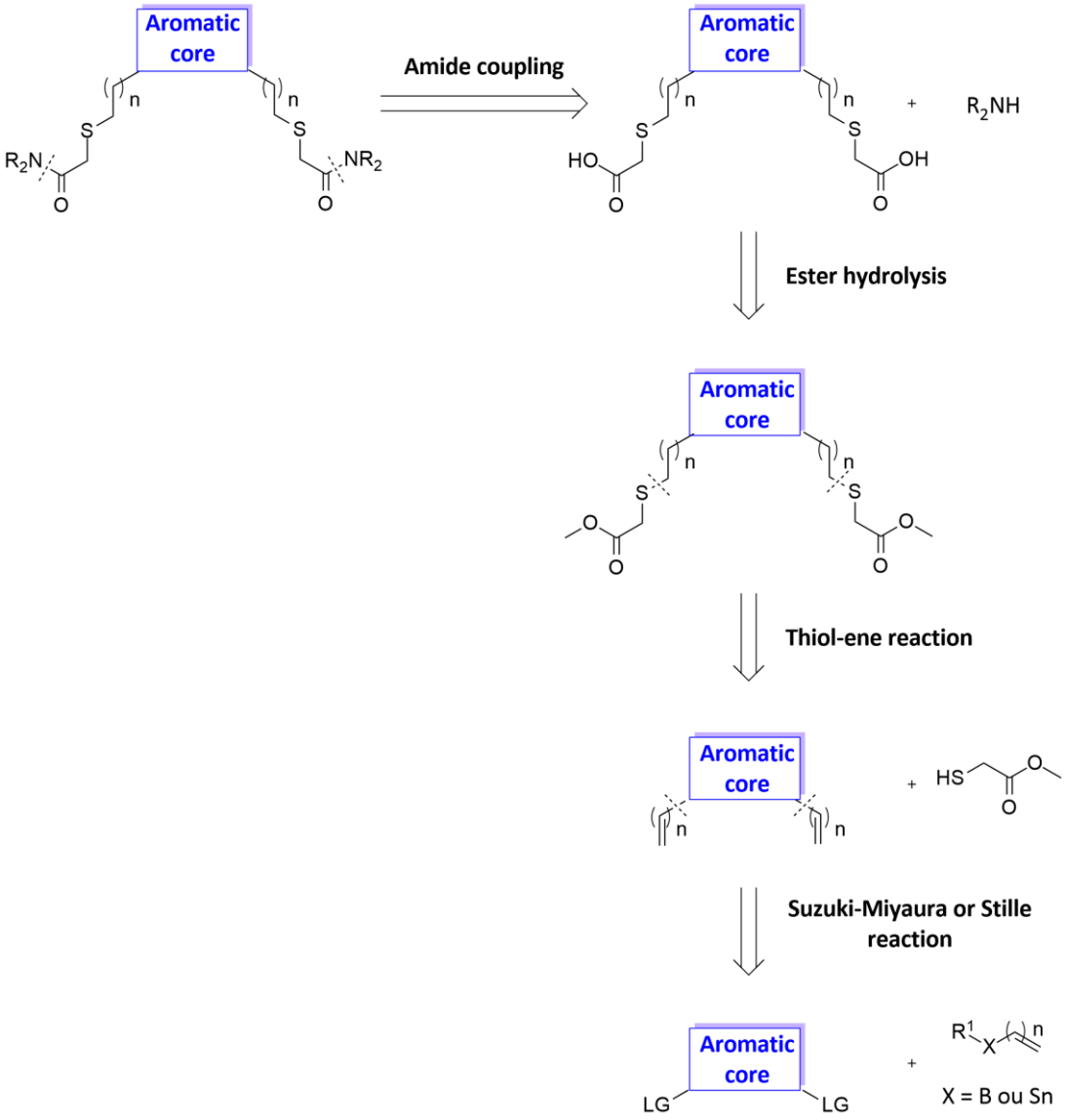

Scheme II.1. Proposed synthetic pathway for the synthesis of benzene and naphthalene derivatives. LG: leaving group; in blue the aromatic core; in orange the positively charged moiety.

In order to form a new C-C bond between the aromatic ring and the future side chain, two different palladium-catalyzed cross-coupling reactions (either a Suzuki-Miyaura or a Stille reaction) were used. These palladium-catalyzed cross-coupling reactions involve the reaction of organic halides or pseudohalides (for example triflates) (R-X) with alkenyl and aryl organometallics (R'-M) in presence of a catalytic amount of Pd (0) complex to furnish the alkenyl- and aryl-substituted compounds (R-R') (Scheme II.2). In both reactions, the transition metal-catalyzed coupling reaction occurs by a sequence of: (a) oxidative addition, (b) transmetalation (usually rate determining step), and (c) reductive elimination. Various phosphine ligands (L) are effective in stabilizing the Pd(0) intermediates, but the stoichiometry, size, and electronic effect of the phosphines all contribute to the reactivity of catalysts toward oxidative addition and reductive elimination.[479,480]

The main difference between these two reactions resides in the metal present in the organometallic reagent used for transmetalation: while in Suzuki-Miyaura is boron [organoboranes, boronic acids: $RB(OH)_2$ or boronate esters: $R'B(OR'')_2$], in Stille is tin (mixed stannanes, $R'SnR''_3$).[479,480] Another difference between the Suzuki's and Stille's cross-coupling mechanism is the need of the boronic acid activation with base. This activation of the boron atom enhances the polarisation of the organic ligand, and facilitates transmetallation.[479] The main drawbacks of Stille reaction when compared with Suzuki-Miyaura reaction are the toxicity of the tin compounds used, and their low polarity, which makes them poorly soluble in water.[480]

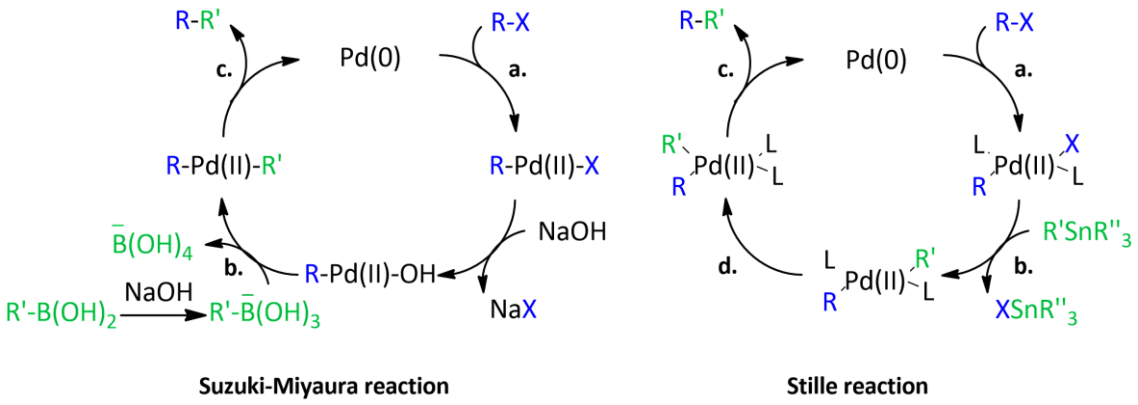

Scheme II.2. Mechanisms of Suzuki-Miyaura and Stille reactions: a. Oxidative addition, b. transmetalation, c. reductive elimination, and d. trans-cis isomerazation.

In the following step, the double bond in the side chain reacted with the thiol of an organosulfur compound. The thiol-ene reaction can proceed under a variety of conditions including: (a) a radical pathway, (b) via catalytic processes mediated by nucleophiles, acids, bases or (c) in the absence of an added catalyst in highly polar

solvents. A wide range of olefines and thiols can be employed although reactivity can vary considerably depending on reaction mechanism, substitution pattern at the C=C bond, the S-H bond strength and its cleavage mechanism (i.e. homolytic vs. heterolytic lysis). Such reactions are generally extremely rapid (even at ambient temperature and pressure), and tolerant to the presence of air/oxygen and moisture.[481] Although the wide variety of mechanisms, the thiol-ene reaction has been frequently conducted under radical conditions, either thermal or photochemically induced. Under such conditions it proceeds via a typical chain process with initiation, propagation and termination steps (Scheme II.3). Initiation involves the treatment of a thiol (RSH) with photoinitiator (under irradiation) or radical initiator (under thermal conditions) resulting in the formation of a thiyl radical (RS•). Propagation is a two-step process involving first the direct addition of the thiyl radical across the C=C bond of the olefine (yielding an intermediate carbon-centred radical) followed by chain transfer to a second molecule of thiol to give the thiol-ene addition product with anti-Markovnikov orientation and the concomitant generation of a new thiyl radical. Possible termination reactions involve typical radical–radical coupling processes.[481]

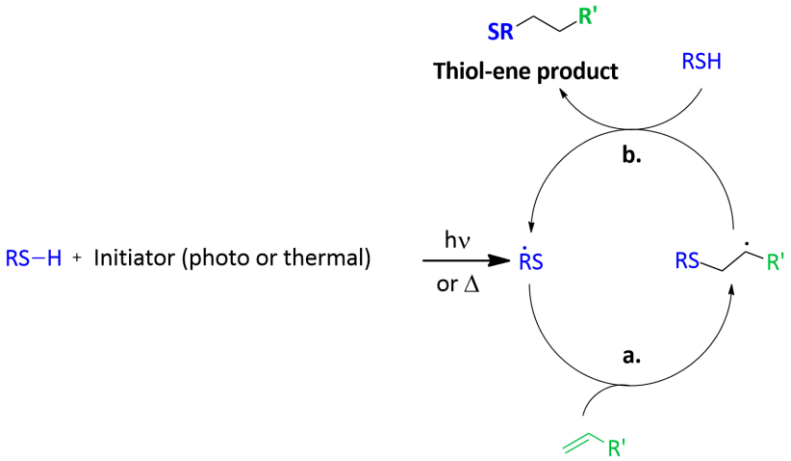

Scheme II.3. Mechanism for the radical thiol-ene reaction: a. Initiation and b. Propagation.

In order to obtain the final compounds, the methyl ester of the side chain was hydrolysed and the resulting carboxylic acid reacted with an amine through an amide coupling.

2.1.2. Synthesis discussion

Bis-allylbenzene **II.21** was synthetized starting from: (a) 1,3-dihydroxibenzene **II.22**, that was converted to the corresponding ditriflate **II.23** in 76% yield; or (b) using the commercially available 1,3-dibromobenzene **II.24.** Then, **II.23** reacted through a Stille

reaction (using allyltributylstannane **II.25** as organometallic reagents and 1,1'-bis(diphenylphosphino)ferrocene **II.26** as ligand) while **II.24** reacted through Suzuki-Miyaura reaction using allyl boronic acid pinacol ester **II.27** as organometallic reagent. (Scheme II.4).

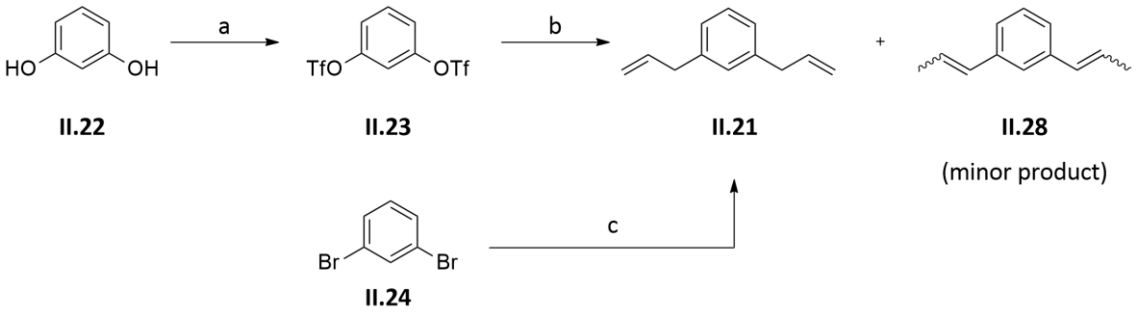

Scheme II.4. Synthesis of compound **II.21**. Reagents and conditions: a) $(CF_3SO_2)_2O$, TEA, DCM, 0 °C to rt, 6 h, 76%; b) **II.25**, **II.26**, $Pd(PPh_3)_2Cl_2$, LiCl, DMF, reflux, 26 h, **II.21**: 21% and **II.28**: 7% (according to ^{1}H-NMR); c) **II.27**, $Pd(PPh_3)_4$, $K_3PO_4.H_2O$, dioxane, reflux, o/n, **II.21**: 64%.

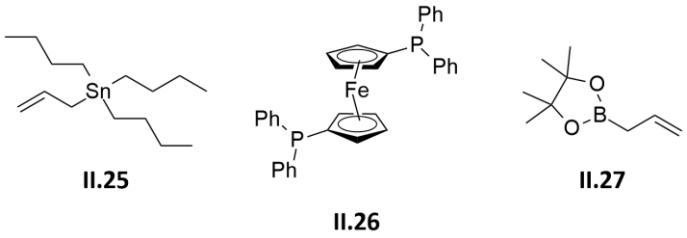

Figure II.4. Organometallic reagents and ligand used.

As exemplified in Scheme II.4, the Stille reaction presented a worst yield and **II.21** was impossible to purify (from the mixture of isomers) by column chromatography. In other hand, the Suzuki-Miyaura reaction represents a better option due to: (a) the higher yield, and (c) the formation of the minor product **II.28** was not observed.

The formation of compound **II.28** is due to a sequential homobimetallic catalysis. Homobimetallic catalysis is a recent concept designed to describe a condition where a transition metal catalyst, with the metal in a certain oxidation state, catalyzes a given reaction to yield a product, which *in situ* undergoes a subsequent transformation, catalyzed by another complex of the same metal, but in a different oxidation state.[482] In the present case, the formation of compound **II.28** involves a Stille cross-coupling reaction followed by an *in situ* palladium-catalyzed conjugative isomerization (Scheme II.5).

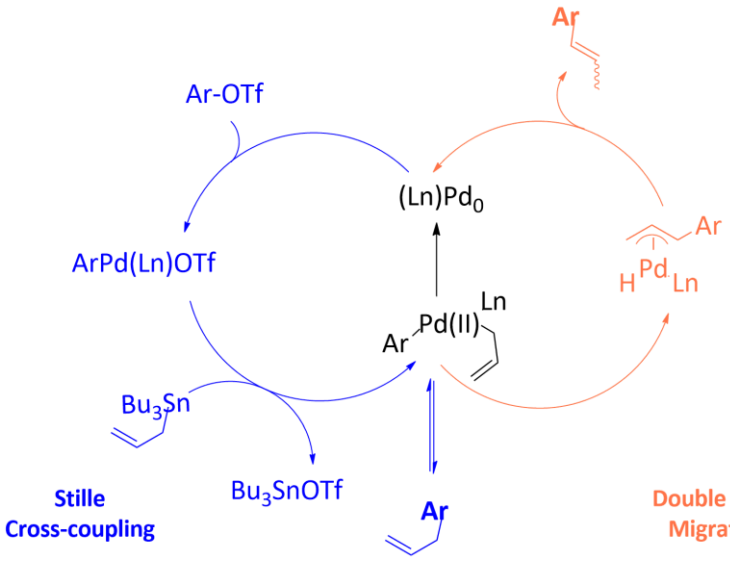

Scheme II.5. Proposed reaction mechanism for the formation of compounds **II.28** and **II.32** (reproduced from [482]).

Bis-allylnaphthalene **II.29** was synthetized starting from 2,7-dihydroxynaphthalene **II.30**, that was converted to the corresponding ditriflate **II.31** in 92% yield. Then, **II.31** reacted through a Stille reaction (using the same reaction conditions used in **II.21** synthesis) or through Suzuki-Miyaura reaction (using the same boronic acid as organometallic reagent and two different bases) (Scheme II.6).

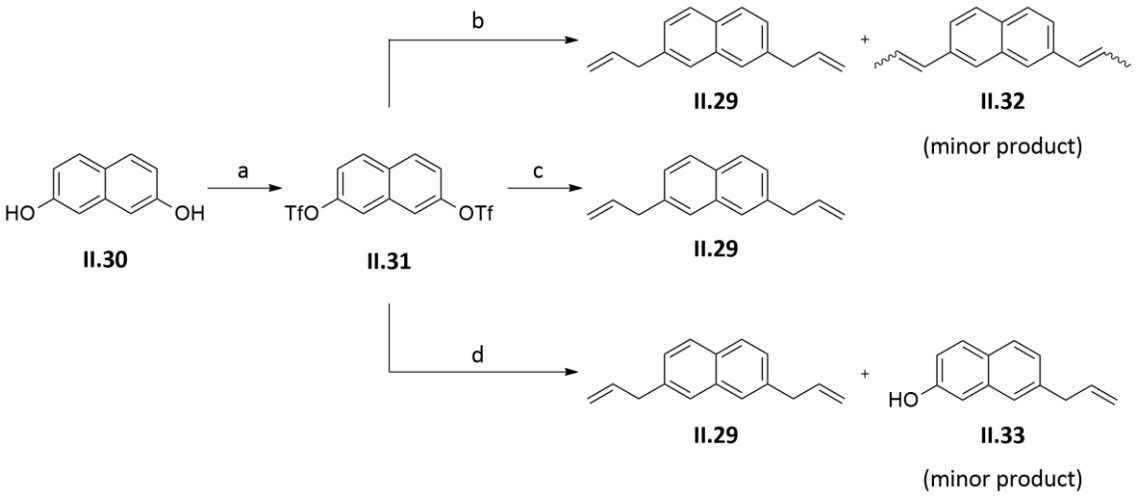

Scheme II.6. Synthesis of compound **II.29**. Reagents and conditions: a) $(CF_3SO_2)_2O$, TEA, DCM, 0 °C to rt, 4 h, 92%; b) **II.25**, **II.26**, $Pd(PPh_3)_2Cl_2$, LiCl, DMF, reflux, 26 h, **II.29**: 47% and **II.32**: 16% (according to ^{1}H-NMR); c) **II.27**, $Pd(PPh_3)_4$, CeF, THF, reflux, 48 h, 20%; d) **II.27**, $Pd(PPh_3)_4$, $K_3PO_4.H_2O$, dioxane, reflux, o/n, **II.29**: 64% and **II.33**: 15%.

As exemplified in Scheme II.6, the Stille reaction presented the same disadvantages reported in the benzene derivative synthesis. As seen previously, the isomerization of double bond in Stille reaction to afford the compound **II.32** is due to a sequential homobimetallic catalysis. Two different reaction conditions of the Suzuki-Miyaura reaction were tested. A better yield was obtained when potassium phosphate tribasic monohydrate was used as base. In addition, in this reaction conditions product **II.33** was obtained as minor product. In order to evaluate the influence of the side chain number, compound **II.33** was used in the synthesis of a molecule containing only one side chain.

In order to access the influence of the length of the side chain, bis-vinylnaphthlene **II.34** was synthetized from the commercially available 2,7-dibromonaphthalene **II.35** and **II.31** were used as starting material using the conditions presented in Table II.1.

Table II.1. Conditions explored in the Suzuki-Miyaura reaction to obtain compound **II.34**.

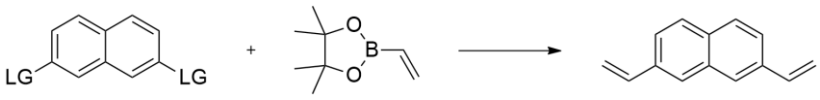

II.31, LG = OTf
II.35, LG = Br

II.34

Entry	Substrate	Pd catalyst	Base	Reaction conditions	Yield
1	**II.31**	$Pd(PPh_3)_4$	$K_3PO_4 \bullet H_2O$	Dioxane, reflux, o/n	58%
2	**II.35**	$Pd(PPh_3)_4$	$K_3PO_4 \bullet H_2O$	Dioxane, reflux, o/n	Vestigial
3	**II.35**	$Pd(PPh_3)_2Cl_2$	$NaCO_3$ 1M	Dioxane, 80 °C, o/n	84%

As exemplified in Table II.1, three different conditions were tested for the Suzuki-Miyaura reaction. A better yield was obtained when **II.35**, bis(triphenylphosphine)palladium(II) dichloride as catalyst and an aqueous solution of sodium carbonate 1 M was used as base (entry 3).

With the allyl and vinyl aromatic compounds in hand, the synthesis proceeded with the thiol-ene reaction of the alkene aromatic compounds with the thiol substrate, under thermal (using AIBN **II.36**) or photochemical conditions (using DPAP **II.37**).

II.36 **II.37**

Figure II.5. Chemical structures of AIBN **II.36** and DPAP **II.37**.

To obtain the thiol-substituted benzene derivative **II.38**, photochemical conditions were used (Scheme II.7) and compound **II.21** was initially reacted with thioglicolic acid **II.39** but the desired product was obtained in low yield (13%) because it was difficult to follow-up the reaction and the purification revealed to be very difficult. Alternatively, compound **II.21** was reacted in the same conditions with methyl thioglycolate **II.40** and the corresponding methyl ester **II.41** was obtained in moderate yield (54%). Subsequent hydrolysis resulted in the desired compound **II.38** with an overall yield of 52% over two steps.

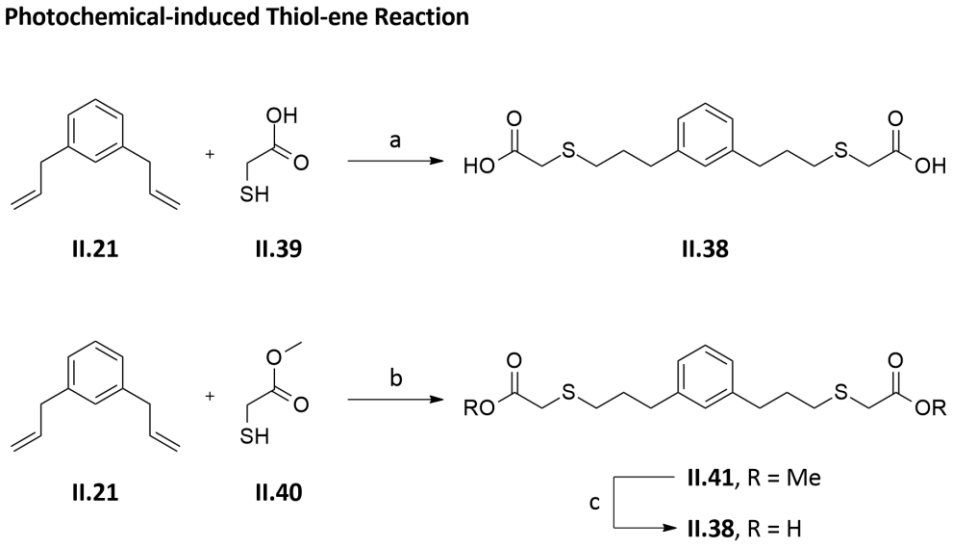

Scheme II.7. Synthesis of compound **II.38**. Reagents and conditions: a) **II.37**, DCE, hv, rt, 1 h, 13%; b) **II.37**, DCE, hv, rt, 1 h, 54%; c) LiOH, H_2O: THF (1:1), rt, 4 h, 96% (52% over two steps).

As exemplified in Scheme II.8, bis-allylnaphathelene **II.29** was reacted with thiol substrates in both thermal and photochemical conditions. Once again, both thermal- and photochemical-induced thiol-ene reaction with thioglicolic acid **II.39** originated the desired product **II.42** in low yields (10% and 20%, respectively). Alternatively, compound **II.29** was reacted with methyl thioglycolate **II.40** under photochemical conditions, and the corresponding methyl ester **II.43** was obtained in excellent yield (92%). Subsequent hydrolysis resulted in the desired compound **II.42** with an overall yield of 84% over two steps.

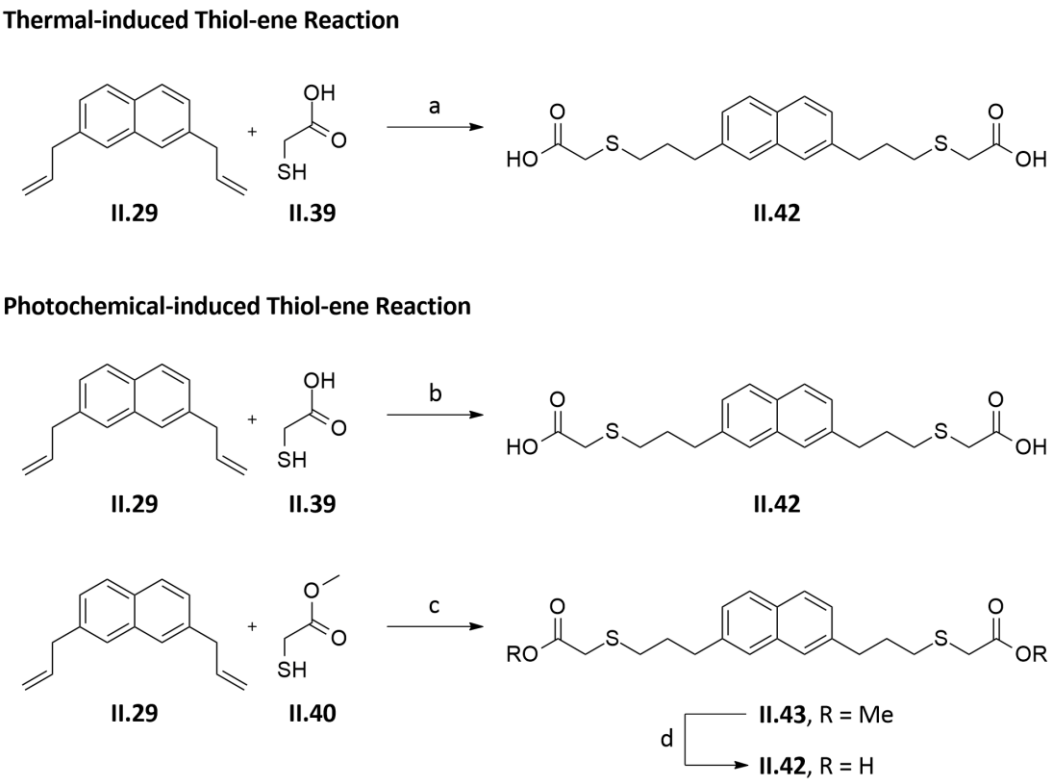

Scheme II.8. Synthesis of compound **II.42**. Reagents and conditions: a) **II.36**, DCE, 90 °C, 70 h, 10%; b) **II.37**, DCE, hv, rt, 1 h, 20%; c) **II.37**, DCE, hv, rt, 1 h, 92%; d) LiOH, H_2O: THF (1:1), rt, 4 h, 91% (84% over two steps).

Based on the previous results, the naphthalene derivative with only one side-chain **II.45** was obtained with an overall moderate yield (65%) applying photochemical conditions and the two steps strategy described before (Scheme II.9). In a similar manner, the naphthalene derivative with shorter side-chains **II.47** was obtained in a more modest yield (28% over two steps, Scheme II.10).

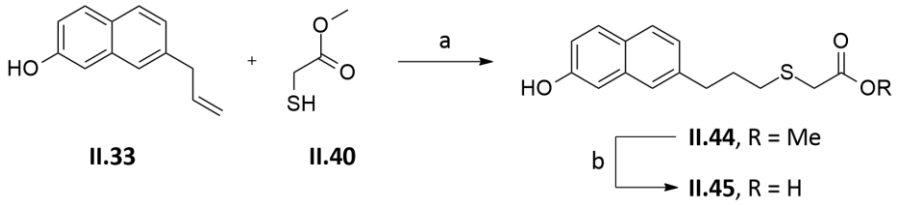

Scheme II.9. Synthesis of compound **II.45**. Reagents and conditions: a) **II.37**, DCE, hv, rt, 15 min, 77%; b) LiOH, H_2O: THF (1:1), rt, 4 h, 84% (65% over two steps).

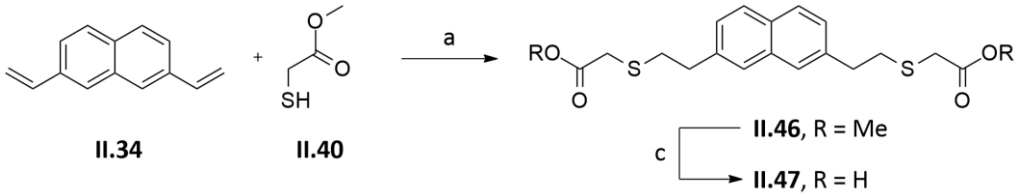

Scheme II.10. Synthesis of compound **II.47**. Reagents and conditions: a) **II.37**, DCE, hv, rt, 4 h, 51%; b) LiOH, H_2O: THF (1:1), rt, 3 h, 54% (28% over two steps).

The synthesis of the final benzene (**II.16**) and naphthene (**II.17**, **II.18**, **II.48**) derivatives were obtained using an uronium-based coupling reagent (TBTU), to obtain the activated carboxylic acid, and a non-nucleophilic base (DIPEA) as displayed in Schemes II.11 and II.12.

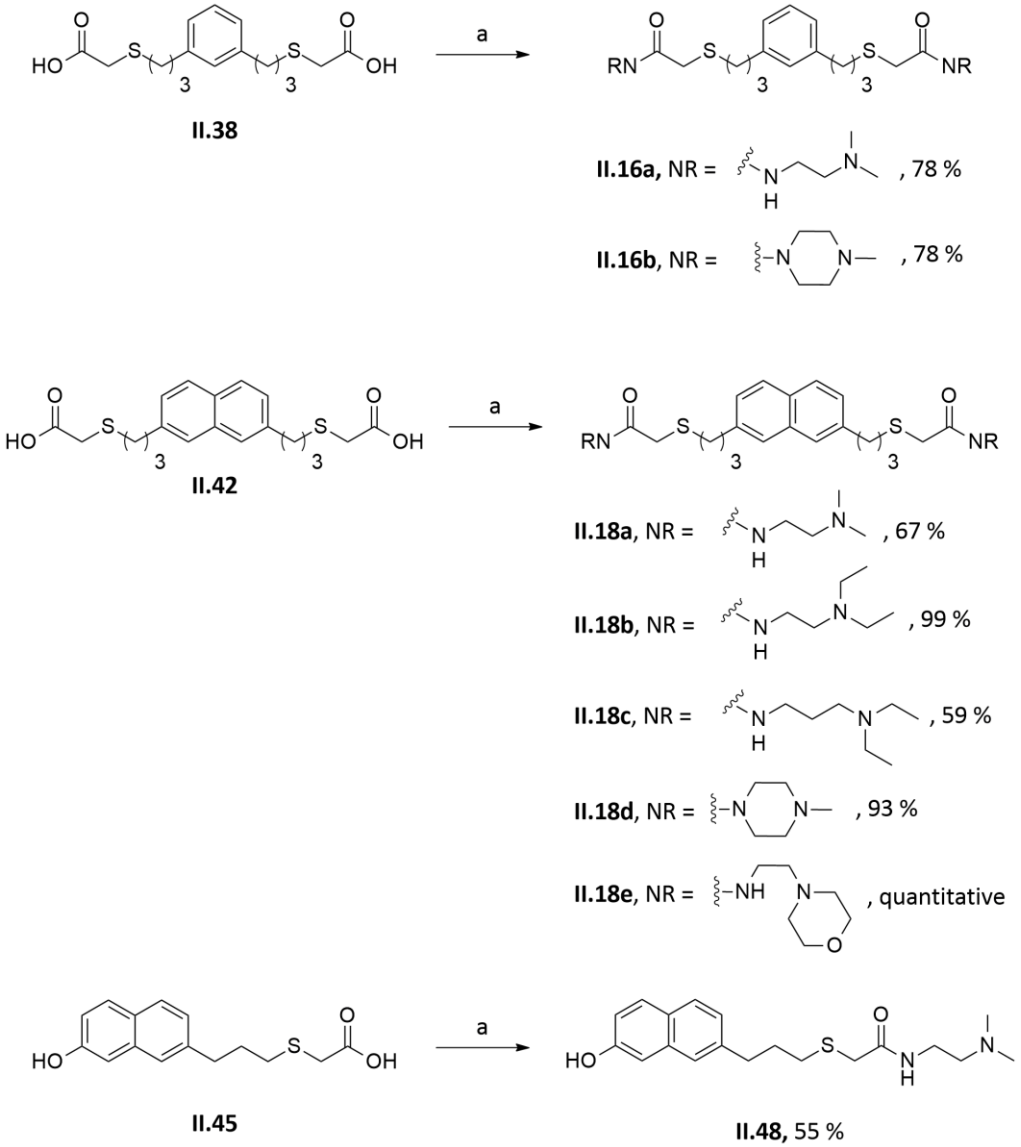

Scheme II.11. Synthesis of benzene (**II.6**) and naphthalene (**II.17, II.48**) derivatives. Reagents and conditions: a) 1. TBTU, DIPEA, DCM, rt, 15 min; 2. Amine, DCM, rt, o/n.

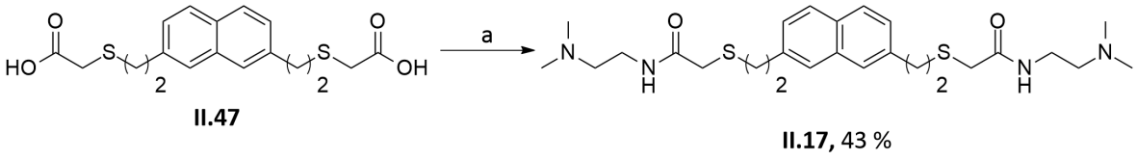

Scheme II.12. Synthesis of naphthalene derivative **II.17**. Reagents and conditions: a) 1. TBTU, DIPEA, DCM, rt, 15 min; 2. Amine, DCM, rt, o/n.

2.2. Synthesis of ligands based on the 2,7-biphenyl naphthalene core

2.2.1. Retrosynthetic analysis

Although the compounds belonging to this series share the naphtalene core, they presented differences in the synthetic approach. In a retrosynthetic analysis is possible to observe that the desired compounds were obtained by a two-step route that only share the first step (Scheme II.13). The first step was the formation of a new C-C bond between naphtalene and the other aromatic ring via Suzuki-Miyaura cross-coupling reaction. In the following step, nucleophilic substitution or Chan-Lam coupling reaction were employed in order to obtain the final compounds.

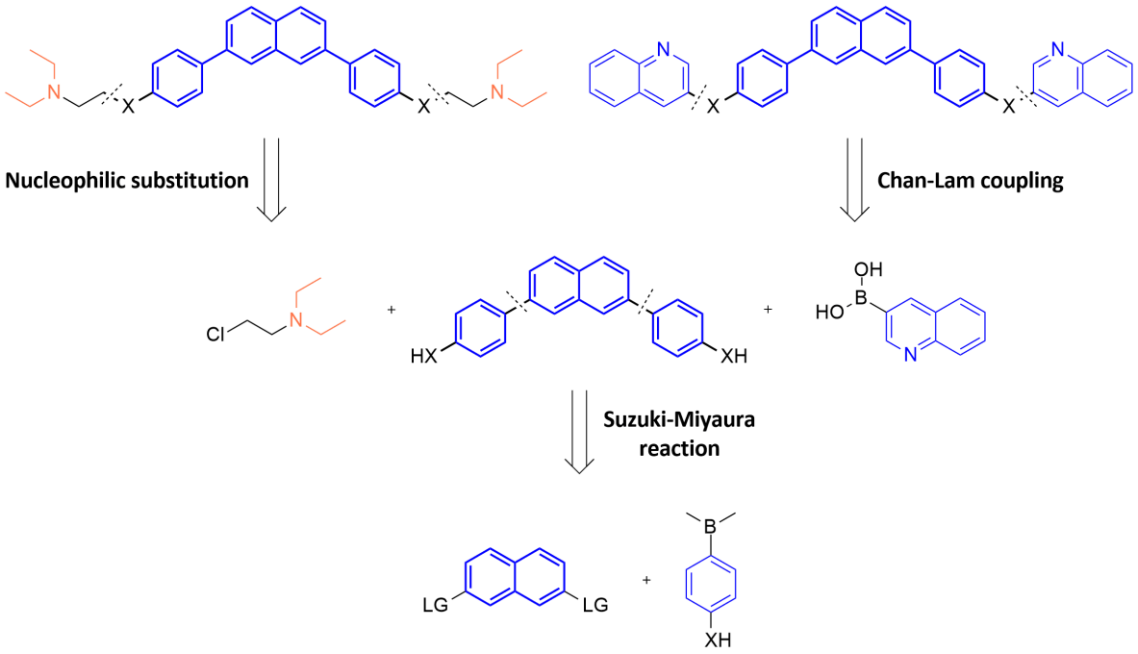

Scheme II.13. Proposed synthetic pathway for the synthesis of 2,7-biphenyl naphthalene derivatives. (X: S or O; LG: leaving group; in blue the aromatic core; in orange the basic group of side chains)

In Chan-Lam coupling reaction, the aryl carbon-heteroatom bond formation occurs via an oxidative coupling of boronic acids, stannanes or siloxanes (Ar^1-Y) with NH or OH (Ar-X) containing compounds in air. The proposed general mechanism for this coupling reaction (Scheme II.14) shows that Ar^1-Y initially undergoes transmetalation (a.) to generate an intermediate, which then coordinates with Ar-X (b.). In the presence of atmospheric oxygen or another primary oxidant, complex previously formed undergoes oxidation (c.), forming a Cu(III) intermediate, which undergoes reductive elimination (d.), yielding the coupling product and a Cu(I) complex. The latter can be reconverted into bis-μ-hydroxo Cu(II) complex in the presence of dioxygen and water (e.).[483]

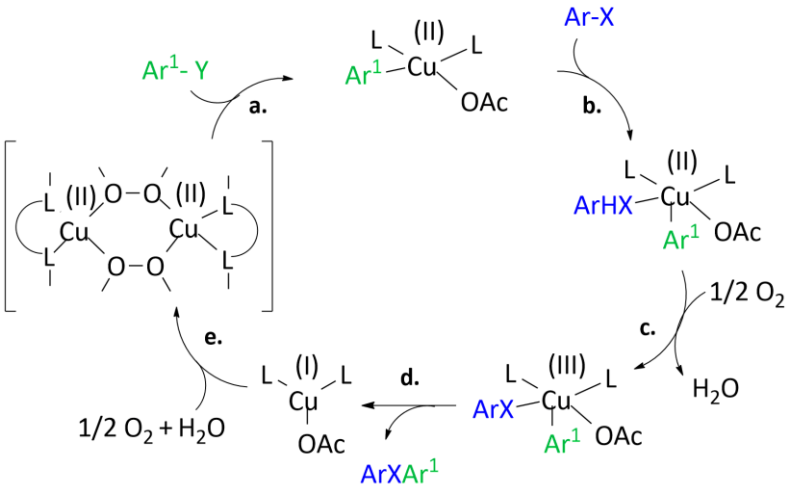

Scheme II.14. Mechanisms of Chan-Lam coupling: a. transmetalation, b. coordination, c. oxidation, d. reductive elimination, and e. complexation.

2.2.2. Synthesis discussion

Similarly to the synthesis of the compounds described in section 2.1.2., the first synthetic step of all compounds comprising four aromatic rings as aromatic core was the formation of a new C-C bond through a palladium-catalyzed cross-coupling reactions.

As demonstrated in Table II.2, the synthesis of compound **II.49** was attempted starting from (4-mercaptophenyl)boronic acid **II.50** using different reaction conditions. However, the desired product was never obtained.

Table II.2. Reaction conditions tried to synthesise compound **II.49.**

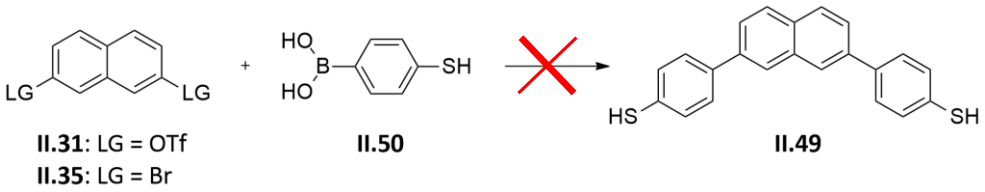

II.31: LG = OTf
II.35: LG = Br

II.50

II.49

Entry	Substrate	Pd catalyst	Base	Reaction conditions
1	**II.31**	$Pd(PPh_3)_4$	$K_3PO_4 \cdot H_2O$	Dioxane, reflux, 16 h
2	**II.35**	$Pd(PPh_3)_4$	Cs_2CO_3	DME/EtOH/H_2O, 150 °C, 150 W, 15 min
3	**II.35**	$Pd(PPh_3)_2Cl_2$	Na_2CO_3 1M	Dioxane, 80 °C, 14 h
4	**II.35**	$Pd(PPh_3)_4$	Na_2CO_3 1M	Toluene/H_2O, 100 °C, 50 min

In contrast, the synthesis of compound **II.51**, starting from (4-hydroxyphenyl)boronic acid **II.52** was straightforward and the compound was obtained in very good yield (85%, Scheme II.15).

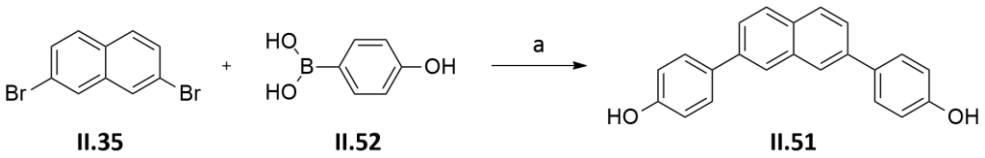

II.35

II.52

II.51

Scheme II.15. Synthesis of compound **II.51**. Reagents and conditions: a) $Pd(PPh_3)_2Cl_2$, Na_2CO_3 1M, dioxane, 80 °C, o/n, 85%.

Finally, the synthesis of final compound **II.19** occurred via nucleophile substitution (Scheme II.16), in which an sp^3-hybridized electrophile must have a leaving group in order to the reaction occur. On the other hand, the synthesis of final compound **II.20**, occurred via a Chan-Lam coupling (Scheme II.16) using 3-quinolineboronic acid pinacol ester.

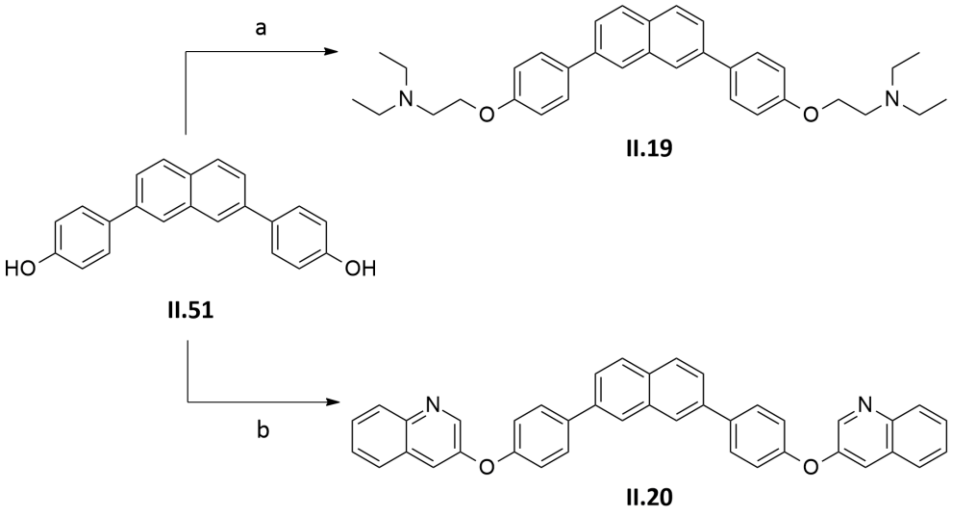

Scheme II.16. Synthesis of compounds **II.19** and **II.20.** Reagents and conditions: a) $Cl(CH_2)_2N(CH_2CH_3)_2$, K_2CO_3, acetone, reflux, o/n, 22%; b) 3-quinolineboronic acid pinacol ester, $Cu(OAc)_2$, pyridine, molecular sieves 3 Å, DCM, rt, o/n, 12%.

2.3. Antiproliferative activity and Structure-Activity Relationship

Short-term antiproliferative assays were carried out using a panel of human cancer cell lines and IC_{50} values were determined using cisplatin as control (Table II.3). The human cancer cell lines used were: (a) breast adenocarcinoma cell line (MCF-7) that has wild-type *K-RAS* and is a telomerase-positive cell lines;[484,485] (b) colorectal adenocarcinoma cell line (HT-29) that has wild-type *k-RAS* and is a telomerase-positive cell lines;[226,486] (c) non-small cell lung carcinoma cell line (NCI-H460) that has a mutated *k-RAS* and is a telomerase-positive cell lines.[487]

Cytotoxicity assays were carried out using a non-malignant human skin fibroblast cell line (CRL-1502) and colorectal adenocarcinoma cell line (CaCo-2). Despite CaCo-2 being a cancer cell line is a well-accepted model to characterize the safety profile of compounds.[488]

Table II.3. Short-term antiproliferative activity evaluated with a panel of malignant and nonmalignant cell lines.

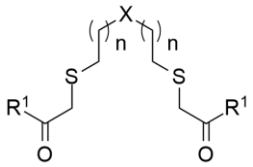

II.16-II.18

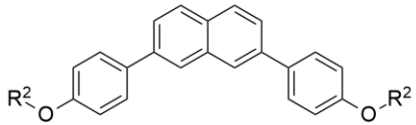

II.19-II.20

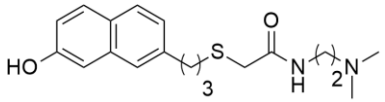

II.48

					IC_{50}(μM)[a]						
	X	**n**	**R^1**	**R^2**	**MCF-7**	**HT-29**	**NCI-H460**	**CRL-1502**	**CaCo-2**	**cLogP[c]**	**MW**
II.16a	Ben.	2	$NH(CH_2)_2N(CH_3)_2$	-	> 15	6.82 ± 0.33	> 15	> 20	> 20	2.63	482.76
II.16b	Ben.	2	*N*-MePpz	-	>20	> 20	> 20	ND[b]	> 20	2.98	346.50
II.17	Naph.	1	$NH(CH_2)_2N(CH_3)_2$	-	>20	5.39 ± 1.27	>20	ND[b]	> 20	2.78	504.77
II.18a	Naph.	2	$NH(CH_2)_2N(CH_3)_2$	-	5.15 ± 1.44	2.09 ± 0.50	4.97 ± 1.39	6.09 ± 1.30	> 20	3.81	532.82
II.18b	Naph.	2	$NH(CH_2)_2N(CH_2CH_3)_2$	-	4.13 ± 0.45	1.35 ± 0.32	3.28 ± 0.29	9.00 ± 5.48	> 20	5.32	588.93
II.18c	Naph.	2	$NH(CH_2)_3N(CH_2CH_3)_2$	-	13.2 ± 3.32	2.27± 0.10	6.95 ± 0.30	4.73 ± 3.57	> 20	5.86	616.98
II.18d	Naph.	2	*N*-MePpz	-	8.45 ± 2.51	2.04 ± 0.75	3.68 ± 0.81	> 20	> 20	4.03	556.84
II.18e	Naph.	2	$NH(CH_2)_2$*N*-Mor	-	> 20	≥ 20	> 20	ND[b]	> 20	3.51	616.89
II.19	-	-	-	$(CH_2)_2N(CH_2CH_3)_2$	2.25 ± 1.69	1.01 ± 0.57	1.44 ± 0.63	ND[b]	7.87 ± 0.35	8.31	510.72
II.20	-	-	-	3-quinolyl	>20	>20	>20	ND[b]	> 20	9.25	566.66
II.48	-	-	-	-	> 15	2.59 ± 0.55	9.39 ± 1.82	12.54 ± 0.40	> 20	2.98	346.50
Cisplatin	-	-	-	-	> 20	> 20	2.48 ± 1.55	ND[b]	> 20	ND[b]	ND[b]

[a] Values represent the mean ± SD for at least 3 independent experiments; [b] ND: not determined;[c] Calculated values using the software available at http://www.molinspiration.com.

The results showed that most of the compounds presented higher antiproliferative activity against HT-29 cells comparatively with the other cancer cell lines used. It is noteworthy that compounds **II.16a** and **II.17** only presented antiproliferative against this cell line. Toward both MCF-7 and HT-29 cells, compounds **II.18a**-**II.18d** and **II.19** presented lower IC_{50} values than cisplatin. However toward NCI-H460, only compound **II.19** presented better antiproliferative activity than cisplatin.

Based on the antiproliferative activity of the compounds over the three cancer cell lines, some SAR elucidation can be made (Figure II.6). Comparing the ligands based on benzene and naphthalene core, naphthalene aromatic core was preferred to benzene (**II.16a** vs. **II.18a**). The presence of two side chains proved to have a beneficial effect (**II.18a** vs. **II.48**), except in the case of HT-29 cancer cell line were the antiproliferative activity is similar for **II.18a** and **II.48**. The antiproliferative activity of compounds was also affected by the length of the chain: (a) between the aromatic ring and the sulfur atom [three carbon chain was preferred over two carbon side chain (**II.17** vs. **II.18a**)], and (b) between the two nitrogens [two carbon chain was preferred over three carbon side chain (**II.18b** vs. **II.18c**)]. The variation of the terminal amine group also showed to influence as compounds presenting dimethylamine or diethylamine (**II.18a** and **II.18b**) were the more cytotoxic while the less basic morfoline analogue **II.18e** presented the lower antiproliferative activity. Within naphthalene derivatives, it is also interesting to notice that compound **II.18d** was the only compound that presented good antiproliferative activity towards the three cancer cell lines and no cytotoxicity towards CRL-1502 and CaCo-2 in the tested concentration range.

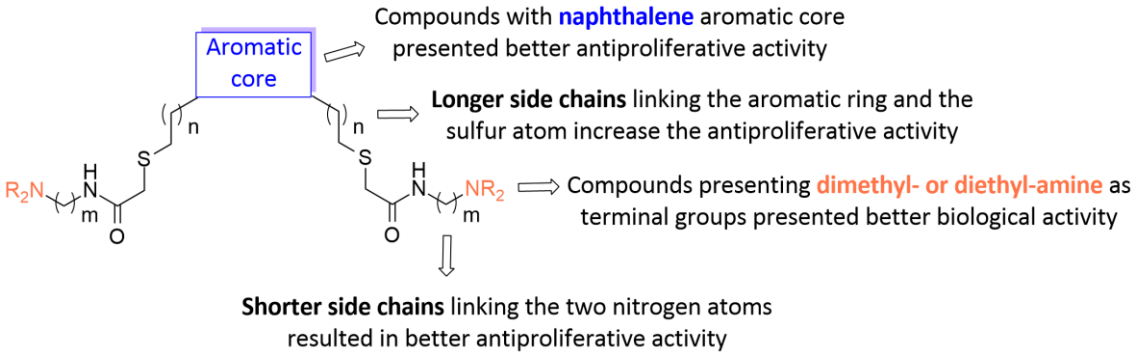

Figure II.6. SAR for benzene and naphthalene derivatives.

Within all the tested compounds, compound **II.19** with a higher aromatic surface core presented the lower IC_{50} values in the three cancer cell lines. The drawback of this compound was the cytotoxicity over CaCo-2 cell line. The substitution of the amine side chains of **II.19** for quinoline rings **II.20** resulted in lack of activity toward all the cell lines tested.

2.4. Investigation of the Mechanism of Action

2.4.1. Compounds as G4 ligands

The ability of the synthesised compounds to bind and stabilise G4 DNA and dsDNA was investigated using a FRET melting assay, with ligand concentrations ranging from 0.1 to 5 μM. Three different DNA sequences were used (a) 26-mer double-stranded hairpin loop sequence (T-loop) representing dsDNA (Table II.4); (b) 21-mer DNA G4 from region in human *k-RAS* oncogene promoter (KRas21R) (Table II.5); (c) 21-mer DNA G4 from the human telomeric sequence (F21T) (Table II.6).

The analysis of FRET melting data revealed that only compound **II.19** showed a weak stabilization of DNA sequences tested.

The poor stabilizing ability of the synthesised compounds can be explained by (a) the small aromatic surface of the naphthalene (which is smaller than the G-quartet), and (b) the flexibility of the structure. Analysing the ligands presented in Figures II.1 and II.2, it is possible to realize that the ligands with higher stabilizing ability presented a "bent" shape where the benzene or naphthalene is flanked by at least one aromatic ring increasing the aromatic surface for π-π interactions and the rigidity of the structure. The better G4 stabilizing ability presented by the compound with the bigger aromatic surface (**II.19**) is in agreement with the previously stated**.** However, it also important to notice that the majority of the compounds also presented modest G4 stabilizing ability. In fact, the more successful G4 ligands incorporating naphthalene described in literature are naphthalimido and naphthalene diimides that presented a bigger aromatic surface.[213,214,217]

Table II.4. FRET-melting temperature variations (ΔT_m[a]) of T-loop at 0.2 µM, stabilized by different derivatives in K^+ cacodylate buffer (pH 7.4, 60 mM K^+). Values represent the mean ± SD for a triplicated experience.

	[Ligand]/ µM						
	0.1	**0.5**	**1**	**2**	**3**	**4**	**5**
II.18a	0.77 ± 0.16	1.00 ± 0.19	0.75 ± 0.17	0.79 ± 0.19	0.95 ± 0.18	1.23 ± 0.18	1.08 ± 0.17
II.18b	0.40 ± 0.17	0.09 ± 0.19	0.14 ± 0.17	- 0.09 ± 0.18	- 0.06 ± 0.17	- 0.11 ± 0.18	- 0.13 ± 0.17
II.18c	0.02 ± 0.19	- 0.28 ± 0.21	- 0.47 ± 0.27	- 0.70 ± 0.22	- 0.97 ± 0.22	- 0.84 ± 0.29	- 0.95 ± 0.25
II.18d	- 0.74 ± 0.63	0.05 ± 0.64	- 0.41 ± 0.71	- 0.49 ± 0.19	- 0.59 ± 0.21	- 0.65 ± 0.20	- 0.62 ± 0.28
II.18e	0.02 ± 0.17	- 0.13 ± 0.19	- 0.14 ± 0.17	- 0.40 ± 0.18	- 0.61 ± 0.17	- 0.51 ± 0.17	- 0.54 ± 0.19
II.19	- 0.59 ± 0.18	0.04 ± 0.21	0.27 ± 0.22	0.88 ± 0.19	2.04 ± 0.19	4.04 ± 0.17	6.25 ± 0.17
II.48	0.45 ± 0.20	0.53 ± 0.21	0.33 ± 0.19	0.52 ± 0.20	0.26 ± 0.21	0.40 ± 0.19	0.50 ± 0.20

Table II.5. FRET ΔT_m[a] of KRas21R at 0.2 µM, stabilized by different derivatives in K^+ cacodylate buffer (pH 7.4, 60 mM K^+). Values represent the mean ± SD for a triplicated eperience.

	[Ligand]/ µM						
	0.1	**0.5**	**1**	**2**	**3**	**4**	**5**
II.18a	0.68 ± 0.24	0.82 ± 0.32	0.83 ± 0.23	0.85 ± 0.23	1.04 ± 0.25	1.81 ± 0.23	1.79 ± 0.23
II.18b	0.22 ± 0.27	0.84 ± 0.27	- 0.14 ± 0.25	- 0.01 ± 0.25	0.00 ± 0.25	0.75 ± 0.26	0.91 ± 0.24
II.18c	- 0.51 ± 0.25	- 0.36 ± 0.25	- 0.52 ± 0.24	- 0.70 ± 0.25	0.47 ± 0.23	0.23 ± 0.23	0.07 ± 0.23
II.18d	- 0.77 ± 0.25	- 0.84 ± 0.25	- 0.93 ± 0.25	- 1.06 ± 0.25	- 1.04 ± 0.25	- 0.93 ± 0.26	- 0.03 ± 0.30
II.18e	0.03 ± 0.25	- 0.03 ± 0.26	- 0.75 ± 0.25	- 0.94 ± 0.24	- 0.85 ± 0.25	- 0.84 ± 0.25	- 0.12 ± 0.25
II.19	- 0.16 ± 0.33	- 1.14 ± 0.34	- 0.11 ± 0.34	0.98 ± 0.35	1.94 ± 0.36	2.03 ± 0.35	4.06 ± 0.35
II.48	0.03 ± 0.28	0.78 ± 0.27	0.34 ± 0.28	0.16 ± 0.27	0.11± 0.30	0.81 ± 0.25	0.85 ± 0.25

Table II.6. FRET ΔT_m[a] of F21T at 0.2 µM, stabilized by different derivatives in K^+ cacodylate buffer (pH 7.4, 60 mM K^+). Values represent the mean ± SD for a triplicated experience.

	[Ligand]/ µM						
	0.1	**0.5**	**1**	**2**	**3**	**4**	**5**
II.18a	1.87 ± 0.27	2.05 ± 0.29	1.36 ± 0.27	2.22 ± 0.25	2.79 ± 0.26	2.89 ± 0.27	2.87± 0.29
II.18b	- 0.33 ± 0.24	0.44 ± 0.24	- 0.19 ± 0.22	- 0.46 ± 0.22	- 0.57 ± 0.22	- 0.99 ± 0.27	-1.22 ± 0.23
II.18c	- 0.13 ± 0.21	- 0.41 ± 0.24	- 0.98 ± 0.22	- 0.99 ± 0.22	- 1.11 ± 0.22	- 1.04 ± 0.21	0.60 ± 0.24
II.18e	- 0.08 ± 0.26	- 0.24 ± 0.27	- 0.13 ± 0.25	- 0.21 ± 0.24	- 0.20 ± 0.25	- 0.13 ± 0.26	- 0.12± 0.30
II.19	- 0.01 ± 0.40	- 1.05 ± 0.45	- 1.01 ± 0.39	1.08 ± 0.40	0.95 ± 0.37	0.08 ± 0.52	2.17 ± 0.43
II.48	- 0.25 ± 0.21	- 0.24 ± 0.22	- 0.13 ± 0.22	- 0.29 ± 0.21	- 0.38± 0.20	- 0.53 ± 0.21	- 0.22 ± 0.23

2.4.2. Apoptosis

It is well established that chemotherapeutic agents act by triggering mechanisms of cell death by apoptosis. In this context, apoptosis induction was assessed by flow cytometry analysis using the Guava Nexin assay. As illustrated in Figure II.7, exposure of HT-29 cells to compounds **II.18a**, **II.18b** and **II.19** at the IC_{50} concentration, for 48 h, resulted in a significant increase of apoptosis levels ($p<0.05$). In particular, compound **II.19** at IC_{50} concentration was able to increase apoptosis up to 50%, as compared to vehicle control exposure ($p<0.005$). When cells were exposed to the same compounds at 2-fold IC_{50} concentration, the percentage of cells undergoing apoptosis further increased, especially for compound **II.19**. Taken together, these results suggest that induction of apoptosis is an important mechanism underlying compounds effects.

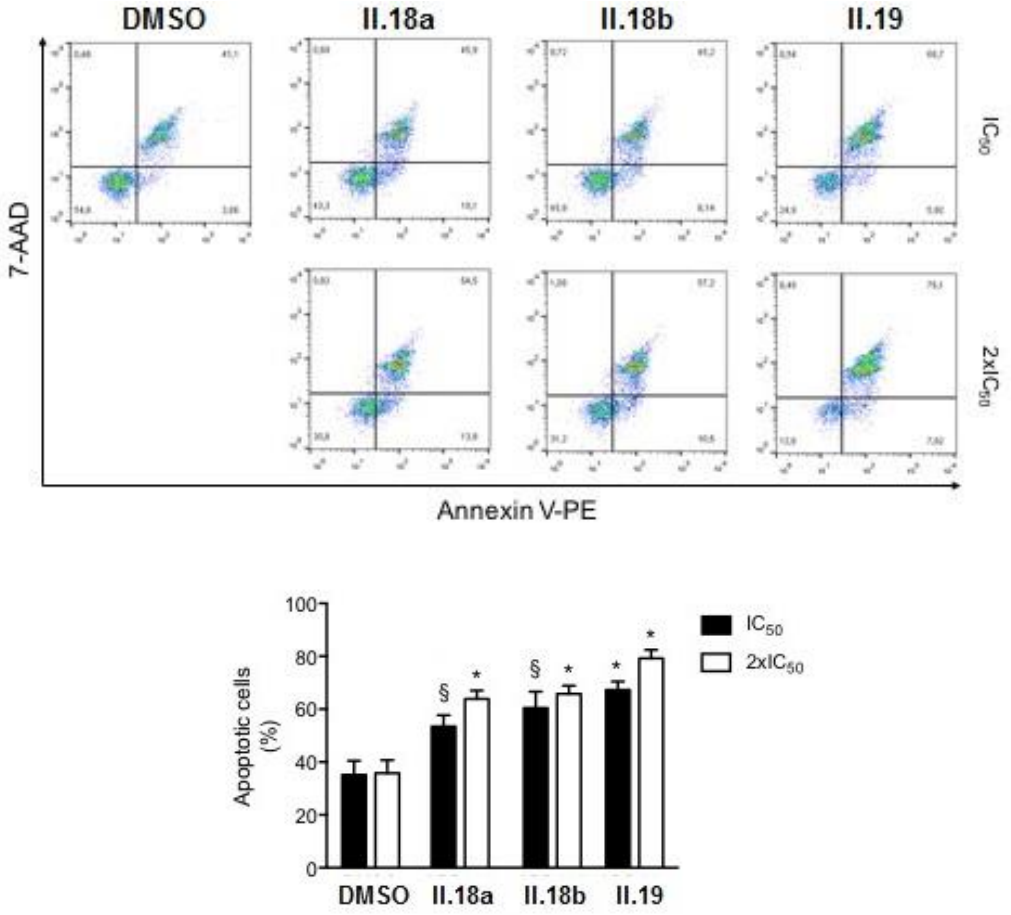

Figure II.7. Apoptosis induction of HT-29 cells (measured by flow cytometry analysis) after exposure to **II.18a**, **II.18b** and **II.19** at the IC_{50} and 2-fold IC_{50} concentrations, for 48 h. DMSO was used as vehicle control. Results are expressed as percentage of apoptotic cells ± SEM, from at least 3 independent experiments. §$p < 0.05$ and *$p < 0.005$ from respective DMSO treatment.

3. Conclusion

A library of eleven novel simetric compounds presenting three different aromatic cores (benzene, nafthalene and 2,7-biphenyl naphthalene) flanked by side chains with heteroatoms and amine terminal groups were synthesised with moderate to good yields. Based on the antiproliferative activity of the compounds and on the cytotoxicy assays results, some SAR elucidation was made. Among the synthesised compounds, four naphthalene based derivatives (**II.18a-II.18d**) and one 2,7-biphenyl naphthalene derivative (**II.19**) stood out by the their interesting antiproliferative activities over three cancer cell lines, specially against HT-29 where the five compounds presented lower IC_{50} values than cisplatin. Within the four naphthalene based derivatives, it is also interesting to notice that despite compound **II.18d** not presenting the lower IC_{50} values, it was the only compound that presented good antiproliferative activity towards the three cancer cell lines and no citotocixicity towards CRL-1502 and CaCo-2 in the tested concentration range. Within all the tested compounds, compound **II.19** with a higher aromatic surface core presented the lowest IC_{50} values in the three cancer cell lines. The drawback of this compound was its citotoxicity over CaCo-2 cell line. These good results have encourage the search for the mechanism of action of these molecules. As they were inicially designed to act as G4 ligands, a FRET-melting assay was carried out. However, the antiproliferative activity did not seem to result from its action as G4 ligands since the compounds tested only presented a minor effect on G4 stabilization. Their poor action as G4 stabilizers can be explained by the small aromatic surface of these compounds (compared to the G-quartet) and by the flexibility of the compounds. In order to obtain better and more selective G4 stabilizers, molecules with bigger aromatic surface or with a higher electronic density in the aromatic rings should be synthesised. Based on the antiproliferative activity of the compounds, **II.18a**, **II.18b** and **II.19** were choosen to assess apoptosis induction. In agreement with the lower IC_{50} values of compound **II.19** toward HT-29 cell line, this compound presented particularly interesting results as at IC_{50} concentration it was able to increase apoptosis up to 50%, as compared to vehicle control exposure. When cells were exposed to the same compounds at 2-fold IC_{50} concentration, the percentage of cells undergoing apoptosis further increased. Taken together, these results suggest that induction of apoptosis is an important mechanism underlying compounds antiproliferaive effects.

CHAPTER III

III. SYNTHESIS AND BIOLOGICAL EVALUATION OF POLYAROMATIC FUSED COMPOUNDS AS G4 LIGANDS

1. Introduction

Despite the variety of polyaromatic fused scaffolds present in compounds evaluated as G4 ligands, benzo[*h*][1,6]naphthyridin-2(1*H*)-one scaffold (a tricyclic aromatic scaffold) was never been used for this purpose. As illustrated in Figure III.1., this tricyclic scaffold is the core structure in Torin1 (**III.1a**) and Torin2 (**IIII.1b**), a selective ATP-competitive mammalian target of rapamycin (mTOR) kinase inhibitor.[489,490] More recently, our group demonstrated that these compounds are extremely potent antimalarial drugs. Torin2 has single-digit nanomolar potency in both liver and blood stages of infection *in vitro* and is likewise effective against both stages *in vivo*, with a single oral dose sufficient to clear liver stage infection Parasite elimination and perturbed trafficking of liver stage parasitophorous vacuole membrane-resident proteins are both specific aspects of Torin-mediated *Plasmodium* liver stage inhibition, indicating that Torins have a distinct mode of action compared with currently used antimalarials.[491]

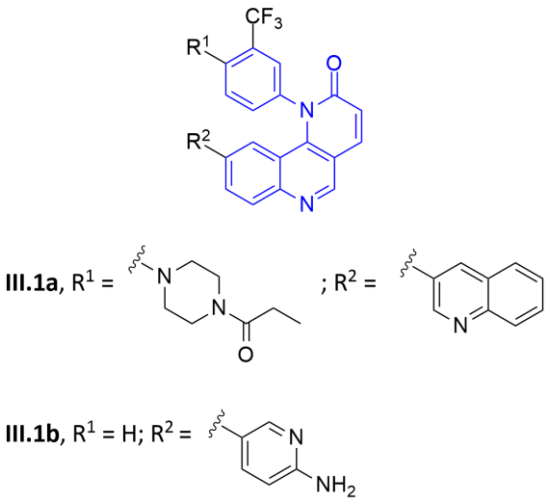

Figure III.1. Torin1 (**III.1a**) and Torin2 (**III.1b**).

The benzo[*h*][1,6]naphthyridin-2(1*H*)-one scaffold, chosen due to its extended aromatic core scaffold and thus potential to establish interactions through π-π stacking. In order to explore the importance of this aromatic core as G4 ligand, this chapter will focus on the synthesis and evaluation of the G4 stabilizing ability of a library of compounds (Figure III.2) with either aromatic (**III.2**) or aliphatic (**III.3** and **III.4**) amine

side chains with different lengths. Besides that, the effect of a cationic center on the aromatic core (**III.4**), which would interact with the negative electrostatic center of the G4 by electrostatic interaction, was also studied.

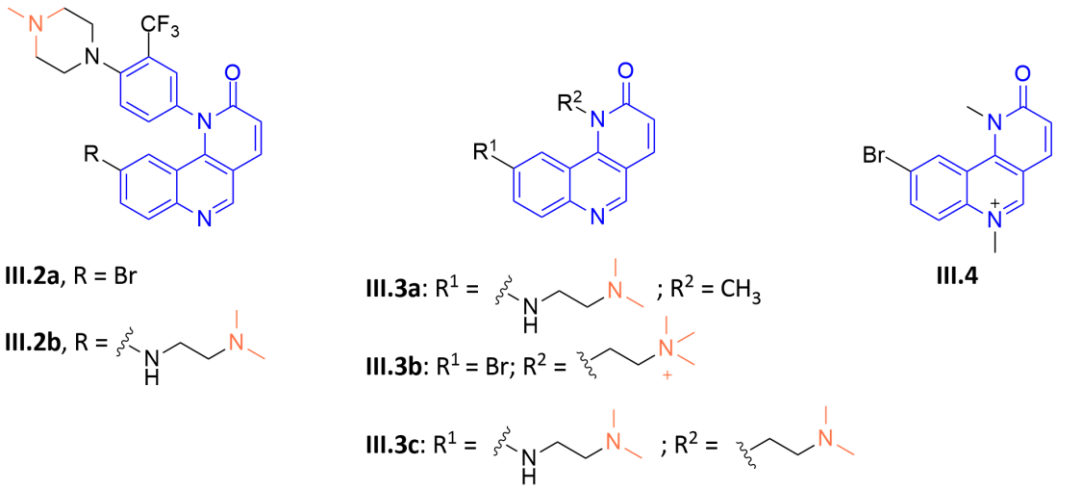

Figure III.2. Library of Torin-based compounds synthesised to be tested as G4 ligands (in blue the aromatic core; in orange the basic group of of side chains).

2. Methods, Results and Discussion

2.1. Retrosynthetic analysis

The compounds of this series were obtained according the proposed synthetic pathway illustrated in Scheme III.1.

These compounds share an aromatic core that was accomplished through a Gould-Jacobs quinoline synthesis and subsequent chlorination of the 4-hydroxyquinoline. The Gould-Jacobs quinoline synthesis (Scheme III.2) involved: (a) the condensation of aniline **III.5** with diethyl(2-ethoxymethylene)malonate **III.6** to afford an enamine **II.7**, and (b) the intramolecular cyclization to quinolin-4-one nucleus **III.8**.[492]

In contrast with the synthesis of **III.3** and **III.4** (which used commercially available amines), synthesis of **III.2** started with a three-reaction sequence to obtain the aromatic side arm. The fluorine was first substituted by nucleophilic aromatic displacement with piperazine to give the corresponding substituted product. This reaction took place by a two-step reaction: in the first step, the nucleophile (in this case an amine group) attacked the carbon bearing the leaving group forming a carbanion intermediate (addition); in the second step of the reaction, the leaving group departed, reestablishing

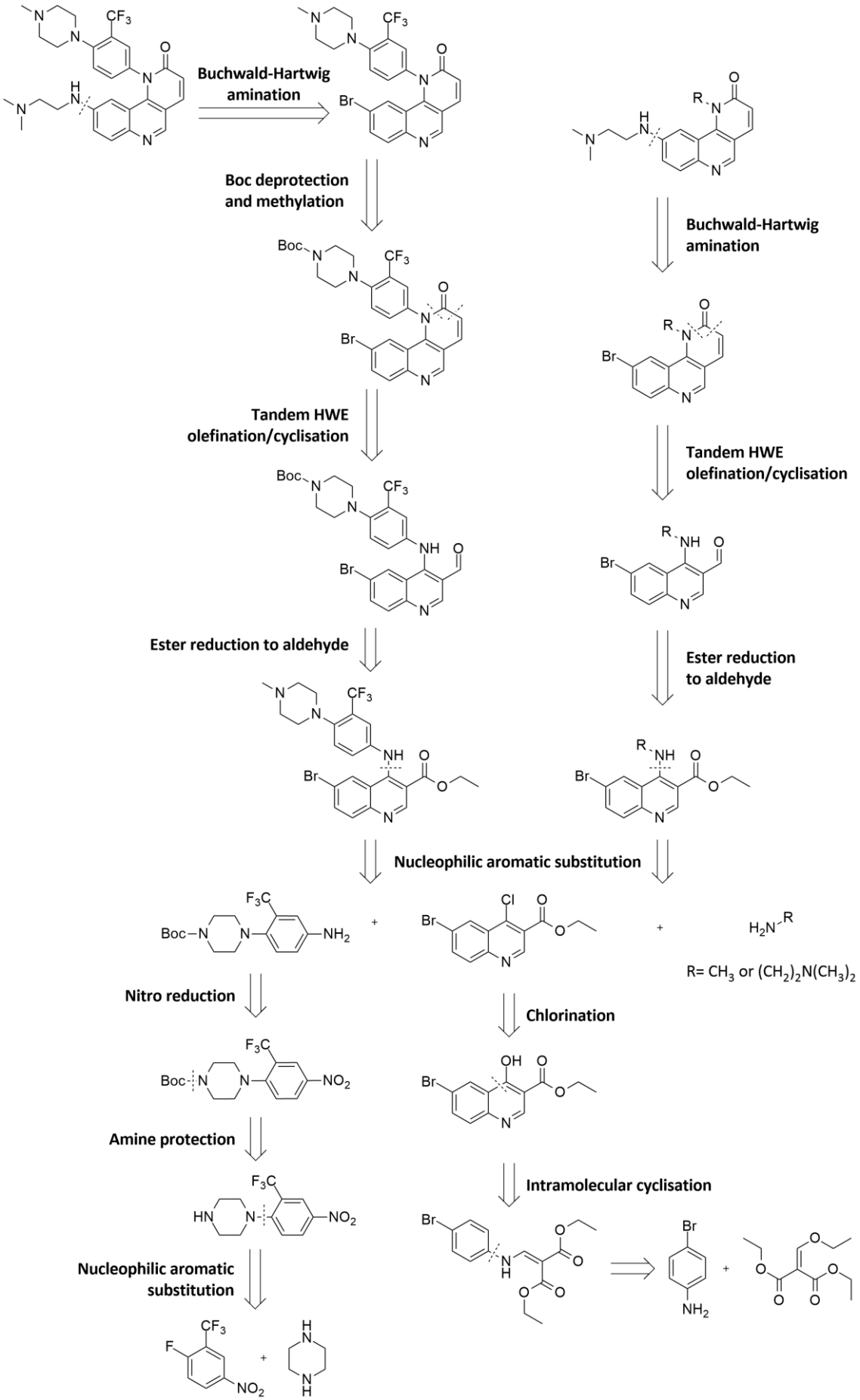

Scheme III.1. Proposed synthetic pathway for the synthesis of Torin-based compounds.

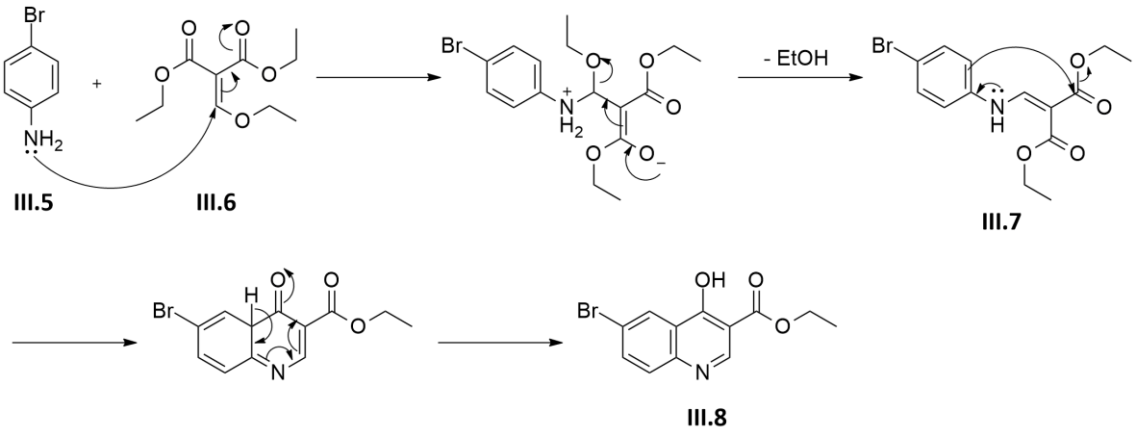

Scheme III.2. Mechanism of Gould-Jacobs quinoline synthesis.

the aromaticity of the ring (elimination). Although being a poorer leaving group than chloride or bromide, fluorine reacts faster than them in nucleophilic aromatic substitution because it accelerates the rate-determining step (addition) by its large inductive effect. Being the most electronegative element in the periodic table, it stabilizes the anionic intermediate, assisting the acceptance of electrons by the benzene ring. The presence of two electron-withdrawing groups in *ortho* and *para* to the halogen also contribute to this reaction by activating the benzene ring.[493] Subsequently, the amine group was protected with Boc group, which was choosen due to its stablility to bases and nucleophiles as well as to catalytic hydrogenation.[494] In the last step, the nitro functional group was reduced by catalytic hydrogenation to give the corresponding aniline.

The synthesis of both **III.2**, **III.3** and **III.4** proceeded with a nucleophilic aromatic substitution at C-4 of the quinoline ring **III.9** with an aniline or amine, respectively (Scheme III.3). In this case, the carbanion intermediate was stabilized by resonance. The reaction took place in the desired position mainly because the most stable intermediate is formed since resonance contributor obtained has the greatest electron density on nitrogen. In addition, the ester group in *ortho* position to the halogen also have a contribution to the reaction.[493]

Reduction of the ester to aldehyde needs to be performed before proceed to the Tandem Horner-Wadsworth-Emmons (HWE) olefination/cyclisation. However, this is a real problem in synthetic chemistry inasmuch as the aldehydes are more readily reduced than the ester, the reduction carries on to the alcohol oxidation level. In order to try to solve this situation, there are two options: (a) use selective reduction reagentes (e.g. DIBAL) or (b) reduce the compound to alcohol, and oxidize the alcohol back to the aldehyde.[495]

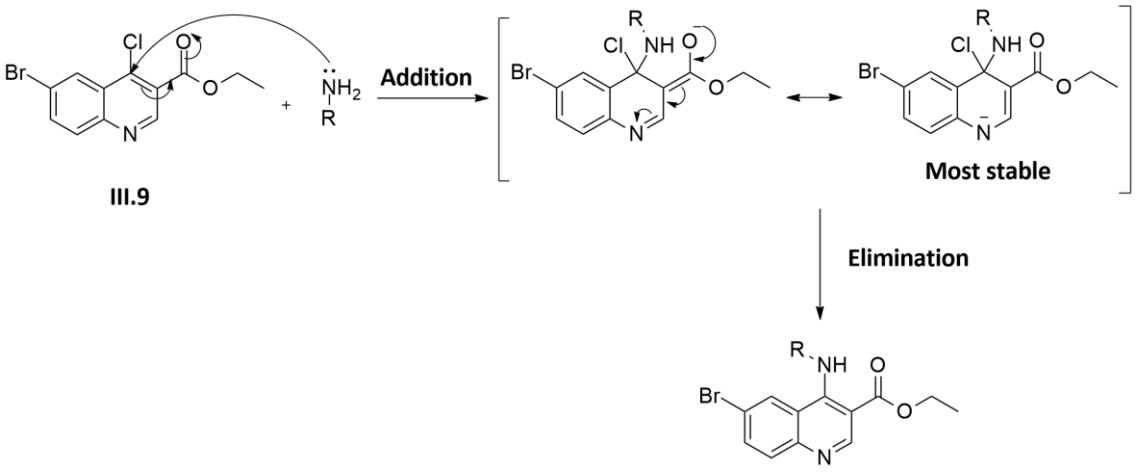

Scheme III.3. Mechanism of nucleophilic aromatic substitution.

DIBAL can perform the oxidation of esters to aldehydes in a single step. It exists as a bridged dimer and it becomes a reducing agent only after it has formed a Lewis acid–base complex. DIBAL reduces esters even at – 70 °C, and at this temperature the tetrahedral intermediate may be stable. Only in the aqueous work-up does it collapse to the aldehyde when excess DIBAL has been destroyed so that no further reduction is possible.[495]

Ester reduction to primary alcohol followed by its oxidation is the other alternative. To reduce the ester, different nucleophilic reducing agents, such as: lithium aluminum hydride ($LiAlH_4$), sodium borohydride ($NaBH_4$) or lithium borohydride ($LiBH_4$), can be employed.[496]

The alcohol oxidation can be done using different approaches. The most commonly used methods for oxidizing alcohols are based around metals in high oxidation states, often chromium (VI) or manganese(VII), which mechanistically are quite similar because both rely on the formation of a bond between the hydroxyl group and the metal. Due to the toxicity associated with the use of these heavy metals, new methodologies for the oxidation of alcohols to aldehydes have been developed. An important modern reagent (discovered in 1983) is known as the Dess–Martin periodinane (DMP). This reagent has several advantages over Cr(VI)-based oxidizing reagents, including: relative easy preparation, near 1 to 1 stoichiometry, shorter reaction times, simplified workups, and lower toxicity.[495,496]

The tandem HWE olefination/cyclisation was used to obtain the tricyclic core scaffold. The HWE olefination (Scheme III.4) consists in the synthesis of olefins from the condensation between carbonyl compounds (both aldehydes and ketones) and carboanions derived from phosphonates. Despite the similarity of HWE olefination reaction mechanism to the mechanism of the Wittig reaction, the former reaction conditions have obvious advantages over the original Wittig Reaction, such as: (a) the

higher nucleophilicity and the basicity of phosphonate-stablized carbanion compared to the corresponding phosphonium ylides; (b) the easy removal of dialkylphosphate salt (by-product of this reaction) by simple aqueous extraction. Although this reaction give preferencially *E*-olefins, both *Z*-olefins and *E*-olefins are possible products, and the ratio depends on the stereochemical outcome of the initial addition and the ability of the intermediate to equilibrate. For disubstituted olefins (from aldehydes), the *E*:*Z* ratio increases: (a) at higher reaction temperatures; (b) cation order of $Li^+ > Na^+ > K^+$; (c) with increasing α-substitution of the aldehyde.[497]

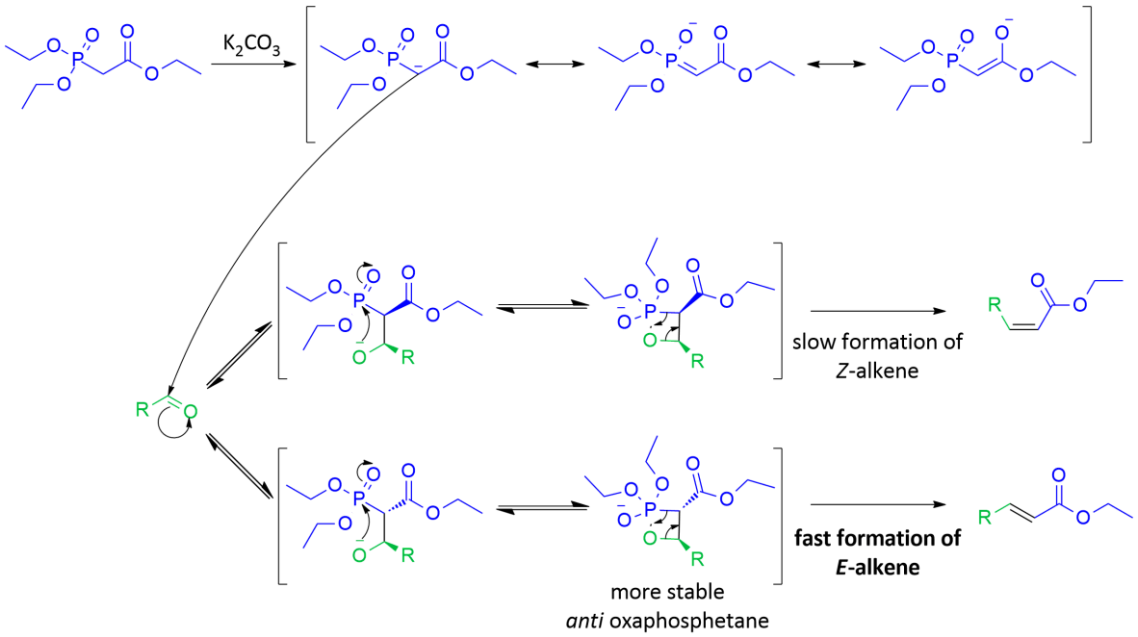

Scheme III.4. Mechanism of HWE (in green the carbonyl compounds; in blue carboanions derived from phosphonates).

The HWE olefination is followed by straightforward intramolecular *N*-acylation of the amine, proton loss, and electronic reorganisation to provide the annulated product **III.10** (Scheme III.5). It is important to refer that only the *E*-olefin is able to be converted to the annulated product.

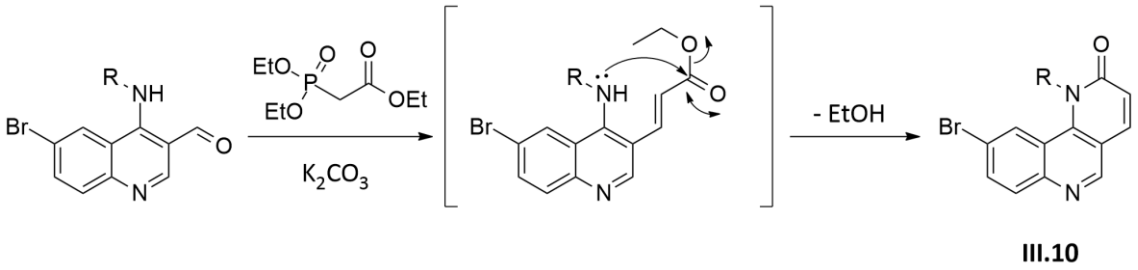

Scheme III.5. Mechanism of tandem HWE olefination/cyclisation.

As can be seen in the retrosynthetical Scheme III.1, in order to synthesise **III.2**, Boc deprotection took place followed by the amine methylation. *tert*-Butyl carbamates are cleaved under anhydrous acidic conditions with the production of *tert*-butyl cations. The most common removal conditions for Boc are 25-50% TFA in DCM, but other acids, such as 1 M trimethylsilyl chloride, phenol in DCM, and 4 M HCl in dioxane have been successfully used. Scavengers such as thiophenol and triethylsilane (TES) may prevent nucleophilic substrates from being alkylated.[494]

Amine methylation (also required of the synthesis of **III.3b** and **III.4**) can be done using different methodologies, such as: (a) nucleophilic substitution with methyl triflate; or (b) Eschweiler–Clarke reaction.[498] The latter reaction allows the preparation of tertiary methylamines from secondary amines via treatment with formaldehyde in the presence of formic acid (Scheme III.6). The formate anion acts as hydride donor to reduce the imine or iminium salt, so that the overall process is a reductive amination. The formation of quaternary amines is not possible.

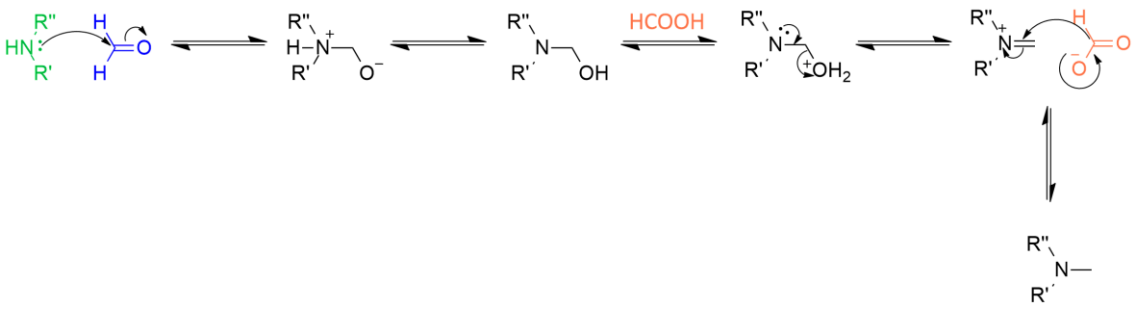

Scheme III.6. Mechanism of Eschweiler–Clarke reaction.

The preparation of **III.2b**, **III.3a** and **III.3c** required the formation of a C-N bond. Traditional methods for the synthesis of arylamines, such as nucleophilic aromatic substitution and Ullmann-type couplings, are typically conducted using relatively harsh reaction conditions and have limited generality. On the other hand, the palladium-catalyzed C-N bond formation of arylamines (Buchwald-Hartwig amination) can be

conducted under relatively mild conditions, is regioselective, and does not require activating groups.[499] In this reaction (Scheme III.7), aryl halides or pseudohalides (Ar-X) and primary or secondary amines (R_2NH) react to form an aryl amines (Ar-NR_2). It starts with the oxidative addition, in common with most palladium-catalyzed coupling mechanisms. In the next step, the amine nucleophile is coordinated to the metal and deprotonated by the base. The catalytic cycle is closed by reductive elimination, yielding the final arylated amine product while regenerating the active catalyst. As in the previous examples of cross-coupling reactions, various ligands can be used.[500]

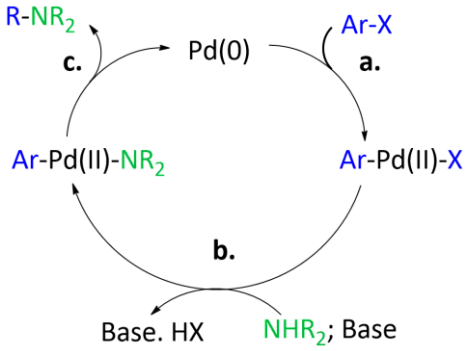

Scheme III.7. Mechanisms of Buchwald-Hartwig amination: a. Oxidative addition, b. amine binding and deprotonation, c. reductive elimination.

2.2. Synthesis discussion

2.2.1. Synthesis of starting materials **III.9** and **III.11**

The synthesis of ethyl 6-bromo-4-chloroquinoline-3-carboxylate **III.9** (Scheme III.8) was accomplish starting from the condensation of 4-bromoaniline **III.5** with malonate **III.6** to afford enamine **III.7** in excellent yield (99%). This enamine underwent a thermally induced intramolecular cyclisation in diphenyl ether to form the corresponding 4-hydroxiquinoline **III.8**, which was then reacted with phosphoryl chloride to afford **III.9** in excellent yield.

To synthesise **III.11** (Scheme III.9)**,** the fluorine of **III.12** was first substituted by nucleophilic aromatic displacement with piperazine (**III.13**) to give the corresponding substituted product **III.14** in excellent yield (95%) followed by the amine protection with Boc_2O in the presence of a catalytic amount of DMAP affording compound **III.15** in excellent yield (96%). The effect of DMAP is rationalized in terms of increasing the nucleophilicity of an intermediate *N*-Boc-DMAP complex (nucleophilic catalysis) compared with that of the anhydride. Simultaneously CO_2 gas is released driving the

reaction towards completion.[501] In the last step, the nitro functional group was reduced by catalytic hydrogenation to give the corresponding aniline **III.11**.

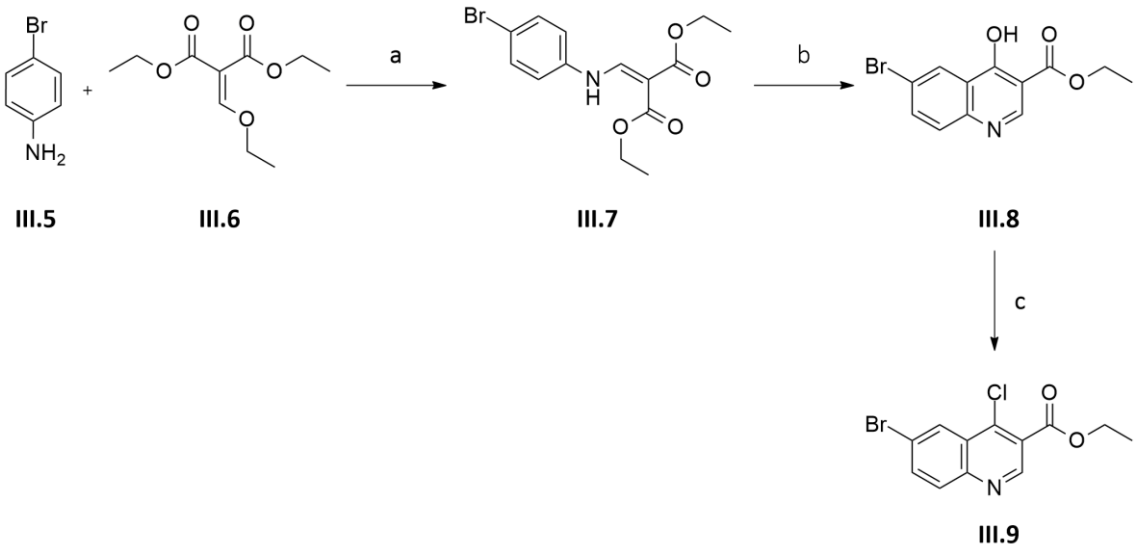

III.5 **III.6** **III.7** **III.8** **III.9**

Scheme III.8. Synthesis of compound **III.9**. Reagents and conditions: a) 115 °C, 1.5 h, 99%; b) Ph_2O, 250 °C, 2 h, 80%; c) $POCl_3$, 0 to 115 °C, 2.5 h, 100%.

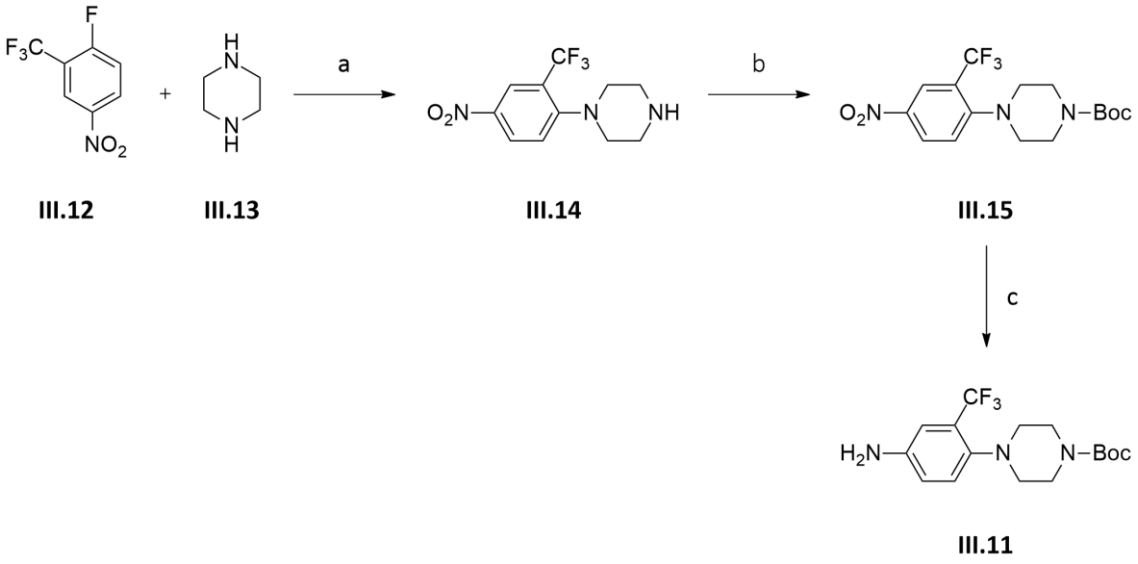

III.12 **III.13** **III.14** **III.15** **III.11**

Scheme III.9. Synthesis of compound **III.11**. Reagents and conditions: a) K_2CO_3, DMSO, 90 °C, o/n, 96%; b) Boc_2O, DMAP, rt, o/n, 94%; c) H_2, Pd/C, rt, o/n, 97%.

2.2.2. Synthesis of intermediates **III.16, III.17** and **III.18** through nucleophilic aromatic substitution

To obtain compounds **III.16**, **III.17** and **III.18** it was performed a nucleophilic aromatic substitution at the C-4 of the quinoline ring by reaction with the corresponding amines (Scheme III.10).

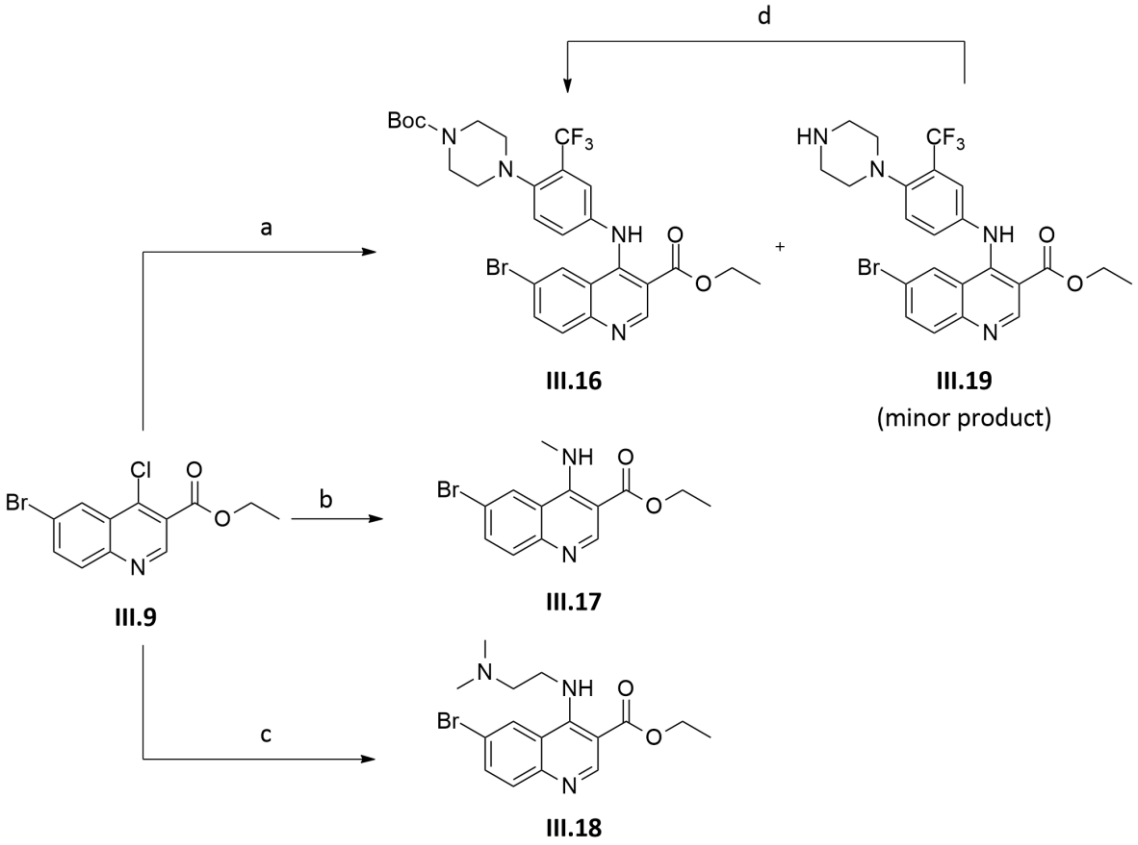

Scheme III.10. Synthesis of **III.16, III.17** and **III.18**. Reagents and conditions: a) **III.11**, dioxane, 110 °C, o/n, **III.16**: 65% and **III.19**: 17%; b) Methylamine solution 2.0 M in methanol, dioxane, 110 °C, o/n, 99%; c) *N*,*N*-dimethylethylenediamine, dioxane, 110 °C, o/n, 95%; d) Boc_2O, DMAP, rt, o/n, 75%.

In the reaction to obtain **III.16**, it occurred a partial thermal deprotection of the Boc group, originating compound **III.19** as a minor by-product (20% yield), which has been already described in literature.[502] Therefore compound **III.19** was reprotected with Boc (Scheme III.10).

2.2.3. Synthesis of intermediates **III.20, III.21** and **III.22** through ester reduction to alcohol

As oxidation of alcohol to aldehyde in the previously reported synthesis of Torin1[489,490] was not reproducible, the ester redution to alcohol was performed using $LiAlH_4$ (Scheme III.11). Since $LiAlH_4$ reacts violently with protic solvents, esters were reacted with $LiAlH_4$ in an aprotic dry solvent (THF) affording the corresponding alcohols **III.20**, **III.21** and **III.22,** in moderated to excellent yields (62-96%).

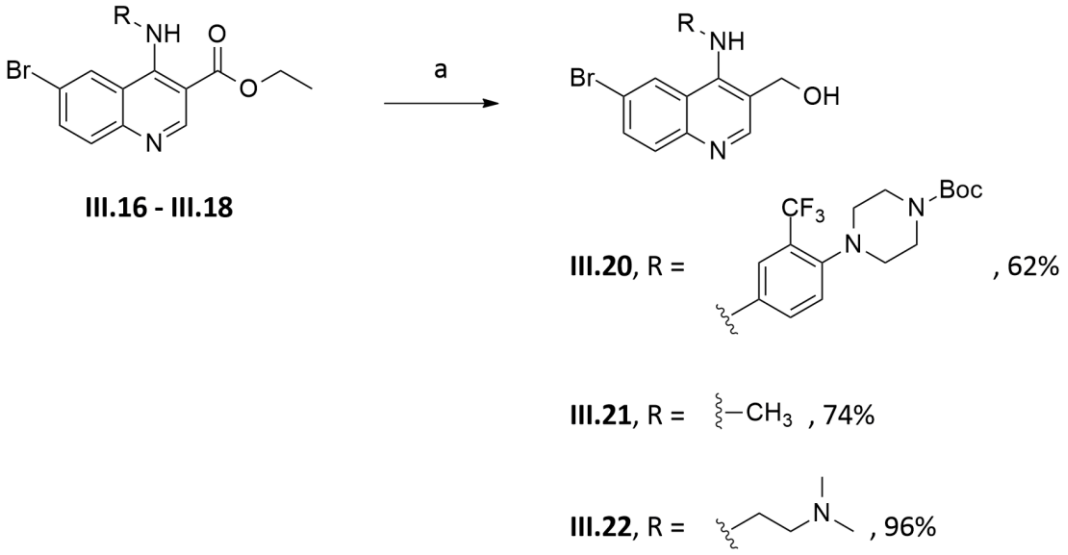

Scheme III.11. Synthesis of **III.20, III.21** and **III.22**. Reagents and conditions: a) $LiAlH_4$, THF, rt, 1 h.

2.2.4. Synthesis of compounds **III.23, III.24** and **III.25** through alcohol oxidation and tandem HWE olefination/cyclisation

The oxidation of alcohol to aldehyde in the previously reported synthesis of Torin1 have been done with MnO_2 .[489,490] MnO_2 could be advantageous if the molecule had more than an alcohol group since this oxidant is highly chemioselective (allylic, benzylic, and propargylic alcohols are oxidized faster than saturated alcohols). However, the molecules only presented an alcohol group and the oxidations with MnO_2 presentes other disadvantages such as the need of a large excess of reagent for complete conversion of the alcohol, long reaction times, and the difficulty associated with obtaining highly activated MnO_2.[496] For those reasons, *o*-iodooxybenzoic acid (IBX, **III.26**), a periodinane that is also an intermediary in DMP synthesis, was choosen as oxidizing reagents.[503] **III.26** was obtained by oxidation of 2-iodobenzoic acid (**III.27**) as displayed in Scheme III.12.

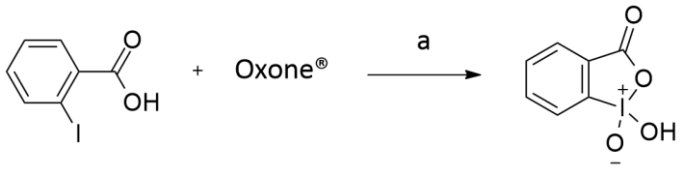

III.27 **III.26**

Scheme III.12. IBX synthesis. Reagents and conditions: a) H_2O, 70 °C (3 h) to 0 °C (1 h), 79%.

As exemplified in Scheme III.13, the oxidation of **III.20** to aldehyde **III.28** was performed with good yields. The synthesis of compounds **III.29** and **III.30** was more challenging. The oxidation of **III.21** with IBX in the previous conditions gave poor yields, however the yield improved when trifluoroacetic acid was added to the reaction. In fact, secondary amines must be temporarily protonated *in situ* with acid since the propensity for IBX to selectively act on the amine moiety to give the respective imine is truly remarkable.[504,505] Under this conditions, aldehydes **III.29** and **III.30** were obtained with excellent yields. Having the aldehydes in hand, the HWE olefination/cyclisation was tried. Starting with aldehyde **III.28**, the tandem HWE olefination/cyclisation was performed and **III.23** with good yields. Compounds **III.24** and **III.25** were obtained in low yields being the *Z*-alkenes (**III.31** and **III.32**, respectively) the other products of the reactions. Alternativelly, higher reaction temperature (150 °C) using a solvent with an higher boiling point (DMF) was tested but only degradation products were formed. In order to obtain the annulated product, isomerization and cyclisation of *E*-alkene proceeded in a basic reaction media in ethanol.

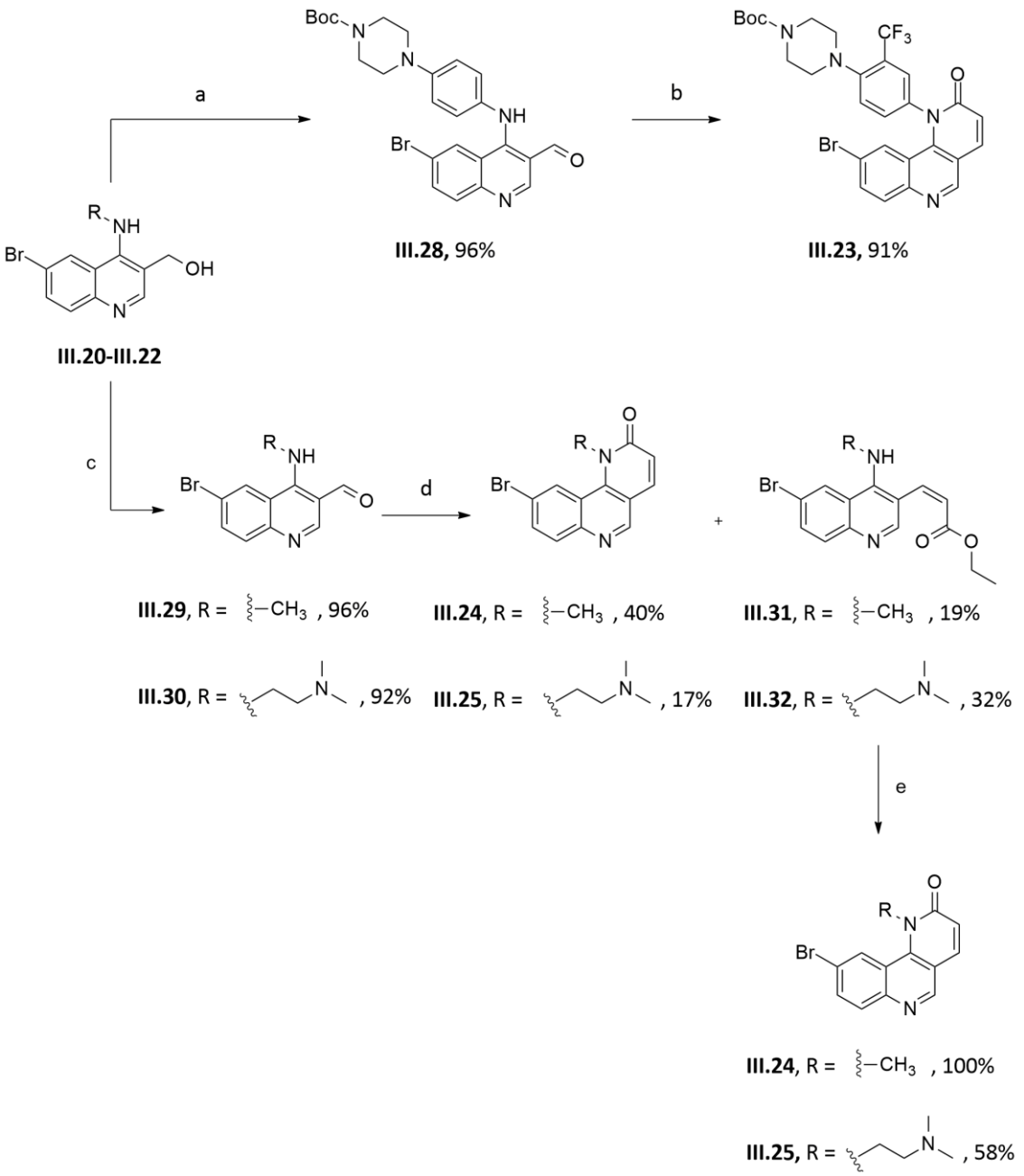

Scheme III.13. Synthesis of compounds **III.23, III.24, III.25**. Reagents and conditions: a) IBX, DMF, rt, 3 h; b) Triethyl phosphonoacetate, K_2CO_3, EtOH, 100 °C, o/n; c) IBX, TFA, DMF, rt, 3 h; d) Triethyl phosphonoacetate, K_2CO_3, EtOH, 100 °C, o/n; e) K_2CO_3, EtOH, 125 °C, o/n.

2.2.5. Synthesis of the target compounds

To synthesise **III.2a**, the Boc deprotected compound was easily obtained using TFA in DCM. This product was directly used in the Eschweiler–Clarke procedure to obtain **III.2a** (Scheme III.14).

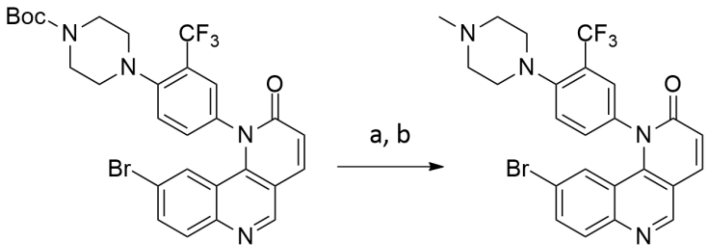

III.23 **III.2a**

Scheme III.14. Synthesis of **III.2a**. Reagents and conditions: a) TFA, DCM, rt, 3h; b) $(CH_2O)_n$, HCOOH, MeOH, reflux, 24 h, 52%.

Buchwald-Hartwig amination was employed to prepare **III.2b.** As the proper choice of catalyst (Pd source, ligand choice), base, and solvent are crucial for the success of a given amination, different conditions were tested as shown in Table III.1. The ligands tested in this synthesis were CyJohnPhos (**III.33**), (R)-Binap (**III.34**) and Xantphos (**III.35**) (Figure III.3).

Table III.1. Reaction conditions explored to obtain compound **III.2b.** Reagents and conditions: a) $NH_2CH_2CH_2N(CH_3)_2$, $Pd(OAc)_2$, toluene, 100 ^oC.

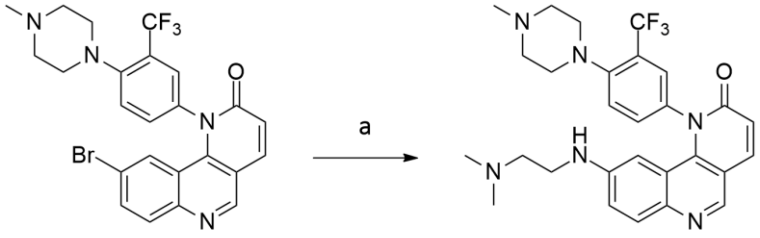

III.2a **III.2b**

Entry	Ligand	Base	Reaction time	Yield
1	**III.33**	Na^tOBu	48 h	12%
2	**III.34**	Cs_2CO_3	24 h	No reaction
3	**III.35**	K_2CO_3	24 h	35%

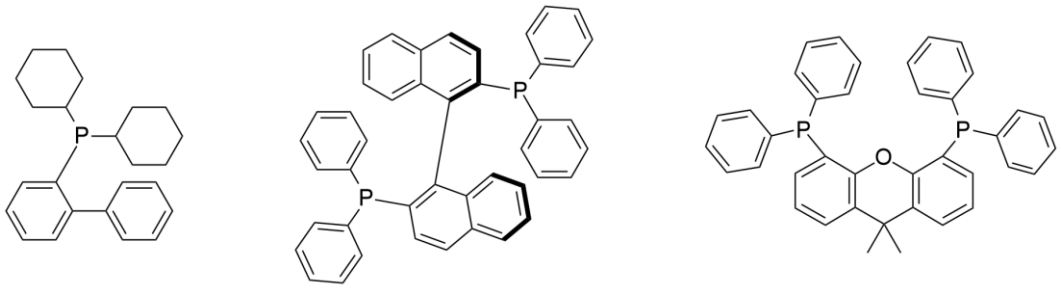

III.33 **III.34** **III.35**

Figure III.3. Ligands used in the Buchwald-Hartwig amination.

A better yield was obtained when Xantphos was used as ligand and potassium carbonate was used as base. As exemplified in Schemes III.15 and III.16, methyl trifluoromethanesulfonate was choosen as methylating agent to synthesise **III.3b** and **III.4.** While **III.3b** was obtained in very low yield, **III.4** was obtained with good yield. Buchwald-Hartwig amination was choosen to synthesise **III.3a** and **III.3c.** To obtain these compounds, solvent and temperature used in **III.2b** synthesis were changed after an unsuccessful atempt to obtain **III.3a.**

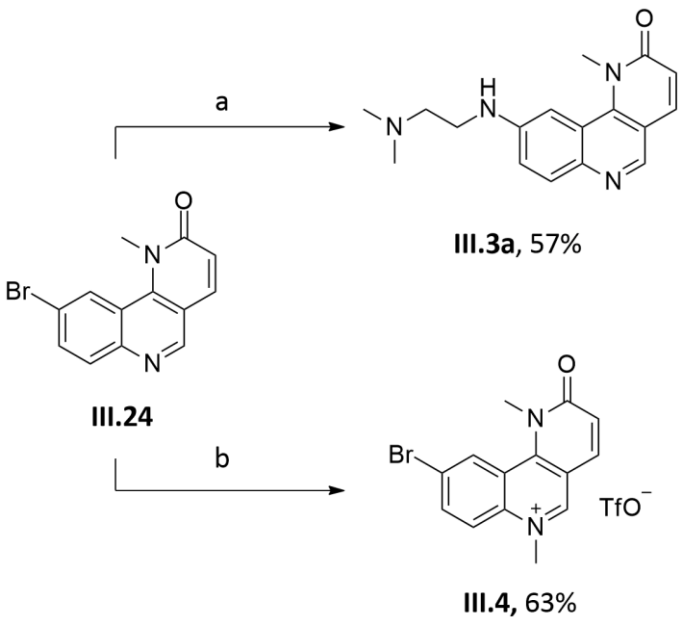

Scheme III.15. Synthesis of **III.3a** and **III.4**. Reagents and conditions: a) $NH_2CH_2CH_2N(CH_3)_2$, $Pd(OAc)_2$, **III.35**, K_2CO_3, dioxane, 120 °C, o/n; b) $CF_3SO_2OCH_3$, toluene, rt, o/n.

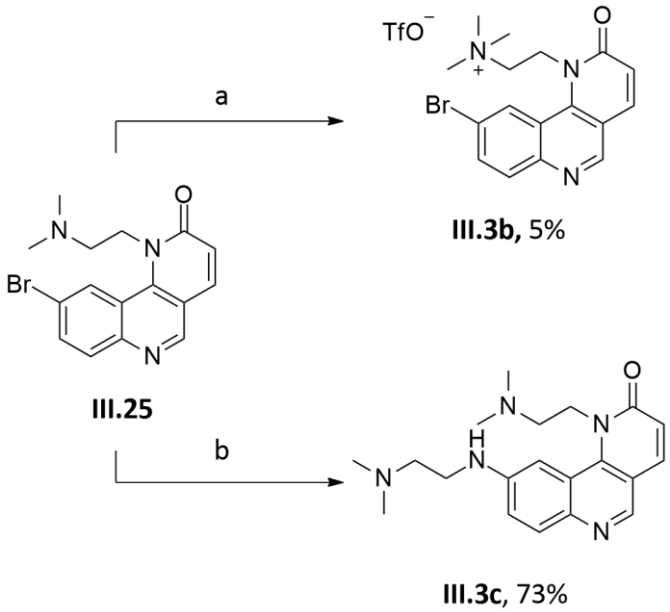

Scheme III.16. Synthesis of **III.3b** and **III.3c**. Reagents and conditions: a) $CF_3SO_2OCH_3$, toluene, rt, o/n; b) $NH_2CH_2CH_2N(CH_3)_2$, $Pd(OAc)_2$, **III.35**, K_2CO_3, dioxane, 120 °C, o/n.

2.3. Compounds as G4 ligands

The ability of the synthesised compounds to stabilize G4 and their selectivity to G4s over dsDNA was investigated using FRET-melting assay, with ligand concentrations ranging from 0.1 to 5 µM. Three different DNA sequences were used (a) 26-mer double-stranded hairpin loop sequence (T-loop) representing dsDNA (Table III.2); (b) 21-mer DNA G4 from region in human *k-RAS* oncogene promoter (KRas21R) (Table III.3); (c) 21-mer DNA G4 from the human telomeric sequence (F21T) (Table III.4).

These compouds are better G4 stabilizers than the compounds described in the previous chapter.

All compounds present a similar ΔT_m trend of KRas21R≈F21T>T-loop, suggesting that they are better G4 DNA stabilizers when compared with dsDNA.

Analising the effect of the different side chains on position N^1 (**III.2b**, **III.3a** and **III.3c**) revealed that the: (a) compound with the smaller side chain **III.3a** presented the worst G4 DNA stabilizing ability; (b) compound **III.2b** presented a better G4 DNA ability when compared with **III.3a** (probably due to the increase of the aromatic surface that could be good for the interaction with the G-quartet); (c) compound with an aliphatic side chain **III.3c** presented a better G4 stabilization ability when compared with the compound with a higher aromatic surface **III.2b** and the best dsDNA stabilizing ability within these three compounds**.** The better results observed for **III.3c** can be explained

Table III.2. FRET ΔT_m of T-Loop at 0.2 µM, stabilized by different derivatives in K^+ cacodylate buffer (pH 7.4, 60 mM K^+). Values represent the mean ± SD for a triplicated experience.

	[Ligand]/µM						
	0.1	**0.5**	**1**	**2**	**3**	**4**	**5**
III.2a	1.04 ± 0.23	1.12 ± 0.25	1.00 ± 0.21	1.06 ± 0.20	1.06 ± 0.21	- 1.97 ± 0.22	- 2.13 ± 0.22
III.2b	- 0.86 ± 0.34	0.28 ± 0.37	- 1.54 ± 0.58	- 0.67 ± 0.36	- 0.62 ± 0.36	- 1.12 ± 0.35	- 1.63 ± 0.33
III.3a	0.01 ± 0.18	0.07 ± 0.18	0.26 ± 0.18	0.44 ± 0.21	0.52 ± 0.18	0.66± 0.18	0.56 ± 0.19
III.3b	- 0.56 ± 0.24	- 0.53 ± 0.25	- 0.70 ± 0.24	- 0.66 ± 0.24	- 0.67 ± 0.22	- 0.73 ± 0.23	- 0.48 ± 0.27
III.3c	- 0.10 ± 0.18	0.43 ± 0.19	0.68 ± 0.19	1.69 ± 0.29	1.62 ± 0.21	1.85 ± 0.20	2.77 ± 0.17
III.4	- 0.10 ± 0.23	- 0.10 ± 0.21	- 0.31 ± 0.24	- 0.19 ± 0.21	- 0.21 ± 0.21	- 0.17 ± 0.21	- 0.16 ± 0.21

Table III.3. FRET ΔT_m of KRas21R at 0.2 µM, stabilized by different derivatives in K^+ cacodylate buffer (pH 7.4, 60 mM K^+). Values represent the mean ± SD for a triplicated experience.

	[Ligand]/µM						
	0.1	**0.5**	**1**	**2**	**3**	**4**	**5**
III.2a	0.66 ± 0.31	0.76 ± 0.29	0.71 ± 0.28	2.67 ± 0.30	2.90 ± 0.29	3.76 ± 0.28	5.83± 0.32
III.2b	2.16 ± 0.52	1.28 ± 0.53	2.01 ± 0.51	2.27 ± 0.46	1.10 ± 0.65	4.17 ± 0.48	3.97± 0.58
III.3a	0.96 ± 0.23	1.64 ± 0.24	0.86 ± 0.24	0.63 ± 0.27	0.91 ± 0.24	0.93 ± 0.23	0.87 ± 0.24
III.3b	0.10 ± 0.24	- 0.16 ± 0.24	- 0.02 ± 0.24	- 0.02 ± 0.25	0.98 ± 0.25	1.20 ± 0.27	0.72± 0.25
III.3c	0.67 ± 0.25	0.98 ± 0.24	1.86 ± 0.24	2.98 ± 0.24	3.98 ± 0.24	4.77 ± 0.24	6.97 ± 0.25
III.4	0.22 ± 0.24	0.22 ± 0.24	0.16 ± 0.25	0.02 ± 0.25	0.07 ± 0.24	0.07 ± 0.24	0.05± 0.25

Table III.4. FRET ΔT_m of F21T at 0.2 µM, stabilized by different derivatives in K^+ cacodylate buffer (pH 7.4, 60 mM K^+). Values represent the mean ± SD for a triplicated experience..

	[Ligand]/µM						
	0.1	**0.5**	**1**	**2**	**3**	**4**	**5**
III.2a	0.78 ± 0.24	1.00 ± 0.24	1.60 ± 0.25	2.09 ± 0.27	5.08 ± 0.28	6.09 ± 0.28	5.38 ± 0.27
III.2b	0.06 ± 0.28	-0.03 ± 0.37	0.19 ± 0.35	0.31 ± 0.37	1.88 ± 0.27	4.03 ± 0.29	4.22 ± 0.30
III.3a	0.00 ± 0.25	0.20 ± 0.27	0.82 ± 0.23	1.13 ± 0.23	1.82 ± 0.23	1.86 ± 0.26	2.07 ± 0.28
III.3b	-0.04 ± 0.28	-0.01 ± 0.28	-0.01 ± 0.28	0.81 ± 0.26	1.88 ± 0.28	0.86 ± 0.28	0.86 ± 0.34
III.3c	0.27 ± 0.29	1.19 ± 0.31	2.40 ± 0.29	4.09 ± 0.28	5.06 ± 0.31	6.04 ± 0.28	7.97 ± 0.33
III.4	-0.06 ± 0.25	0.64 ± 0.26	0.76 ± 0.24	1.66 ± 0.24	1.65 ± 0.24	1.69 ± 0.28	2.60 ± 0.30

by the flexibility of the alkyl chain that allows a better positioning for amine terminal group to interact with the anionic phosphate groups.

In contrast, ΔT_m of compounds with the aromatic ring substituent on position N^1 (**III.2a** and **III.2b**) are compared is possible to observe that the additional amine moiety present in **III.2b** did not seem to have a significant impact on G4 stabilization.

The compound with a cationic center on the aromatic core (**III.4**) only presented a weak stabilizing of F21T what can be explianed by the lack of alkylamine side chains.

3. Conclusion

A library of six novel benzo[*h*][1,6]naphthyridin-2(1*H*)-one derivatives with different terciary amine side chains were synthesised. While the synthesis of compounds with an aromatic side chain (**III.2**) was straightforward, the synthesis of derivatives with alkylamines (**III.3** and **III.4**) presented more challenges.

When tested as G4 ligands, these compounds presented better stabilizing capacity when compared with the compounds described in the previous chapter. This difference can be ascribed to their higher aromatic surface which can allow a better π-π interaction between the G-quartet and the aromatic surface of ligands. Based on FRET-melting assays data, there was possible to perceive some of the structural features that these derivatives present and are important in G4 ligands.

CHAPTER IV

IV. SYNTHESIS OF CYSTEINE-BASED BUILDING BLOCKS OF PNA

1. Introduction

Despite the huge variety of PNA and α-PNA monomers, there is only one presenting a sulphur atom in its structure: a chemically dynamic oligomer in which the nucleobase is attached via a thioester bond and spaced by a variety of α-amino acids (**IV.1**). The most exciting characteristic of this system was its ability to adapt to the DNA complement in terms of the nucleobase sequence. As exemplified in Scheme IV.1, the oligomers efficiently self-assembles by means of reversible covalent thioester bond formation between thioester-functionalized nucleobase (**IV.2**) and simple oligopeptide backbone containing cysteine (**IV.3**). Although, this α-PNA cross-pair with RNA and DNA in Watson-Crick their nucleobase recognition hybridization properties were inferior to *N*-(2-aminoethylglycine)PNA.[506]

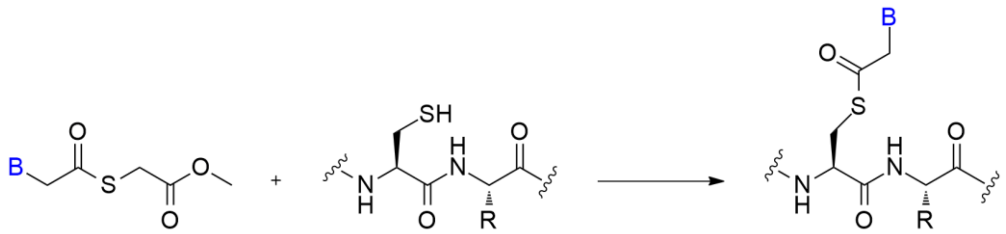

IV.2 **IV.3** **IV.1**

Scheme IV.1. Reversible thioester formation between thioester-functionalized nucleobase and oligopeptide backbone containing cysteine (B: nucleobase; R: amino acid side chain).

This chapter is focus on the development of synthetic strategies to obtain new chimeric amino acids based on cysteine's functionalization with nucleobase side chains, which can be used as building blocks of α-PNAs (**IV.4,** Figure IV.1). Dipeptides incorporating these chimeric amino acids and glycine were also synthesised. The benefits of this strategy are the: (a) chemical diversity it confers to the structures and (b) flexibility of the side chain, which may be important in allowing the oligomer to adopt the appropriate DNA binding conformation.

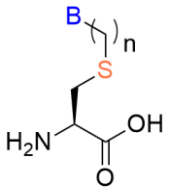

IV.4

Figure IV.1. Chimeric amino acid containing sulphur (n = 1-3, in blue is the nucleobase and in orange is the sulphur atom).

2. Methods, Results and Discussion

2.1. Retrosynthetic analysis

As previously stated in Chapter I (pages 45-46), it is mandatory an orthogonal strategy for the protection of the primary amino group of the backbone and of the exocyclic amino groups of the nucleobases. To synthetise the desired compounds, it was applied the Fmoc/Boc strategy,[393,394] where the Fmoc group was used as the protective group of the amino groups of the amino acids and the Boc group was chosen to protect exocyclic amino groups of the nucleobases.

To obtain the designed chimeric amino acids and dipeptides, three different pathways could be pursued (Scheme IV.2): (a) firstly, reaction of the linking chain with the protected nucleobase followed by the reaction with cysteine, both through nucleophilic substitution; (b) reaction of the linking chain with cysteine followed by the reaction with the protected nucleobase, both through nucleophilic substitution; or (c) reaction of the linking chain with the protected nucleobase through nuclephilic substitution followed by the thiol-ene reaction with cysteine. To obtain the dipeptides containing the chimeric amino acids, a similar pathway can be followed using cysteinyl-glicine dipeptide instead of cysteine amino acid.

N-alkylation of nucleobases is usually conducted using alkyl halides,[507] alkyl tosylates[508] and mesylates.[509] Furthermore, this reaction with other carbon electrophiles such as epoxides,[510] Michael acceptors,[511] carbonates,[512] and allylic esters catalyzed by Pd(0)[513] are also well-known procedures. A few reports describing conditions that are suitable for accessing *N*-alkylated nucleobases from alcohols, have also been reported, mostly using Mitsunobu reaction.[514] This reaction is the dehydrative coupling of mainly primary or secondary alcohol to a pronucleophile, which is mediated

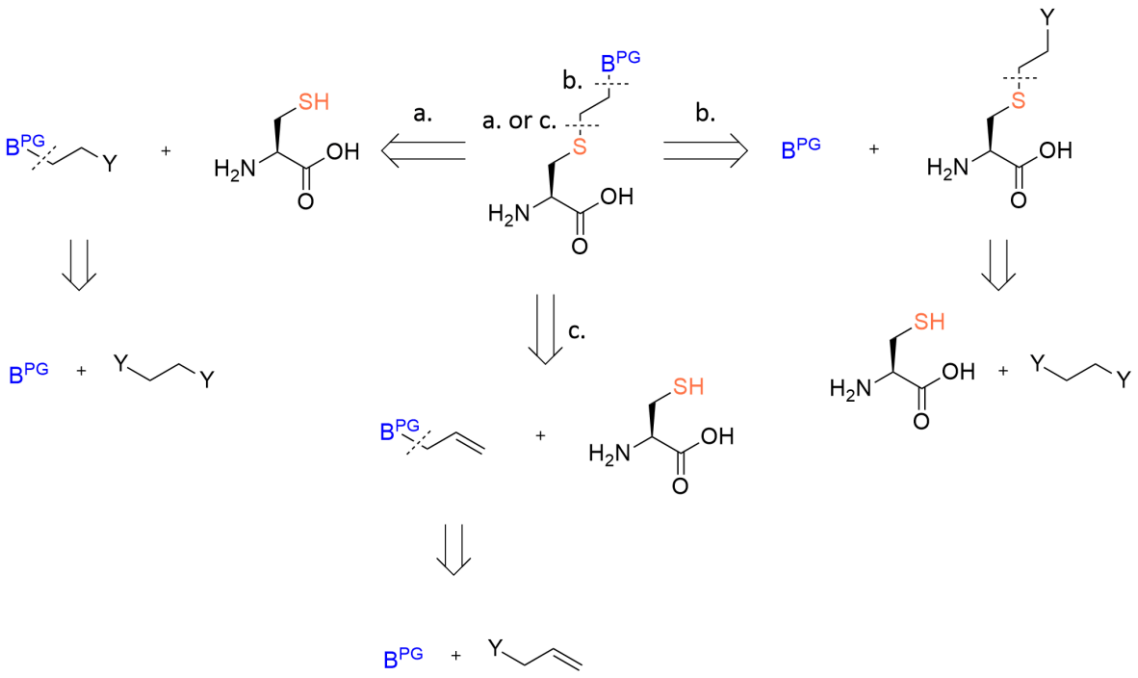

Scheme IV.2. Retrosynthetic scheme for chimeric amino acid synthesis (BPG: Boc-nucleobase nucleobase, Y: Cl, Br, I).

by the reaction between a dialkyl azodicarboxylate (usually DIAD) and a trialkyl- or triaryl-phosphine (usually triphenylphosphine). The Mitsunobu reaction usally proceeds under mild and neutral conditions, and typically at 0 °C to rt.[515]

Relatively to the *S*-alkylation of thiols, due to increasing application of thioethers in various fields, many methods have been reported for the formation C-S bond, mainly using aromatic thiols as starting materials.[516] However, the approaches for the alkylation of the thiol group of cysteine are scarcer. *S*-alkylation of cysteine or cysteine derivatives is mainly obtain through substitution nucleophilic bimolecular (S_N2) or thiol-ene reactions.

S-alkylation of unprotected and protected cysteine amino acids via S_N2 requires the formation of thiolate anions. Thiols are much more acidic and nucleophilic in comparison to alcohols, and these properties can be explained by the weakness of the S-H bond and the greater likelihood that the negative charge will be distributed within sulphur 3d orbitals. Relatively to cysteine, it can be considered a triprotic acid in which the pKa of thiol group has been determined to be 8.2 (Scheme IV.3).[517]

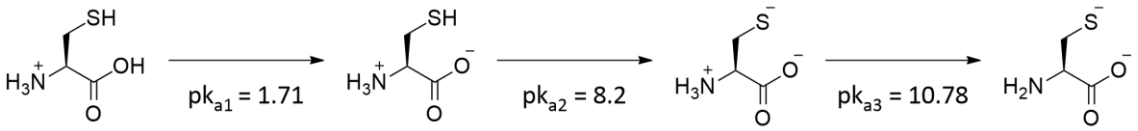

IV.5

Scheme IV.3. Protonation states of cysteine (pKa values depend on temperature, ionic strength, and the microenvironment of the ionisable group).[517,518]

To obtain the cysteine thiolate (**IV.5**) different bases have been employed in literature.[519-528] However, unsatisfactory yields, poor selectivity, problems with solubility and purification, formation of side-products and racemisation were among the difficulties encountered.[522]

Alternatively, thiol-ene reaction (previously discussed in Chapter II, pages 67-68) can also be used in *S*-alkylation of cysteines.[524,529-531] In order to obtain the chimeric amino acid, first the linking chain reacted with protected nucleobase to form a nucleobase allyl derivative. As these derivatives are considered to be of great importance in pharmaceutical industry,[532] literature offers multiple examples of procedures dedicated to *N*-allylation of nucleobases or its derivatives by reaction with: (a) allyl bromide using different bases;[532-534] (b) hexamethyldisilazane to form 2,4-bis((trimethylsilyl)oxy) derivative which will then react with allyl bromide;[533] (c) *N*,*N*-dimethylformamide diallyl acetal;[533] (d) triallyl phosphite;[534] (e) allyl acetate through Pd(0)-catalyzed allylation;[535] or (f) 1,2-dibromoproane to alkylate the nucleobase followed by dehydrobromination.[535] The main problem reported for the majority of this procedure is the formation of a mixture of regioisomers.[533,535] Having the *N*-allylated nucleobase in hand, it can react with cysteine via thiol-ene reaction. To synthesise the cysteine-based building blocks, reaction were conducted under radical conditions which mechanism is described in Scheme IV.4 (both thermal and photochemically induced). In order to obtain the final compounds, both S_N2 and thiol-ene reactions were tried.

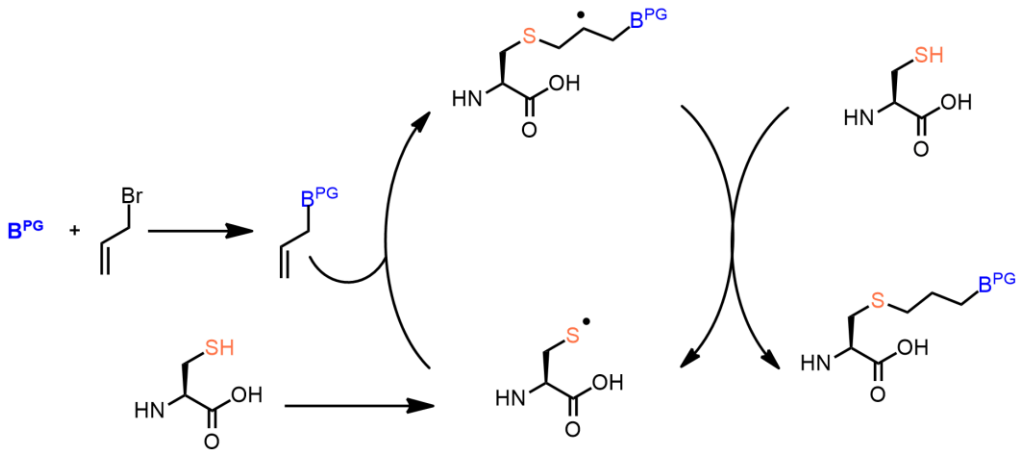

Scheme IV.4. Mechanism of synthesis of target compounds via radical thiol-ene reaction.

2.2. Synthesis discussion

2.2.1. Preparation of Fmoc-cysteine (**IV.6**) and Fmoc-cysteinyl-glicine dipeptides (**IV.7**)

According to the protecting groups strategy selected to synthesise the chimeric amino acids and dipeptides, *N*-Fmoc-*S*-Trt-L-cysteine **IV.8** was used as starting material. As exemplified in Scheme IV.5a, the trityl group was deprotected with TFA and TES as scavenger to prevent retritylation. Silanes are usually most efficient in removing the trityl cations as they reduce them to inert triphenylmethane.[494]

Fmoc-cysteinyl-glicine dipeptides (**IV.7**, Scheme IV.5b) were synthesized starting from *N*-Fmoc-*S*-Trt-L-cysteine **IV.8** and glycine ethyl ester hydrochloride (**IV.9a**) or glycine benzyl ester hydrochloride (**IV.9b**). These starting materials were chosen having in mind the concept of orthogonality: (a) trityl, as seen previously, is usually removed in acidic conditions; (b) ethyl ester is removed under basic conditions; and (c) benzyl ester can be removed by catalytic hydrogenolysis. Comparing the two protected glycine amino acids used, the ethyl ester is more affordable but epimerization and degradation of cysteine can occur under the basic conditions of deprotection, while glycine benzyl ester is more expensive but the deprotection under catalytic hydrogenolysis is less prone to epimerization.[494]

Amide coupling to obtain **IV.10a** and **IV.10b** were performed using TBTU/HOBt as coupling agents and DIPEA as base, which provides fast couplings and reduces racemization.[536] Finally, the thiol group was deprotected to afford the desired dipeptides **IV.7a** and **IV.7b** in very good yields.

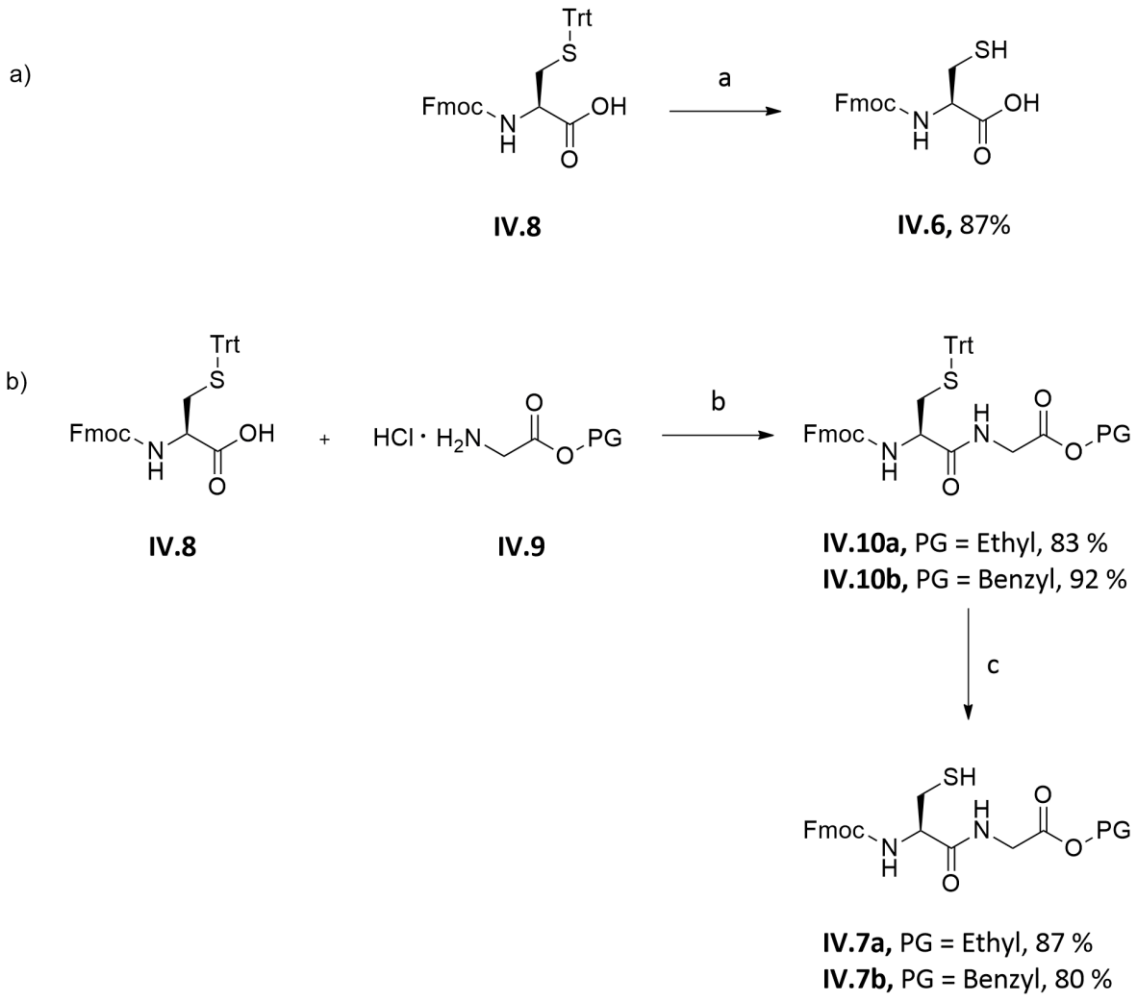

Scheme IV.5. Synthesis of a) **IV.6** and b) **IV.7**. Reagents and conditions: a) TFA, TES, DCM, rt, 3h; b) TBTU, HOBt, DIPEA, DMF, rt, o/n; c) TFA, TES, DCM, rt, 3h.

2.2.2. Boc-protection of the exocyclic amine group of nucleobases

Boc-protection of cytosine and adenine (respectively **IV.11** and **IV.12**, Scheme IV.6) was accomplished through a two-step procedure already described in literature.[537,538] First the tris-Boc compounds **IV.13** and **IV.14** were synthesised, followed by the selective deprotection, under basic conditions, of N^1 in cytosine and N^9 in adenine, to afford the bis-Boc compounds **IV.15** and **IV.16** in good overall yields. To overcome guanine drawbacks (such as its insolubility in almost all solvents and its polyfunctional nature with imidazole, amide, and guanidine substructures), 2-amino-6-chloropurine **IV.17**, a guanine analogue, was used as starting material. Bis-Boc-protection of the exocyclic amine of 2-amino-6-chloropurine (to obtain **IV.18**) was performed following the above described methodology. As seen before, this procedure has the tris-Boc derivative **IV.19** as intermediary (Scheme IV.4).[537,538] Thymine does not need any protection.

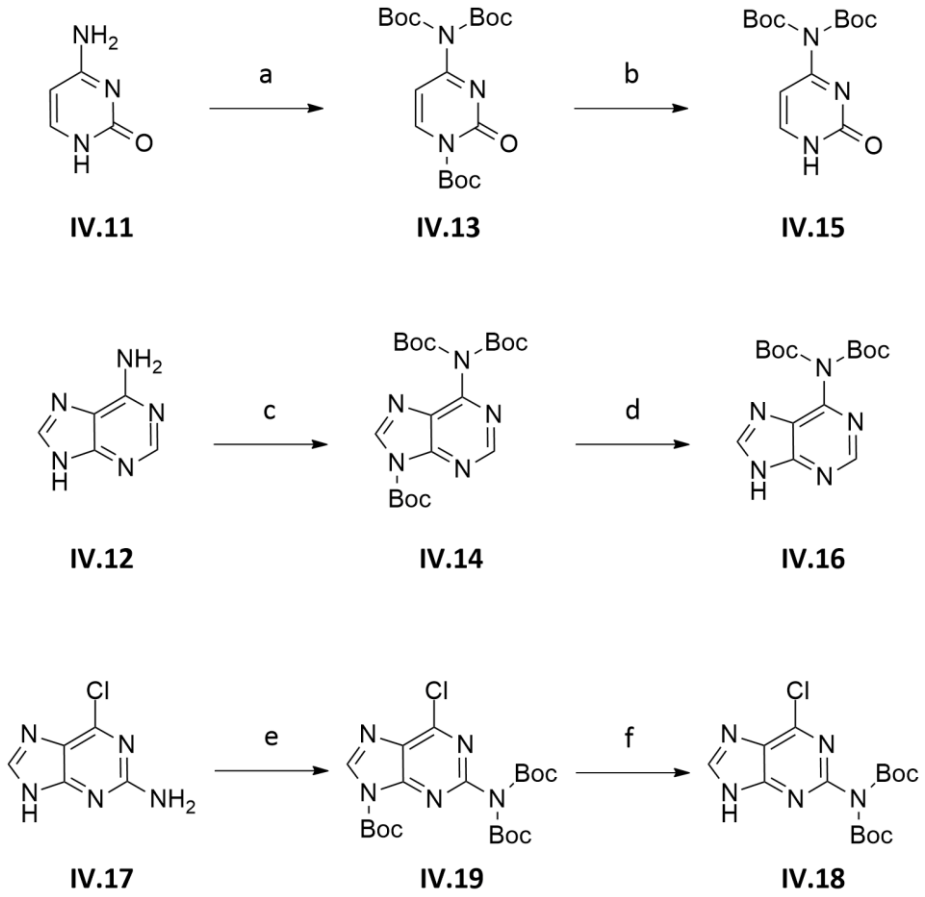

Scheme IV.6. *N*-protection of cytosine, adenine and guanine with Boc. Reagents and conditions: a) Boc_2O, DMAP, THF, rt, o/n, 90%; b) $NaHCO_3$, MeOH, 50 °C, 1 h, 83%; c) Boc_2O, DMAP, THF, rt, o/n, 93%; d) $NaHCO_3$, MeOH, 50 °C, 1 h, 75%; e) Boc_2O, DMAP, THF, rt, o/n, 68%; f) $NaHCO_3$, MeOH, 50 °C, 1 h, 95%.

2.2.3. Synthesis of final chimeric amino acids and dipeptides

During the search for the ideal reaction conditions to obtain the final chimeric cysteines, **IV.16** was the nucleobase elected in the majority of the cases. In addition, not only **IV.6** and **IV.7a** but also unprotected cysteine (**IV.20**) and acetylcysteine (**IV.21**), were used as reagents. These reagents were choosen since they are cheaper reagents and do not the need the additional step of trityl removal.

2.2.3.1. Starting with *N*-alkylation of nucleobases followed by *S*-alkylation of cysteine through S_N2 reaction (Pathway a)

Firstly, the *N*-hydroxymethylation of bis-Boc adenine **IV.16** was tried. The *N*-hydroxymethylation has been already described for *N*-unsubstituted benzimidazoles

with formaldehyde and paraformaldehyde.[539] Besides that, 9-hydroxymethyladenine was obtained by chance when methoxyethoxymethyl chloride was added to an alkaline aqueous solution of adenine.[540] The planned design would be to convert the hydroxyl group of the expected product **IV.22** in a good leaving group (mesilate, triflate or halogen).

Two reaction conditions (Table IV.1) were tried to obtain **IV.22**, but in both cases, although **IV.16** was partially consumed during the reaction with the formation of several compounds, the ^{1}H NMR spectra of the crude did not present the CH_2 peak compatible with the hydroxymethylene.

Table IV.1. Reactions condition tried for *N*-hydroxymethylation of bis-Boc adenine **IV.16**.

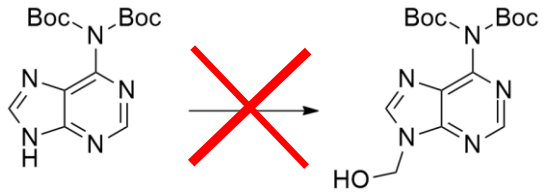

IV.16 **IV.22**

Entry	Base	Alkylating agent	Reaction conditions
1	-	Formaldehyde solution (37% in H_2O)	EtOH, rt, 20 h
2	NaOH 1M	Paraformaldehyde	Absolute EtOH, rt, 48 h

Alternatively, as exemplified in Scheme IV.7, *N*-alkylation of bis-Boc adenine **IV.16** was successfully accomplish with 1-bromo-2-chloroethane **IV.23,** affording the expected product **IV.24** in moderate yield.

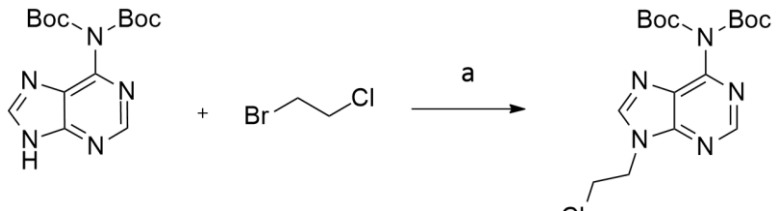

IV.16 **IV.23** **IV.24**

Scheme IV.7. Synthesis of compound **IV.24**. Reagents and conditions: a) K_2CO_3, DMF, rt, o/n, 71%.

Then, *S*-alkylation with **IV.24** was tried using different basic conditions. To synthesise the cysteine derivative **IV.25** (Table IV.2), TMG (entry 1 and 2) was tested as a base as described in literature.[522] However, *S*-alkylation did not occur neither with **IV.20** nor with **IV.6**. *S*-alkylation of **IV.21** was also tried using sodium methoxide (entry 3) but without any success.

Table IV.2. Reaction conditions tried to obtain compound **IV.25**.

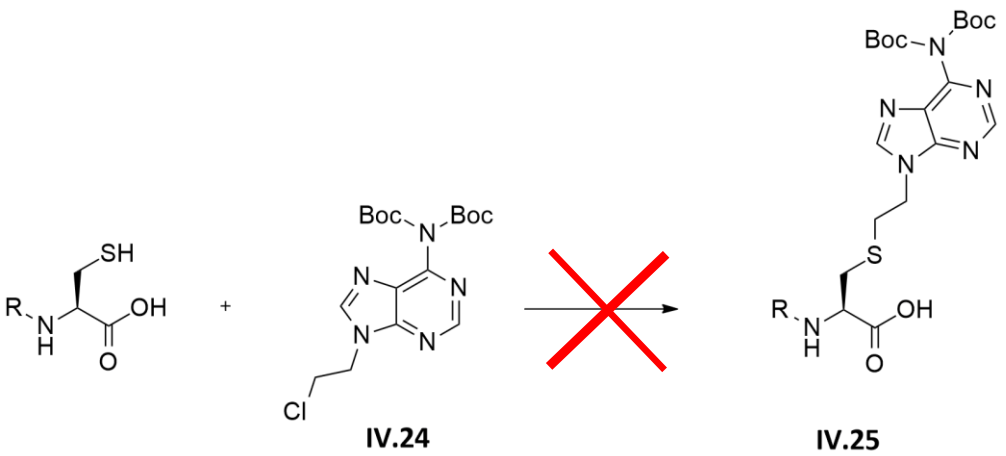

Entry	R	Base	Reaction conditions
1	H **(IV.20)**	TMG	MeOH:THF, rt, 24 h
2	Fmoc **(IV.6)**	TMG	MeOH:DMF, rt, 24 h
3	Ac **(IV.21)**	$NaOCH_3$	MeOH, rt, 30 h

To syntheside the dipeptide derivative **IV.26** (Table IV.3), DIPEA was used as base in entries 1-3). Since the product was not obtained when only the base was used (entry 1), the reaction conditions were replicated but with the addition of sodium iodide (entry 2). With the addition of this salt, the substitution of chloride by iodine in **IV.24** should occur via S_N2 because iodide is a stronger nucleophile than chloride – Finkelstein reaction.[541] As iodide is also a better leaving group than chloride it was expected that the following S-alkylation reaction worked better with this modification. Since **IV.26** was not obtain again, a third attempt (entry 3) was done using a higher reaction temperature, but once again the desired product was not obtained. Finally, potassium carbonate was also tried as base (entry 4) but again without success.

Table IV.3. Reaction conditions tried to obtain compound **IV.26**.

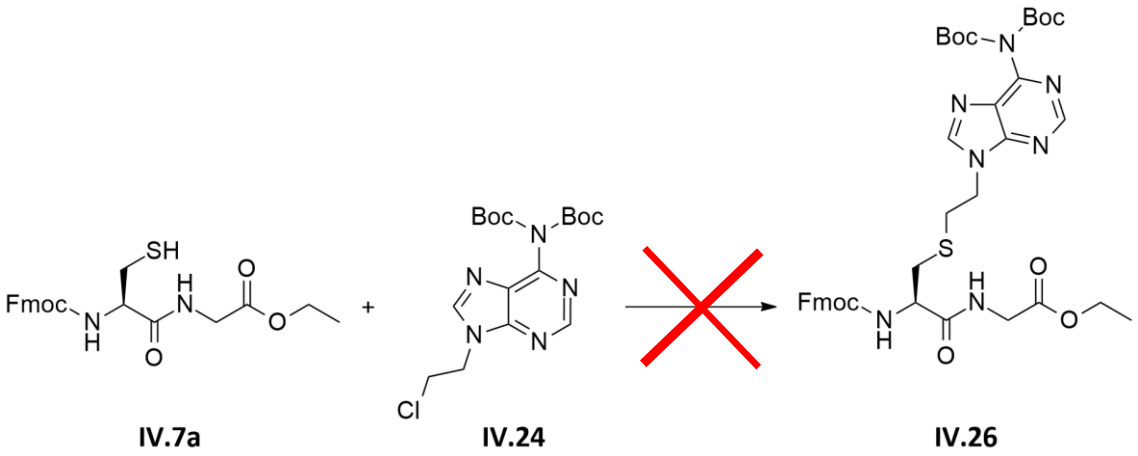

IV.7a **IV.24** **IV.26**

Entry	Base	NaI	Reaction conditions
1	DIPEA	-	DMF, rt, 24 h
2	DIPEA	☑	DMF, rt, 24 h
3	DIPEA	☑	DMF, 50 °C, 7 h
4	K_2CO_3	☑	DMF, rt, o/n

2.2.3.2. Starting with *S*-alkylation of cysteine followed by *N*-alkylation of nucleobases through S_N2 reaction (Pathway b)

As the final products were not obtained using the reaction conditions reported in the previous section, it was decided to test pathway b, in which the first step involves the *S*-alkylation of cysteine with the linking chain.

As exemplified in Table IV.4, *S*-alkylation of cysteine was attempted with bromochloromethane **IV.27**.

Table IV.4. Reaction conditions tried in the S-alkylation of cysteine with **IV.27**.

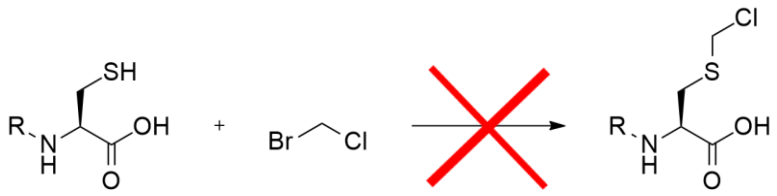

IV.27 **IV.28**

Entry	R	Base	Equiv. of alkylating agent	Reaction conditions
1	H **(IV.20)**	TMG	1	MeOH:THF, 50 °C, 2 h
2	H **(IV.20)**	TMG	20	MeOH:THF, 50 °C, 2 h
3	Fmoc **(IV.6)**	K_2CO_3	2	DMF, 0 °C to rt, o/n

In this case, two different bases were used. Using the reaction conditions described in literature for TMG[522] (entry 1), the desired product was not obtained and instead it occurred double alkylation resulting in a cysteine dimer liked through a methylene brigde. In order to try to avoid the formation of this product, an excess of alkylating agent was used (entry 2). However, in this case a complex mixture of products were obtained maybe due to the formation of *O*- or *N*-alkylated side-products. The *S*-alkylation of **IV.6** was also tried using potassium carbonate (entry 3) but the desired product **IV.28** was not obtained.

Alternatively, cysteine *S*-alkylation was attempted using 1-bromo-2-chloroethane **IV.23** (Table IV.5).

Table IV.5. Reaction conditions tried in the S-alkylation of cysteine with **IV.23.**

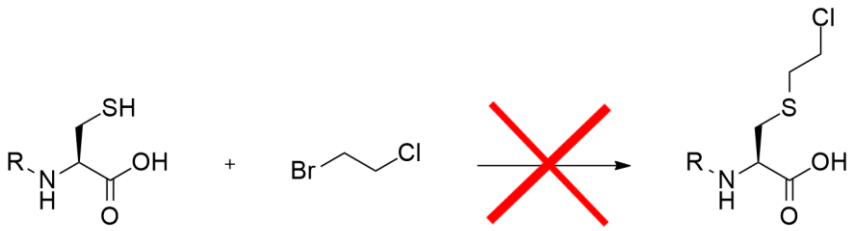

IV.23 **IV.29**

Entry	R	Base	Reaction conditions
1	H **(IV.20)**	TMG	MeOH:THF, 50 °C, 3 h
2	Ac **(IV.21)**	$NaOCH_3$	MeOH, reflux, 3 h
3	Ac **(IV.21)**	TEA	DMF, rt, 3 h

In this case three different conditions were tested (Table IV.5) but **IV.29** was not formed. Using the reaction conditions described in literature for TMG[522] (entry 1), a complex mixture of products were obtained maybe due to the formation of *O*- or *N*-alkylated side-products. Based in literature reports, sodium methoxide[528] and triethylamine[521] were also tried as base (entry 2 and 3, respectively) but again without success.

2.2.3.3. Starting with *N*-allylation of nucleobases via S_N2 reaction followed by thiol-ene reaction with cysteine (Pathway c)

As it was not possible to obtain the desired final chimeric products using the reaction pathways described in the previous sections, a pathway c was tested.

2.2.3.3.1. *N*-allylation of nucleobases

The first step of this synthetic pathway consists in the regioselective synthesis of *N*-allyl derivatives of nucleobases. *N*-allylation of bis-Boc citosine **IV.15**, bis-Boc adenine **IV.16** and thymine **IV.30** was performed by using allyl bromide and potassium carbonate as base (Scheme IV.8). In line with the higher acidity of N^1-H versus N^3-H of **IV.15**,[542] selective allylation took place at amide nitrogen N^1 originating **IV.31**. In the case of *N*-allylation of **IV.16** and **IV.30**, two regioisomers were obtained. In both cases, the major product were the desired one (**IV.32** and **IV.33**) and they were isolated from their by-products (**IV.34** and **IV.35**) using flash column chromatography.

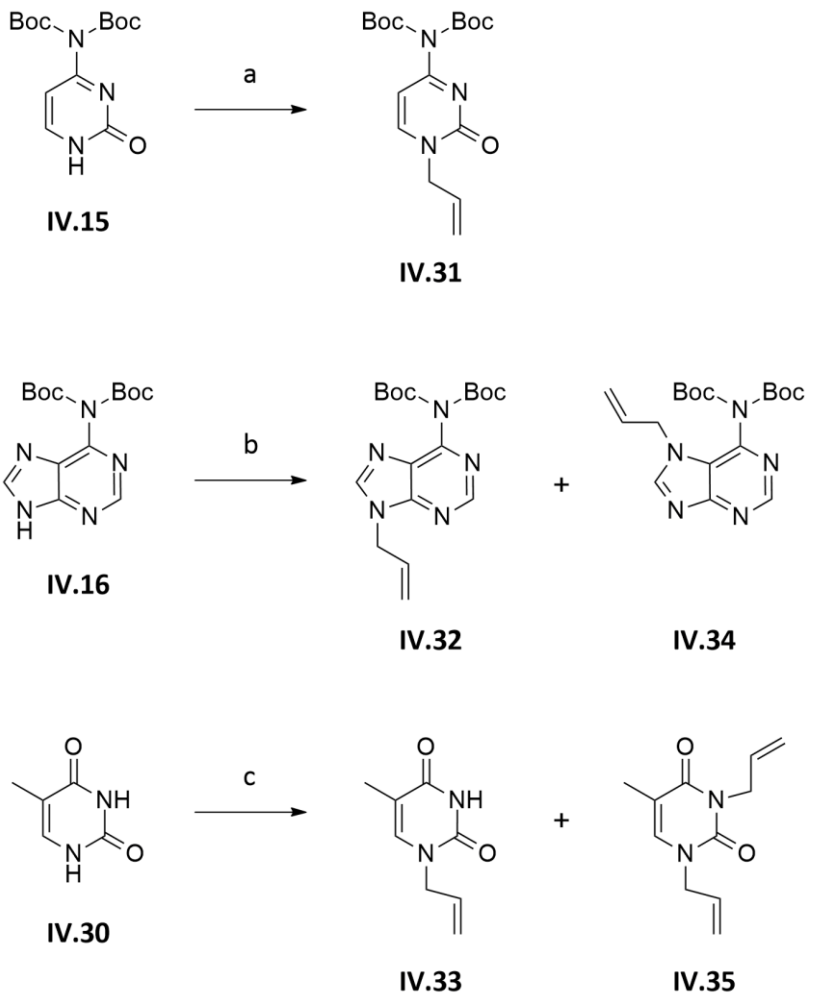

Scheme IV.8. *N*-allylation of **IV.15**, **IV.16** and **IV.30**. Reagents and conditions: a) $BrCH_2CHCH_2$, K_2CO_3, DMF, rt, o/n, 68%; b) $BrCH_2CHCH_2$, K_2CO_3, DMF, rt, o/n, **IV.32**: 58% and **IV.34**: 36%; c) $BrCH_2CHCH_2$, K_2CO_3, DMF, rt, o/n, **IV.3**: 60% and **IV.35**: 20%.

The development of an easy and successful synthesis of *N*-allylated-Boc-protected guanine was the major challenge. Two different reaction conditions (Table IV.6) were tried to obtain the *N*-allylation of **IV.18**.

Table IV.6. Reaction conditions explored to obtain compound **IV.36**.

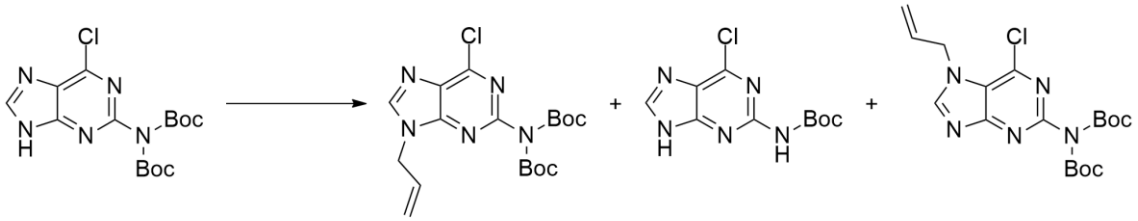

IV.18 **IV.36** **IV.37** **IV.38**

Entry	Base	Reagents and conditions	Yield		
			IV.36	IV.37	IV.38
1	NaH	$BrCH_2CHCH_2$, THF, 0 °C to rt, o/n	20%	22%	-
2	K_2CO_3	$BrCH_2CHCH_2$, DMF, 0 °C to rt, o/n	51%	-	26%

Using the conditions described in entry 1, the desired compound **IV.36** was obtained as minor product and an interesting occurrence was the cleavage of one of the Boc group of the bis-Boc compound **IV.36** to afford the N^2- Boc-protected compound **IV.37**. The isolation of this product had been already described in literature using NaOH in EtOH at room temperature.[538] Despite that, there are very few methods for the selective deprotection of di-Boc protected to mono-Boc protected amines.[543-545] The mechanism proposed in literature[543-545] based on the formation of a six-membered chelate seems to be applicable to this situation (Scheme IV.9). So, the initial chelation between the metal ion and two oxygen of the carbonyl group is followed by abstraction of proton from the methyl group led to the loss of isobutene, CO_2 and formation of mono-Boc-protected group.

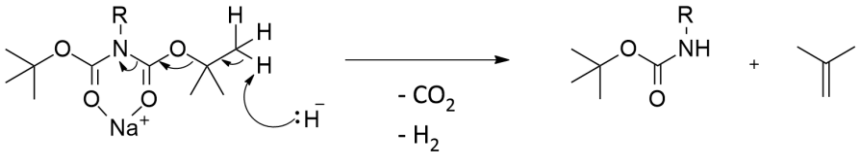

IV.18 **IV.37**

Scheme IV.9. Mechanism of selective deprotection of a Boc group in the presence of sodium ion.

When potassium carbonate was used as base (entry 2), **IV.36** was obtained with a better yield. Under this conditions, the N^7-allyl derivative **IV.38** was obtained as minor product.

Having compound **IV.36** in hand, the next step would be conversion of the 6-chloro moiety to a 6-oxo function of guanine. Some methods described in the past for this conversion have employed vigorous acidic (such as refluxing hydrochloric acid)[546] or basic conditions (such as refluxing NaOH solution)[547] that could easily remove both Boc protecting groups. Milder conditions include treatment of protected 2-amino-6-halopurine with trimethylamine in the presence of 3-hydroxypropionitrile and 1,8-diazabicycloundec-7-ene which lead to the corresponding guanine via intermediate 6-trimethylammonium **IV.39** and 6-(2-cyanoethoxy) derivatives.[548] Alternatively, the same authors explored the use of a ethanolic solution of trimethylamine (35% in EtOH/H_2O, 95:5) at 0 °C to room temperature, and they were able to obtain directly the desired final compound (instead of the ammonium salt) with good yields.[537] Having in mind these reports, this reaction condition (Table IV.7, entry 1) was used for the conversion of **IV.36** into the guanine derivative **IV.40.**

Table IV.7. Reaction conditions to obtain compound **IV.40** using an ethanolic solution of trimethylamine.

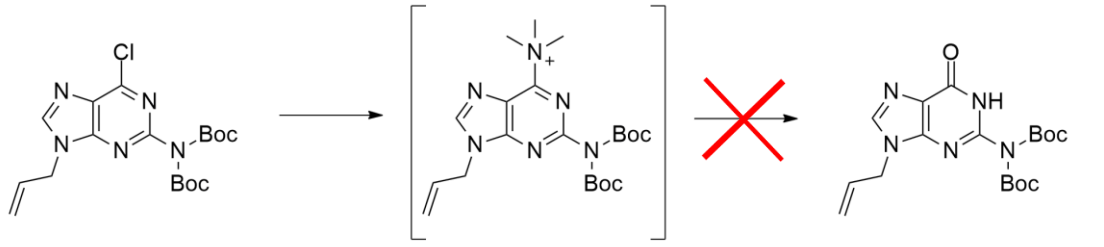

Exact mass: 411.17 g.mol^{-1} | Exact mass: 433.26 g.mol^{-1} | Exact mass: 391.19 g.mol^{-1}

IV.36 | **IV.39** | **IV.40**

Entry	Solvent	Conditions
1	Ethanolic solution of trimethylamine (35% in EtOH/H_2O, 95:5)	0 °C to rt, o/n
2	Ethanolic solution of trimethylamine (35% in EtOH/H_2O, 95:5) + H_2O (1:1, v/v)	0 °C to rt, o/n

In order to access if **IV.40** was formed, mass spectrometry analysis played an important role. The product formed when using the reaction conditions described in entry 1 did not afford compound **IV.40**, contrary to what is described in literature.[537] Knowing the nucleophiles presented in the reaction media, other possible products from this reaction would be **IV.41** or **IV.42** (the product of the reaction of **IV.39** and ethanolic solution of trimethylamine which have been already described in literature as by-product).[548]

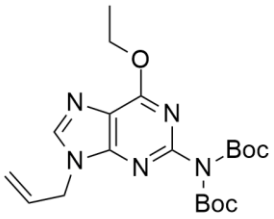

Exact mass: 419.22 g.mol^{-1}

IV.41

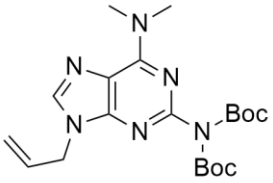

Exact mass: 418.23 g.mol^{-1}

IV.42

Figure IV.2. Possible products from the reaction between **IV.36** and the ethanolic solution of trimethylamine.

The mass spectrum (which presented a peak at 419.28) and ^{1}H NMR spectrum (which presented a broad singlet at 3.49 ppm, a value similar to the chemical shift of the dimethyl group of 2-amino-6-*N*,*N*-dimethylaminopurine derivative described in literature[549]) indicated that the compound formed was **IV.42**. In order to try to obtain the desired product, the amount of water was increased to avoid the reaction of the trimethylammonium compound with trimethylamine (entry 2, Table IV.7), but neither the desired product nor the reported by-products were isolated.

Some authors reported the high volatility of the ethanolic solution of trimethylamine as a drawback of this method. Therefore, they have explored the use of bicyclic tertiary amine DABCO, which has a higher melting point. In addition, the resulting intermediate **IV.43** was easily hydrolysed in refluxing water or by using aqueous sodium hydroxide in dichloromethane at room temperature to provide the 9-substituted guanine.[550] Therefore, these reaction conditions were tried but **IV.40** was again not obtained (entry 1, Table IV.8).[550] Alternatively, the amount of water and DABCO were increased and the solvent was changed to THF (entry 2 and 3, Table IV.8). However, once again, the product was not detected by mass spectrometry.

Table IV.8. Reaction conditions to obtain compound **IV.40** using DABCO.

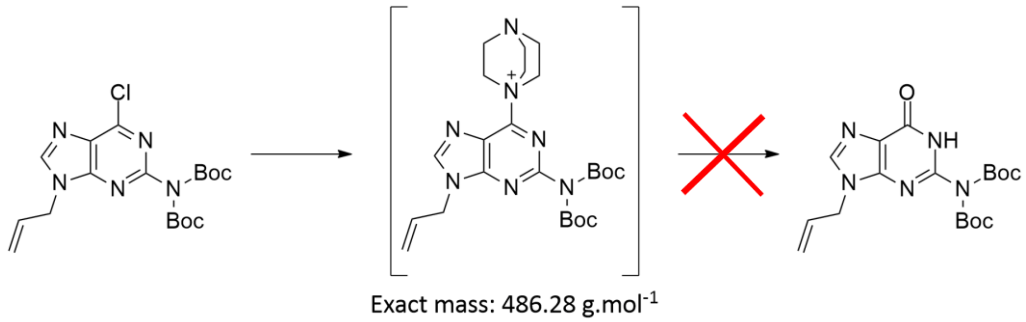

Exact mass: 486.28 g.mol^{-1}

IV.36 **IV.43** **IV.40**

Entry	Equiv. of DABCO	Solvent	Water	Conditions
1	1	DMSO	4 equiv.	rt, o/n
2	1.2	THF	Excess	rt, o/n
3	2.4	THF	Excess	rt, o/n

As it was not possible to obtain **IV.40** in the previous attempts, an alternative route was tried. In this pathway (Scheme IV.10), the first step was the *N*-allylation of unprotected 4-chloro guanine **IV.17**, followed by the convertion of the 6-chloro moiety of **IV.44** into the 6-oxo function of guanine (**IV.45**), using refluxing hydrochloric acid.[386]

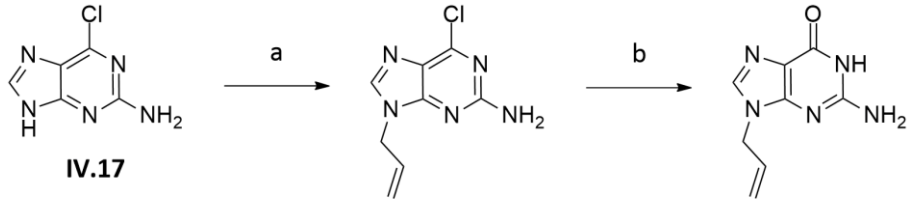

IV.17 **IV.44** **IV.45**

Scheme IV.10. *N*-allylation of **IV.17** and conversion of the *N*-allylated product (**IV.44**) into **IV.45**. Reagents and conditions: a) $BrCH_2CHCH_2$, K_2CO_3, DMF, rt to 50 °C, o/n, 68%; b) 1 N aqueous HCl, rt to reflux, 2 h, 71%.

Having the *N*-allylated 4-chloro guanine derivative **IV.45**, Boc-protection of the exocyclic amine was performed by following the previously described methodology.[537,538] In a first attempt (entry 1, Table IV.9), only 2.2 equivalents of Boc_2O were used in order to try to protect exclusively the exocyclic amine. However, three compounds were obtained: bis-Boc **IV.40**, mono-Boc **IV.46**, and tris-Boc **IV.47** protected

derivatives. In order to improve the yield of **IV.40**, 4 equivalents of Boc_2O (entry 2, Table IV.9) were used leading to the formation of the desired bis-Boc derivative **IV.40** in moderate yield (45%).

Table IV.9. Reaction conditions for Boc-protection of the exocyclic amine of **IV.46**. Reagents and conditions: DMAP, THF, rt.

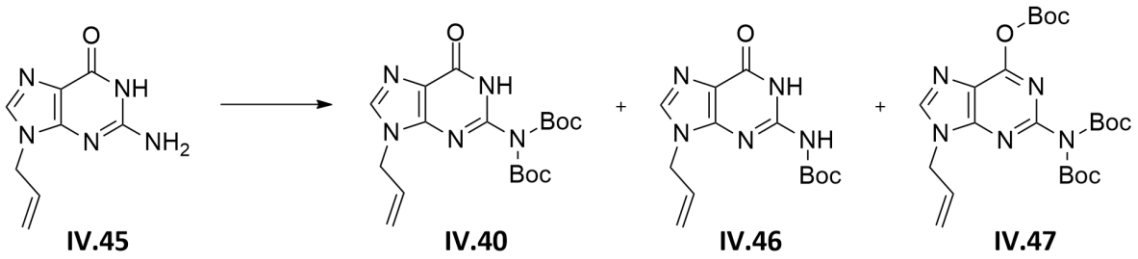

Entry	Equiv. of Boc_2O	Reaction time	Yield		
			IV.40	IV.46	IV.47
1	2.2	4 h	20%	16%	12%
2	4	24 h	45%	42%	7%

In an attempt to avoid the formation of product **IV.47**, the O^6-protection of **IV.45** (Scheme IV.11) with benzyl group, which deprotection could easily be achieved either by hydrogenation or acidolysis with TFA,[394] was also tried.

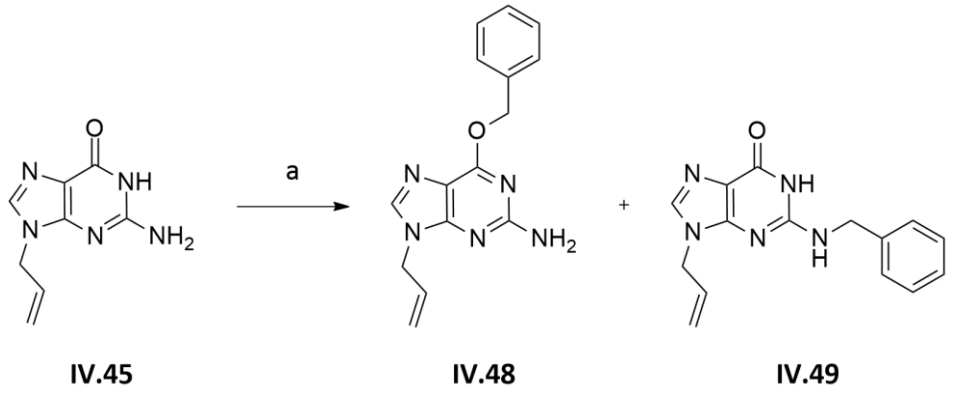

Scheme IV.11. *O*-benzylation of **IV.45**. Reagents and conditions: a) $C_6H_5CH_2Br$, NaH, DMF, rt, o/n, **IV.48**: 16% and **IV.49**: 26%.

Due to the low yield of the desired compound **IV.48**, its Boc protection of the exocyclic amine was not performed since this this method would not present any advantage over

the previous one. This low yield can be explained by the formation of by-products such as N^2-benzylate product **IV.49**.

2.2.3.3.2. Thermally induced thiol-ene reactions

Given the successful thermally induced coupling of cysteine with different alkenes reported in literature,[524] thiol-ene of *N*-protected cysteines and different alkenes was carried out in refluxing dichloroethane (DCE) in the presence of AIBN, the radical initiator. As exemplified in Table IV.10, initially diferent reaction conditions were screened with commercially available reagents (entry 1-3) in order to find the optimized conditions.

Table IV.10. Reaction conditions used in thermally induced thiol-ene reactions of *N*-protected cysteines with different alkenes. Reagents and conditions: a) AIBN, DCE.

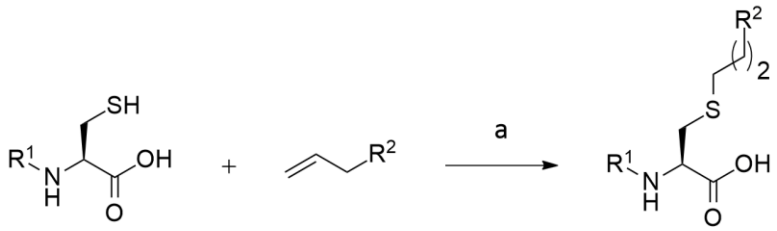

IV.50

Entry	R^1	R^2	Product	Ratio thiol/ene	Temperature (°C)	Time (h)	Yield
1	Ac **(IV.21)**	$(CH_2)_4CH_3$	**IV.50a**	1:3	80	1.5	62%
2	Ac **(IV.21)**	OH	**IV.50b**	1:3	80	2	100%
3	Fmoc **(IV.6)**	OH	**IV.50c**	1:3	80	3.5	100%
4	Fmoc **(IV.6)**	T **(IV.33)**	**IV.50d**	1:1	90	5	31%
5	Fmoc **(IV.6)**	T **(IV.33)**	**IV.50d**	1:3	90	3	57%
6	Fmoc **(IV.6)**	T **(IV.33)**	**IV.50d**	3:1	90	5	63%
7	Fmoc **(IV.6)**	$C(Boc)_2$ **(IV.31)**	**IV.50e**	1:3	90	3	21%
8	Fmoc **(IV.6)**	$A(Boc)_2$ **(IV.32)**	**IV.50f**	1:3	80	3	42%

Thermally thiol-ene reaction worked well when *N*-protected cysteines were used. Comparing different *N*-protected cysteines, the reaction with **IV.21** (entry 2) was faster than the reaction using **IV.6** (entry 3) but the yield was excellent in both cases. Besides that, it was observed that a better yield was obtained when one of the reagents was in excess (entries 4, 5 and 6). Since yields obtained when the thiol/ene ratio was 3:1 or 1:3

were similar, the remaining reactions were done with a thiol/ene ratio of 1:3 because the reaction was faster (entries 5 and 6). The reaction duration is important since thermal deprotection of Boc can occur (as seen in chapter III, page 98). This can also explain why **IV.50e** and **IV.50f** presented a lower yield compared with the reactions of unprotected thymine (entries 6-8).

When thiol-ene reactions between dipetides and alkenes were tried (Table IV.11), the results were quite different. In these conditions, the only product successfully obtained was **IV.51a** (entry 1). Even though, this reaction took longer reaction times and presented a lower yield when compared with the correspondent reaction with cysteine **IV.21** (entry 1, Table IV.10).

Table IV.11. Reaction conditions used in thermally induced thiol-ene reaction of dipeptides with different alkenes. Reagents and conditions: a) AIBN, DCE.

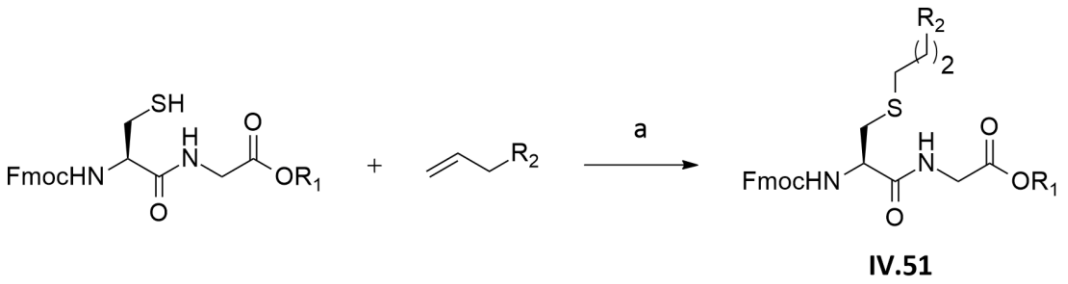

IV.51

Entry	R^1	R^2	Product	Ratio thiol/ene	Temperature (°C)	Time (h)	Yield
1	Et **(IV.7a)**	OH	**IV.51a**	1:3	80	20	21%
2	Et **(IV.7a)**	Br	**IV.51b**	1:3	90	19	-
3	Et **(IV.7a)**	Br	**IV.51b**	1:3	90	3	-
4	Et **(IV.7a)**	T **(IV.33)**	**IV.51c**	1:3	90	23	-
5	Et **(IV.7a)**	$C(Boc)_2$ **(IV.31)**	**IV.51d**	1:3	90	23	-
6	Et **(IV.7a)**	$A(Boc)_2$ **(IV.32)**	**IV.51e**	1:3	90	20	-
7	Bn **(IV.7b)**	T **(IV.33)**	**IV.51f**	1:3	90	23	-
8	Bn **(IV.7b)**	$C(Boc)_2$ **(IV.31)**	**IV.51g**	1:3	90	23	-

When allyl bromide was used (entries 2 and 3, Table IV.11), the desired thiol-ene coupling product **IV.51b** was not obtained and instead it was obtained the *S*-alkylated dipeptide **IV.52** in low yield (19%). The mechanism that can explain the formation of this product is displayed in Scheme IV.12.

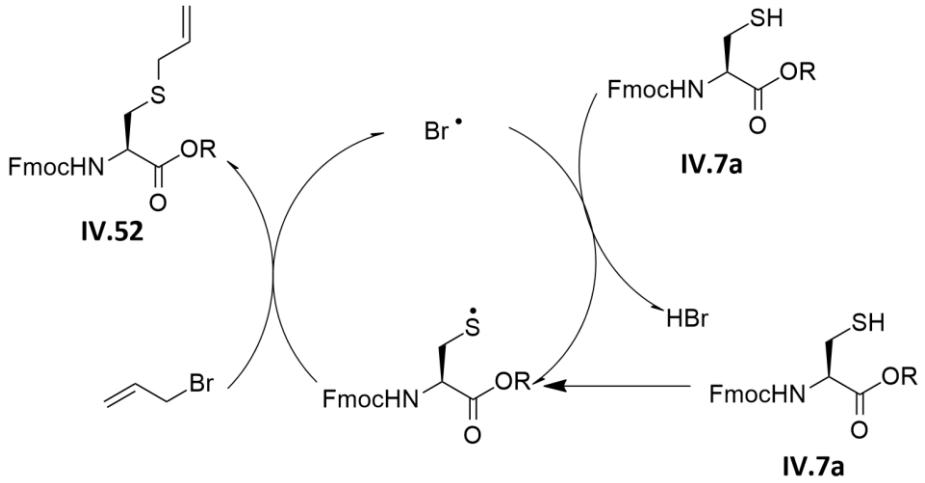

Scheme IV.12. Proposed mechanism for the formation of **IV.52** (R= GlyOEt).

The inability to obtain chimeric dipeptides with nucleobase side chains (entries 4-8, Table IV.11) can be related either with thermal deprotection of Boc or with thermal decomposition of the dipeptide due to the extended reaction times.

2.2.3.3.3. Photochemically induced thiol-ene reactions

Otherwise, experiments under photochemical conditions were also performed. Similarly to what occurred with the thermally induced reactions, the conditions were initially optimized with cysteines bearing different protecting groups and with different alkenes. As exemplified in Tables IV.12 and IV.13, the reactions occurred at room temperature by irradiation at maximum wavelength of 365 nm, under inert atmosphere, and in the presence of DPAP as sensitizer.[551]

These reaction conditions gave better yields and are shorter than thermally-induced ones. Besides that, the excess of alkene turned out to be a key element in this approach since reactions with a thiol/ene ratio of 1:3 presented consistently better yields (entries 3 and 6, Table IV.12).

Table IV.12. Reaction conditions used in photochemically induced thiol-ene reaction of *N*-protected cysteines with different *N*-allylated Boc-protected nucleobases. Reagents: a) DPAP, DCE.

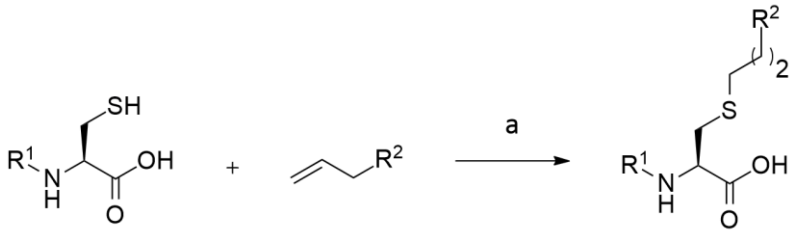

IV.50

Entry	R^1	R^2	Product	Ratio thiol/ene	Conc. [M]	Time (h)	Yield
1	Ac **(IV.21)**	$(CH_2)_4CH_3$	**IV.50a**	1:3	0.6	1	100%
2	Fmoc **(IV.6)**	T **(IV.33)**	**IV.50d**	1:1	0.6	4	66%
3	Fmoc **(IV.6)**	T **(IV.33)**	**IV.50d**	1:3	0.6	2	87%
4	Fmoc **(IV.6)**	T **(IV.33)**	**IV.50d**	3:1	0.3	2	57%
5	Fmoc (**IV.6)**	$C(Boc)_2$ **(IV.31)**	**IV.50e**	1:1	0.6	3	57%
6	Fmoc **(IV.6)**	$C(Boc)_2$ **(IV.31)**	**IV.50e**	1:3	0.6	2	78%
7	Fmoc **(IV.6)**	$C(Boc)_2$ **(IV.31)**	**IV.50e**	3:1	0.3	4	47%
8	Fmoc **(IV.6)**	G(Boc) **(IV.46)**	**IV.50g**	1:3	0.6	3	30%

Using the photochemically induced thiol-ene reaction, it was possible to obtain the final chimeric dipeptides, functionalized with all nucleobases, in moderate yields (Table IV.13).

Table IV.13. Reaction conditions tried photochemically induced thiol-ene reaction of dipeptides with different *N*-allylated Boc-protected nucleobases. Reagents: a) DPAP, DCE.

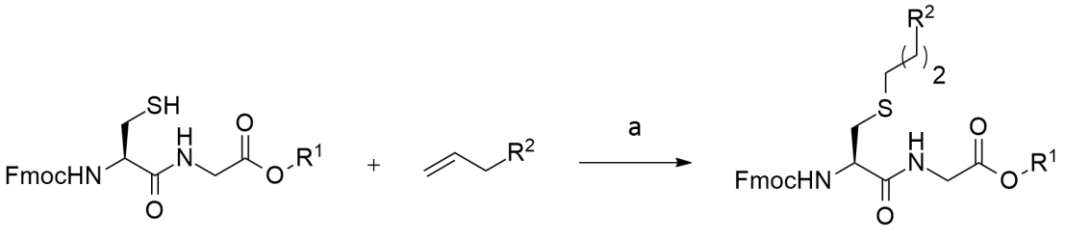

IV.51

Entry	R^1	R^2	Product	Ratio thiol/ene	Time (h)	Yield
1	Et **(IV.7a)**	T **(IV.33)**	**IV.51c**	1:3	2	51%
2	Et **(IV.7a)**	$A(Boc)_2$ **(IV.32)**	**IV.51e**	1:3	3	48%
3	Bn **(IV.7b)**	T **(IV.33)**	**IV.51f**	1:3	3	49%
4	Bn **(IV.7b)**	$C(Boc)_2$ **(IV.31)**	**IV.51g**	1:3	3	62%
5	Bn **(IV.7b)**	$A(Boc)_2$ **(IV.32)**	**IV.51h**	1:3	3	57%
6	Bn **(IV.7b)**	G(Boc) **(IV.46)**	**IV.51i**	1:3	3	44%

Relatively to chimeric dipeptides, two routes could be followed (Scheme IV.13): (a) the thiol-ene reaction was performed between the dipeptide and the *N*-allylated nucleobase or (b) the chimeric cysteine amino acid was initially synthesise and then coupled with glycine, Comparing the overall yields of the two routes (36% vs. 53%, respectively), route b proved to be more efficient.

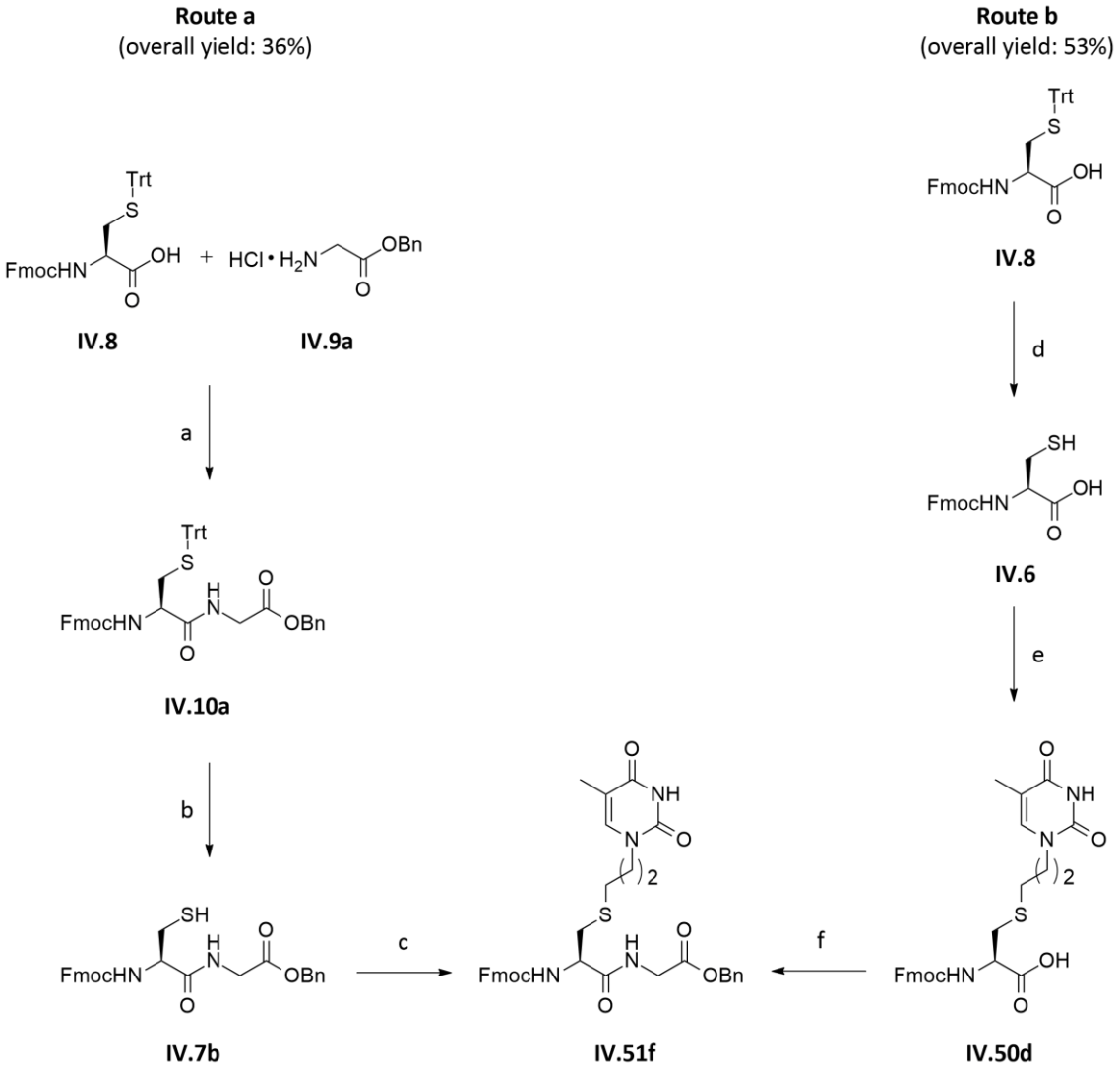

Scheme IV.13. Comparison of two synthetic pathways to obtain **IV.51f**. Reagents and conditions: a) TBTU, HOBt, DIPEA, DMF, rt, o/n, 92%; b) TFA, TES, DCM, rt, 3h, 80%; c) **IV.33**, DPAP, DCE, hv, rt, 3h, 49%; d)TFA, TES, DCM, rt, 3h, 87%; e) **IV.33**, DPAP, DCE, hv, rt, 2h, 87%; f) **IV.9a**, TBTU, HOBt, DIPEA, DMF, rt, o/n, 70%

3. Conclusion

Chimeric cysteine and cysteine-based dipeptides, functionalized with all nucleobases were successfully accomplished yielding a library of 10 new α-PNA building blocks. The formation of the C-S bond was the most challenging step of this synthesis but was successfully overpassed when the thiol-ene reaction was used. The first step of this pathway consisted in the regioselective synthesis of *N*-allyl derivatives of nucleobases. Then, both thermally and photochemically induced thiol-ene conditions were tried either with cysteine or cysteinyl-glycine dipeptides. Photochemically induced thiol-ene

reactions proved to be a better option since they gave better yields in shorter reactions times particularly for reactions with dipeptides as the chimeric products were only obtained in these conditions.

CHAPTER V

V. GENERAL CONCLUSIONS AND FUTURE PERSPECTIVES

The dream of modern drug research is to discover biologically active molecules that are absolutely specific and able to act efficiently only on the molecular targets responsible for the disease progression. In order to try to target nucleic acids in that way, different approches were used such as G4 ligands and oligonucleotide analogues.

The main goal of this thesis was to develop novel DNA ligands, more specifically, (i) to study new scaffolds that could act as G4 ligands (Chapter II and Chapter III) and (ii) to design and prepare novel monomers of α- PNA with increased structural diversity (Chapter IV).

The design of the G4 ligands was based on the structural features usually identified as favorable for the nucleic acid-molecule interaction. A library of eleven novel simetric compounds presenting three different aromatic cores (benzene, nafthalene and 2,7-biphenyl naphthalene) flanked by side chains with heteroatoms and amine terminal groups were synthesised with moderate to good yields. Based on the antiproliferative activity of the compounds and on the cytotoxicity assays results, some SAR elucidation was made. Among the synthesised compounds, four naphthalene based derivatives (**II.18a-II.18d**) and one 2,7-biphenyl naphthalene derivative (**II.19**) stood out by the their interesting antiproliferative activities over three cancer cell lines, specially against HT-29 where the five compounds presented lower IC_{50} values than cisplatin. Within all the tested compounds, compound **II.19** with a higher aromatic surface core presented the lowest IC_{50} values in the three cancer cell lines. **II.19** is an excellent starting point for further optimization. The activity results herein reported for these naphthalene derivatives have encouraged the search for the mechanism of action of these compounds. As they were inicially designed to act as G4 ligands, a FRET-melting assay was carried out. However, the antiproliferative activity did not seem to result from its action as G4 ligands since the compounds tested only presented a minor effect on G4 stabilization. Their poor action as G4 stabilizers can be explained by the small aromatic surface of these compounds (compared to the G-quartet) and by the flexibility of the compounds. In order to obtain better and more selective G4 stabilizers, molecules with bigger aromatic surface should be synthesised. For example, it would be interesting to synthesise compounds with where the naphthalene ring will be flanked by aromatic rings, such as benzimidazole, instead of the alkyl chain. Based on the antiproliferative activity of the compounds, **II.18a**, **II.18b** and **II.19** were choosen to assess apoptosis induction. In agreement with the lower IC_{50} values of compound **II.19** toward HT-29 cell line, this compound presented particularly interesting results as at IC_{50} concentration it was able to increase apoptosis up to 50%, as compared to vehicle control exposure. When cells were exposed to the same compounds at 2-fold IC_{50} concentration, the

percentage of cells undergoing apoptosis further increased. In addition, the percentage of HT-29 apoptotic cells is related to the IC_{50} values of **II.18a** and **II.18b**. Taken together, these results suggest that induction of apoptosis is an important mechanism underlying compounds effects.

In order to identify compounds with improved G4 stabilizing ability, a library of six novel benzo[*h*][1,6]naphthyridin-2(1*H*)-one derivatives with different terciary amine side chains were synthesised. While the synthesis of compounds with an aromatic side chain (**III.2**) was straightforward, the synthesis of derivatives with alkylamines (**III.3** and **III.4**) presented more challenges. When tested as G4 ligands, these compounds presented better stabilizing capacity when compared with the compounds described in the previous chapter. This difference can be ascribed to their higher aromatic surface which can allow a better π-π interaction between the G-quartet and the aromatic surface of ligands. Despite containing this important structural feature, the ability of these Torin-based ligands to stabilize G4 did not reach the binding efficiency reported for other polyaromatic ligands, thus highlighting the need to continue the optimization of the Torin scaffold as putative G4 ligands. Based on FRET-melting assays data, it would be interesting to synthesise compounds: (a) with a cationic center on the aromatic core and two alkyl side chains with terminal terciary amine groups in positions N^1 and C^9; or (b) similar to **III.2b** but with an more flexible alkylamine instead of the methyl piperazine to try to improve the interaction of the amine tertiary group with the phosphate groups of DNA. Besides that, other Torin derivatives with alkyl amine substituents in other positions N^1 and C^{10} or cationic derivatives with akyl amine substituents in N^1 and N^{13} could also be interesting molecules.

Chimeric cysteine and cysteine-based dipeptides, functionalized with all nucleobases were also successfully accomplished. To form the C-S bond, we used the reaction of the adequately protected allyl nucleobases with cysteine or cysteinyl-glycine dipeptides under thermally and photochemically induced thiol-ene conditions. The photochemically induced thiol-ene reactions proved to be a better option since they gave better yields in shorter reactions times particularly for reactions with dipeptides as these chimeric products were only obtained in these conditions. These chimeric products can be used with different purposes. The more obvious is its use in the synthesis of α-PNA analogues. Its sequence can be based, for example, on clinically relevant aptamers (short ssDNA segments). The strength of the interaction between the newly-developed α-PNA aptamer analogues and their complementary DNA strands, as well as, their protein targets can be evaluated applying several physico-chemical methodologies. The chimeric amino acids can also be used to synthesise fluorescein-labelled α-PNAs, candidates for molecular recognition in biosensor design. Alternativelly, these chimeric aminoacids can also be important in controlling the spatial

arrangement of peptides and construction of conformationally rigid, cyclic peptides without the need for covalent-bond reinforcement such already reported.[552]

In conclusion, this thesis opened new perspectives and reinforced previously existing perceptions over the structural feactures that G4 ligand should have. With regards to non-fused aromatic ligands, this work confirmed that the presence of more than one aromatic core (such as benzene or naphtalene) seems to be essential to: (a) have an aromatic surface big enough to selectively interact with the G-quartet; (b) give some rigidity to the structure. Respecting the polyaromatic fused compounds, a new scaffold was tested as G4 ligand and the FRET-melting data give precious information to be used in the design of new derivatives of this scaffold. Besides that, it is also essential to highlight the very good antiproliferative results obtained with the naphthalene 2,7-biphenyl naphthalene derivatives. The synthesis of new α-PNA monomers containing sulfur was also an achivement. From a chemical point of view, this work is also interesting for the variety of reactions that were employed where the click thiol-ene reactions stood out due to its use in the synthesis of compounds from different chapters of this thesis.

CHAPTER VI

VI. EXPERIMENTAL SECTION

1. Chemistry

All chemicals and solvents were of analytical reagent grade and were purchased from Alfa Aesar or Sigma-Aldrich.

Thin layer chromatography (TLC) was performed using Merck silica gel 60F254 aluminium plates. All reactions were monitored by TLC. Flash column chromatography was performed using Merck silica gel 60 (230-400 mesh ASTM) eluting with various solvent mixtures and using an air aquarium pump to apply pressure.

NMR spectra were obtained on a Bruker 400 Ultra-Shield instrument (^{1}H 400 MHz, ^{13}C 101 MHz) and on a Bruker 300 Avance spectrometer (^{1}H 300 MHz, ^{13}C 75 MHz). using deuterated chloroform, methanol or dimethylsulfoxide as solvents; chemical shifts are expressed in parts per million (ppm, δ) referenced to the solvent used and the proton coupling constants (*J*) in hertz (Hz). Multiplicities are given as: s (singlet), bs (broad singlet), d (doublet), dd (double doublet), dt (double triplet), t (triplet), q (quartet), quint (quintuplet) and m (multiplet).

Mass analyses were determined using a Micromass Quattro Micro API spectrometer, equipped with Waters 2695 HPLC Module and Waters 2996 Photodiode Array Detector, by LCLEM, Faculty of Pharmacy from the University of Lisbon, Portugal. High resolution mass spectra were performed in Unidade de Espectrometria de Masas (HMRS), Santiago de Compostela, Spain. Elemental analysis (for C, H, and N) were determined using a FLASH 2000 analyser, performed by LCLEM, Faculty of Pharmacy from the University of Lisbon, Portugal.

Melting points were determined using a Kofler Bock Monoscop M and are uncorrected.

The household UVA lamp apparatus was equipped with four 15 W tubes (1.5 x 27 cm each). Photoinduced reactions were carried out in a glass vial (diameter: 1 cm; wall thickness: 0.65 mm), sealed with a natural rubber septum, located 2.5 cm away from the UVA lamp (irradiation on sample: 365 nm, 1.04 W/m^{2}).

2. Synthesis

2.1. Synthesis of compounds described in Chapter II

2.1.1. General methods

General procedure A for triflation reaction. To a suspension of an aromatic alcohol (1 equiv.) in DCM (0.6 M) at 0 ^{o}C was added triethylamine (2.2 equiv.). After 15 min, trifluorometanesulfonic anhydride (2.2 equiv.) was slowly added to the reaction mixture. Then, the reaction mixture was allowed to warm to rt. After 4-6 h, the reaction was poured into water and extracted with DCM. The organic phase was washed with water, brine and dried with anhydrous Na_2SO_4. The solvent was removed under reduced pressure and the crude product was purified by flash column chromatography.

General procedure B for the Suzuki cross-coupling reaction: To a solution of triflate or bromide (1 equiv.) in 1,4-dioxane (0.2 M) at rt in a sealed tube, were added allylboronic acid pinacol ester (2.6 equiv.), $K_3PO_4 \bullet H_2O$ (3 equiv.) and tetrakis(triphenylphosphine)palladium(0) (6 mol%). After degassing during 5 min, the reaction mixture was refluxed at 110 ^{o}C o/n before being cooled at rt, diluted in Et_2O and filtered through a pad of celite. The filtrate was concentrated under reduced pressure and the crude product was purified by flash column chromatography.

General method C for the thiol-ene reaction: Thiol (2.8 or 4 equiv.) and DPAP (0.1 equiv.) were added to an alkene (1 equiv.). All the reagents were dissolved in DCE (solvent was degassed for 15 min prior to use) (0.6 M). The solution was irradiated at rt for 15 min-3 h under magnetic stirring and then concentrated under reduced pressure. The crude product was purified by flash column chromatography.

General Procedure D for ester hydrolysis: To a solution of methyl ester (1 equiv.) in THF:H_2O (1:1) (0.2 M) was added LiOH (2.5 or 5 equiv.). The reaction mixture was then stirred at rt during 4 h. After THF evaporation, the reaction mixture was acidified with 1N aqueous HCl and the aqueous phase was extracted with DCM. The combined organic phases were washed with water, brine and dried with anhydrous Na_2SO_4. The solvent was then removed under reduced pressure to afford the desired compounds.

General procedure E for amide synthesis: To a suspension of acid (1.1 equiv.) in dry DCM (0.25 M) was added DIPEA (2 equiv.) and TBTU (2.2 equiv.). After 10 min, the amine (2 equiv.) was added. The reaction mixture was then stirred at rt and under nitrogen

atmosphere o/n. Then, the reaction was diluted with EtOAc and the organic phase was washed with water. The aqueous phased was acidified with 10% aqueous $KHSO_4$ and extracted with EtOAc. After that, the aqueous phase was basified with NaOH 1N and extracted again with EtOAc. The combined organic phases were washed with water, brine and dried with anhydrous Na_2SO_4. The solvent was removed under reduced pressure to afford the desired compounds.

2.1.2. Synthesis of compounds **II.23** and **II.31**

1,3-phenylene bis(trifluoromethanesulfonate) (II.23)

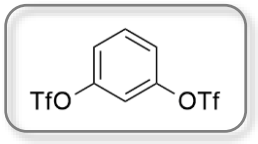

1,3-dihydroxybenzene **II.22** (220 mg, 3.63 mmol) reacted with trifluorometanesulfonic anhydride (672 µL, 4.00 mmol) was treated under the conditions described in general procedure A. The crude product was purified by flash column chromatography (hexane/EtOAc, 95:5) to afford **II.23** as a colorless oil (514 mg, 76%). ^{1}H NMR (400 MHz, $CDCl_3$) δ 7.59 (t, *J* = 8.4 Hz, 1H, H_5), 7.37 (dd, *J* = 8.4, 2.0 Hz, 2H, H_4, H_6), 7.26 (s, 1H, H_2).

Naphthalene-2,7-diyl bis(trifluoromethanesulfonate) (II.31)

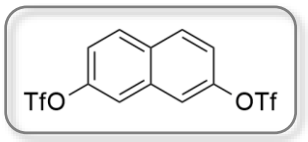

To a suspension of 2,7-dihydroxynaphthalene **II.30** (1 g, 6.24 mmol) reacted with trifluorometanesulfonic anhydride (2.56 mL, 13.74 mmol) under the conditions described in general procedure A. The crude product was purified by flash column chromatography (hexane/EtOAc, 95:5) to afford **II.31** as a white solid (2.44 g, 92%). M.p. 60-61 ºC; ^{1}H NMR (400 MHz, $CDCl_3$) δ 8.01 (d, *J* = 8.8 Hz, 2H, H_4, H_5), 7.81 (d, *J* = 2 Hz, 2H, H_1, H_8), 7.48 (dd, *J* = 8.8, 2 Hz, 2H, H_3, H_6). Analytical date were in agreement with those already published.[553]

2.1.3. Synthesis of compounds **II.21**, **II.29**, **II.33** and **II.34**

1,3-diallylbenzene (II.21)

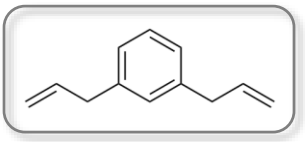

1,3-dibromobenzene **II.24** (500 mg, 2.12 mmol) was coupled with allylboronic acid pinacol ester (1.03 mL, 5.51 mmol) under the conditions described in general procedure B. The crude product was purified by flash column chromatography (hexane 100%) to afford **II.21** as a colorless oil (214 mg, 64%). ^{1}H NMR (400 MHz, $CDCl_3$) δ 7.22 (t, J = 7.4 Hz, 1H, H_5), 7.03 (d, *J* = 8.1 Hz, 3H, H_2, H_4, H_6), 5.97 (ddt, *J* = 16.9, 10.1,

6.7 Hz, 2H, C*H*=CH_2), 5.12 – 5.03 (m, 4H, CH=CH_2), 3.38 (t, *J* = 8.0 Hz, 4H, CH_2CH=CH_2). ^{13}C NMR (101 MHz, $CDCl_3$) δ 140.3 (C_1, C_3), 137.6 (*C*H=CH_2), 129.0 (C_5), 128.6 (C_6), 126.5 (C_2,C_4), 115.9 (CH=*C*H_2), 40.3 (*C*H_2CH=CH_2). Analytical date were in agreement with those already published.[554]

2,7-diallylnaphthalene (II.29)

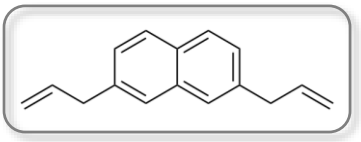

II.31 (800 mg, 1.89 mmol) was coupled with allylboronic acid pinacol ester (919 µL, 4.90 mmol) under the conditions described in the general procedure B. The crude product was purified by flash column chromatography (hexane/EtOAc, 9:1) to afford **II.29** as a colorless oil (251 mg, 64%). ^{1}H NMR (400 MHz, $CDCl_3$) δ 7.74 (d, *J* = 8.4 Hz, 2H, H_4, H_5), 7.57 (s, 2H, H_1, H_8), 7.28 (d, *J* = 8.4 Hz, 2H, H_3, H_6), 6.04 (m, 2 H, C*H*=CH_2), 5.13 (d, *J* = 10.4 Hz, 2H, CH=CH_{trans}), 5.10 (d, *J* = 2.4 Hz, 2H, CH=CH_{cis}), 3.54 (d, *J* = 6.6 Hz, 4H, CH_2CH=CH_2). ^{13}C NMR (101 MHz, $CDCl_3$) δ 137.8 (C_2, C_7), 137.5 (*C*H=CH_2), 134.0 (C_9), 131.0 (C_{10}), 127.8 (C_4, C_5), 127.0 (C_3, C_6), 126.4 (C_1, C_8), 116.1 (CH=*C*H_2), 40.5 (*C*H_2CH=CH_2). Analytical date were in agreement with those already published.[555]

7-allylnaphthalen-2-ol (II.33)

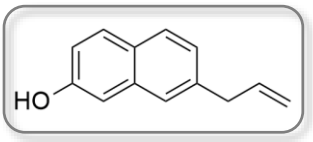

II.33 was obtained as a minor product of the previous reaction. White solid (53 mg, 15%). M.p. 128-133 °C; ^{1}H NMR (400 MHz, $CDCl_3$) δ 8.11 (s, 1H, H_1), 7.92 (d, *J* = 8.4 Hz, 1H, H_4), 7.83 (d, *J* = 8.4 Hz, 2H, H_3, H_5), 7.73 (s, 1H, H_8), 7.36 (d, *J* = 8.4 Hz, 1H, H_6), 6.16 – 6.02 (m, 1H, C*H*=CH_2), 5.22 – 5.12 (m, 2H, CH=CH_2), 3.59 (d, *J* = 6.4 Hz, 2H, CH_2CH=CH_2). ^{13}C NMR (101 MHz, $CDCl_3$) δ 138.8 (C_2), 138.2 (C_7), 137.4 (*C*H=CH_2), 134.1 (C_9), 131.5 (C_{10}), 128.4 (C_3), 127.9 (C_4), 127.7 (C_6), 127.2 (C_8), 125.9 (C_1), 125.3 (C_5), 116.3 (CH=*C*H_2), 40.5 (*C*H_2CH=CH_2). MS (ESI) *m/z* 185 $[M+H]^+$.

2,7-divinylnaphthalene (II.34)

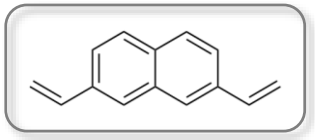

To a solution of 2,7-dibromonaphthalene **II.35** (300 mg, 1.05 mmol, 1 equiv.) in dry 1,4-dioxane (0.1 M) at rt were added vinylboronic acid pinacol ester (463 µL, 2.73 mmol, 2,6 equiv.), Na_2CO_3 1M (6 equiv.) and bis(triphenylphosphine)palladium(II) dichloride (10 mol%). After degassing during 5 min, the reaction mixture was stirred at 80 °C o/n before being cooled at rt, diluted in Et_2O and filtered through a pad of celite. The filtrate was concentrated under reduced pressure and the crude product was purified by flash column chromatography (hexane 100%) to afford compound **II.34** as a white solid (158 mg, 84%). M.p. 75-76 °C; ^{1}H NMR

(400 MHz, $CDCl_3$) δ 7.76 (d, *J* = 8.6 Hz, 2H, H_4, H_5), 7.72 (s, 2H, H_1,H_8), 7.60 (d, *J* = 8.6 Hz, 2H, H_3, H_6), 6.87 (dd, *J* = 17.6, 10.8 Hz, 2H, C*H*=CH_2), 5.87 (d, *J* = 17.6 Hz, 2H, CH=CH_{trans}), 5.34 (d, *J* = 10.8 Hz, 2H, CH=CH_{cis}). ^{13}C NMR (101 MHz, $CDCl_3$) δ 137.0 (*C*H=CH_2), 135.5 (C_2, C_7), 133.8 (C_9), 133.0 (C_{10}), 128.1 (C_4, C_5), 126.6 (C_3, C_6), 123.4 (C_1, C_8), 114.4 (CH=*C*H_2). Analytical date were in agreement with those already published.[556]

2.1.4. Synthesis of compounds **II.41**, **II.43**, **II.44** and **II.46**

Dimethyl 2,2'-((1,3-phenylenebis(propane-3,1-diyl))bis(sulfanediyl))diacetate (II.41)

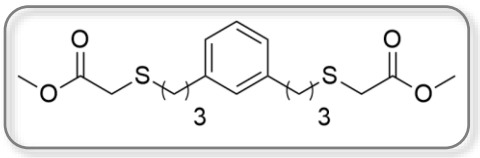

II.21 (214 mg, 1.35 mmol) was coupled with methyl thioglicolate (483 µL, 5.40 mmol) for 1 h under the conditions described in the general procedure C. The crude product was purified by flash column chromatography (hexane/EtOAc, 9:1) to afford **II.41** as an oil (269 mg, 54%). ^{1}H NMR (400 MHz, $CDCl_3$) δ 7.20 (t, *J* = 7.4 Hz, 1H, H_5), 7.01 (d, *J* = 8.0 Hz, 3H, H_2, H_4, H_6), 3.71 (s, 6H, CH_3), 3.23 (s, 4H, SCH_2C=O), 2.66 (dt, J = 17.6, 7.4 Hz, 8H, ArC$H_2$$CH_2$$CH_2S, ArCH_2$$CH_2CH_2$S), 1.96 – 1.86 (m, 4H, ArCH_2C$H_2$$CH_2$S). ^{13}C NMR (101 MHz, $CDCl_3$) δ 171.1 (*C*=O), 141.5 (C_1, C_3), 128.8 (C_5), 128.6 (C_6), 126.2 (C_2,C_4), 52.5 (*C*H_3), 34.7 (Ar*C*$H_2$$CH_2$$CH_2$S), 33.5 (S*C*$H_2$C=O), 32.2 (Ar$CH_2$$CH_2$*C*$H_2$S), 30.6 (Ar$CH_2$*C*$H_2$$CH_2$S).

Dimethyl 2,2'-((naphthalene-2,7-diylbis(propane-3,1-diyl))bis(sulfanediyl))diacetate (II.43)

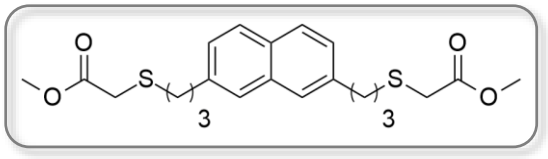

II.29 (250 mg, 1.20 mmol) was coupled with methyl thiolate (429 µL, 4.80 mmol) for 1 h under the conditions described in the general procedure C. The crude product was purified by flash column chromatography (hexane/EtOAc, 9:1) to afford **II.43** as a white solid (466 mg, 92%). ^{1}H NMR (400 MHz, $CDCl_3$) δ 7.73 (d, *J* = 8.2 Hz, 2H, H_4, H_5), 7.55 (s, 2H, H_1, H_8), 7.27 (d, *J* = 8.2 Hz, 2H, H_3, H_6), 3.70 (s, 6H, CH_3), 3.24 (s, 4H, SCH_2C=O), 2.87 (t, *J* = 7.6 Hz, 4H, ArC$H_2$$CH_2$$CH_2$S), 2.67 (t, *J* = 7.2 Hz, 4H, Ar$CH_2$$CH_2CH_2$S), 2.08 – 1.94 (m, 4H, ArCH_2C$H_2$$CH_2$S). ^{13}C NMR (101 MHz, $CDCl_3$) δ 171.1 (*C*=O), 139.0 (C_2, C_7), 133.8 (C_9), 130.8 (C_{10}), 127.9 (C_4, C_5), 126.7 (C_3, C_6), 126.2 (C_1, C_8), 52.5 (*C*H_3), 34.9 (Ar*C*$H_2$$CH_2$$CH_2$S), 33.5 (S*C*$H_2$C=O), 32.2 (Ar$CH_2$$CH_2$*C*$H_2$S), 30.5 (Ar$CH_2$*C*$H_2$$CH_2$S).

Methyl 2-((3-(7-hydroxynaphthalen-2-yl)propyl)thio)acetate (II.44)

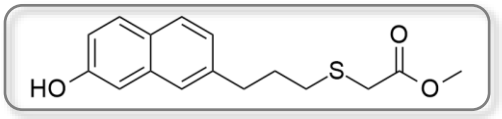

II.33 (53 mg, 0.29 mmol) was coupled with methyl thiolate (69 µL, 0.78 mmol) for 15 min under the conditions described in the general

procedure C**.** The crude product was purified by preparative TLC (hexane/EtOAc, 8:2) to afford **II.44** as a light yellow solid (64 mg, 77%). M.p. 57-60 °C; ^{1}H NMR (400 MHz, $CDCl_3$) δ 8.10 (s, 1H, H_1), 7.92 (d, J = 8.4 Hz, 1H, H_3), 7.82 (d, J = 8.4 Hz, 2H, H_4, H_5), 7.72 (s, 1H, H_8), 7.35 (d, J = 8.4 Hz, 1H, H_6), 3.72 (s, 3H, CH_3), 3.26 (s, 2H, SCH_2C=O), 2.92 (t, J = 7.4 Hz, 2H, ArCH_2CH$_2$CH$_2$S), 2.71 (t, J = 7.2 Hz, 2H, ArCH$_2$CH$_2$CH_2S), 2.10 – 2.01 (m, 2H, ArCH_2CH_2CH$_2$S). ^{13}C NMR (101 MHz, $CDCl_3$) δ 171.1 (C=O), 139.5 (C_7), 138.8 (C_2), 134.0 (C_9), 131.4 (C_{10}), 128.4 (C_3), 127.9 (C_4), 127.5 (C_6), 127.1 (C_8), 125.80 (C_1), 125.3 (C_5), 52.5 (CH$_3$), 34.9 (ArCH$_2$CH$_2$CH$_2$S), 33.6 (SCH$_2$C=O), 32.2 (ArCH$_2$CH$_2$$CH_2$S), 30.5 (ArCH$_2$$CH_2CH_2$S).

Dimethyl 2,2'-((naphthalene-2,7-diylbis(ethane-2,1-diyl))bis(sulfanediyl))diacetate (II.46)

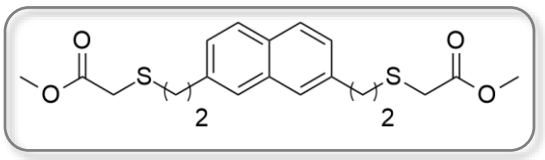

II.34 (158 mg, 0.88 mmol) was coupled with methyl thiolate (315 µL, 3.52 mmol) for 3 h under the conditions described in the general procedure C. The crude product was purified by flash column chromatography (hexane/EtOAc, 8:2) to afford **II.46** as a light yellow oil (177 mg, 51%). ^{1}H NMR (400 MHz, $CDCl_3$) δ 7.75 (d, J = 8.4 Hz, 2H, H_4, H_5), 7.60 (s, 2H, H_1,H_8), 7.30 (d, J = 8.4 Hz, 2H, H_3, H_6), 3.74 (s, 6H, CH_3), 3.25 (s, 4H, SCH_2C=O), 3.09 – 3.03 (m, 4H, ArCH_2CH$_2$S), 3.01 – 2.95 (m, 4H, ArCH$_2$CH_2S). ^{13}C NMR (101 MHz, $CDCl_3$) δ 171.0 (C=O), 137.9 (C_2, C_7), 133.8 (C9), 131.2 (C_{10}), 128.0 (C_4, C_5), 126.8 (C_3, C_6), 126.6 (C_1, C_8), 52.5 (CH$_3$), 35.9 (ArCH$_2$CH$_2$S), 34.1 (ArCH$_2$$CH_2$S), 33.7 (S$CH_2$C=O).

2.1.5. Synthesis of compounds **II.38**, **II.42**, **II.45** and **II.47**

2,2'-((1,3-phenylenebis(propane-3,1-diyl))bis (sulfanediyl))diacetic acid (II.38)

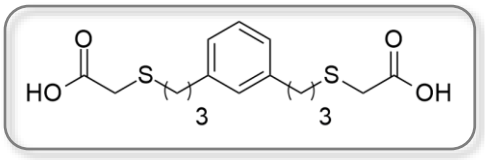

II.41 (269 mg, 0.73 mmol) was treated under the conditions described in the general procedure D to afford **II.38** as an incolor oil (238 mg, 96%). ^{1}H NMR (400 MHz, $CDCl_3$) δ 7.20 (t, J = 7.4 Hz, 1H, H_5), 7.00 (d, J = 8.3 Hz, 3H, H_2, H_4, H_6), 3.24 (s, 4H, SCH_2C=O), 2.68 (q, J = 7.4 Hz, 8H, ArCH_2CH$_2$CH$_2$S, ArCH$_2$CH$_2$CH_2S), 1.96 – 1.86 (m, 4H, ArCH$_2$CH_2CH$_2$S). ^{13}C NMR (101 MHz, $CDCl_3$) δ 177.9 (C=O), 141.6 (C_1, C_3), 128.6 (C_2), 128.5 (C_5), 126.4 (C_4, C_6), 34.7 (ArCH_2CH$_2$CH$_2$S), 34.5 (SCH_2C=O), 33.2 (ArCH$_2$CH$_2$CH_2S), 31.4 (ArCH$_2$CH_2CH$_2$S). MS (ESI) *m/z* 341 [M-H]$^-$.

2,2'-((naphthalene-2,7-diylbis(propane-3,1-diyl))bis (sulfanediyl))diacetic acid (II.42)

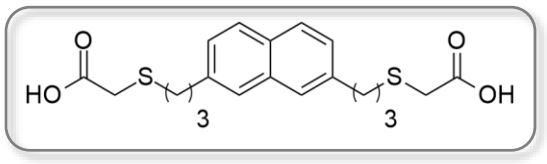

II.43 (563 mg, 1.34 mmol) was treated under the conditions described in the general procedure D to afford **II.42** as a white solid (479 mg, 91%). M.p. 132-135 ^{o}C; ^{1}H NMR (400 MHz, $CDCl_3$) δ 7.74 (d, *J* = 8.8 Hz, 2H, H_4, H_5), 7.63 (s, 2H, H_1, H_8), 7.24 (d, *J* = 8.8 Hz, 2H, H_3, H_6), 3.21 (s, 4H, SCH_2C=O), 2.91 (t, *J* = 6.4 Hz, 4H, ArCH_2CH$_2$CH$_2$S), 2.66 (t, *J* = 7.0 Hz, 4H, ArCH$_2$CH$_2$CH_2S), 2.08 – 1.98 (m, 4H, ArCH$_2$CH_2CH$_2$S). ^{13}C NMR (101 MHz, $CDCl_3$) δ 177.8 (*C*=O), 138.5 (C_2, C_7), 133.7 (C_9), 130.8 (C_{10}), 127.9 (C_4, C_5), 126.9 (C_3, C_6), 126.7 (C_1, C_8), 34.2 (Ar*C*H$_2$CH$_2$CH$_2$S), 31.5 (S*C*H$_2$C=O), 31.0 (ArCH$_2$CH$_2$*C*H$_2$S), 29.8 (ArCH$_2$*C*H$_2$CH$_2$S). MS (ESI) *m/z* 391 $[M-H]^-$.

2-((3-(7-hydroxynaphthalen-2-yl)propyl)thio)acetic acid (II.45)

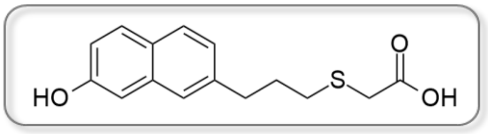

II.44 (71 mg, 0.24 mmol) was treated under the conditions described in the general procedure D to afford **II.45** as an off-white solid (57 mg, 84%). M.p. 127-130 ^{o}C; ^{1}H NMR (400 MHz, DMSO-d_6) δ 8.28 (s, 1H, H_1), 8.00 (d, *J* = 8.4 Hz, 1H, H_4), 7.93 (d, *J* = 8.4 Hz, 1H, H_3), 7.89 (d, *J* = 8.4 Hz, 1H, H_5), 7.82 (s, 1H, H_8), 7.42 (d, *J* = 8.4 Hz, 1H, H_6), 3.26 (s, 2H, S*C*H$_2$C=O), 2.85 (t, *J* = 7.4 Hz, 2H, ArCH_2CH$_2$CH$_2$S), 2.64 (t, *J* = 7.2 Hz, 2H, ArCH$_2$CH$_2$CH_2S), 2.01 – 1.87 (m, 2H, ArCH$_2$CH_2CH$_2$S). ^{13}C NMR (101 MHz, DMSO-d_6) δ 171.8 (*C*=O), 139.7 *(*C_7), 137.5 (C_2), 133.6 (C_9), 131.0 (C_{10}), 128.4 (C_4), 127.7 (C_6, C_5), 126.7 (C_8), 125.2 (C_1), 124.7 (C_3), 34.3 (Ar*C*H$_2$CH$_2$CH$_2$S), 33.3 (S*C*H$_2$C=O), 31.4 (ArCH$_2$CH$_2$*C*H$_2$S), 30.2 (ArCH$_2$*C*H$_2$CH$_2$S).

2,2'-((naphthalene-2,7-diylbis(ethane-2,1-diyl))bis (sulfanediyl))diacetic acid (II.47)

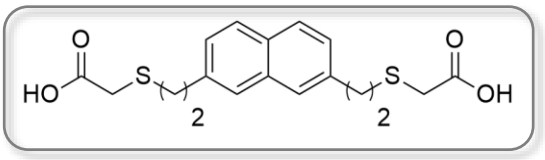

II.46 (150 mg, 0.38 mmol) was treated under the conditions described in the general procedure D to afford **II.47** as an incolor oil (75 mg, 54%). ^{1}H NMR (400 MHz, $CDCl_3$) δ 7.72 (d, *J* = 8.3 Hz, 2H, H_4, H_5), 7.59 (s, 2H, H_1,H_8), 7.27 (d, *J* = 8.3 Hz, 2H, H_3, H_6), 3.23 (s, 4H, SCH_2C=O), 3.02 (dd, J = 15.1, 6.6 Hz, 8H, ArCH_2CH$_2$S, ArCH$_2$CH_2S). ^{13}C NMR (101 MHz, $CDCl_3$) δ 175.2 (*C*=O), 137.7 (C_2, C_7), 133.7 (*C*9), 131.1 (C_{10}), 128.0 (C_4, C_5), 126.8 (C_3, C_6), 126.7 (C_1, C_8), 35.7 (Ar*C*H$_2$CH$_2$S), 34.1 (ArCH$_2$*C*H$_2$S), 33.7 (S*C*H$_2$C=O).

2.1.6. Synthesis of compounds **II.16a-b**, **II.42**, **II.17**, **II.18a-e** and **II.48**

2,2'-((1,3-phenylenebis(propane-3,1-diyl))bis(sulfanediyl))bis(*N*-(2-(dimethylamino) ethyl)acetamide) (II.16a)

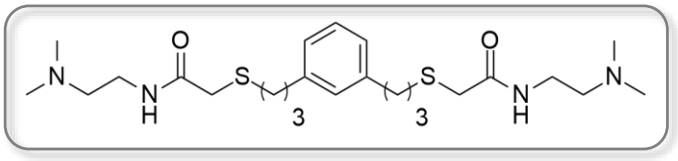

II.38 (75 mg, 0.22 mmol) was coupled with *N*,*N*-dimethylethylenediamine (43 µL,0.40 mmol) according to the general procedure E to afford **II.16a** as a salmon-coloured solid (75 mg, 78%). ^{1}H NMR (400 MHz, $CDCl_3$) δ 7.26 (bs, 2H, N*H*), 7.17 (t, *J* = 7.5 Hz, 1H, H_5), 7.00 – 6.92 (m, 3H, H_2, H_4, H_6), 3.32 (dd, *J* = 11.4, 5.8 Hz, 4H, NHCH_2CH$_2$NMe$_2$), 3.20 (s, 4H, SCH_2C=O), 2.65 (t, *J* = 7.4 Hz, 4H, ArCH_2CH$_2$CH$_2$S), 2.53 (t, *J* = 7.4 Hz, 4H, ArCH$_2$CH$_2$CH_2S), 2.39 (t, *J* = 5.8 Hz, 4H, NHCH$_2$CH_2NMe$_2$), 2.19 (s, 12H, CH_3), 1.87 (quint, *J* = 7.4 Hz, 4H, ArCH$_2$CH_2CH$_2$S). ^{13}C NMR (101 MHz, $CDCl_3$) δ 169.0 (*C*=O), 141.4 (C_1, C_3), 128.7 (C_2), 128.6 (C_5), 126.2 (C_4, C_6), 57.8 (NHCH$_2$*C*H$_2$NMe$_2$), 45.2 (*C*H$_3$), 37.1 (NH*C*H$_2$CH$_2$NMe$_2$), 36.1 (S*C*H$_2$C=O), 34.7 (Ar*C*H$_2$CH$_2$CH$_2$S), 32.4 (ArCH$_2$CH$_2$*C*H$_2$S), 30.7 (ArCH$_2$*C*H$_2$CH$_2$S). MS (ESI) *m/z* 483 $[M+H]^+$. HRMS-ESI: *m/z* $[M + H]^+$ calcd for $C_{24}H_{42}N_4O_2S_2$: 483.2822, found: 483.2822.

2,2'-((1,3-phenylenebis(propane-3,1-diyl))bis(sulfanediyl))bis(1-(4-methylpiperazin-1-yl)ethanone) (II.16b)

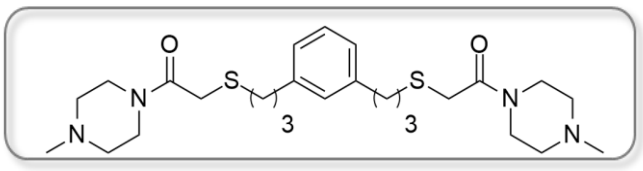

II.38 (75 mg, 0.22 mmol) was coupled with 1-methylpiperazine (44 µL,0.40 mmol) according to the general procedure E to afford **II.16b** as a coulorless oil (75 mg, 78%). ^{1}H NMR (300 MHz, $CDCl_3$) δ 7.19 (t, *J* = 7.8 Hz, 1H, H_5), 7.03-6.97 (m, 3H, H_2, H_4, H_6), 3.63 (t, *J* = 5.0 Hz, 4H, N(CH$_2$CH$_2$)NMe), 3.51 (t, *J* = 5.0 Hz, 4H, N(CH$_2$CH$_2$)NMe), 3.31 (s, 4H, SCH_2C=O), 2.67 (dt, *J* = 14.6, 7.5 Hz, 8H, ArCH_2CH$_2$CH$_2$S, ArCH$_2$CH$_2$CH_2S), 2.44 (t, *J* = 5.0 Hz,4H, N(CH$_2$CH$_2$)NMe), 2.37 (t, *J* = 5.0 Hz,4H, N(CH$_2$CH$_2$)NMe), 2.30 (s, 6H, CH_3), 1.93 (quint, *J* = 7.5 Hz, 4H, ArCH$_2$CH_2CH$_2$S). ^{13}C NMR (75 MHz, $CDCl_3$) δ 167.9 (*C*=O), 141.6 (C_1, C_3), 128.8 (C_2), 128.5 (C_5), 126.2 (C_4, C_6), 55.1 (N(CH$_2$CH$_2$)NMe), 54.8 (N(CH$_2$CH$_2$)NMe), 46.4 (N(CH$_2$CH$_2$)NMe), 46.1 (*C*H$_3$), 41.8 (N(CH$_2$CH$_2$)NMe), 34.8 (Ar*C*H$_2$CH$_2$CH$_2$S), 33.4 (S*C*H$_2$C=O), 31.9 (ArCH$_2$CH$_2$*C*H$_2$S), 30.9 (ArCH$_2$*C*H$_2$CH$_2$S). MS (ESI) *m/z* 507 $[M+H]^+$. Anal. Calcd for $C_{26}H_{43}N_4O_2S_2 \cdot 0.25H_2O$: C, 61.07; H, 8.40; N, 10.96. Found: C, 61.02; H, 8.62; N, 10.70.

2,2'-((naphthalene-2,7-diylbis(ethane-2,1-diyl))bis(sulfanediyl))bis(*N*-(2-(dimethylamino)ethyl)acetamide) (II.17)

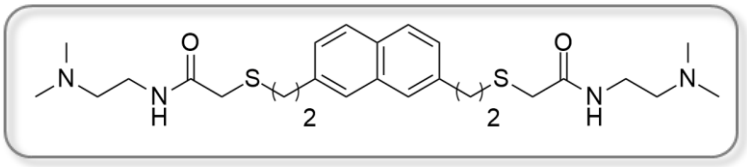

II.47 (75 mg, 0.22 mmol) was coupled with *N*,*N*-dimethylethylenediamine (27 µL, 0.25 mmol) according to the general procedure E to afford II.17 as a brown oil (27 mg, 43%).^{1}H NMR (400 MHz, $CDCl_3$) δ 7.74 (d, *J* = 9.1 Hz, 2H, H_4, H_5), 7.57 (s, 2H, H_1, H_8), 7.27 (d, *J* = 9.1 Hz, 2H, H_3 and H_6), 7.21 (bs, 2H, N*H*), 3.34 (dd, *J* = 11.4, 5.8 Hz, 4H, NHCH_2CH$_2$NMe$_2$), 3.25 (s, 4H, SCH_2C=O), 3.04 (t, *J* = 7.6 Hz, 4H, ArCH_2CH$_2$S), 2.89 (t, *J* = 7.6 Hz, 4H, ArCH$_2$CH_2S), 2.41 (t, *J* = 5.8 Hz, 4H, NHCH$_2$CH_2NMe$_2$), 2.22 (s, 12H, CH_3). ^{13}C NMR (101 MHz, $CDCl_3$) δ 169.0 (*C*=O), 137.8 (C_2, C_7), 133.7 (C_9), 131.1 (C_{10}), 128.0 (C_4, C_5), 126.7 (C_3, C_6), 126.6 (C_1, C_8), 57.9 (NHCH$_2$*C*H$_2$NMe$_2$), 45.2 (*C*H$_3$), 37.1 (NH*C*H$_2$CH$_2$NMe$_2$), 36.3 (S*C*H$_2$C=O), 35.9 (Ar*C*H$_2$CH$_2$S), 34.4 (ArCH$_2$*C*H$_2$S). MS (ESI) *m/z* 505 [M+H]$^+$. HRMS-ESI: *m/z* [M + H]$^+$ calcd for $C_{26}H_{41}N_4O_2S_2$: 505.2665, found: 505.2662.

2,2'-((Naphthalene-2,7-diylbis (propane-3,1-diyl))bis(sulfanediyl)) bis(*N*-(2-(dimethylamino)ethyl)acetamide) (II.18a)

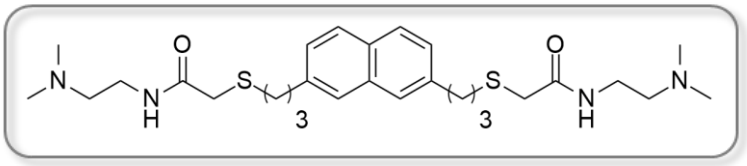

II.42 (75 mg, 0.19 mmol) was coupled with *N*,*N*-dimethylethylenediamine (38 µL, 0.35 mmol) according to the general procedure E to afford **II.18a** as a light yellow solid (62 mg, 67%). M.p. 93-95 °C. ^{1}H NMR (400 MHz, $CDCl_3$) δ 7.73(d, *J* = 8.4 Hz, 2H, H_4, H_5), 7.54 (s, 2H, H_1, H_8), 7.26 (d, *J* = 8.4 Hz, 4H, H_3, H_6, N*H*), 3.34 (dd, *J* = 11.2, 5.8 Hz, 4H, NHCH_2CH$_2$NMe$_2$), 3.24 (s, 4H, SCH_2C=O), 2.87 (t, *J* = 7.4 Hz, 4H, ArCH_2CH$_2$CH$_2$S), 2.59 (t, *J* = 7.4 Hz, 4H, ArCH$_2$CH$_2$CH_2S), 2.40 (t, *J* = 5.8 Hz, 4H, NHCH$_2$CH_2NMe$_2$), 2.21 (s, 12H, CH_3), 2.07-1.95 (m, 4H, ArCH$_2$CH_2CH$_2$S). ^{13}C NMR (101 MHz, $CDCl_3$) δ 169.0 (*C*=O), 138.9 (C_2, C_7), 133.8 (C_9), 130.8 (C_{10}), 127.9 (C_4, C_5), 126.7 (C_3, C_6), 126.2 (C_1, C_8), 57.9 (NHCH$_2$*C*H$_2$NMe$_2$), 45.2 (*C*H$_3$), 37.2 (NH*C*H$_2$CH$_2$NMe$_2$), 36.2 (S*C*H$_2$C=O), 34.9 (Ar*C*H$_2$CH$_2$CH$_2$S), 32.4 (ArCH$_2$CH$_2$*C*H$_2$S), 30.6 (ArCH$_2$*C*H$_2$CH$_2$S). MS (ESI) *m/z* 533 [M+H]$^+$. Anal. Calcd for $C_{28}H_{44}N_4O_2S_2$●0.25H_2O: C, 62.65; H, 8.37; N, 10.44. Found: C, 62.27; H, 8.15; N, 10.20.

2,2'-((Naphthalene-2,7-diylbis (propane-3,1-diyl))bis(sulfanediyl)) bis(*N*-(2-(diethylamino)ethyl)acetamide) (II.18b)

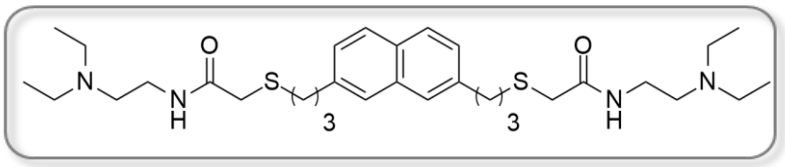

II.42 (100 mg, 0.25 mmol) was coupled with *N*,*N*-diethylethylenediamine (65 µL, 0.46 mmol) according to the general procedure E to afford **II.18b** as an orange oil (136 mg, 99%). ^{1}H NMR (400 MHz, $CDCl_3$) δ 7.72 (d, *J* = 7.8 Hz, 2H, H_4, H_5), 7.53 (s, 2H, H_1, H_8), 7.44 (s, 2H, N*H*), 7.25 (d, *J* = 7.8 Hz, 2H, H_3, H_6), 3.31 (dd, *J* = 11.2, 5.6 Hz, 4H, NHCH_2CH$_2$NEt$_2$), 3.23 (s, 4H, SCH_2C=O), 2.85 (t, *J* = 7.4 Hz, 4H, ArCH_2CH$_2$CH$_2$S), 2.69 – 2.43 (m, 16H, ArCH$_2$CH$_2$CH_2S, NHCH$_2$CH_2NEt$_2$, NCH_2CH$_3$), 2.03 – 1.96 (m, 4H, ArCH$_2$CH_2CH$_2$S), 1.00 (t, *J* = 7.0 Hz, 12H, NCH$_2$CH_3). ^{13}C NMR (101 MHz, $CDCl_3$) δ 168.9 (*C*=O), 138.9 (C_2, C_7), 133.8 (C_9), 130.8 (C_{10}), 127.9 (C_4, C_5), 126.7 (C_3, C_6), 126.3 (C_1, C_8), 51.4 (NHCH$_2$*C*H$_2$NEt$_2$), 46.8 (N*C*H$_2$CH$_3$), 37.2 (NH*C*H$_2$CH$_2$NEt$_2$), 36.3 (S*C*H$_2$C=O), 35.0 (Ar*C*H$_2$CH$_2$CH$_2$S), 32.5 (ArCH$_2$CH$_2$*C*H$_2$S), 30.7 (ArCH$_2$*C*H$_2$*C*H$_2$S), 11.9 (NCH$_2$*C*H$_3$). MS (ESI) *m/z* 589 [M+H]$^+$

2,2'-((Naphthalene-2,7-diylbis (propane-3,1-diyl))bis (sulfanediyl))bis(*N*-(3-(diethylamino)propyl)acetamide) (II.18c)

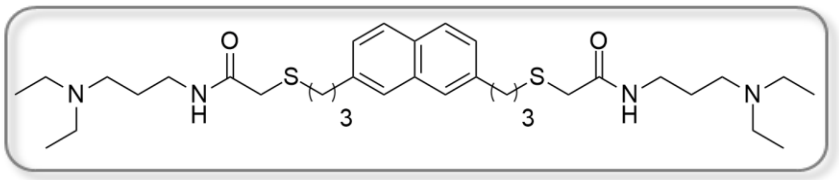

II.42 (75 mg, 0.19 mmol) was coupled with 3-(diethylamino)propylamine (55 µL, 0.35 mmol) according to the general procedure E to afford **II.18c** as an orange oil (64 mg, 59%). ^{1}H NMR (400 MHz, $CDCl_3$) δ 7.94 (bs, 2H, N*H*), 7.72 (d, *J* = 8.2 Hz, 2H, H_4, H_5), 7.53 (s, 2H, H_1, H_8), 7.25 (d, *J* = 8.2 Hz, 2H, H_3, H_6), 3.33 (dd, *J* = 12.0, 6 Hz, 4H, NHCH_2CH$_2$CH$_2$NEt$_2$), 3.20 (s, 4H, SCH_2C=O), 2.85 (t, *J* = 7.6 Hz, 4H, ArCH_2CH$_2$CH$_2$S), 2.53 (m, 16H, ArCH$_2$CH$_2$CH_2S, NHCH$_2$CH$_2$CH_2NEt$_2$, NCH_2CH$_3$), 1.98 (m, 4H, ArCH$_2$CH_2CH$_2$S), 1.63 (m, 4H, NHCH$_2$CH_2CH$_2$NEt$_2$), 1.02 (t, *J* = 7.1 Hz, 12H, NCH$_2$CH_3). ^{13}C NMR (101 MHz, $CDCl_3$) δ 169.0 (*C*=O), 138.9 (C_2, C_7), 133.8 (C_9), 130.8 (C_{10}), 127.9 (C_4, C_5), 126.7 (C_3, C_6), 126.3 (C_1, C_8), 51.9 (NHCH$_2$CH$_2$*C*H$_2$NEt$_2$), 46.9 (N*C*H$_2$CH$_3$), 39.8 (NH*C*H$_2$CH$_2$CH$_2$NEt$_2$), 36.3 (S*C*H$_2$C=O), 35.0 (Ar*C*H$_2$CH$_2$CH$_2$S), 32.5 (ArCH$_2$CH$_2$*C*H$_2$S), 30.6 (ArCH$_2$*C*H$_2$*C*H$_2$S), 26.0 (NHCH$_2$*C*H$_2$CH$_2$NEt$_2$), 11.5 (NCH$_2$*C*H$_3$). MS (ESI) *m/z* 617 [M+H]$^+$ HRMS-ESI: *m/z* [M + H]$^+$ calcd for $C_{34}H_{57}N_4O_2S_2$: 617.3917, found: 617.3917.

2,2'-((naphthalene-2,7-diylbis(propane-3,1-diyl))bis(sulfanediyl))bis(1-(4-methyl piperazin-1-yl)ethanone) (II.18d)

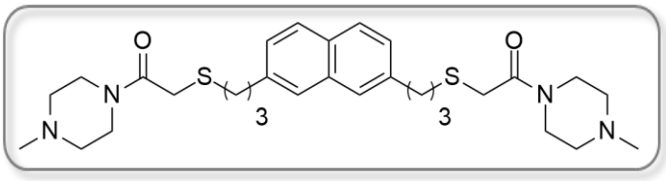

II.42 (100 mg, 0.25 mmol) was coupled with 1-methylpiperazine (51 µL, 0.46 mmol) according to the general procedure E to afford **II.18d** as an white solid (120 mg, 93%). ^{1}H NMR (400 MHz, $CDCl_3$) δ 7.74 (d, *J* = 8.4 Hz, 2H, H_4, H_5), 7.57 (s, 2H, H_1, H_8), 7.29 (d, *J* = 8.4 Hz, 2H, H_3, H_6), 3.64 (s, 4H, N(CH_2CH_2)NMe), 3.56 – 3.50 (m, 4H, N(CH_2CH_2)NMe), 3.34 (s, 4H, SCH_2C=O), 2.89 (t, *J* = 7.6 Hz, 4H, ArC$H_2CH_2CH_2$S), 2.70 (t, *J* = 7.2 Hz, 4H, Ar$CH_2CH_2CH_2$S), 2.48 – 2.41 (m, 4H, N(CH_2CH_2)NMe), 2.40 – 2.35 (m, 4H, N(CH_2CH_2)NMe), 2.31 (s, 6H, CH_3), 2.10 – 2.01 (m, 4H, Ar$CH_2CH_2CH_2$S). ^{13}C NMR (101 MHz, $CDCl_3$) δ 167.9 (*C*=O), 139.1 (C_2, C_7), 133.9 (C_9), 130.8 (C_{10}), 127.8 (C_4, C_5), 126.8 (C_3, C_6), 126.3 (C_1, C_8), 55.2 (N(CH_2CH_2)NMe), 54.8 (N(CH_2CH_2)NMe) 46.5 (N(CH_2CH_2)NMe), 46.1 (N*C*H_3), 41.86 (N(CH_2CH_2)NMe), 35.0 (Ar*C*$H_2CH_2CH_2$S), 33.5 (S*C*H_2C=O), 31.9 (Ar$CH_2CH_2CH_2$S), 30.73 (Ar$CH_2CH_2CH_2$S). MS (ESI) *m/z* 557 $[M+H]^+$. HRMS-ESI: *m/z* $[M + H]^+$ calcd for $C_{30}H_{44}N_4O_2S_2$: 557.2977, found: 557.2978.

2,2'-((Naphthalene-2,7-diylbis (propane-3,1-diyl))bis (sulfanediyl))bis(*N*-(2-morpholinoethyl)acetamide) (II.18e)

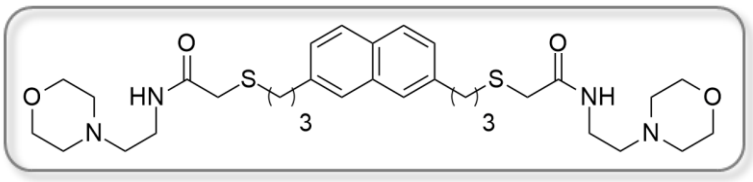

II.42 (75 mg, 0.19 mmol) was coupled with 4-(2-aminoethyl)morpholine (46 µL, 0.35 mmol) according to the general procedure E to afford **II.18e** as an orange oil (107 mg, 100%). ^{1}H NMR (400 MHz, $CDCl_3$) δ 7.70 (d, *J* = 8.4 Hz, 2H, H_4, H_5), 7.50 (s, 2H, H_1, H_8), 7.31 (s, 2H, N*H*), 7.22 (d, *J* = 8.4 Hz, 2H, H_3, H_6), 3.61 (s, 8H, N(CH_2CH_2)$_2$O), 3.32 (dd, *J* = 6, 11.2 Hz, 4H, NHCH_2CH_2NEt$_2$O), 3.21 (s, 4H, SCH_2C=O), 2.83 (t, *J* = 7.4 Hz, 4H, ArC$H_2CH_2CH_2$S), 2.55 (t, *J* = 7.2 Hz, 4H, Ar$CH_2CH_2CH_2$S), 2.41 (t, *J* = 6 Hz, 4H, NHCH$_2$CH_2NEt$_2$O), 2.36 (s, 8H, N(CH_2CH_2)$_2$O), 1.97 (m, 4H, Ar$CH_2CH_2CH_2$S). ^{13}C NMR (101 MHz, $CDCl_3$) δ 168.8 (*C*=O), 138.7 (C_2, C_7), 133.7 (C_9), 130.7 (C_{10}), 127.8 (C_4, C_5), 126.6 (C_3, C_6), 126.1 (C_1, C_8), 66.9 (N(CH_2CH_2)$_2$O), 56.8 (NHCH$_2$*C*H$_2$NEt$_2$O), 53.2 (N(*C*H_2CH_2)$_2$O), 36.1 (S*C*H$_2$C=O), 35.9 (NH*C*H$_2$CH$_2$NEt$_2$O), 34.8 (Ar*C*$H_2CH_2CH_2$S), 32.3 (Ar$CH_2CH_2CH_2$S), 30.6 (2xAr$CH_2CH_2CH_2$S). MS (ESI) *m/z* 617 $[M+H]^+$. HRMS-ESI: *m/z* $[M + H]^+$ calcd for $C_{32}H_{49}N_4O_4S_2$: 617.3190, found: 617.3187.

_N_-(2-(dimethylamino)ethyl)-2-((3-(7-hydroxynaphthalen-2-yl)propyl)thio)acetamide (II.48)

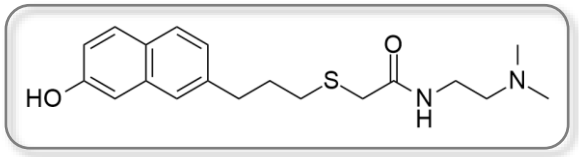

II.45 (37 mg, 0.13 mmol) was coupled with *N*,*N*-dimethylethylenediamine (12 µL, 0.12 mmol) according to the slightly modified general procedure E (where only 1.1 equiv. of TBTU, 1 equiv. of DIPEA and 1 equiv. of amine was used) to afford **II.48** as an off-white solid (23 mg, 55%). M.p. > 320 °C; ^{1}H NMR (400 MHz, $CDCl_3$) δ 8.10 (s, 1H, H_1), 7.92 (d, J = 8.4 Hz, 1H, H_4), 7.82 (d, J = 8.4 Hz, 2H, H_3, H_5), 7.70 (s, 1H, H_8), 7.33 (d, J = 8.4 Hz, 1H, H_6), 7.26 (s, 1H, N*H*), 3.34 (dd, J = 11.3, 5.6 Hz, 2H, NHCH_2CH$_2$NMe$_2$), 3.25 (s, 2H, SCH_2C=O), 2.91 (t, J = 7.4 Hz, 2H, ArCH_2CH$_2$CH$_2$S), 2.61 (t, J = 7.2 Hz, 2H, ArCH$_2$CH$_2$CH_2S), 2.40 (t, J = 5.9 Hz, 2H, NHCH_2CH$_2$NMe$_2$), 2.23 (s, 6H, CH_3), 2.08 – 1.99 (m, 2H, ArCH$_2$CH_2CH$_2$S). ^{13}C NMR (101 MHz, $CDCl_3$) δ 169.1 (*C*=O), 139.3 (*C*$_7$), 138.8 (*C*$_2$), 134.0 (*C*$_9$), 131.4 (C$_{10}$), 128.4 (*C*$_4$), 128.0 (*C*$_5$), 127.5 (*C*$_6$), 127.1 (*C*$_8$), 125.8 (*C*$_1$), 125.3 (*C*$_3$), 57.9 (NHCH$_2$*C*H$_2$NMe$_2$), 45.2 (*C*H$_3$), 37.1 (NH*C*H$_2$CH$_2$NMe$_2$), 36.3 (S*C*H$_2$C=O), 35.0 (Ar*C*H$_2$CH$_2$CH$_2$S), 32.5(ArCH$_2$CH$_2$*C*H$_2$S), 30.6 (ArCH$_2$*C*H$_2$CH$_2$S). HRMS-ESI: *m/z* [M + K]$^+$ calcd for $C_{19}H_{26}N_2O_2SK$: 384.1506, found: 384.1516.

2.1.7. Synthesis of compounds **II.51**, **II.19** and **II.20**

4,4'-(naphthalene-2,7-diyl)diphenol (II.51)

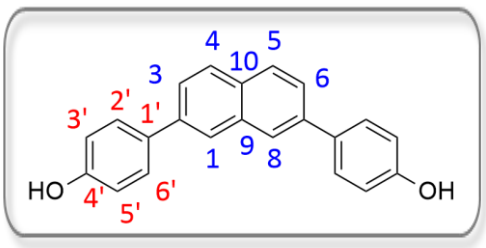

To a solution of 2,7-dibromonaphthalene **II.35** (100 mg, 0.35 mmol, 1 equiv.) in 1,4-dioxane (0.1 M) at rt were added phenylboronic acid **II.52** (125 mg, 0.91 mmol, 2.6 equiv.), 1 M aqueous Na_2CO_3 (6 equiv.) and bis(triphenylphosphine)palladium(II) dichloride (10 mol%). After degassing during 5 min, the reaction mixture was stirred at 80 °C o/n before being cooled to rt, diluted with EtOAc and filtered through a pad of celite. The filtrate was concentrated under reduced pressure and the crude product was purified by preparative TLC (tolune/EtOH, 9:1) to afford compound **II.51** (93 mg, 85%) as a off-white solid. M.p. 245-247 °C; ^{1}H NMR (400 MHz, MeOD) δ 8.03 (s, 2H, H_1, H_8), 7.87 (d, J = 8.4 Hz, 2H, H_4, H_5), 7.68 (d, J = 8.4 Hz, 2H, H_3, H_6), 7.61 (d, J = 8.4 Hz, 4H, $H_{2'}$, $H_{6'}$), 6.91 (d, J = 8.4 Hz, 2H, $H_{3'}$, $H_{5'}$). ^{13}C NMR (101 MHz, MeOD) δ 158.3 (*C*-OH), 140.1 (*C*$_2$, *C*$_7$), 135.7 (*C*$_9$), 133.7 (*C*$_{1'}$), 132.5 (*C*$_{10}$), 129.3 (*C*$_{2'}$, *C*$_{6'}$), 129.0 (*C*$_4$, *C*$_5$), 125.9 (*C*$_3$, *C*$_6$), 125.7 (*C*$_1$, *C*$_8$), 116.7 (*C*$_{3'}$, *C*$_{5'}$). MS (ESI) *m/z* 352 [M+K]$^+$.

2,2'-((naphthalene-2,7-diylbis(4,1-phenylene)) bis(oxy))bis(N,N-diethylethanamine) (II.19)

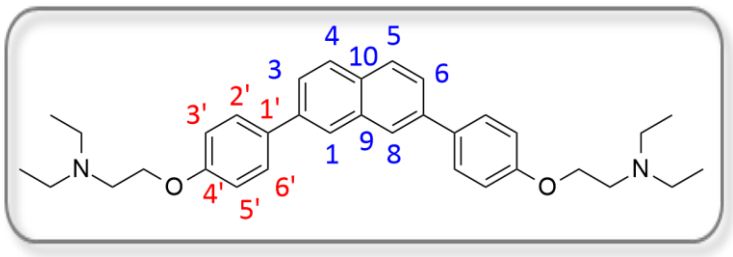

To a suspension of alcohol **II.51** (43 mg, 0.14 mmol, 1 equiv.) in dry acetone (0.075 M) was added K_2CO_3 (3 equiv.) and 2-chloro-*N,N*-diethylethylamine hydrochloride (142 mg, 0.84 mmol, 6 equiv.) was added. The reaction mixture was stirred at reflux o/n. Reaction solvent was evaporated, EtOAc was added to the reaction mixture and the organic phase was washed with water. The aqueous phased was basified with NaOH 1N and extracted again with EtOAc. The combined organic phases were washed with water, brine and dried with anhydrous Na_2SO4. The solvent was removed under reduced pressure and the crude product was purified by alumina preparative TLC (EtOAc/MeOH, 9:1) to afford compound **II.19** as yellow-pale solid (16 mg, 22%). M.p. 88-89 °C; ^{1}H NMR (400 MHz, $CDCl_3$) δ 8.01 (s, 2H, H_1, H_8), 7.88 (d, J = 8.4 Hz, 2H, H_4, H_5), 7.71 – 7.62 (m, 6H, H_3, H_6. $H_{2'}$, $H_{6'}$), 7.03 (d, J = 8.4 Hz, 4H, $H_{3'}$, $H_{5'}$), 4.13 (t, J = 6.4 Hz, 4H, $OCH_2CH_2N(Et)_2$), 2.93 (t, J = 6.4 Hz, 4H, $OCH_2CH_2N(Et)_2$), 2.68 (q, J = 7.2 Hz, 8H, CH_2CH_3), 1.11 (t, J = 7.2 Hz, 12H, CH_2CH_3). ^{13}C NMR (101 MHz, $CDCl_3$) δ 158.7 ($COCH_2CH_3N$), 138.7 (C_2, C_7), 134.2 (C_9), 133.7 ($C_{1'}$), 131.3 (C_{10}), 128.5 ($C_{2'}$, $C_{6'}$), 128.2 (C_4, C_5), 125.4 (C_3, C_6), 125.3 (C_1, C_8), 115.07 ($C_{3'}$, $C_{5'}$), 66.7 (OCH_2CH_2N), 51.9 (OCH_2CH_2N), 48.0 (NCH_2CH_3), 11.9 (NCH_2CH_3). MS (ESI) *m/z* 511 $[M+H]^+$. HRMS-ESI: *m/z* $[M + K]^+$ calcd for $C_{34}H_{43}N_2O_2$: 511.3319, found: 511,3316.

2,7-bis(4-(quinolin-3-yloxy)phenyl)naphthalene (II.20)

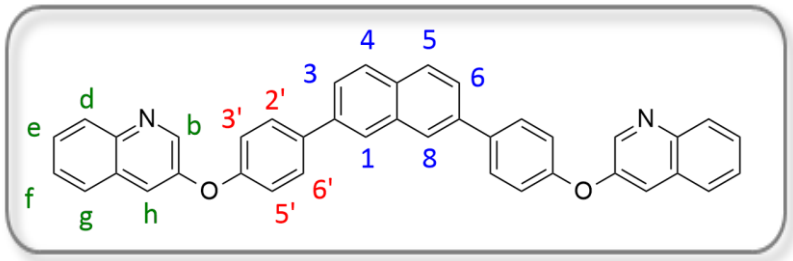

Pyridine (5 equiv.) was added to a solution of **II.51** (70 mg, 0.22 mmol, 1 equiv.), 3-quinolineboronic acid pinacol ester (172 mg, 0.66 mmol, 3 equiv.), copper(II) acetate (1.0 equiv.), and powdered 4 A molecular sieves in dry DCM (0.1 M). The reaction mixture was then stirred at room temperature during 24 hours at room temperature. After completion, was diluted in DCM and filtered through a pad of celite. The solvent was removed under reduced pressure and the crude product was purified by preparative TLC (hexane/EtOAc, 7:3) to afford **II.20** (15 mg, 12%) as a white solid. ^{1}H NMR (300 MHz, $CDCl_3$) δ 8.88 (d, J = 2.7 Hz, 2H, H_b), 8.13 (m, 4H, H_1, H_4, H_5, H_8), 7.97 (d,

J = 8.6 Hz, 2H, H_g), 7.74 (m, 8H, $H_{2'}$, $H_{6'}$, H_d, H_f), 7.67 – 7.62 (m, 4H, H_3, H_6, H_h), 7.55 (dd, J = 11.6, 4.6 Hz, 2H, H_e), 7.25 – 7.20 (d, J = 8.7 Hz, 4H, $H_{3'}$, $H_{5'}$).

2.2. Synthesis of compounds described in Chapter III

2.2.1. General methods

General procedure F for the nucleophilic aromatic substitution. To a solution of ethyl 6-bromo-4-chloroquinoline-3-carboxylate (1 equiv.) in dry 1,4-dioxane (0.2 M) at rt was added the amine (1.1 to 3.1 equiv.). The resulting solution was stirred at 110 °C in a sealed tube under nitrogen atmosphere for 12 h. After completion of the reaction, the reaction mixture was cooled to rt and 1 N aqueous NaOH was added to neutralise the solution, followed by dilution with water (pH ~ 8) and extraction with EtOAc. The combined organic phases were washed with water, brine and dried with anhydrous Na_2SO_4. The solvent was removed under reduced pressure to afford the desired compounds.

General procedure G for ester reduction. To a solution of ester (1 equiv.) in dry THF (0.1 M) at 0 °C was added $LiAlH_4$ (1.2 to 3 equiv.). The reaction mixture was stirred at rt during 1 h. After completion of the reaction, the reaction was quenched with 5% aqueous $KHSO_4$. The aqueous mixture was extracted with EtOAc and the combined organic phases were washed with water, brine and dried with anhydrous Na_2SO_4. The solvent was removed under reduced pressure. The crude product was purified by flash column chromatography.

General procedure H for alcohol oxidation and Horner-Wadsworth-Emmons reaction. To a solution of alcohol (1 equiv.) in dry DMF (0.1 M) at room temperature was added IBX (1.5 equiv.) and TFA (1.5 equiv.). The reaction mixture was then stirred, at room temperature under N_2 atmosphere, during 3 h before being diluted with EtOAc. The organic phase was washed with 5% aqueous $NaHCO_3$, water, brine and dried with anhydrous Na_2SO_4. The solvent was evaporated under reduced pressure and the crude aldehyde was used in the next step without further purification. To a solution of aldehyde in dry ethanol (0.2 M), at room temperature in a sealed tube, was added K_2CO_3 (3 equiv.) and triethyl phosphonoacetate (1.2 equiv.). The reaction mixture was stirred at 100 °C o/n under nitrogen atmosfere before being cooled to room temperature and all volatiles were removed under reduced pressure. The crude mixture was dissolved in EtOAc and the organic phase was consecutively washed with 5% aqueous $KHSO_4$, water,

brine and dried with anhydrous Na_2SO_4. The solvent was removed under reduced pressure and the crude Z-alkene was used in the next step without further purification. To a solution of the Z-alkene in dry ethanol (0.2 M), at room temperature in a sealed tube, was added K_2CO_3 (3 equiv.). The reaction mixture was stirred at 120 °C o/n under nitrogen atmosfere before being cooled to room temperature and all volatiles were removed under reduced pressure. The crude mixture was dissolved in EtOAc and the organic phase was consecutively washed with 5% aqueous $KHSO_4$, water, brine and dried with anhydrous Na_2SO_4. The solvent was removed under reduced pressure and the crude product was purified to afford the desired compounds.

General procedure I for Buchwald-Hartwig reaction. To a solution of bromide (1 equiv.) in dioxane (0.1 M) at rt were added amine (1.6 equiv.), K_2CO_3 (10 equiv.), palladium(II) acetate (10 mol%) and xantphos (0.2 equiv.). After degassing during 5 min, the reaction mixture was stirred at 120 °C o/n before being cooled at rt, diluted in EtOAc and filtered through a pad of celite. The filtrate was concentrated under reduced pressure and the crude product was purified to afford the desired compounds.

General procedure J for *N*-methylation. To a suspension of **III.24** or **III.25** (1 equiv.) in dry toluene (0.5 M), ethyl trifluoromethanesulfonate (6 equiv.) was added dropwise under N_2 atmosphere. The reaction mixture was stirred at rt during 48 h. MeOH was added to the reaction mixture and the solvent was removed under reduced pressure. Then, Et_2O was added to the crude product and the precipitate was filtered using a Büchner funnel to afford the desired compounds.

2.2.2. Synthesis of compound **III.9**

Diethyl {[(4-bromophenyl)amino]methylene}malonate (III.7)

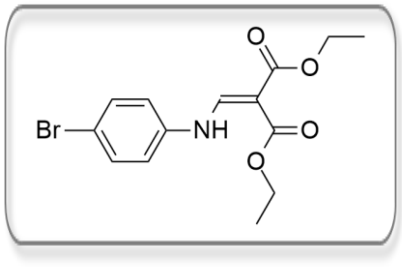

4-bromoaniline **III.5** (3.00 g, 17.4 mmol, 1 equiv.) and diethyl(2-ethoxymethylene)malonate **III.6** (4.30 mL, 21.0 mmol, 1.2 equiv.) reacted in a sealed tube at 115 °C during 1.5 h. After cooling to room temperature, EtOAc was added to the reaction. The precipitate was filtered using a Büchner funnel and dried to afford **III.7** (5.89 g, 99%) as a white solid. M.p. 100-102 °C; ^{1}H NMR (300 MHz, $CDCl_3$) δ 11.03 (d, *J* = 13.0 Hz, 1H, N*H*), 8.48 (d, *J* = 13.0 Hz, 1H, NC*H*CH(CO_2Et)$_2$), 7.49 (d, *J* = 8.8 Hz, 2H, H_2, H_6), 7.5 (d, J = 8.8 Hz, 2H, H_3, H_5), 4.42-4.22 (m, 4H, CH_2), 1.45-1.26 (m, 6H, CH_3). Analytical date were in agreement with those already published.[557]

Ethyl 6-bromo-4-hydroxyquinoline-3-carboxylate (III.8)

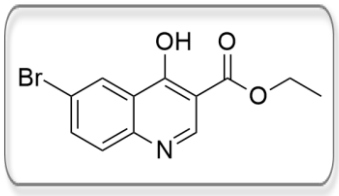

III.7 (5.33 g, 15.6 mmol, 1 equiv.) was added to diphenyl ether (31 mL). The mixture was refluxed for 2 h and then allowed to cool to room temperature. Hexane was added to th reaction mixture, and the precipite was filtered under vacuum and dried to afford **III.8** (3.70 g, 80%) as a white solid. M.p. > 320 ºC; ^{1}H NMR (400 MHz, DMSO-d_6) δ 8.59 (s, 1H, H_2), 8.23 (d, J = 2.1 Hz, 1H, H_5), 7.61 (d, J = 8.2 Hz, 1H, H_8), 7.01 (dd, J = 8.2, 2.1 Hz, 1H, H_7), 4.23 (q, J = 7.1 Hz, 2H, CH_2), 1.28 (t, *J* = 7.1 Hz, 3H, CH_3). Analytical date were in agreement with those already published.[187]

Ethyl 6-bromo-4-chloroquinoline-3-carboxylate (III.9)

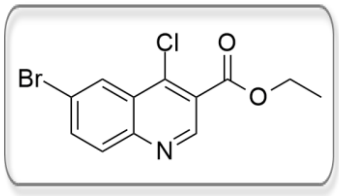

$POCl_3$ (3.6 mL) was added dropwise to **III.8** (1.50 g, 5.07 mmol, 1 equiv.) under an nitrogen atmosphere at 0 ºC. The reaction mixture reacted in a sealed tube at 115 ºC during 2 h. Then it was cooled to room temperature and carefully poured onto ice. Under agitation, NH_3 25% was added until pH = 7. The aqueos phase was extracted with DCM. The organic phase was washed with brine and dried with anhydrous Na_2SO_4. The solvent was removed under reduced pressure to afford **III.9** (1.59 g, 100%) as a light yellow solid. ^{1}H NMR (500 MHz, $CDCl_3$) δ 9.21 (s, 1H, H_2), 8.47 (d, 1.5 Hz, 1H, H_5), 8.02 (d, 9.0 Hz, 1H, H_8), 7.95 (dd, 1.5 Hz, 9.0 Hz, 1H, H_7), 4.40 (q, 7.0 Hz, 2H, CH_2), 1.60 (t, 7.0 Hz, 3H, CH_3).

2.2.3. Synthesis of compound **III.11**

1-(4-nitro-2-(trifluoromethyl)phenyl)piperazine (III.14)

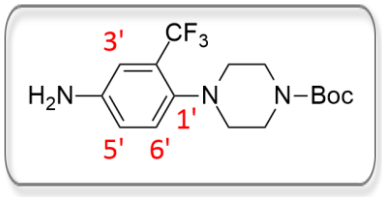

Piperazine **III.13** (494 mg, 5.74 mmol, 2 equiv.) was added to a mixture of 2-fluoro-5-nitrobenzotrifluoride **III.12** (394 µL, 2.87 mmol, 1 equiv.) and potassium carbonate (1.5 equiv.) in DMSO (1 M). The reaction mixture was stirred o/n at 90 ºC. After completion of the reaction, the mixture was diluted with EtOAc and the organic phase was washed with water and brine and dried with anhydrous Na_2SO_4. The solvent was removed under reduced pressure to afford compound **III.14** (757 mg, 96%) as orange oil. ^{1}H NMR (400 MHz, $CDCl_3$) δ 8.51 (d, *J* = 2.0 Hz, 1H, $H_{3'}$), 8.33 (dd, *J* = 8.8, 2.0 Hz, 1H, $H_{5'}$), 7.29 (d, *J* = 8.8 Hz, 1H, $H_{6'}$), 3.13 (d, *J* = 3.0 Hz, 4H, CH_2), 3.07 (d, *J* = 3.0 Hz, 4H, CH_2). ^{13}C NMR (101 MHz, $CDCl_3$) δ 157.3 ($C_{1'}$), 142.2 ($C_{4'}$), 128.0 (C$H_{5'}$), 124.7 ($C_{3'}$), 124.6 (CF_3), 122.5 ($C_{6'}$), 121.9 ($C_{2'}$), 53.8 (CH_2), 45.9 (CH_2).

***tert*-butyl 4-(4-nitro-2-(trifluoromethyl)phenyl)piperazine-1-carboxylate (III.15)**

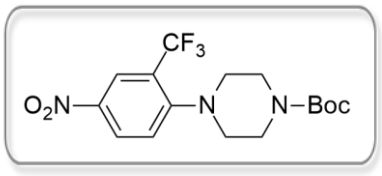

To a solution of **III.14** (700 mg, 2.54 mmol, 1 equiv.) and DMAP (0.1 equiv) in dry THF (0.2 M), was added Boc_2O (876 µL, 3.82 mmol, 1.5 equiv.) under a nitrogen atmosphere. The reaction mixture was stirred o/n at rt. After evaporation of the solvent, EtOAc was added and the organic phase was washed with 1N aqueous HCl, brine and dried with anhydrous Na_2SO_4. The solvent was removed under reduced pressure to afford compound **III.15** (897 mg, 94%) as an orange solid. M.p. 100-102 °C ;^{1}H NMR (400 MHz, $CDCl_3$) δ 8.52 (s, 1H, $H_{3'}$), 8.35 (d, J = 8.8 Hz, 1H, $H_{5'}$), 7.29 (d, J = 8.8 Hz, 1H, $H_{6'}$), 3.60 (s, 4H, CH_2), 3.05 (s, 4H, 2xCH_2), 1.48 (s, 9H, Boc). Analytical date were in agreement with those already published.[558]

***tert*-butyl 4-(4-amino-2-(trifluoromethyl)phenyl)piperazine-1-carboxylate (III.11)**

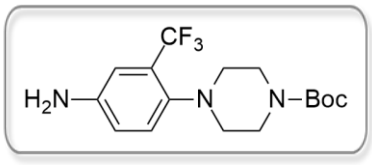

A solution of **III.15** (850 mg, 2.26 mmol, 1 equiv.) in MeOH/EtOAc (1:1, 0.1 M) was treated with 15% Pd/C (10% w/w). The reaction was stirred o/n under an H_2 at atmospheric pressure and rt. After completion of the reaction, the mixture was filtered through a celite bed. The solvent was removed under reduced pressure to afford compound **III.10** (762 mg, 97%). as a light yellow solid. M.p. 140-142 °C; ^{1}H NMR (400 MHz, $CDCl_3$) δ 7.13 (d, J = 8.4 Hz, 1H, H_6), 6.91 (s, 1H, $H_{3'}$), 6.79 (d, J = 8.4 Hz, 1H, $H_{5'}$), 3.76 (s, 2H, NH_2), 3.51 (s, 4H, CH_2), 2.76 (s, 4H, CH_2), 1.48 (s, 9H, Boc). Analytical date were in agreement with those already published.[558]

2.2.4. Synthesis of compounds **III.16, III.17** and **III.18**

Ethyl 6-bromo-4-((4-(4-(tert-butoxycarbonyl)piperazin-1-yl)-3-(trifluoromethyl)phenyl)amino)quinoline-3-carboxylate (III.16)

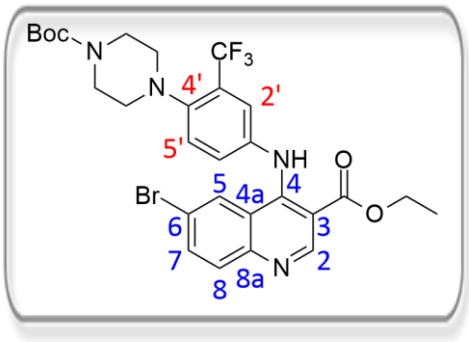

III.9 (1.27 g, 4.04 mmol) was coupled with **III.11** (1.47 g, 4.25 mmol, 1.1 equiv.) under the conditions described in general procedure F to afford **III.16** as a light yellow solid (1.63 g, 65%). M.p. 162-164 °C; ^{1}H NMR (400 MHz, $CDCl_3$) δ 10.50 (s, 1H, NH), 9.27 (s, 1H, H_2), 7.88 (d, J = 8.6 Hz, 1H, H_8), 7.71 (d, J = 8.6 Hz, 1H, H_7), 7.62 (s, 1H, H_5), 7.35 (s, 1H, $H_{2'}$), 7.28 (d, J = 8.8 Hz, 1H, $H_{5'}$), 7.13 (d, J = 8.8 Hz, 1H, $H_{6'}$), 4.45 (q, J = 6.9 Hz, 2H, CH_3), 3.56 (s, 4H, CH_{2Ppz}), 2.86

(s, 4H, CH_{2Ppz}), 1.47 (m, 12H, CH_2CH_3, Boc). Analytical date were in agreement with those already published.[559]

Ethyl 6-bromo-4-((4-(piperazin-1-yl)-3-(trifluoromethyl)phenyl)amino)quinoline-3-carboxylate (III.19)

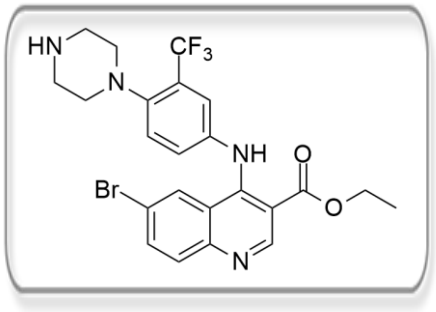

III.19 was obtained as minor product of the previous reaction. The aqueous phase was acidified until pH ~ 6 and further extracted with EtOAc. The solvent was removed under reduced pressure to afford **III.19** as a yellow solid (359 mg, 17%). M.p. 240-242 ^oC; ^1H NMR (300 MHz, $CDCl_3$) δ 10.48 (s, 1H, Quin-N*H*-Ph), 9.26 (s, 1H, H_2), 7.88 (d, *J* = 8.9 Hz, 1H, H_8), 7.71 (dd, *J* = 8.9, 2.1 Hz, 1H, H_7), 7.61 (d, *J* = 2.1 Hz, 1H, H_5), 7.35-7.25 (m, 2H, $H_{2'}$, $H_{5'}$), 7.14 (dd, *J* = 8.4, 2.3 Hz, 1H, $H_{6'}$), 4.44 (q, *J* = 7.1 Hz, 2H, CH_2CH_3), 3.21 (s, 4H, CH_{2Ppz}), 3.09 (s, 4H, CH_{2Ppz}), 1.45 (t, *J* = 7.1 Hz, 3H, CH_3).^{13}C NMR (75 MHz, $CDCl_3$) δ 168.2 (*C*=O), 151.7 (C_2), 151.0 (C_4),149.6 (C_{8a}), 148.3 ($C_{4'}$), 139.7 ($C_{1'}$), 134.8 (C_7), 132.0 (C_8), 129.0 ($C_{3'}$), 128.7 (C_5), 126.2 ($C_{6'}$), 125.6 ($C_{2'}$), 121.6 (CF_3), 121.1 ($C_{5'}$), 120.4 (C_{4a}), 118.7 (C_6), 107.9 (C_3), 61.8 (CH_2CH_3), 52.4 (C_{Ppz}), 45.1 (C_{Ppz}), 14.4 (CH_3). MS (ESI) *m/z* 523 $[M+H]^+$.

Ethyl 6-bromo-4-(methylamino)quinoline-3-carboxylate (III.17)

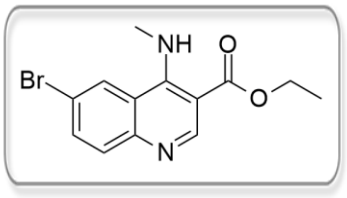

III.9 (1.59 g, 5.05 mmol) was coupled with a methylamine solution 2.0 M in methanol (4.10 mL, 10.36 mmol, 2.1 equiv.) under the conditions described in general procedure F to afford **III.17** as a light yellow solid (1.54 g, 99%). Mp 113-116 ^oC; ^1H NMR (300 MHz, $CDCl_3$) δ 9.45 (s, 1H, N*H*), 9.04 (s, 1H, H_2), 8.43 (d, *J* = 1.9 Hz, 1H, H_5), 7.78 (d, *J* = 8.9 Hz, 1H, H_8), 7.69 (dd, *J* = 8.9, 1.9 Hz, 1H, H_7), 4.36 (q, *J* = 7.1 Hz, 2H, CH_2CH_3), 3.47 (d, *J* = 5.6 Hz, 3H, NHCH_3), 1.40 (t, *J* = 7.1 Hz, 3H, CH_2CH_3). ^{13}C NMR (75 MHz, $CDCl_3$) δ 168.9 (*C*=O), 156.4 (C_4), 152.0 (C_2), 150.0 (C_{8a}), 134.2 (C_7), 131.7 (C_8), 128.5 (C_5), 120.6 (C_{4a}), 117.2 (C_6), 102.9 (C_3), 60.9 (CH_2CH_3), 35.5 ($NHCH_3$), 14.4 (OCH_2CH_3). MS (ESI) *m/z* 309 and 310 $[M+H]^+$.

Ethyl 6-bromo-4-((2-(dimethylamino)ethyl)amino)quinoline-3-carboxylate (II.18)

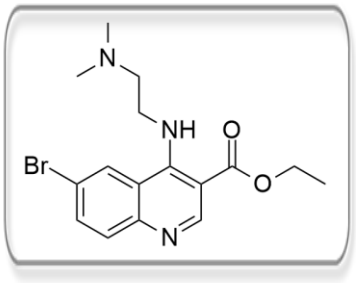

III.9 (1.59 g, 5.05 mmol) was coupled with *N,N*-dimethylethylenediamine (1.93 mL, 17.69 mmol, 3.5 equiv.) under the conditions described in general procedure F to afford **III.18** as light yellow solid (1.75 g, 95%). M.p. 119-122 °C; ^{1}H NMR (300 MHz, $CDCl_3$) δ 9.42 (s, 1H, N*H*), 9.06 (s, 1H, H_2), 8.37 (d, *J* = 1.7 Hz, 1H, H_5), 7.79 (d, *J* = 8.9 Hz, 1H, H_8), 7.70 (dd, *J* = 8.9, 1.7 Hz, 1H, H_7), 4.38 (q, J = 7.1 Hz, 2H, CH_2CH$_3$), 3.84 (dd, J = 10.9, 5.8 Hz, 2H, NCH_2CH$_2$NMe$_2$), 2.61 (t, J = 6.0 Hz, 2H NCH$_2$CH_2NMe$_2$), 2.35 (s, 6H, N(CH_3)$_2$), 1.41 (t, J = 7.1 Hz, 3H, CH$_2$CH_3). ^{13}C NMR (75 MHz, $CDCl_3$) δ 168.3 (*C*=O), 155.7 (C_4), 152.2 (C_2), 149.9 (C_{8a}), 134.2 (C_7), 131.6 (C_8), 128.5 (C_5), 121.0 (C_{4a}), 117.2 (C_6), 103.6 (C_3), 60.9 (*C*H$_2$CH$_3$), 59.4 (NCH$_2$*C*H$_2$NMe$_2$), 46.6 (N*C*H$_2$CH$_2$NMe$_2$), 45.5 (N(*C*H$_3$)$_2$), 14.5 (CH$_2$*C*H$_3$). MS (ESI) *m/z* 366 and 368 $[M+H]^+$.

2.2.5. Synthesis of compounds **III.20, III.21** and **III.22**

***Tert*-butyl 4-(4-((6-bromo-3-(hydroxymethyl)quinolin-4-yl)amino)-2-(trifluoromethyl)phenyl)piperazine-1-carboxylate (III.20)**

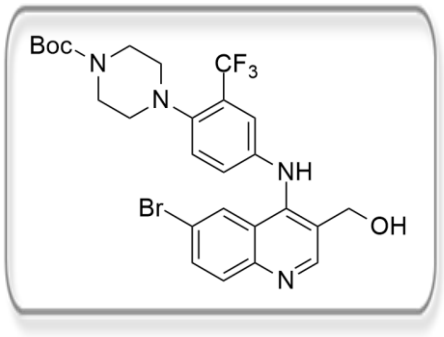

III.16 (1.63 g, 2.62 mmol) was treated with $LiAlH_4$ (298 mg, 7.85 mmol, 3 equiv.) under the conditions described in the general procedure G. The crude product was purified by flash column chromatography (hexane/EtOAc, 7:3) to afford **III.20** as a yellow solid (941 mg, 62%). M.p. 202-204 °C. ^{1}H NMR (300 MHz, $CDCl_3$) δ 8.58 (s, 1H, H_2), 7.89 (d, *J* = 9.0 Hz, 1H, H_8), 7.80 (d, *J* = 2.1 Hz, 1H, H_5), 7.69 (dd, *J* = 9.0, 2.1 Hz, 1H, H_7), 7.49 (s, 1H, N*H*), 7.16 (d, *J* = 8.6 Hz, 1H, $H_{5'}$), 7.12 (d, *J* = 2.6 Hz, 1H, $H_{2'}$), 6.81 (dd, *J* = 8.6, 2.6 Hz, 1H, $H_{6'}$), 4.81 (s, 2H, CH_2OH), 3.53 (s, 4H, CH_{2Ppz}), 2.85 – 2.73 (m, 4H, CH_{2Ppz}), 1.47 (s, 9H, Boc).

(6-bromo-4-(methylamino)quinolin-3-yl)methanol (III.21)

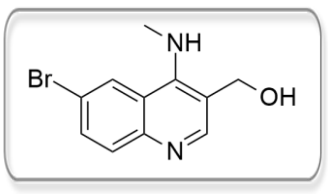

III.17 (1.53 g, 4.94 mmol) was treated with $LiAlH_4$ (281 mg, 7.40 mmol, 1.5 equiv.) under the conditions described in the general procedure G. The crude product was purified by flash column chromatography (EtOAc/MeOH, 95:5) to afford **III.21** as a yellow solid (975 mg, 74%). M.p. 182-184 °C. ^{1}H NMR (300 MHz, $CDCl_3$) δ 8.41 (s, 1H, H_2), 8.38 (d, *J* = 2.1 Hz, 1H, H_5), 7.76 (d, *J* = 8.9 Hz, 1H, H_8),

7.68 (dd, *J* = 8.9, 2.1 Hz, 1H, H_7), 6.32 (br s, 1H, N*H*), 4.82 (s, 2H, CH_2OH), 3.41 (d, J = 5.4 Hz, 3H, CH_3).

(6-bromo-4-((2-(dimethylamino)ethyl)amino)quinolin-3-yl)methanol (III.22)

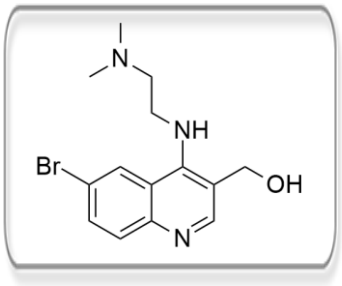

III.18 (1.74 g, 4.76 mmol) was treated with $LiAlH_4$ (217 mg, 5.71 mmol, 1.2 equiv.) under the conditions described in the general procedure G to afford the compound **III.22** as a light yellow solid (1.49 g, 96%). M. p.: 103-105 °C.^{1}H NMR (300 MHz, $CDCl_3$) δ 8.49 (s, 1H, H_2), 8.17 (d, *J* = 2.2 Hz, 1H, H_5), 7.85 (d, *J* = 9.0 Hz, 1H, H_8), 7.68 (dd, *J* = 9.0, 2.2 Hz, 1H H_7), 5.08 (s, 1H, N*H*), 4.80 (d, *J* = 3.4 Hz, 2H, CH_2OH), 3.69 (dd, *J* = 11.1, 5.5 Hz, 2H, NCH_2CH_2NMe_2), 2.50 (t, *J* = 5.5 Hz, 2H, NCH_2CH_2NMe_2), 2.17 (s, 6H, N(CH_3)$_2$). ^{13}C NMR (75 MHz, $CDCl_3$) δ 152.1 (C_2), 151.4 (C_4), 148.1 (C_{8a}), 132.5 (C_7), 131.5 (C_8), 126.0 (C_5), 122.7 (C_{4a}), 119.4 (C_3), 118.5 (C_6), 60.92 (*C*H$_2$OH), 59.42 (N*C*H$_2$CH$_2$NMe_2), 45.73 (NCH$_2$*C*H$_2$NMe_2), 44.85 (N(*C*H$_3$)$_2$).

2.2.6. Synthesis of compounds **III.23, III.24** and **III.25**

***Tert*-butyl 4-(4-(9-bromo-2-oxobenzo[h][1,6]naphthyridin-1(2H)-yl)-2-(trifluoromethyl)phenyl)piperazine-1-carboxylate (III.23)**

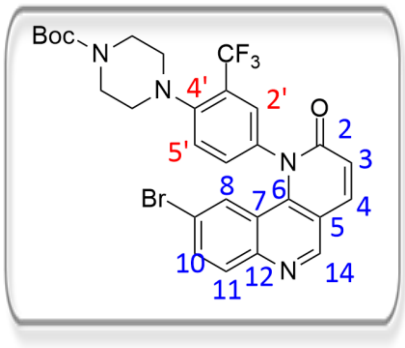

To a solution of **III.20** (385 mg, 0.66 mmol) in dry DMF (0.1 M) at rt was added IBX (241 mg, 0.86 mmol, 1.3 equiv.). The reaction mixture was then stirred, at rt under nitrogen atmosphere, during 3 h before being diluted with EtOAc. The organic phase was washed with 5% aqueous $NaHCO_3$, water, brine and dried with anhydrous Na_2SO_4. The solvent was evaporated under reduced pressure and the crude aldehyde was used in the next step without further purification. To a solution of aldehyde in dry ethanol (0.1 M), at rt in a sealed tube, was added K_2CO_3 (3 equiv.) and triethyl phosphonoacetate (1.2 equiv.). The reaction mixture was stirred at 100 °C o/n before being cooled to rt and all volatiles were removed under reduced pressure. The crude mixture was dissolved in EtOAc and the organic phase was consecutively washed with 5% aqueous $KHSO_4$, water, brine and dried with anhydrous Na_2SO_4. The solvent was removed under reduced pressure to afford compound **III.23** as a light yellow solid (349 mg, 87% over 2 steps). M.p. 223-235 °C; ^{1}H NMR (300 MHz, $CDCl_3$) δ 8.98 (s, 1H, H_{14}), 8.02 – 7.94 (m, 2H, H_4, H_{11}), 7.69 (dd, *J* = 8.9, 2.1 Hz, 1H, H_{10}), 7.61 (d, *J* = 8.5 Hz, 1H, $H_{5'}$), 7.58 (d, *J* = 2.4 Hz, 1H, $H_{2'}$), 7.53 (dd, *J* = 8.5, 2.4 Hz, 1H, $H_{6'}$),

6.97 (d, *J* = 9.5 Hz, 1H, H_3), 6.67 (d, *J* = 2.1 Hz, 1H, H_8), 3.64 (s, 4H, CH_{2Ppz}), 3.11 – 2.97 (m, 4H, CH_{2Ppz}), 1.50 (s, 9H, Boc).

9-bromo-1-methylbenzo[*h*][1,6]naphthyridin-2(1*H*)-one (III.24)

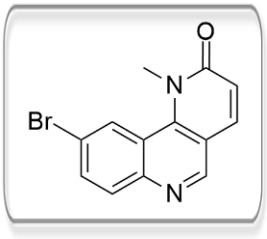

III.21 reacted under the conditions described in the general procedure H to afford the compound **III.24** as a brown solid. M.p. 180-183 °C; ^{1}H NMR (300 MHz, $CDCl_3$) δ 8.88 (s, 1H, H_{14}), 8.68 (d, *J* = 2.0 Hz, 1H, H_8), 8.01 (d, *J* = 8.9 Hz, 1H, H_{11}), 7.90 – 7.78 (m, 2 H, H_4, H_{10}), 6.87 (d, *J* = 9.3 Hz, 1H, H_3), 4.09 (s, 3H, CH_3). ^{13}C NMR (75 MHz, $CDCl_3$) δ 164.1 (*C*=O), 150.7 (C_{14}), 148.1 (C_{12}), 143.2 (C_6), 137.9 (C_4), 133.5 (C_{11}), 132.3 (C_{10}), 127.5 (C_8), 122.2 (C_3), 119.9 (C_9), 119.8 (C_7), 114.0 (C_5), 38.3 (NCH_3).

9-bromo-1-(2-(dimethylamino)ethyl)benzo[*h*][1,6]naphthyridin-2(1*H*)-one (III.25)

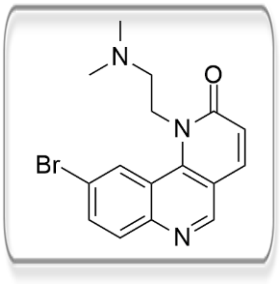

III.22 reacted under the conditions described in the general procedure H to afford the compound **III.25** as a off-white solid. ^{1}H NMR (300 MHz, $CDCl_3$) δ 8.88 (s, 1H, H_{14}), 8.68 (d, *J* = 2.0 Hz, 1H, H_8), 8.01 (d, *J* = 8.9 Hz, 1H, H_{11}), 7.90 – 7.78 (m, 2 H, H_4, H_{10}), 6.86 (d, *J* = 9.3 Hz, 1H, H_3), 4.63 (t, 2H, $CH_2CH_2NMe_2$), 3.06 (t, 2H, $CH_2CH_2NMe_2$), 2.39 (s, 6H, $N(CH_3)_2$).

2.2.7. Synthesis of the target compounds

9-bromo-1-(4-(4-methylpiperazin-1-yl)-3-trifluoromethyl)phenyl) benzo[*h*][1,6]naphthyridin-2(1*H*)-one (III.2a)

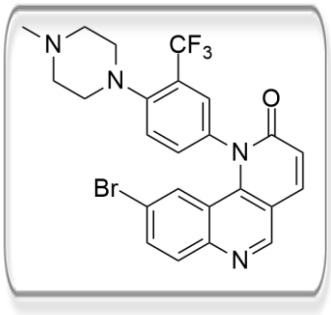

To a solution of **III.23** (340 mg, 0.56 mmol, 1 equiv.) in dry DCM (0.2 M) was slowly added TFA (10 equiv.) at 0 °C. The resulting mixture was stirred at 0 °C during 10 minutes at rt during 3 h. The solvent was evaporated, methanol was added followed by evaporation, and then ether was added and evaporated to afford the corresponding TFA salt which was used in the next step without further purification. To a solution of the TFA salt (1 equiv.) in dry methanol (3 ml) and paraformaldehyde (4 equiv.) was added formic acid (4 equiv.). The reaction mixture was refluxed for 24 h. After cooling to rt, the reaction mixture was partitioned between ether and water. The aqueous phase was basified with Na_2CO_2 2N until pH=12 andthen extracted with ether. The combined organic phases were washed with brine, dried with anhydrous Na_2SO_4 and the solvent removed under reduced pressure to afford **III.2a** as a

light brown solid (158 mg, 52%). M.p. 177-180 °C; ^{1}H NMR (300 MHz, $CDCl_3$) δ 8.98 (s, 1H, H_{14}), 8.01 – 7.93 (m, 2H, H_4, H_{11}), 7.71 – 7.63 (m, 2H, H_{10}, $H_{5'}$), 7.56 (d, *J* = 2.4 Hz, 1H, $H_{2'}$), 7.51 (dd, *J* = 8.4, 2.4 Hz, 1H, $H_{6'}$), 6.97 (d, *J* = 9.5 Hz, 1H, H_3), 6.69 (d, *J* = 2.0 Hz, 1H, H_8), 3.14 (dt, *J* = 11.6, 6.0 Hz, 4H, CH_{2Ppz}), 2.67 (s, 4H, CH_{2Ppz}), 2.41 (s, 3H, CH_3). ^{13}C NMR (75 MHz, $CDCl_3$) δ 163.2 (C=O), 154.2 ($C_{4'}$), 150.9 (C_{14}), 148.3 (C_{12}), 141.7 (C_6), 139.5 (C_4), 135.8 ($C_{1'}$), 133.3 (C_{10}), 133.2 ($C_{6'}$), 132.5 (C_{11}), 129.3 ($C_{3'}$), 128.0 (C_8), 127.8 ($C_{2'}$), 126.3 ($C_{5'}$), 122.9 (C_3), 121.5 (CF_3), 120.2 (C_7), 118.7 (C_9), 113.8 (C_5), 53.5 (C_{Ppz}), 55.4 (C_{Ppz}), 46.1 (CH_3). MS (ESI) *m/z* 517 $[M+H]^+$.

9-((2-(dimethylamino)ethyl)amino)-1-(4-(4-methylpiperazin-1-yl)-3-(trifluoromethyl)phenyl)benzo[h][1,6]naphthyridin-2(1H)-one (III.2b)

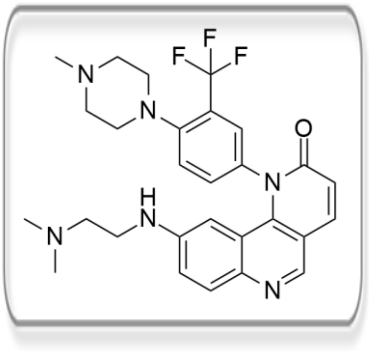

III.2a (33 mg, 0.06 mmol, 1 equiv.) was coupled with *N*,*N*-dimethylethylenediamine (11 µL, 0.10 mmol, 1.5 equiv.), according to the slightly modified general procedure I (where toluene (0.2 M) was used as solvent and the reaction proceeded at 100 °C). The crude product was purified by preparative TLC (EtOAc/MeOH , 95:5) to afford **III.2b** as a brown solid (12 mg, 35%). ^{1}H NMR (300 MHz, $CDCl_3$) δ 8.69 (s, 1H, H_{14}), 7.91 (d, *J* = 9.4 Hz, 1H, H_4), 7.85 (d, *J* = 9.0 Hz, 1H, H_{11}), 7.69 (d, *J* = 2.0 Hz, 1H, $H_{2'}$), 7.52 – 7.48 (m, 2H, $H_{5'}$, $H_{6'}$), 7.01 (dd, *J* = 9.0, 2.4 Hz, 1H, H_{10}), 6.86 (d, *J* = 9.4 Hz, 1H, H_3), 5.94 (d, *J* = 2.4 Hz, 1H, H_8), 4.53 (s, 1H, N*H*), 3.07 (ddd, *J* = 15.7, 11.1, 6.0 Hz, 4H, CH_{2Ppz}), 2.62 (br s, 4H, CH_{2Ppz}), 2.49 – 2.30 (m, 7H, CH_2CH_2, NCH_3), 2.16 (s, 6H, $N(CH_3)_2$).

9-((2-(dimethylamino)ethyl)amino)-1-methylbenzo[*h*][1,6]naphthyridin-2(1*H*)-one (III.3a)

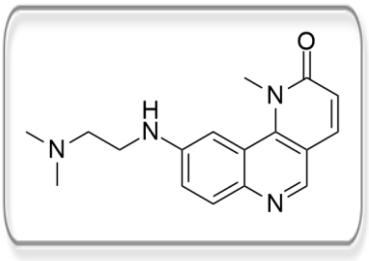

III.24 (50 mg, 0.17 mmol) was coupled with *N*,*N*-dimethylethylenediamine (30 µL, 0.28 mmol), according to general procedure I. The crude product was purified by preparative TLC (DCM/MeOH, 9:1) to afford **III.3a** as a dark yellow solid (29 mg, 57%). M.p. 155-157 °C; ^{1}H NMR (300 MHz, $CDCl_3$) δ 8.62 (s, 1H, H_{14}), 7.94 (d, *J* = 9.0 Hz, 1H, H_{11}), 7.80 (d, *J* = 9.3 Hz, 1H, H_4), 7.38 (d, J = 2.2 Hz, 1H, H_8), 7.19 (dd, *J* = 9.0, 2.4 Hz, 1H, H_{10}), 6.80 (d, *J* = 9.3 Hz, 1H, H_3), 4.90 (s, 1H, N*H*), 4.10 (s, 3H, NCH_3), 3.27 (s, 2H, $NHCH_2CH_2NMe_2$), 2.75 – 2.62 (m, 2H, $NHCH_2CH_2NMe_2$), 2.32 (s, 6H, $N(CH_3)_2$). ^{13}C NMR (75 MHz, $CDCl_3$) δ 164.9 (*C*=O), 146.1 (C_{14}), 146.0 (C_9), 143.7 (C_{12}), 142.8 (C_6), 138.3 (C_4), 131.5 (C_{11}), 121.2 (C_3), 120.8 (C_{10}), 120.3 (C_7), 114.3 (C_5), 102.3 (C_8), 57.7 ($NHCH_2CH_2NMe_2$), 45.2 ($N(CH_3)_2$)., 41.0 ($NHCH_2CH_2NMe_2$), 38.40 (NCH_3).

2-(9-bromo-2-oxobenzo[*h*][1,6]naphthyridin-1(2*H*)-yl)-*N,N,N*-trimethylethanaminium trifluoromethanesulfonate (III.3b)

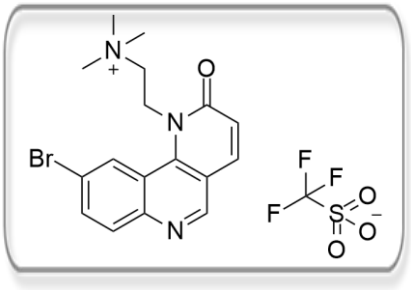

III.25 (100 mg, 0.29 mmol) reacted with methyl trifluoromethanesulfonate (196 µL, 1.73 mmol), according to general procedure J. The filtrate was evaporated and purified by preparative TLC (DCM/MeOH/TEA, 85:15:0.1) to afford **III.3b** as a yellow solid (8 mg, 5%).

1-(2-(dimethylamino)ethyl)-9-((2-(dimethylamino)ethyl)amino)benzo[*h*][1,6]naphthyridin-2(1*H*)-one (III.3c)

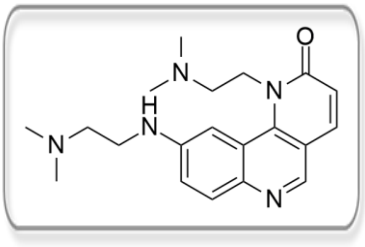

III.25 (145 mg, 0.17 mmol) was coupled with *N,N*-dimethylethylenediamine (73 µL, 0.67 mmol), according to general procedure I. The crude product was purified by flash column chromatography (DCM/MeOH, 95:5) to afford **III.3c** as a yellow solid (107 mg, 73%). ^{1}H NMR (300 MHz, $CDCl_3$) δ 8.59 (s, 1H, H_{14}), 7.93 (d, J = 9.0 Hz, 1H, H_{11}), 7.77 (d, J = 9.3 Hz, 1H, H_4), 7.60 (s, 1H, H_8), 7.20 (dd, J = 7.0, 1.8 Hz, 1H, H_{10}), 6.77 (d, J = 9.3 Hz, 1H, H_3), 4.97 (s, 1H, N*H*), 4.70 (t, 2H, NCH_2CH$_2$NMe$_2$), 3.50 – 3.33 (m, 2H, NHCH_2CH$_2$NMe$_2$), 3.04 (t, 2H, NCH$_2$CH_2NMe$_2$), 2.73 – 2.59 (m, 3H, NHCH$_2$CH_2NMe$_2$), 2.33 (d, J = 12.4 Hz, 12H, NCH_3). ^{13}C NMR (75 MHz, $CDCl_3$) δ 164.7 (C=O), 146.9 (C_{12}), 146.3 (C_{14}), 143.8 (C_6), 138.8 (C_9), 131.7 (C_{11}), 121.3 (C_3), 120.7 (C_{10}), 119.9 (C_7), 114.3 (C_5), 102.4 (C_8), 57.9 (NHCH$_2$*C*H$_2$NMe$_2$), 57.4 (NCH$_2$*C*H$_2$NMe$_2$), 47.6 (N*C*H$_2$CH$_2$NMe$_2$), 45.9 (NCH$_2$CH$_2$N(*C*H$_3$)$_2$), 45.2 (NHCH$_2$CH$_2$N(*C*H$_3$)$_2$), 40.9 (NH*C*H$_2$CH$_2$NMe$_2$).

9-bromo-1,6-dimethyl-2-oxo-1,2-dihydrobenzo[h][1,6]naphthyridin-6-ium trifluoromethanesulfonate (III.4)

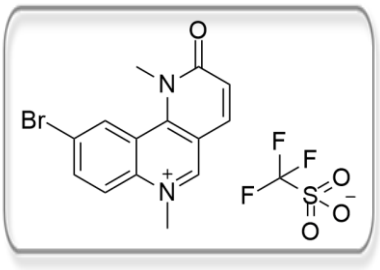

III.24 (85 mg, 0.29 mmol) reacted with methyl trifluoromethanesulfonate (200 µL, 1.76 mmol), according to general procedure J to afford **III.4** as an off-white solid (89 mg, 67%). M.p. 164-167 °C; ^{1}H NMR (300 MHz, MeOD) δ 9.53 (s, 1H, H_{14}), 9.11 (d, J = 1.6 Hz, 1H, H_8), 8.40 – 8.31 (m, 2H, H_{10}, H_{11}), 8.17 (d, J = 9.6 Hz, 1H, H_4), 7.01 (d, J = 9.6 Hz, 1H, H_3), 4.54 (s, 3H, N$^+$CH_3), 4.14 (s, 3H, NCH_3). 13C NMR (75 MHz, MeOD) δ 164.8 (*C*=O), 151.2 (C_{14}), 150.8 (C_6), 139.2 (C_{12}), 139.1 (C_4), 138.7 (C_{11}), 131.3 (C_8), 124.4 (C_3), 123.3 (C_9), 122.1 (C_7), 121.9 (C_{10}), 114.7 (C_5), 45.4 (N$^+$*C*H$_3$), 39.5 (N*C*H$_3$).

2.3. Synthesis of compounds described in Chapter III

2.3.1. General methods

General procedure K for trityl deprotection. TFA (11 equiv.) and TES (3 equiv.) were added to a solution of trityl protected Fmoc-cysteine or dipeptide in DCM and the mixture was stirred at rt for 3 h under nitrogen atmosphere. The solvent was evaporated under reduced pressure and the crude residue was washed with toluene and after each washing it was evaporated to dryness. The solid residue was washed with pentane and the precipitate was filtered to afford the desired compounds.

General procedure L for dipeptide synthesis. *N*-protected-amino acid (1.2 equiv.) and acid-protected amino acid (1.0 equiv.) were dissolved in DMF. Then TBTU (1.2 equiv.), HOBt (1.2 equiv.), and DIPEA (1.2 equiv.) were added. The reaction mixture was stirred at rt o/n. After completion of the reaction, water as added to the reaction mixture and the product was extracted with EtOAc. The organic phase was washed with 5 % aqueous $KHSO_4$, saturated aqueous $NaHCO_3$, water, brine, dried with anhydrous Na_2SO_4 The solvent was removed under reduced pressure and the crude product was purified to afford the desired compounds.

General Procedure M for Boc-Protection of Nucleobases. To a solution of nucleobase (1.0 equiv.) and DMAP (0.1 equiv.) in dry THF (0.2 M) was added Boc_2O (4.0 equiv.) and the reaction mixture was stirred overnight at rt, under a nitrogen atmosphere. After the reaction reach completation, the solvent was evaporated and the crude product was redissolved in AcOEt. The organic phase was washed subsequently with 5% aqueous $KHSO_4$, saturated aqueous $NaHCO_3$, water and brine, dried with anhydrous Na_2SO_4 and concentrated under reduced pressure. The crude product was purified by flash column chromatography.

General Procedure N for selective *N*-Boc deprotection. To a solution of tris-*N*-Boc-nucleobase (1 equiv.) dissolved in MeOH (0.1 M) was added saturated aqueous $NaHCO_3$ (half of MeOH volume). The turbid solution was stirred at 50 °C for 1 h, at which point clean conversion to bis-Boc protected nuclabase was observed by TLC. After evaporation of MeOH, water was added to the reaction mixture (pH=4) and the pH of the mixture was adjusted to ca. 7. The aqueous phase was then extracted with DCM and the combined organic phases were washed with water and brine, dried with anhydrous Na_2SO_4, and concentrated under reduced pressure to afford the desired compounds.

General Procedure O for *N*-allylation of nucleobases. To a suspension of K_2CO_3 (3 equiv.) in dry DMF was added nucleobase (1 equiv.) at 0 °C under nitrogen atmosphere. After 15 min, allyl bromide (1.2 equiv.) was added dropwise and stirring was continued at rt o/n. After reaction completation, water was added and the product was extracted with EtOAc. The organic layer was washed with 5% aqueous $KHSO_4$, water and brine, dried with anhydrous Na_2SO_4 and concentrated under reduced pressure. The crude product was purified by flash column chromatography.

General procedure P for thermaly-induced thiol-ene reaction. The DCE was degassed under nitrogen atmosphere in a sonicator bath for 15 min prior to use. DCE was added to a thiol (1 equiv.), an alkene (3 equiv.), AIBN (0.5 equiv.) and the mixture was brought to reflux. The solution was allowed to cool to rt and the solvent was removed under reduced pressure.

General procedure Q for photochemically-induced thiol-ene reactions. The DCE was degassed under nitrogen atmosphere in a sonicator bath for 15 min prior to use. DCE was added to a thiol (1 equiv.), an alkene (3 equiv.) and 0.1 equivalents of DPAP. The mixture was irradiated at rt under magnetic stirring. Then, the solvent was removed under reduced pressure.

2.3.2. Synthesis of compounds **IV.6** and **IV.7**

_N_-(9-Fluorenylmethoxycarbonyl)-L-cysteine (IV.6)

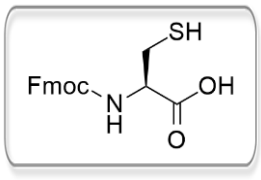

N-(9-Fluorenylmethoxycarbonyl)-*S*-trityl-L-cysteine **IV.8** (100 mg, 0.17 mmol) was treated under the conditions described in the general procedure K to afford the compound **III.6** as a white solid (53 mg, 87%). M.p. 112-115 °C; ^{1}H NMR (400 MHz, $CDCl_3$) δ 7.77 (d, *J* = 7.5 Hz, 2H, H_{arom}), 7.61 (d, *J* = 7.3 Hz, 2H, H_{arom}), 7.41 (t, *J* = 7.4 Hz, 2H, H_{arom}), 7.33 (t, *J* = 8.3 Hz, 2H, H_{arom}), 5.67 (d, *J* = 7.6 Hz, 1H, N*H*), 4.72 (s, 1H, H_α), 4.46 (d, *J* = 6.0 Hz, 2H, CH_{2Fmoc}), 4.24 (t, *J* = 6.6 Hz, 1H, CH_{Fmoc}), 3.13 – 2.95 (m, 2H, CH_2SH), 1.46 (t, *J* = 8.8 Hz, 1H, S*H*). Analytical date were in agreement with those already published.[560]

(*R*)-ethyl 2-(2-((((9H-fluoren-9-yl)methoxy)carbonyl)amino)-3-(tritylthio)propanamido)acetate (III.10a)

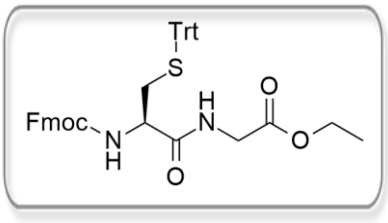

N-(9-Fluorenylmethoxycarbonyl)-*S*-trityl-L-cysteine **IV.8** (1.00 g, 1.71 mmol) and glycine ethyl ester hydrochloride (199 mg, 1.42 mmol) reacted under the conditions descrived in general procedure L. The crude product was purified by flash column chromatography (hexane/EtOAc, 3:7) to afford **III.10a** as white solid (790 mg, 83%). M.p. 77-81 °C; ^{1}H NMR (400 MHz, $CDCl_3$) δ 7.75 (t, *J* = 7.8 Hz, 2H, $H_{aromFmoc}$), 7.57 (d, *J* = 6.8 Hz, 2H, $H_{aromFmoc}$), 7.43-7.36 (m, 8H, $H_{aromFmoc}$, $H_{aromTrt}$), 7.29 – 7.19 (m, 11H, $H_{aromFmoc}$, $H_{aromTrt}$), 6.32 (s, 1H, NH_{gly}), 4.97 (d, J = 5.2 Hz, 1H, NH_{cys}), 4.39 (d, J = 6.8 Hz, 2H, CH_{2Fmoc}), 4.21-4.10 (m, 4H, H_{Fmoc}, CH_2CH$_3$), 3.99-3.86 (m, 2H, CH_{2gly}), 3.79 (d, J = 6.4 Hz, 1H, H_α), 2.67 (t, J = 5.2 Hz, 2H, CH_2SH), 1.25 (t, J = 6.8 Hz, 3H, CH_3). Analytical date were in agreement with those already published.[561]

(*R*)-benzyl 2-(2-((((9H-fluoren-9-yl)methoxy)carbonyl)amino)-3-(tritylthio)propanamido)acetate (II.10b)

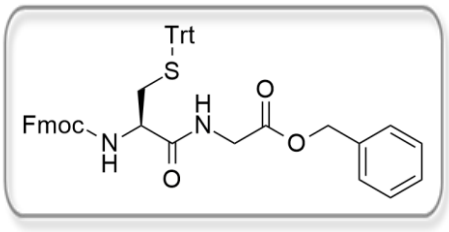

N-(9-Fluorenylmethoxycarbonyl)-*S*-trityl-L-cysteine **IV.8** (697 mg, 1.19 mmol) and glycine benzyl ester hydrochloride (200 mg, 0.99 mmol) reacted under the conditions descrived in general procedure L. The crude product was purified by flash column chromatography (hexane/EtOAc, 3:7) to afford **II.10b** as white solid (671 mg, 92%). M.p. 74-77 °C; ^{1}H NMR (400 MHz, $CDCl_3$) δ 7.66 (t, *J* = 7.0 Hz, 2H, H_{arom}), 7.49 (d, *J* = 6.8 Hz, 2H, H_{arom}), 7.39 – 7.06 (m, 24H, H_{arom}), 6.30 (s, 1H, NH_{gly}), 5.06 (s, 2H, CH_{2Bn}), 4.92 (d, *J* = 6.8 Hz, 1H, NH_{cys}), 4.31 (d, *J* = 6.8 Hz, 2H, CH_{2Fmoc}), 4.11 (t, *J* = 6.8 Hz, 1H, H_{Fmoc}), 3.89 (qd, *J* = 18.4, 4.6 Hz, 2H, CH_{2gly}), 3.72 (d, *J* = 5.6 Hz, 1H, H_∞), 2.59 (s, 2H, CH_2SH). ^{13}C NMR (101 MHz, $CDCl_3$) δ 170.4 (*C*=O), 169.2 (*C*=O), 156.1 (*C*=O), 144.4 ($C_{quartTrt}$), 143.8 ($C_{quatFmoc}$), 143.8 ($C_{quartTrt}$), 141.4 ($C_{quatFmoc}$), 135.1 (C_{quatBn}), 129.7 (C_{arom}), 128.7 (C_{arom}), 128.5 (C_{arom}), 128.2 (C_{arom}), 128.0 (C_{arom}), 127.9 (C_{arom}), 127.4 (C_{arom}), 127.2 (C_{arom}), 127.1 (C_{arom}), 125.2 (C_{arom}), 120.1 (C_{arom}), 67.4 (CH_{2Fmoc}, CH_{2Bn}), 53.9 (CH_α), 47.2 (CH_{Fmoc}), 41.5 (CH_{2gly}), 33.7 (CH_2SH). MS (ESI) 755.34 $[M+Na]^+$.

(*R*)-ethyl 2-(2-((((9H-fluoren-9-yl)methoxy)carbonyl)amino)-3-mercaptopropanamido)acetate (IV.7a)

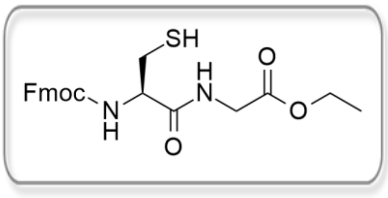

IV.10a (200 mg, 0.30 mmol) was treated under the conditions described in the general procedure K to afford the compound **III.7a** as a white solid (111 mg, 87%). M.p. 133-136 °C; ^{1}H NMR (400 MHz, DMSO-d_6) δ 8.46 (t, *J* = 5.4 Hz, 1H, NH_{gly}), 7.90 (d, *J* = 7.2 Hz, 2H, $H_{aromFmoc}$), 7.74 (dd, *J* = 7.0, 4.2 Hz, 2H, $H_{aromFmoc}$), 7.62 (d, *J* = 8.0 Hz, 1H, NH_{cys}), 7.42 (t, *J* = 7.2 Hz, 2H, $H_{aromFmoc}$), 7.33 (t, *J* = 7.4 Hz, 2H, $H_{aromFmoc}$), 4.34 – 4.21 (m, 3H, CH_{Fmoc}, CH_{2Fmoc}), 4.17-4.12 (m, 1H, $H_{\propto}$), 4.08 (q, *J* = 7.0 Hz, 2H, CH_2CH$_3$), 3.90 – 3.77 (m, 2H, CH_{2gly}), 2.88-2.80 (m, 1H, CH_2SH), 2.71 – 2.62 (m, 1H, CH_2SH), 2.33 (t, *J* = 8.2 Hz, 1H, CH$_2$SH), 1.18 (t, *J* = 7.0 Hz, 3H, CH_3). ^{13}C NMR (101 MHz, DMSO-d_6) δ 170.7 (*C*=O), 169.7 (*C*=O), 156.0 (*C*=O), 143.8 ($C_{quatFmoc}$), 140.7 ($C_{quatFmoc}$), 127.7 (*C*H$_{arom}$), 127.1 (*C*H$_{arom}$), 125.4 (*C*H$_{arom}$), 120.1 (*C*H$_{arom}$), 65.8 (*C*H$_{2Fmoc}$), 60.5 (*C*H$_2$CH$_3$), 57.2 (*C*H$_\alpha$), 46.6 (*C*H$_{Fmoc}$), 40.8 (*C*H$_{2gly}$), 26.2 (*C*H$_2$SH), 14.1 (*C*H$_3$). MS (ESI) 451 [M+Na]$^+$. Anal. Calcd $C_{22}H_{24}N_2O_5S{\cdot}0{,}1H_2O$ for: C, 61.40; H, 5.68; N, 6.51; S, 7.45. Found: C, 61.77; H, 5.83; N, 6.40; S, 7.06.

(*R*)-benzyl 2-(2-((((9H-fluoren-9-yl)methoxy)carbonyl)amino)-3-mercaptopropanamido)acetate (IV.7b)

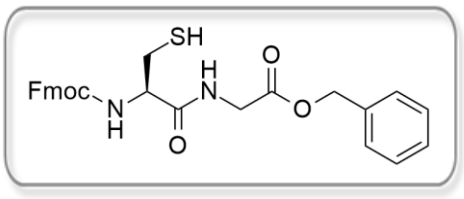

IV.10b (200 mg, 0.27 mmol) was treated under the conditions described in the general procedure K to afford the compound **III.7a** as a white solid (107 mg, 80%)**.** M.p. 128-130 °C; ^{1}H NMR (400 MHz, DMSO-d_6) δ 8.51 (t, J= 5.8 Hz, NH_{gly}), 7.90 (d, *J* = 7.6 Hz, 2H, $H_{aromFmoc}$), 7.74 (dd, *J* = 6.6, 5 Hz, 2H, $H_{aromFmoc}$), 7.64 (d, *J* = 8.0 Hz, 1H, NH_{cys}), 7.42 (t, *J* = 7.4 Hz, 2H, $H_{aromFmoc}$), 7.33 (m, 7H, $H_{aromFmoc,}$ H_{aromBn}), 5.11 (s, 2H, CH_{2Bn}), 4.34 – 4.29 (m, 1H, CH_{Fmoc}), 4.27-4.21 (m, 2H, CH_{2Fmoc}), 4.17-4.12 (m, 1H, H_α), 4.00 – 3.82 (m, 2H, CH_{2gly}), 2.79 (s, 1H, CH_2SH), 2.67 (s, 1H, CH_2SH), 2.32 (s, 1H, SH). ^{13}C NMR (101 MHz, DMSO-d_6) δ 170.7 (*C*=O), 169.6 (*C*=O), 156.0 (*C*=O), 143.8 ($C_{quatFmoc}$), 140.7 ($C_{quatFmoc}$), 135.8 (C_{quatBn}), 128.4 (C_{arom}), 128.1 (C_{arom}), 128.0 (C_{arom}), 127.7 (C_{arom}), 127.1 (C_{arom}), 125.4 (C_{arom}), 120.1 (C_{arom}), 65.9 (*C*H$_{2Fmoc,}$ *C*H$_{2Bn}$), 57.2 (*C*H$_\propto$), 46.7 (*C*H$_{Fmoc}$), 40.9 (*C*H$_{2gly}$), 26.2 (*C*H$_2$SH). MS (ESI) 513 [M+Na]$^+$. Anal. Calcd for $C_{27}H_{26}N_2O_5S$: C, 66.10; H, 5.34; N, 5.71; S, 6.54. Found: C, 66.35; H, 5.70; N, 5.50; S, 6.51.

2.3.3. Synthesis of compounds **IV.13, IV.14** and **IV.19**

Tris-*N*-Boc-cytosine (IV.13)

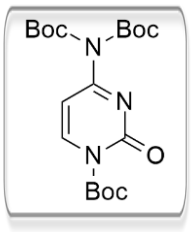

Cytosine **IV.11** (1.00 g, 9.00 mmol) reacted with Boc_2O (8.27 mL, 36.00 mmol) under the conditions described in the general procedure M. The crude product was purified by flash column chromatography (hexane/EtOAc, 25:75) to afford **IV.13** as a pale yellow oil (3.33 g, 90%). ^{1}H NMR (400 MHz, $CDCl_3$) δ 7.97 (d, *J* = 7.9 Hz, 1 H, H_6), 7.07 (d, J = 7.8 Hz, 1 H, H_5), 1.60 (s, 9 H, N^1-Boc), 1.56 (s, 18 H, Boc of exocyclic amine). Analytical date were in agreement with those already published.[541]

Tris-*N*-Boc-adenine (IV.14)

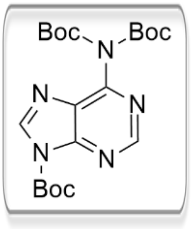

Adenine **IV.12** (1.00 g, 7.40 mmol) was treated with Boc_2O (6.80 mL, 29.60 mmol) under the conditions described in the general procedure M. The crude product was purified by flash column chromatography (hexane/EtOAc, 7:3) to afford **IV.14** as a white foam (3.01 g, 93%). M.p. 53–54 °C; ^{1}H NMR (400 MHz, $CDCl_3$) δ 9.02 (s, 1H, H_2), 8.51 (s, 1H, H_8), 1.71 (s, 9H, N^9-Boc), 1.43 (s, 18H, Boc of exocyclic amine). Analytical date were in agreement with those already published.[537,538]

Tris-*N*-Boc-2-amino-6-chloropurine (IV.19)

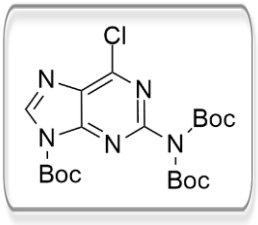

2-amino-6-chloropurine **IV.17** (500 mg, 2.94 mmol) was treated with Boc_2O (2.71 mL, 11.79 mmol) under the conditions described in the general procedure M. The crude product was purified by flash chromatography (elution first with hexane/EtOAc (9:1) to remove unreacted Boc_2O and then with EtOAc, 100%) to afford **IV.19** as a white foam (948 mg, 68%). M.p. 50–51 °C; ^{1}H NMR (400 MHz, $CDCl_3$) δ 8.58 (s, 1H, H_8), 1.69 (s, 9H, C(CH)$_3$ of N^9-Boc), 1.46 (s, 18H, Boc of exocyclic amine). Analytical date were in agreement with those already published.[537,538]

2.3.4. Synthesis of compounds **IV.15, IV.16** and **IV.18**

Bis-*N*-Boc-cytosine (IV.15)

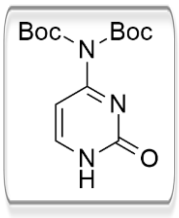

IV.13 (3.33 g, 8.09 mmol) was treated under the conditions described in the general procedure N to afford the compound **III.15** as a white solid (2.11 g, 83%). M.p. > 320 ºC; ^{1}H RMN (400 MHz, $CDCl_3$) δ 7.68 (d, *J* = 7.1 Hz, 1 H, H_6), 7.26 (s, 1 H, N*H*), 7.12 (d, *J* = 7.1 Hz, 1 H, H_5), 1.56 (s, 18 H, Boc). Analytical date were in agreement with those already published.[541]

Bis-*N*-Boc-adenine (IV.16)

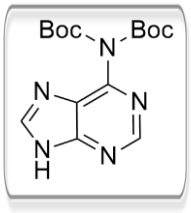

IV.14 (3.01 g, 6.91 mmol) was treated under the conditions described in the general procedure N to afford the compound **IV.16** as a white solid (1.73 g, 75%). M.p. 147-149 ºC; ^{1}H RMN (400 MHz, $CDCl_3$) δ 8.81 (s, 1 H, H_2) 8.35 (s, 1 H, H_8), 1.55 (s, 18 H, s, 18H, Boc). Analytical date were in agreement with those already published.[537,538]

Bis-*N*-Boc-2-amino-6-chloropurine (IV.18)

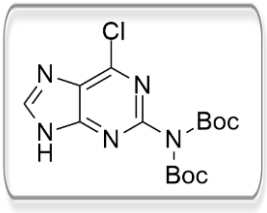

IV.19 (948 mg, 2.02 mmol) was treated under the conditions described in the general procedure N to afford the compound **IV.18** as a waxy solid (709 mg, 96%). ^{1}H NMR (400 MHz, $CDCl_3$) δ 8.36 (s, 1H, H_8), 1.51 (s, 18H, Boc). Analytical date were in agreement with those already published.[537,538]

2.3.5. Synthesis of compound **IV.24**

Bis-*tert*-butyl (9-(2-chloroethyl)-9*H*-purin-6-yl)carbamate (IV.24)

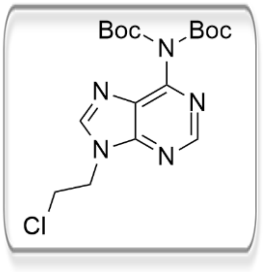

To a suspension of **IV.16** (200 mg, 0.60 mmol, 1 equiv.) in dry DMF (0.2 M) at rt was added K_2CO_3 (3 equiv.) and 1-bromo-2-chloroethane (60 µL, 0.72 mmol, 1.2 equiv.). The reaction mixture was stirred at rt under nitrogen atmosphere o/n. The reaction was diluted with ethyl acetate and washed with 1N HCl, water, brine and dried with anhydrous Na_2SO_4. The solvent was removed under reduced pressure. The crude product was purified by flash column chromatography (hexane/EtOAc,3:7) to afford **IV.24** as a white solid (169 mg, 71%). ^{1}H NMR (400 MHz, $CDCl_3$) δ 8.83 (s, 1H, H_2), 8.16 (s, 1H, H_8), 4.61 (t, *J* = 5.5 Hz, 2H, NCH_2), 3.93 (t, *J* = 5.5 Hz, 2H, CH_2Cl), 1.40 (s, 18H, Boc).

2.3.6. Synthesis of compounds **IV.31**, **IV.32** and **IV.33**

***N*^{1}-allyl-bis-Boc-cytosine (IV.31)**

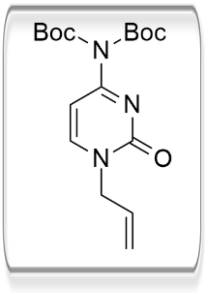

IV.15 (330 mg, 1.06 mmol) reacted with allyl bromide (110 µL, 1.27 mmol) under the conditions described in general procedure O. The crude product was purified by flash column chromatography (hexane/EtOAc, 2:8) to afford **IV.31** as a white solid (254 mg, 68%). M.p. 78-70 ^{0}C; ^{1}H NMR (400 MHz, $CDCl_3$) δ 7.50 (d, *J* = 7.3 Hz, 1H, H_6), 7.02 (d, *J* = 7.3 Hz, 1H, H_5), 5.98-5.88 (m, 1H, C*H*=CH_2), 5.30 (d, *J* = 10.2 Hz, 1H, CH=CH_{cis}), 5.26 (d, *J* = 17.1 Hz, 1H, CH=CH_{trans}), 4.48 (d, *J* = 6.0 Hz, 2H, NCH_2), 1.56 (s, 18H, Boc). ^{13}C NMR ($CDCl_3$) δ 162.4 (C_4), 155.1 (*C*=O), 149.7 (*C*=O_{Boc}), 147.3 (C_6), 131.8 (*C*H=CH_2), 119.7 (CH=*C*H_2), 96.6 (C_5), 85.1 ($C_{quatBoc}$), 52.3 (N*C*H_2), 27.8 (*C*H_3). MS (ESI) *m/z* 374 [M+Na]$^+$. HRMS-ESI: *m/z* [M + Na]$^+$ calcd for $C_{17}H_{25}N_3NaO_5$: 374.1686, found: 374.1678.

***N*^{9}-allyl-bis-Boc-adenine (IV.32)**

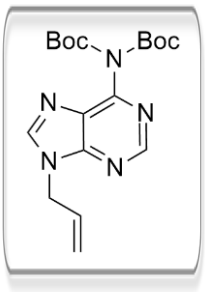

IV.16 (200 mg, 0.60 mmol) reacted with allyl bromide (62 µL, 0.72 mmol) under the conditions described in general procedure O. The crude product was purified by flash column chromatography (hexane/EtOAc, 2:8) to afford **IV.32** as a white solid (129 mg, 58%). M.p. 74-77 ^{0}C; ^{1}H NMR (400 MHz, $CDCl_3$) δ 8.85 (s, 1H, H_2), 8.07 (s, 1H, H_8), 6.10-5.99 (m, 1H, C*H*=CH_2), 5.33 (dd, *J* = 10.2, 0.4 Hz, 1H, CH=CH_{cis}), 5.21 (d, *J* = 17.2, 0.4 Hz, 1H, CH=CH_{trans}), 4.89 (d, *J* = 5.6 Hz, 2H, NCH_2), 1.43 (s, 18H, Boc). ^{13}C NMR (101 MHz, $CDCl_3$) δ 153.3 (C_4), 152.3 (C_2), 150.5 (C_6), 150.4 (*C*=O_{Boc}), 144.7 (C_8), 131.3 (*C*H=CH_2), 128.8 (C_5), 119.7 (CH=*C*H_2), 83.8 ($C_{quatBoc}$), 46.2 (N*C*H_2), 27.9 (*C*H_3). MS (ESI) *m/z* 398 [M+Na]$^+$. Anal. Calcd for $C_{22}H_{33}N_5O_4$: C, 57.59; H, 6.71; N, 18.65. Found: C, 57.96; H, 6.85; N, 18.37.

***N*^{7}-allyl-bis-Boc-adenine (IV.34)**

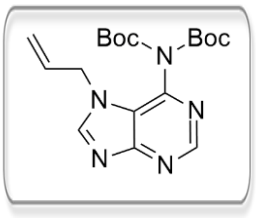

IV.34 was obtained as a minor product of the previous reaction.White solid (81 mg, 36%). ^{1}H NMR (400 MHz, $CDCl_3$) δ 9.04 (s, 1H, H_2), 8.24 (s, 1H, H_8), 6.01 – 5.92 (m, 1H, C*H*=CH_2), 5.33 (d, *J* = 10.3 Hz, 1H, CH=CH_{cis}), 5.20 (d, *J* = 17.1 Hz, 1H, CH=CH_{trans}), 4.82 (d, *J* = 5.6 Hz, 2H, NCH_2), 1.38 (s, 18H, Boc). ^{13}C NMR (101 MHz, CDCl3) δ 163.7 (C_4), 157.1 (C_6), 152.9 (C_2), 150.1 (*C*=O_{Boc}), 148.8 (C_8), 144.2 (C_5), 131.1 (*C*H=CH_2), 120.1 (CH=*C*H_2), 84.6 ($C_{quatBoc}$), 49.3 (N*C*H_2), 28.0 (*C*H_3).

N^1-allylthymine (IV.33)

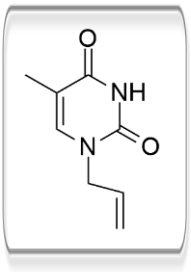

Thymine **IV.30** (1.00g, 7.93 mmol) reacted with allyl bromide (822 µL, 9.52 mmol) under the conditions described in general procedure O. The crude product was purified by flash column chromatography (hexane/EtOAc, 7:3) to afford **IV.33** as a white solid (792 mg, 60%). M.p. 95-97 ºC; ^{1}H NMR ($CDCl_3$) δ 9.01 (br s, 1H, N*H*), 6.97 (s, 1H, C*H*=C(CH_3)), 5.91 – 5.81 (m, 1H, C*H*=CH_2), 5.30 (d, J = 10.2 Hz, 1H, CH=CH_{cis}), 5.26 (d, J = 17.8 Hz, 1H, CH=CH_{trans}), 4.33 (d, J = 5.8 Hz, 2H, NCH_2), 1.92 (s, 3H, CH_3). ^{13}C NMR ($CDCl_3$) δ 164.3 (C^4=O), 150.9 (C^2=O), 139.8 (C_6), 131.8 (*C*H=CH_2), 119.4 (CH=CH_2), 111.1 (*C*-5), 49.9 (N*C*H_2), 12.5 (C*C*H_3). MS (ESI) *m/z* 190 $[M+Na]^+$. Analytical date were in agreement with those already published.[532,533]

N^1,N^3-diallylthymine (IV.35)

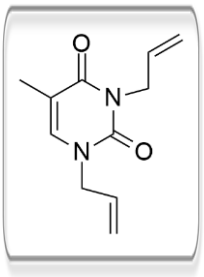

IV.35 was obtained as a minor product of the previous reaction. Incolor oil (322 mg, 20%). ^{1}H NMR (400 MHz, $CDCl_3$) δ 6.96 (s, 1H, H_6), 5.88 (ddd, *J* = 16.6, 10.6, 5.7 Hz, 2H, C*H*=CH_2), 5.34 – 5.13 (m, 4H, CH=CH_2), 4.58 (d, *J* = 5.7 Hz, 2H, N^3CH_2), 4.35 (d, *J* = 5.7 Hz, 2H, N^1CH_2), 1.93 (s, 3H, CH_3). ^{13}C NMR (101 MHz, $CDCl_3$) δ 163.6 (C^4=O), 151.3 (C^2=O), 137.9 (C_6), 132.1 (N^1CH_2*C*H=CH_2), 131.9 (N^3CH_2*C*H=CH_2), 119.2 (N^1CH_2CH=*C*H_2), 118.0 (N^3CH_2CH=*C*H_2), 110.3 (C_5), 50.9 (N^1*C*H_2), 43.6 (N^3*C*H_2), 13.2 (*C*H_3). Analytical date were in agreement with those already published.[562]

2.3.7. Synthesis of compound **IV.36**

N^9-allyl-N^2,$N^{2'}$-bis-Boc-2-amino-6-chloropurine (IV.36)

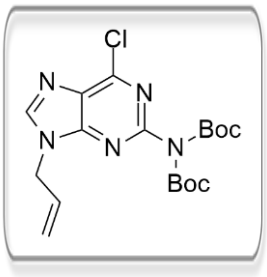

IV.18 (50 mg, 0.14 mmol) reacted with allyl bromide (14 µL, 0.16 mmol) under the conditions described in general procedures O. The crude product was purified by preparative TLC (hexane/EtOAc, 2:8) to afford **IV.36** as white solid (28 mg, 51%). ^{1}H NMR ($CDCl_3$) δ 8.15 (s, 1H, H_8), 6.10 – 5.96 (m, 1H, C*H*=CH_2), 5.37 (d, *J* = 10.2 Hz, 1H, CH=CH_{cis}), 5.24 (d, *J* = 17.0 Hz, 1H, CH=CH_{trans}), 4.88 (d, *J* = 5.8 Hz, 2H, NCH_2), 1.44 (s, 18H, Boc). ^{13}C NMR ($CDCl_3$) δ 152.7 (C_4), 152.1 (C_6), 151.4 (*C*=O_{Boc}), 150.7 (C_2), 145.9 (C_8), 131.0 (*C*H=CH_2), 130.1 (C_5), 120.2 (CH=*C*H_2), 83.8 ($C_{quatBoc}$), 46.5 (N*C*H_2), 28.0 (*C*H_3). MS (ESI) *m/z* 432 $[M+Na]^+$.

N^7-allyl-N^2,$N^{2'}$-bis-Boc-2-amino-6-chloropurine (IV.38)

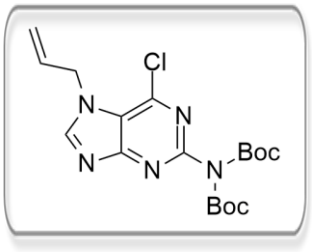

IV.38 was obtained as minor product of the previous reaction. White soild (15 mg, 27%). ^{1}H NMR (400 MHz, $CDCl_3$) δ 8.26 (s, 1H, H_8), 6.09 (ddd, *J* = 22.2, 10.4, 5.6 Hz, 1H, C*H*=CH_2), 5.39 (d, *J* = 10.4 Hz, 1H, CH=CH_{cis}), 5.17 – 5.08 (m, 3H, CH=CH_{trans} and NCH_2), 1.44 (s, 18H, Boc).

N^2-mono-Boc-2-amino-6-chloropurine (IV.37)

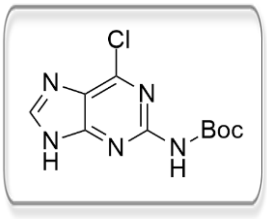

To a suspension of NaH 60 % dispersion in mineral oil (1.1 equiv.) in dry THF was added **IV.18** (50 mg, 0.14 mmol, 1 equiv.) at 0 °C under nitrogen atmosphere. After 15 minutes, allyl bromide (13 µL, 0.15 mmol, 1.1 equiv.) was added dropwise. The reaction mixture was stirred at rt o/n. After reaction completation, it was quenched with water. After THF evaporation, the pH of the mixture was adjusted to ca. 7 and extracted with DCM. The combined organic phases were washed with water and brine, dried with anhydrous Na_2SO_4, and concentrated under reduced pressure. The crude product was purified by preparative TLC (hexane/EtOAc, 2:8) to afford **IV.37** as a white solid (12 mg, 22%). M.p. decompose at 200 °C; ^{1}H NMR (400 MHz, $CDCl_3$) δ 8.44 (s, 1H, H_8), 7.81 (br s, 1H, N*H*), 1.57 (s, 9H, Boc). Analytical date were in agreement with those already published.[538]

2.3.8. Synthesis of compound **IV.45**

N^9-allyl-2-amino-6-chloropurine (IV.44)

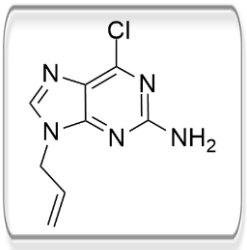

2-amino-6-chloropurine **IV.17** (400 mg, 2.36 mmol) reacted with allyl bromide (245 µL, 2.83 mmol) under the conditions described in general procedure O. The crude product was purified by flash column chromatography (hexane/EtOAc, 1:1) to afford **IV.44** as a white solid (334 mg, 68%). M.p. 149-151 °C; ^{1}H NMR (400 MHz, $CDCl_3$) δ 7.77 (s, 1H, H_8), 6.07 – 5.93 (m, 1H, C*H*=CH_2), 5.32 (d, *J* = 10.1 Hz, 1H, CH=CH_{cis}), 5.20 (d, J = 17.1 Hz, 1H, CH=CH_{trans}), 5.12 (s, 2H, NH_2), 4.70 (d, J = 4.5 Hz, 2H, NCH_2). MS (ESI) *m/z* 210 $[M+H]^+$. Analytical date were in agreement with those already published.[386]

***N*-9-allylguanine (IV.45)**

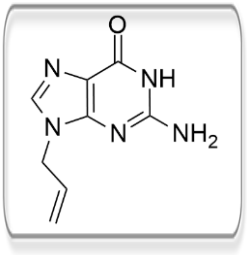

To solution of **IV.44** (334 mg, 1.59 mmol) in 1 N aqueous HCl (9.0 mL) was warmed to a gentle reflux for 2 h. After cooling to rt, the pH of the mixture was adjusted to ca. 7 with solid NaOH, and then cooled in an ice bath for 0.5 h. The precipitate was collected by filtration and dried in vacuo to afford **IV.45** as a white solid (238 mg, 71%). ^{1}H NMR (400 MHz, DMSO-d_6) δ 10.56 (s, 1H, N*H*), 7.64 (s, 1H, H_8), 6.45 (s, 2H, NH_2), 6.20 – 5.85 (m, 1H, C*H*=CH$_2$), 5.17 (d, *J* = 9.8 Hz, 1H, CH=CH_{cis}), 4.96 (d, *J* = 16.9 Hz, 1H, CH=CH_{trans}), 4.58 (s, 2H, NCH_2). Analytical date were in agreement with those already published.[386]

2.3.9. Synthesis of compound **IV.40**

***N*^{9}-allyl-*N*^{2},*N*$^{2'}$-bis-Boc-guanine (IV.40)**

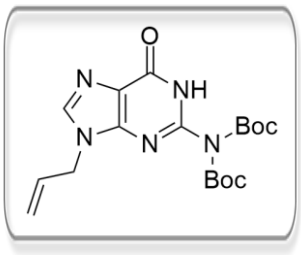

IV.45 (400 mg, 2.09 mmol) was treated with Boc$_2$O (1.92 mL, 8.37 mmol, 4 equiv.) under the conditions described in the general procedure M. The crude product was purified by flash chromatography [elution started with hexane/EtOAc (15:85) and polarity increased gradually until EtOAc/MeOH (95:5)] to afford **IV.40** as a white solid (371 mg, 45%). M.p. 149-152 ^{0}C; ^{1}H NMR (400 MHz, $CDCl_3$) δ 11.32 (s, 1H, N*H*), 7.64 (s, 1H, C_8), 5.96 (ddd, *J* = 16.5, 10.5, 5.0 Hz, 1H, C*H*=CH$_2$), 5.28 (dd, J = 10.5, 0.6 Hz, 1H, CH=CH_{cis}), 5.14 (dd, *J* = 16.5, 0.6 Hz, 1H CH=CH_{trans}), 4.61 (dd, *J* = 5.0, 1.4 Hz, 2H, NC$H_{2)}$, 1.56 (s, 18H, Boc). ^{13}C NMR (101 MHz, $CDCl_3$) δ 155.9 (C=O), 149.2 (*C*=O$_{Boc}$), 148.2 (C_4), 146.3 (C_2), 138.9 (C_8), 131.7 (*C*H=CH$_2$), 121.3 (C_5), 119.1 (CH=*C*H$_2$), 86.3 ($C_{quatBoc}$), 46.0 (N*C*H$_2$), 27.8 (Boc). MS (ESI) *m/z* 414 [M+Na]$^+$.

***N*^{9}-allyl-*N*^{2}-mono-Boc-guanine (IV.46)**

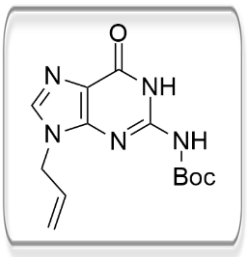

IV.46 was obtained as a minor product of the previous reaction. White solid (253 mg, 42%). M.p. 167-170 ^{0}C. ^{1}H NMR (400 MHz, $CDCl_3$) δ 11.35 (s, 1H, N*H*), 7.63 (s, 1H, NH_{exo}), 7.61 (s, 1H, H_8), 5.95 (m, 1H, C*H*=CH$_2$), 5.27 (d, *J* = 10.4 Hz, 1H, CH=CH_{cis}), 5.12 (d, *J* = 17.2 Hz, 1H, CH=CH_{trans}), 4.61 (d, *J* = 5.6 Hz, 2H, NCH_2), 1.51 (s, 9H, Boc). ^{13}C NMR (101 MHz, $CDCl_3$) δ 155.8 (*C*=O), 152.5 (*C*=O$_{Boc}$), 148.7 (C_4), 147.1 (C_2), 138.6 (C_8), 131.9 (*C*H=CH$_2$), 120.7 (C_5), 118.9 (CH=*C*H$_2$), 84.6 ($C_{quatBoc}$), 45.9 (N*C*H$_2$), 28.1 (Boc). MS (ESI) *m/z* 314 [M+Na]$^+$. Anal. Calcd for $C_{17}H_{25}N_5O_3 \cdot 0.4H_2O$: C, 55,26; H, 6.45; N, 17.91. Found: C, 54.64; H, 6.41; N, 17,20.

N^9-allyl-N^2,$N^{2'}$,O^6-tris-Boc-guanine (IV.47)

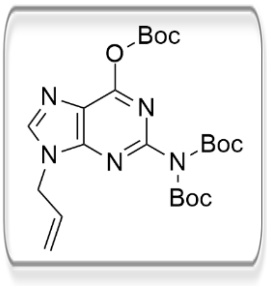

IV.47 was obtained as a minor product of the reaction to obtain **II.40.** White solid (73 mg, 7%).^{1}H NMR (400 MHz, CDCl3) δ 7.80 (s, 1H, H_8), 5.99 (ddd, J = 19.8, 10.0, 5.4 Hz, 1H, C*H*=CH_2), 5.29 (d, J = 10.0 Hz, 1H, CH=CH_{cis}), 5.09 (d, J = 19.8 Hz, 1H, CH=CH_{trans}), 4.76 (dt, J = 5.4, 1.4 Hz, 2H, NCH_2), 1.60 (s, 8H, Boc), 1.43 (s, 18H, Boc of exocyclic amine). MS (ESI) *m/z* 514 $[M+Na]^+$.

2.3.10. Synthesis of compound **IV.48**

N^9-allyl-O^6-benzylguanine (IV.48)

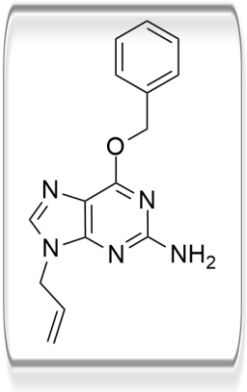

To a suspension of **IV.45** (40 mg, 0.21 mmol, 1 equiv.) in dry DMF (0.2 M), NaH 80 % dispersion in mineral oil (1.1 equiv.) was added under nitrogen atmosphere. After 15 min, benzyl bromide (27 µL, 0.23 mmol, 1.1 equiv.) was added dropwise. The reaction mixture was stirred at rt o/n. After reaction completation, it was quenched with water. The aqueous phase was extracted with EtOAc. The combined organic phases were washed with 5% aqueous KHSO4, water and brine, dried with anhydrous Na_2SO_4, and concentrated under reduced pressure. The crude product was purified by preparative TLC (eluent EtOAc/MeOH, 94:6) to afford **IV.48** as an incolor oil (9.5 mg, 16%). ^{1}H NMR (400 MHz, $CDCl_3$) δ 7.61 (s, 1H, H_8), 7.51 (d, *J* = 7.0 Hz, 2H, H_{benzyl}), 7.39 – 7.27 (m, 3H, H_{benzyl}), 6.07 – 5.93 (m, 1H, C*H*=CH_2), 5.56 (s, 2H, OCH_2), 5.28 (d, *J* = 10.2 Hz, 1H, CH=CH_{cis}), 5.15 (d, *J* = 17.0 Hz, 1H, CH=CH_{trans}), 4.93 (s, 2H, NH_2), 4.67 (d, *J* = 4.9 Hz, 2H, NCH_2). MS (ESI) *m/z* 304 $[M+Na]^+$. Analytical date were in agreement with those already published.[563]

N^9-allyl-N^2-benzylguanine (IV.49)

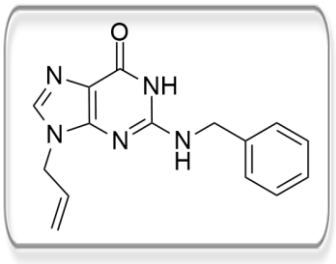

IV.49 was obtained as a major product of the previous reaction. Colorless oil (15 mg, 26%). ^{1}H NMR (400 MHz, $CDCl_3$) δ 7.59 (s, 1H, H_8), 7.40-7.32 (m, 3H, H_{benzyl}), 7.29 (d, J = 8.3 Hz, 2H, H_{benzyl}), 5.99 (ddd, *J* = 16.5, 10.2, 4.7 Hz, 1H, C*H*=CH_2), 5.36 (s, 2H, NCH_2C$_{benzyl}$), 5.30 (d, *J* = 10.2 Hz, 1H, CH=CH_{cis}), 5.19 (d, *J* = 16.5 Hz, 1H CH=CH_{trans}), 5.09 (d, *J* = 17.3 Hz, 2H, N*H*), 4.61 (d, *J* = 4.7 Hz, 2H, NCH_2CH=CH_2). MS (ESI) *m/z* 304 $[M+Na]^+$.

2.3.11. Synthesis of the target compounds

_N_-acetyl-_S_-octyl-_L_-cysteine (IV.50a)

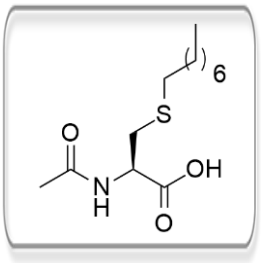

_N_-acetyl-L-cysteine **IV.21** (50 mg, 0.31 mmol) reacted with octene (144 µL, 0.93 mmol) under the conditions described in both general procedure P for 1.5 h (52 mg, 62%) and general procedure Q for 1 h (84 mg, 100%) to afford compound **IV.50a** as a colorless oil. ^{1}H NMR (400 MHz, $CDCl_3$) δ 6.45 (d, J = 6.9 Hz, 1H, NH), 4.76 (dd, J = 12.1, 5.5 Hz, 1H, H_α), 3.03 (d, J = 5.1 Hz, 2H, CCH_2S), 2.54 (t, J = 7.4 Hz, 2H, SCH_2CH$_2$(CH$_2$)$_5$CH$_3$), 2.09 (s, 3H, NC(O)CH_3), 1.57 (dt, J = 14.9, 7.3 Hz, 2H, SCH$_2$CH_2(CH$_2$)$_5$CH$_3$), 1.40 – 1.21 (m, 10H, SCH$_2$CH$_2$(CH_2)$_5$CH$_3$), 0.88 (t, J = 6.8 Hz, 3H, SCH$_2$CH_2(CH$_2$)$_5$CH_3).

***(R)*-2-((((9H-fluoren-9-yl)methoxy)carbonyl)amino)-3-((3-hydroxypropyl)thio) propanoic acid (IV.50c)**

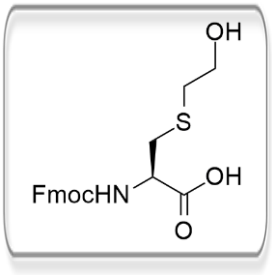

IV.6 (50 mg, 0.15 mmol) reacted with allyl alcohol (30 µL, 0.45 mmol) under the conditions described in general procedure P for 3.5 h to afford compound **IV.50c** as an colorless oil (58 mg, 100%). ^{1}H NMR (400 MHz, $CDCl_3$) δ 7.74 (d, J = 7.4 Hz, 2H, $H_{aromFmoc}$), 7.59 (d, J = 7.3 Hz, 2H, $H_{aromFmoc}$), 7.38 (t, J = 7.2 Hz, 2H, $H_{aromFmoc}$), 7.33 – 7.26 (t, J = 7.9 Hz 2H, $H_{aromFmoc}$), 6.01 (d, J = 7.6 Hz, 1H, NH), 4.63 (s, 1H, H_α), 4.38 (d, J = 6.8 Hz, 2H, CH_{2Fmoc}), 4.21 (t, J = 6.8 Hz, 1H, CH_{Fmoc}), 3.69 (t, J = 5.2 Hz, 2H, SCH$_2$CH$_2$CH_2OH), 3.02 (dd, J = 12.7, 4.7 Hz, CCH_2S), 2.65 (d, J = 6.1 Hz, 2H, SCH_2CH$_2$CH$_2$OH), 1.79 (t, J = 6.1 Hz, 2H, SCH$_2$CH_2CH$_2$OH). MS (ESI) m/z 424 $[M+Na]^+$.

(*R*)-2-((((9H-fluoren-9-yl)methoxy)carbonyl)amino)-3-((3-(5-methyl-2,4-dioxo-3,4-dihydropyrimidin-1(2H)-yl)propyl)thio)propanoic acid (IV.50d)

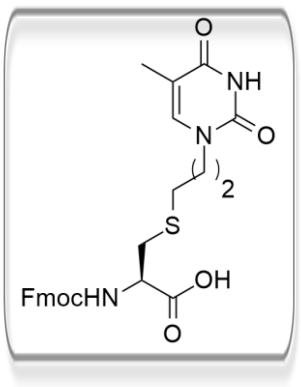

IV.6 (50 mg, 0.15 mmol) reacted with **IV.33** (73 mg, 0.45 mmol) under the conditions described in both general procedure P for 3 h (42 mg, 57%) and general procedure Q for 2 h (65 mg, 87%) to afford compound **IV.50d** as a white solid. ^{1}H NMR (400 MHz, $CDCl_3$) δ 9.93 (s, 1H, N$H_{thymine}$), 7.75 (d, J = 7.5 Hz, 2H, $H_{aromFmoc}$), 7.61 (t, J = 7.4 Hz, 2H, $H_{aromFmoc}$), 7.38 (t, J = 7.4 Hz, 2H, $H_{aromFmoc}$), 7.28 (q, J = 7.4 Hz, 2H, $H_{aromFmoc}$), 6.97 (s, 1H, C$H_{thymine}$), 5.99 (br s, 1H, NH_{cys}), 4.63 (s, 1H, H_α), 4.39 (d, J = 7.1 Hz, 2H, CH_{2Fmoc}), 4.21 (t, J = 7.1 Hz, 1H, CH_{Fmoc}), 3.84 (dd, J = 13.7, 6.5 Hz, 1H, NCH_2CH$_2$CH$_2$SCH$_2$), 3.67 (dd, J = 13.4, 6.8

Hz, 1H, NCH_2CH$_2$CH$_2$SCH$_2$), 3.10 – 3.04 (m, 2H, NCH$_2$CH$_2$CH$_2$SCH_2), 2.59 (t, *J* = 6.4 Hz, 2H, NCH$_2$CH$_2$CH_2SCH$_2$), 1.98 – 1.83 (m, 5H, C$H_{3thymine}$, NCH$_2$CH_2CH$_2$SCH$_2$). MS (ESI) *m/z* 508 [M−H]$^-$.

(*R*)-2-((((9H-fluoren-9-yl)methoxy)carbonyl)amino)-3-((2-(4-(bis(tert-butoxycarbonyl)amino)-2-oxopyrimidin-1(2*H*)-yl)ethyl)thio)propanoic acid (IV.50e)

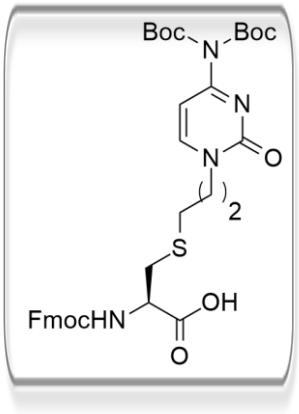

IV.6 (50 mg, 0.15 mmol) reacted with **IV.31** (153 mg, 0.45 mmol) under the conditions described in general procedure Q for 2 h to afford compound **IV.50e** as a white solid (79 mg, 78%). ^{1}H NMR (400 MHz, CDCl$_3$) δ 7.77 (d, *J* = 7.2 Hz, 2H, $H_{aromFmoc}$), 7.62 (s, 2H, $H_{aromFmoc}$), 7.45 – 7.29 (m, 5H, $H_{cytosine}$, $H_{aromFmoc}$), 7.11 (d, *J* = 6.3 Hz, 1H, $H_{cytosine}$), 5.94 (br s, 1H, NH_{cys}), 4.65 (s, 1H, H_{α}), 4.35 (d, *J* = 19.9 Hz, 2H, CH_{2Fmoc}), 4.24 (m, 1H, CH_{Fmoc}), 4.07 (d, *J* = 7.0 Hz, 1H, NCH_2CH$_2$CH$_2$SCH$_2$), 3.88 (m, 1H, NCH_2CH$_2$CH$_2$SCH$_2$), 3.20 – 2.96 (m, 2H, NCH$_2$CH$_2$CH$_2$SCH_2), 2.61 (m, 2H, NCH$_2$CH$_2$CH_2SCH$_2$), 2.04 (m, 2H, NCH$_2$CH_2CH$_2$SCH$_2$), 1.54 (s, 18H, Boc). MS (ESI) *m/z* 694 [M−H]$^-$.

(*R*)-2-((((9H-fluoren-9-yl)methoxy)carbonyl)amino)-3-((3-(2-((tert-butoxycarbonyl)amino)-6-oxo-1*H*-purin-9(6*H*)-yl)propyl)thio) propanoic acid (IV.50g)

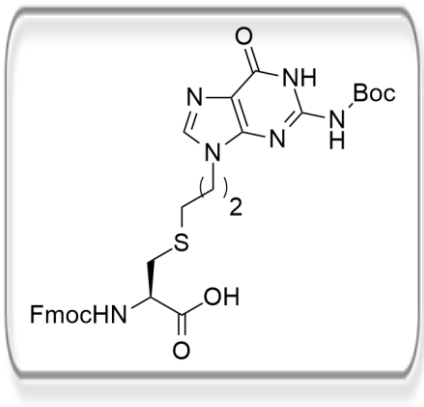

IV.6 (50 mg, 0.15 mmol) reacted with **IV.46** (127 mg, 0.45 mmol) under the conditions described in general procedure Q for 3 h to afford compound **IV.50g** as a white solid (28 mg, 30%). ^{1}H NMR (400 MHz, CDCl$_3$) δ 11.50 (s, 1H, N$H_{guanine}$), 8.56 (s, 1H, N$H_{guanine}$), 7.78 (s, 1H, $H_{8guanine}$), 7.70 (t, J = 6.6 Hz, 2H, $H_{aromFmoc}$), 7.57 (d, *J* = 7.4 Hz, 3H, $H_{aromFmoc}$), 7.36 (t, *J* = 7.4 Hz, 3H, $H_{aromFmoc}$), 6.17 (d, *J* = 7.5 Hz, 1H, NH_{cys}), 4.66 (d, *J* = 6.5 Hz, 1H, H_{α}), 4.46 (dd, J = 10.5, 7.0 Hz, 1H, NCH_2CH$_2$CH$_2$SCH$_2$), 4.38 (dd, *J* = 10.6, 6.7 Hz, 1H, NCH_2CH$_2$CH$_2$SCH$_2$), 4.20 (t, *J* = 6.7 Hz, 1H, CH_{Fmoc}), 4.07 (t, *J* = 6.7 Hz, 2H, CH_{2Fmoc}), 3.16 (dd, *J* = 14.6, 5.1 Hz, 1H, NCH$_2$CH$_2$CH$_2$SCH_2), 3.03 (dd, *J* = 14.0, 4.4 Hz, 1H, NCH$_2$CH$_2$CH$_2$SCH_2), 2.56 (t, *J* = 6.3 Hz, 2H, NCH$_2$CH_2CH$_2$SCH$_2$), 1.57 – 1.42 (m, 2H, NCH$_2$CH$_2$CH_2SCH$_2$).

(*R*)-ethyl 2-(2-((((9H-fluoren-9-yl)methoxy)carbonyl)amino)-3-((3-hydroxypropyl)thio)propanamido)acetate (IV.51a)

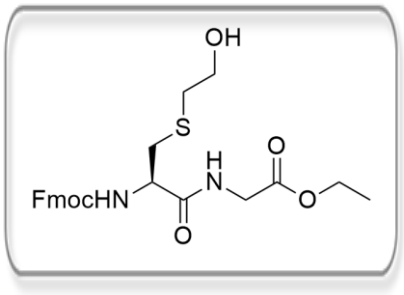

IV.7a (50 mg, 0.12 mmol) reacted with allyl alcohol (24 µL, 0.36 mmol) under the conditions described in general procedure P for 20 h to afford compound **IV.5a** as an colorless oil (12 mg, 21%). ^{1}H NMR (400 MHz, $CDCl_3$) δ 7.76 (d, *J* = 7.5 Hz, 2H, $H_{aromFmoc}$), 7.59 (d, J = 7.5 Hz, 2H, $H_{aromFmoc}$), 7.40 (t, *J* = 7.5 Hz, 2H, $H_{aromFmoc}$), 7.31 (td, *J* = 7.5, 0.9 Hz, 2H, $H_{aromFmoc}$), 7.05 (br s, 1H, NH_{gly}), 5.89 (br s, 1H, NH_{cys}), 4.43 (s, 3H, CH_{2Fmoc}, H_{α}), 4.21 (dd, *J* = 14.4, 7.2 Hz, 3H, CH_{Fmoc}, OCH_2CH$_3$), 4.03 (s, 2H, CH_{2gly}), 3.72 (t, *J* = 5.8 Hz, 2H, SCH$_2$CH$_2$CH_2OH), 3.00 (d, *J* = 8.2 Hz, 1H, CCH_2S), 2.86 (d, *J* = 8.2 Hz, 1H, CCH_2S), 2.72 (s, 2H, SCH_2CH$_2$CH$_2$OH), 1.84 (dt, *J* = 12.0, 6.1 Hz, 2H, SCH$_2$CH_2CH$_2$OH), 1.26 (t, *J* = 7.2, 3H, CH_3).

(*R*)-ethyl 2-(2-((((9H-fluoren-9-yl)methoxy)carbonyl)amino)-3-((2-(5-methyl-2,4-dioxo-3,4-dihydropyrimidin-1(2H)-yl)ethyl)thio) propanamido)acetate (IV.51c)

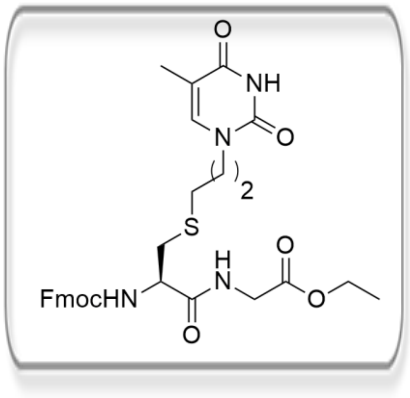

IV.7a (50 mg, 0.12 mmol) reacted with **IV.33** (58 mg, 0.36 mmol) under the conditions described in general procedure Q for 3 h to afford **IV.51c** as a white solid (35 mg, 51%). M.p. 89-91 °C**;** ^{1}H NMR (400 MHz, $CDCl_3$) δ 9.14 (br s, 1H, N$H_{thymine}$), 7.68 (d, *J* = 7.5 Hz, 2H, $H_{aromFmoc}$), 7.53 (d, *J* = 7.2 Hz, 2H, $H_{aromFmoc}$), 7.32 (t, *J* = 7.4 Hz, 2H, $H_{aromFmoc}$), 7.22 (dd, *J* = 14.2, 6.9 Hz, 3H, $H_{aromFmoc}$, NH_{gly}), 6.93 (s, 1H, $H_{6thymine}$), 5.97 (d, *J* = 7.4 Hz, 1H, NH_{cys}), 4.34 (d, *J* = 6.4 Hz, 3H, CH_{2Fmoc}, $H_{\propto}$), 4.13 (dd, *J* = 14.8, 7.4 Hz, 3H, CH_{Fmoc}, OCH_2CH$_3$), 3.98 (d, *J* = 5.9 Hz, 2H, CH_{2gly}), 3.81 (dt, *J* = 12.6, 6.8 Hz, 1H, NCH_2CH$_2$CH$_2$SCH$_2$), 3.64 (dt, *J* = 12.6, 6.8 Hz, 1H, NCH_2CH$_2$CH$_2$SCH$_2$), 2.91 (dd, *J* = 12.9, 6.9 Hz, 1H, NCH$_2$CH$_2$CH$_2$SCH_2), 2.80 (dd, *J* = 12.9, 6.9 Hz, 1H, NCH$_2$CH$_2$CH$_2$SCH_2), 2.56 (s, 2H, NCH$_2$CH$_2$CH_2SCH$_2$), 2.02 – 1.76 (m, 5H, CH$_{3thymine}$, NCH$_2$CH_2CH$_2$SCH$_2$), 1.20 (t, J = 7.1 Hz, 3H, CH$_2$CH_3). ^{13}C NMR (101 MHz, $CDCl_3$) δ 170.7 (*C*=O$_{dip}$), 169.8 (*C*=O$_{dip}$), 164.3 (C^4=O$_{thymine}$), 156.2 (C=O$_{dip}$), 151.0 (C^2=O$_{thymine}$), 143.8 ($C_{quatFmoc}$), 141.4 ($C_{quatFmoc}$), 140.5 ($C_{6thymine}$), 127.9 ($C_{aromFmoc}$), 127.2 ($C_{aromFmoc}$), 125.2 ($C_{aromFmoc}$), 120.1 (*C*H$_{aromFmoc}$), 111.2 (C$_{5thymine}$), 67.3 (*C*H$_{2Fmoc}$), 61.8 (O*C*H$_2$CH$_3$), 54.3 ($C_{\propto}$), 47.3 (N*C*H$_2$CH$_2$CH$_2$SCH$_2$), 47.2 (*C*H$_{Fmoc}$), 41.6 (*C*H$_{2gly}$), 34.4 (NCH$_2$CH$_2$CH$_2$S*C*H$_2$), 29.2 (NCH$_2$CH$_2$CH$_2$S*C*H$_2$), 28.4 (N*C*H$_2$*C*H$_2$CH$_2$SCH$_2$), 14.3 (CH$_2$*C*H$_3$), 12.4 (CH$_{3thymine}$).

(*R*)-ethyl 2-(2-((((9H-fluoren-9-yl)methoxy)carbonyl)amino)-3-((3-(6-(bis(tert-butoxycarbonyl)amino)-9H-purin-9-yl)propyl)thio) propanamido)acetate (IV.51e)

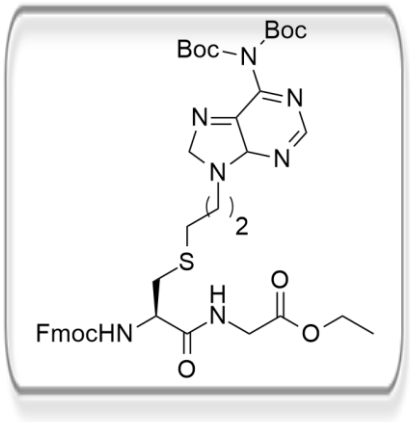

IV.7a (50 mg, 0.12 mmol) reacted with **IV.32** (131 mg, 0.36 mmol) under the conditions described in general procedure Q for 3 h to afford **IV.51e** (45 mg, 48%). ^{1}H NMR (400 MHz, $CDCl_3$) δ 8.86 (s, 1H, $H_{2thymine}$), 8.14 (s, 1H, $H_{8thymine}$), 7.76 (d, *J* = 7.2 Hz, 2H, $H_{aromFmoc}$), 7.59 (d, *J* = 7.2 Hz, 2H, $H_{aromFmoc}$), 7.39 (t, *J* = 7,4 Hz, 1H, $H_{aromFmoc}$), 7.31 (t, *J* = 7,4 Hz, 1H, $H_{aromFmoc}$), 7.04 (s, 1H, NH_{gly}), 5.80 (s, 1H, NH_{cys}), 4.49-4.33 (m, 5H, CH_{2Fmoc}, $H_{\propto}$, NCH_2CH$_2$CH$_2$SCH$_2$), 4.21 (dd, *J* = 14.5, 7.2 Hz, 3H, CH_{Fmoc}, OCH_2CH$_3$), 4.04 (s, 2H, CH_{2gly}), 2.98 (s, 1H, NCH$_2$CH$_2$CH$_2$SCH_2), 2.86 (s, 1H, NCH$_2$CH$_2$CH$_2$SCH_2), 2.61 (s, 2H, CH$_2$CH$_2$CH_2SCH$_2$), 2.24 (s, 2H, NCH$_2$CH_2CH$_2$SCH$_2$), 1.45 (s, 18H, Boc), 1.27 (t, *J* = 7.2 Hz, 3H, CH_3). ^{13}C NMR (101 MHz, $CDCl_3$) δ 170.4 (*C*=O), 169.5 (*C*=O), 160.5 ($C_{2adenine}$), 153.5 ($C_{4adenine}$), 152.2 ($C_{8adenine}$), 150.7 (*C*=O_{Boc}), 150.5 ($C_{6adenine}$), 143.7 ($C_{quatFmoc}$), 141.5 ($C_{quatFmoc}$), 128.9 ($C_{5adenine}$), 127.9 ($C_{aromFmoc}$), 127.2 ($C_{aromFmoc}$), 125.2 ($C_{aromFmoc}$), 120.2 ($C_{aromFmoc}$), 84.0 ($C_{quat\ t\text{-}BuBoc}$), 67.3 (*C*H$_{2Fmoc}$), 61.9 (O*C*H$_2$CH$_3$), 54.3 (*C*-H$_{\propto}$), 47.2 (*C*H$_{Fmoc}$), 42.8 (N*C*H$_2$CH$_2$CH$_2$SCH$_2$), 41.6 (*C*H$_{2gly}$), 34.2 (NCH$_2$CH$_2$CH$_2$S*C*H$_2$), 29.2 (NCH$_2$CH$_2$CH$_2$SCH$_2$), 29.1 (NCH$_2$CH$_2$CH$_2$SCH$_2$), 28.0 (C(*C*H$_3$)$_3$)., 14.3 (OCH$_2$*C*H$_3$). MS (ESI) *m/z* 826.48 [M+Na]$^+$.

(R)-benzyl 2-(2-((((9H-fluoren-9-yl)methoxy)carbonyl)amino)-3-((3-(5-methyl-2,4-dioxo-3,4-dihydropyrimidin-1(2H)-yl)propyl) thio)propanamido)acetate (IV.51f)

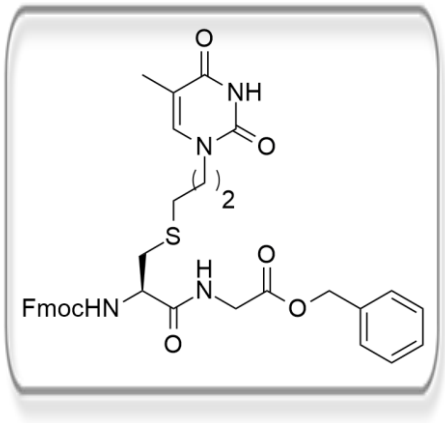

IV.7b (50 mg, 0.11 mmol) reacted with **IV.33** (52 mg, 0.33 mmol) under the conditions described in general procedure Q for 3 h to afford **IV.51f** (34 mg, 49%).^{1}H NMR (400 MHz, $CDCl_3$) δ 8.54 (s, 1H, NH_{tymine}), 7.76 (d, *J* = 7.6 Hz, 2H, $H_{aromFmoc}$), 7.60 (d, *J* = 7.2 Hz, 2H, $H_{aromFmoc}$), 7.44 – 7.24 (m, 9H, $H_{aromFmoc}$, H_{aromBn}), 7.19 (s, 1H, NH_{gly}), 6.99 (s, 1H, CH_{tymine}), 5.89 (s, 1H, NH_{cys}), 5.19 (s, 2H, CH_{2Bn}), 4.42 (d, *J* = 5.6 Hz, 3H, C$H_{2Fmoc,}$ $H_{\propto}$), 4.22 (t, *J* = 6.6 Hz, 1H, CH_{Fmoc}), 4.09 (q, ,2H, CH_{2gly}), 3.88 (s, 1H, NCH_2CH$_2$CH$_2$SCH$_2$), 3.71-3.65 (m, 1H, NCH_2CH$_2$CH$_2$SCH$_2$), 2.96 (s, 1H, NCH$_2$CH$_2$CH$_2$SCH_2), 2.85 (s, 1H, NCH$_2$CH$_2$CH$_2$SCH_2), 2.62 (s, 2H, CH$_2$CH$_2$CH_2SCH$_2$), 1.97 (s, 2H, NCH$_2$CH_2CH$_2$SCH$_2$), 1.89 (s, 3H, $CH_{3tymine}$). ^{13}C NMR (101 MHz, $CDCl_3$) δ 170.6 (*C*=O_{dip}), 169.6 (*C*=O_{dip}), 164.0 (C_4=$O_{thymine}$), 156.2 (*C*=O_{dip}) , 151.1 (C_2=$O_{thymine}$), 143.8 ($C_{quatFmoc}$),

141.5 ($C_{quatFmoc}$), 140.4 ($C_{6thymine}$), 135.1 (C_{quatBn}), 128.8 (C_{arom}), 128.8 (C_{arom}), 128.6 (C_{arom}), 127.9 (C_{arom}), 127.2 (C_{arom}), 125.2 (C_{arom}), 120.2 (C_{arom}), 111.2 ($C_{5thymine}$), 67.6 (CH_{2Bn}), 67.3 (CH_{2Fmoc}), 54.3 (C_{α}), 47.3 ($NCH_2CH_2CH_2SCH_2$), 47.2 (CH_{Fmoc}), 41.7 (CH_{2gly}), 34.4 ($NCH_2CH_2CH_2SCH_2$), 29.3 ($NCH_2CH_2CH_2SCH_2$), 28.4 ($NCH_2CH_2CH_2SCH_2$), 12.5 ($CH_{3tymine}$). MS (ESI) *m/z* 679 $[M+Na]^+$.

(*R*)-benzyl 2-(2-((((9H-fluoren-9-yl)methoxy)carbonyl)amino)-3-((3-(4-(bis(tert-butoxycarbonyl)amino)-2-oxopyrimidin-1(2H)-yl) propyl)thio)propanamido)acetate (IV.51g)

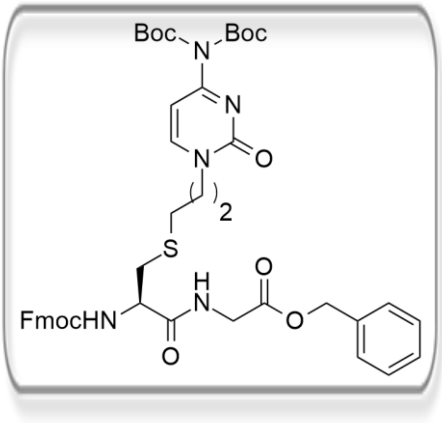

IV.7b (50 mg, 0.11 mmol) reacted with **IV.31** (112 mg, 0.33 mmol) under the conditions described in general procedure Q for 3 h to afford **IV.51g** (55 mg, 62%). ^{1}H NMR (400 MHz, $CDCl_3$) δ 7.75 (d, *J* = 7.6 Hz, 2H, $H_{aromFmoc}$), 7.60 (d, *J* = 6.8 Hz, 2H, $H_{aromFmoc}$), 7.54 (d, *J* = 7.2 Hz, 1H, $H_{cytosine}$), 7.41 – 7.29 (m, 10 H, $H_{aromFmoc}$, $H_{aromBn,}$ NH_{gly}), 7.02 (d, *J* = 7.2 Hz, 1H, $H_{cytosine}$), 5.85 (s, 1H, NH_{cys}), 5.16 (s, 2H, CH_{2Bn}), 4.41 (d, *J* = 5.8 Hz, 3H, $CH_{2Fmoc,}$ $H_{\propto}$), 4.22 (t, *J* = 5.8 Hz, 1H, CH_{Fmoc}), 4.15-4.00 (m, 3H, $CH_{2gly,}$ $NCH_2CH_2CH_2SCH_2$), 3.89 – 3.82 (m, 1H, $NCH_2CH_2CH_2SCH_2$), 2.91 (d, *J* = 12.8 Hz, $NCH_2CH_2CH_2SCH_2$), 2.61 (s, 2H, $NCH_2CH_2CH_2SCH_2$), 2.05 (s, 2H, $NCH_2CH_2CH_2SCH_2$), 1.54 (s, 18H, Boc). ^{13}C NMR (101 MHz, $CDCl_3$) δ 170.8 (C=O_{dip}), 169.4 (C=O_{dip}), 162.5 ($C_{4cytosine}$), 155.1 (C=O_{dip}), 155.3 (C=$O_{cytosine}$), 149.7 (C=O_{Boc}), 148.2 ($CH_{cytosine}$), 143.8 ($C_{quatFmoc}$), 141.4 ($C_{quatFmoc}$), 135.3 (C_{quatBn}), 128.7 (C_{arom}), 128.6 (C_{arom}), 128.5 (C_{arom}), 127.9 (C_{arom}), 127.2 (C_{arom}), 125.3 (C_{arom}), 120.1 (C_{arom}), 96.6 ($CH_{cytosine}$), 85.1 ($C_{quatBoc}$), 67.3(CH_{2Fmoc}), 67.3 (CH_{2Bn}), 54.20 ($CH_{\propto}$), 49.66 ($NCH_2CH_2CH_2SCH_2$), 47.21 (CH_{Fmoc}), 41.61 (CH_{2gly}), 34.47 ($NCH_2CH_2CH_2SCH_2$), 29.13 ($NCH_2CH_2CH_2SCH_2$), 27.93 ($NCH_2CH_2CH_2SCH_2$), 27.80 (CH_3). Mp: 64-67 °C. MS (ESI) *m/z* 864 $[M+Na]^+$. HRMS: $(M-H)^+$ ($C_{44}H_{52}N_5O_{10}S$) cacld 842.3429, found 842.3414.

(*R*)-benzyl 2-(2-((((9H-fluoren-9-yl)methoxy)carbonyl)amino)-3-((3-(6-(bis(tert-butoxycarbonyl)amino)-9H-purin-9-yl)propyl)thio) propanamido)acetate (IV.51h)

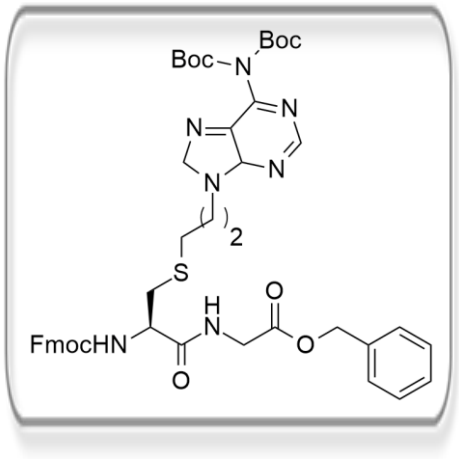

IV.7b (50 mg, 0.11 mmol) reacted with **IV.32** (115 mg, 0.33 mmol) under the conditions described in general procedure Q for 3 h to afford **IV.51h** (50 mg, 57%). ^{1}H NMR (400 MHz, $CDCl_3$) δ 8.85 (s, 1H, H_2), 8.11 (s, 1H, H_8), 7.75 (d, J = 7.6 Hz, 2H, $H_{aromFmoc}$), 7.58 (d, J = 7.2 Hz, 2H, $H_{aromFmoc}$), 7.40-7.28 (m, 9H, $H_{aromFmoc}$, H_{aromBn}), 7.06 (s, 1H, NH_{gly}), 5.79 (s, 1H, NH_{cys}), 5.17 (s, 2H, CH_{2Bn}), 4.48 – 4.25 (m, 5H, C$H_{2Fmoc,}$ C$H_{\propto,}$ NCH_2CH$_2$CH$_2$SCH$_2$), 4.21 (t, J = 6.6 Hz, 1H, CH_{Fmoc}), 4.09 (s, 2H, CH_{2gly}), 2.91 (dd, J = 57.2, 12.4 Hz, 2H, NCH$_2$CH$_2$CH$_2$SCH_2), 2.58 (s, 2H, CH$_2$CH$_2$CH_2SCH$_2$), 2.21 (s, 2H, NCH$_2$CH_2CH$_2$SCH$_2$), 1.42 (d, J = 24.4 Hz, 18H, Boc). ^{13}C NMR (101 MHz, $CDCl_3$) δ 170.5 (C=O$_{dip}$), 169.4 (C=O$_{dip}$), 156.1 (C=O$_{dip}$), 153.5 ($C_{4adenine}$), 152.2 ($C_{2adenine}$), 150.7 ($C_{6adenine}$), 150.5 (C=O$_{Boc}$), 145.1 ($C_{8adenine}$), 143.7 ($C_{quatFmoc}$), 141.4 ($C_{quatFmoc}$), 135.11 (C_{quatBn}), 129.0 ($C_{5adenine}$), 128.8 (C_{arom}), 128.8 (C_{arom}), 128.6 (C_{arom}), 127.9 (C_{arom}), 127.2 (C_{arom}), 125.2 (C_{arom}), 120.2 (C_{arom}), 84.0 (C$_{quatBoc}$), 67.5 (CH_{2Fmoc}), 67.3 (CH_{2Bn}), 54.2 (C$H_{\propto}$), 47.2 (CH_{Fmoc}), 42.7 (NCH_2CH$_2$CH$_2$SCH$_2$), 41.6 (CH_{2gly}), 34.2 (NCH$_2$CH$_2$CH$_2$SCH$_2$), 29.8 (NCH$_2$CH$_2$CH_2SCH$_2$), 29.1 (NCH$_2$CH_2CH$_2$SCH$_2$), 27.9 (CH_3). Mp: 62-65 ^{o}C. MS (ESI) *m/z* 888 [M+Na]$^{+}$. HRMS: (M-H)$^{+}$ ($C_{45}H_{52}N_7O_9S$) cacld 866.3542 found 866.3524.

(*R*)-benzyl 2-(2-((((9H-fluoren-9-yl)methoxy)carbonyl)amino)-3-((3-(2-((tert-butoxycarbonyl)amino)-6-oxo-1H-purin-9(6H)-yl)propyl)thio)propanamido)acetate (IV.51i)

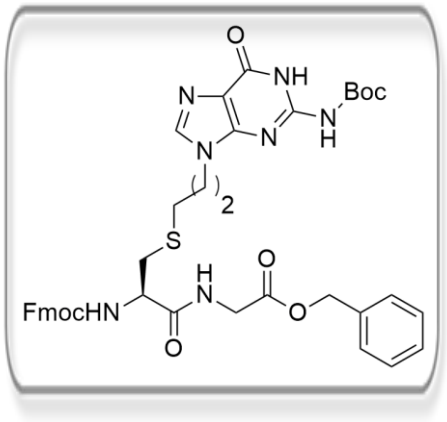

IV.7b (50 mg, 0.11 mmol) reacted with **IV.51i** (89 mg, 0.33 mmol) under the conditions described in general procedure Q for 3 h to afford **IV.51i** (31 mg, 44%). ^{1}H NMR (400 MHz, $CDCl_3$) δ 11.53 (s, 1H, N$H_{1guanina}$), 9.01 (s, 1H, N$H_{exoguanina}$), 7.67 (t, J = 7.4 Hz, 2H, $H_{aromFmoc}$), 7.57 (s, 1H, C$H_{8guanine}$), 7.5 (d, J = 6.8 Hz, 2H, $H_{aromFmoc}$), 7.37-7.21 (m, 10H, $H_{aromFmoc}$, H_{aromBn}, NH_{gly}), 6.49 (s, 1H, NH_{cys}), 5.15 (s, 2H, CH_{2Bn}), 4.54 – 4.33 (m, 3H, C$H_{2Fmoc,}$ $H_{\propto}$), 4.20-4.11 (m, 4H, H_{Fmoc}, C$H_{2gly,}$ NCH_2CH$_2$CH$_2$SCH$_2$), 3.90 (s, 1H, NCH_2CH$_2$CH$_2$SCH$_2$), 3.10 (d, J = 10.4 Hz, 1H, NCH$_2$CH$_2$CH$_2$SCH_2), 2.85 (dd, J = 13.6, 8.4 Hz, 1H, NCH$_2$CH$_2$CH$_2$SCH_2), 2.65–2.50 (m, 2H,

$NCH_2CH_2CH_2SCH_2$), 2.18 – 1.92 (m, 2H, $NCH_2CH_2CH_2SCH_2$), 1.48 (s, 9H, Boc). ^{13}C NMR (101 MHz, $CDCl_3$) δ 169.36 (C=O_{dip}), 165.6 (C=O_{dip}), 156.6 (C=O_{dip}) 155.9 (C=$O_{6guanine}$), 153.3 (C=O_{Boc}), 147.8 (C_4), 143.7 ($C_{quatFmoc}$), 143.6 (C_2), 141.4 ($C_{quatFmoc}$), 135.1 (C_{quatBn}), 128.8 (C_{arom}), 128.5 (C_{arom}), 128.5 (C_{arom}), 127.9 (C_{arom}), 127.1 (C_{arom}), 124.9 (C_{arom}), 120.1 (C_{arom}), 84.0 ($C_{quatBoc}$), 67.5 (CH_{2Fmoc}), 67.1 (CH_{2Bn}), 54.6 (CH_{α}), 47.2 (CH_{Fmoc}), 42.4 ($NCH_2CH_2CH_2SCH_2$), 41.6 (CH_{2gly}), 33.4 ($NCH_2CH_2CH_2SCH_2$), 28.9 ($NCH_2CH_2CH_2SCH_2$), 28.3 ($NCH_2CH_2CH_2SCH_2$), 28.1 (CH_3).

(*R*)-ethyl 2-(2-((((9H-fluoren-9-yl)methoxy)carbonyl)amino)-3-(allylthio)propanamido)acetate (IV.52)

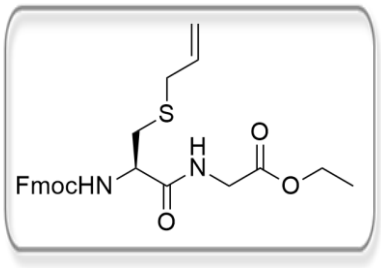

IV.7b (50 mg, 0.11 mmol) reacted with allyl bromide (30µL, 0.33 mmol) under the conditions described in general procedure P for 3 h to afford compound **IV.52** as an colorless oil (12 mg, 21%). ^1H NMR (400 MHz, $CDCl_3$) δ 7.77 (d, J = 7.4 Hz, 2H, $H_{aromFmoc}$), 7.60 (d, J = 7.4 Hz, 2H, $H_{aromFmoc}$), 7.41 (t, J = 7.4 Hz, 2H, $H_{aromFmoc}$), 7.32 (t, J = 7.4 Hz, 2H, $H_{aromFmoc}$), 6.82 (br s, 1H, NH_{gly}), 5.78 (dt, J = 18.2, 8.0 Hz, 1H, CH=CH_2), 5.68 (br s, 1H, NH_{cys}), 5.18 (d, J = 16.7 Hz, 1H, CH=CH_{trans}), 5.13 (d, J = 10.0 Hz, 1H, , CH=CH_{cis}) 4.48 – 4.32 (m, 3H, CH_{2Fmoc} , H_{α}), 4.22 (dd, J = 14.5, 7.1 Hz, 3H, CH_{Fmoc}, OCH_2CH_3), 4.04 (s, 2H, CH_{2gly}), 3.18 (s, 2H, SCH_2CH=CH_2), 2.92 (d, J = 12.3 Hz, 1H, CCH_2S), 2.82 (dd, J = 12.3, 6.3 Hz, 1H, CCH_2S), 1.26 – 1.17 (t, J = 7.1 Hz 3H, CH_3). MS (ESI) 491.18 $[M+Na]^+$.

3. FRET-melting assay procedure

The ability of the test compounds to stabilise G-quadruplex DNA (F21T and KRAS21R) and a self-complementary hairpin DNA (T-Loop) sequences was investigated by using a fluorescence resonance energy transfer (FRET) assay with ligand concentrations ranging from 0.1 to 5 µM. The labelled oligonucleotides contained the donor fluorophore 6-carboxyfluorescein (FAM) and the acceptor fluorophore 6-carboxytetramethylrhodamine (TAMRA). Sequences were as follows: F21T (5'-[FAM]-GGG TTA GGG TAG GGT TAG GG-[TAMRA]-3'), KRas21R (5'-[FAM]-AGG GCG GTG TGG GAA GAG GGA-[TAMRA]-3'), T-loop (5'-[FAM]-TAT AGC TAT ATT TTT TTA TAG CTA TA-[TAMRA]-3'). Each oligonucleotide was initially diluted to 100 µm in nuclease-free water (not DEPC-treated). Stock solutions of 20 µm and subsequent dilutions were obtained in FRET buffer (60 µm KCl, potassium cacodylate, pH 7.4). The FRET probe sequences were diluted from stock to the correct concentration (0.4 µm) and then annealed by heating at 85 ^0C for 10 min, followed by slow cooling to rt in the heating block.

Test compounds were prepared as 10 μm DMSO stock solutions and diluted to 1 μm using 1 μm nuclease-free water (not DEPC-treated). The rest of the dilutions were performed using FRET buffer. Annealed DNA (50 μL) and test compound solution (50 μL) were distributed across 96-well RT-PCR plates. Relevant controls were also performed to check for interference with the assay. Fluorescence readings were made with excitation at λ 450–495 nm and detection at λ 515–545 nm, taken at intervals of 1 ^{o}C in the range 30–95 ^{0}C, with a constant temperature being maintained for 30 s prior to each reading to ensure a stable value. Experiments were performed in triplicate. Final analysis of the data was carried out with GraphPad Prism v.5.0. The advanced curve-fitting function in GraphPad Prism was used for calculation of ΔT_m values.

4. *In cellula* assays

4.1. Cell Culture

Human colorectal adenocarcinoma cell lines (HT-29 and CaCo-2), lung cancer (NCI-H460) and breast cancer (MCF- 7) cell lines and, human normal skin fribroblasts (CRL-1502) cells were acquired from ATCC. Cell lines were cultivated in RPMI-1640 media supplemented with L-glutamine, 10% fetal bovine serum (FBS) and antibiotic antimycotic solution and were grown in an incubator with a 5% CO_2 humidified atmosphere and at 37 ^{o}C.

4.2. Antiproliferative assay

Each cell line was plated in 96-well plates with a density of approximately $5x10^3$ (NCI-H460), $1x10^4$ (HT-29) and $1{,}5x10^4$ (MCF-7) cells/well. Plates were incubated overnight and treated the next day with the samples to be tested. Stock solutions of the compounds were prepared and diluted with the cell culture media containing 0.5% FBS. This same media composition was used for the performance of the assays. Cisplatin stock solution was prepared at 10 mM concentration in phosphate buffer saline (PBS). After 48 h incubation with the compounds, media was removed, cells were washed with PBS and treated for 3 h with fresh media containing 50 μg/mL neutral red. After this period, cells were washed with PBS and the amount of neutral red retained by the cells extracted with an organic solution (19.96 mL distilled water, 20 mL ethanol and 400 μL glacial acetic acid). Plate was gently shake and read at 540 nm in a plate reader. Viability was determined by the ratio of absorbance of treated cells and non-treated cells

(control). For each experimental situation, 3 repliques were done and the average points were used to construct a fitting toxicity curve in GraphPad. From each fitting curve, an IC_{50} was determined and associated error is the standard deviation of the different IC_{50}s produced from independent experiments. Assays performed by Dr. Raquel Frade.

4.3. Toxicity assay

CaCo-2 or CRL-1502 cells were plated in 96-well plates and grown until formation of a monolayer. Monolayers were posteriorly incubated with the compounds for 24 h previously to viability assessment. Viability was determined using the neutral red dye as previously described. Assays performed by Dr. Raquel Frade.

4.4. Apoptosis evaluation

Apoptosis was quantified using the Guava Nexin Reagent kit (Merck Millipore). The Nexin assay uses two distinct dyes, Annexin V to detect phosphatidylserine (PS) on the external membrane of apoptotic cells, and the cell impermeant dye, 7-AAD, as an indicator of membrane structural integrity. For this purpose, HT-29 cells were plated in 24-well plates at $5x10^4$ cells/well. Twenty-four hours after plating, cells were exposed either to DMSO (vehicle control) or to the compounds in test at the IC_{50} and 2-fold IC_{50} concentration for additional 48 h. After that, the culture medium was collected and cells detached with Accutase. Cells were the collected to the same tube and centrifuged at 500 g for 5 min at 4 ^oC. The cell pellet was resuspended in PBS supplemented with 2% FBS. Subsequently, 50 µL of cell suspension were mixed with 50 µL of Guava Nexin reagent and incubated for 20 min, at room temperature in the absence of light. Following the staining procedure, sample acquisition and data analysis of at least 5000 events per sample were performed using the Guava easyCyteTM Flow Cytometer (Merck Millipore) and Nexin software module. Assays performed by Dr. Joana Amaral.

REFERENCES

REFERENCES

1. Pray L. Discovery of DNA structure and function: Watson and Crick. *Nature Education.* **2008**; *1* (1): 100.
2. Clancy S. RNA functions. *Nature Education*. **2008**; *1* (1): 102.
3. Lodish H.; Berk A.; Zipursky S. L.; Matsudaira P.; Baltimore D.; Darnell J. Structure of Nucleic Acids. *Molecular Cell Biology*. New York: W. H. Freeman. **2004**; 4th edition.
4. Watson J. D.; Crick F. H. C. Molecular Structure of Nucleic Acids: A Structure for Deoxyribose Nucleic Acid. *Nature*. **1953**; *171* (4356): 737-738.
5. Amato J.; Iaccarino N.; Randazzo A.; Novellino E.; Pagano B. Noncanonical DNA Secondary Structures as Drug Targets: the Prospect of the i-Motif. *ChemMedchem*. **2014**; *9* (9): 2026-2030.
6. Clancy S. Chemical structure of RNA. *Nature Education*. **2008**; *7* (1): 60.
7. Stefan L.; Bertrand B.; Richard P.; Le Gendre P.; Denat F.; Picquet M. *et al*. Assessing the Differential Affinity of Small Molecules for Noncanonical DNA Structures. *ChemBioChem*. **2012**; *13* (13):1905-1912.
8. Gellert M.; Lipsett M. N.; Davies D. R. Helix formation by guanylic acid. *Proc. Natl. Acad. Sci. U. S. A.* **1962**; *48* (12): 2013-2018.
9. Hardin C. C.; Perry A. G.; White K. Thermodynamic and kinetic characterization of the dissociation and assembly of quadruplex nucleic acids. *Biopolymers*. **2000**; *56* (3): 147-194.
10. Burge S.; Parkinson G. N.; Hazel P.; Todd A. K.; Neidle S. Quadruplex DNA: sequence, topology and structure. *Nucleic Acids Res*. **2006**; *34* (19): 5402-5415.
11. Collie G. W.; Parkinson GN. The application of DNA and RNA G-quadruplexes to therapeutic medicines. *Chem. Soc. Rev.* **2011**; *40* (12): 5867-5892.
12. Georgiades S. N.; Abd Karim N. H.; Suntharalingam K.; Vilar R. Interaction of Metal Complexes with G-Quadruplex DNA. *Angew. Chem., Int. Ed*. **2010**; *49* (24): 4020-4034.
13. Bryan T.; Baumann P. G-Quadruplexes: From Guanine Gels to Chemotherapeutics. *Mol. Biotechnol.* **2011**; *49* (2): 198-208.
14. Mohanty D.; Bansal M. Conformational polymorphism in G-tetraplex structures: strand reversal by base flipover or sugar flipover. *Nucleic Acids Res*. **1993**; *21* (8): 1767-1774.
15. Stegle O.; Payet L.; Mergny J. L.; MacKay D. J. C.; Huppert J. L. Predicting and understanding the stability of G-quadruplexes. *Bioinformatics*. **2009**; *25* (12): i374-i382.
16. Wong H. M.; Stegle O.; Rodgers S.; Huppert J. L. A Toolbox for Predicting G-Quadruplex Formation and Stability. *J. Nucleic Acids*. **2010**; *2010*: 564946.
17. Lorenz R.; Bernhart S. H.; Qin J.; Siederdissen C. H.; Tanzer A.; Amman F. *et al*. 2D Meets 4G: G-Quadruplexes in RNA Secondary Structure Prediction. *IEEE/ACM Trans. Comput. Biol. Bioinf*. **2013**; *10* (4): 832-844.
18. Yaku H.; Fujimoto T.; Murashima T.; Miyoshi D.; Sugimoto N. Phthalocyanines: a new class of G-quadruplex-ligands with many potential applications. *Chem. Commun.* **2012**; *48* (50): 6203-6216.
19. Huppert J. L.; Balasubramanian S. Prevalence of quadruplexes in the human genome. *Nucleic Acids Res*. **2005**; *33* (9): 2908-2916.
20. Balasubramanian S.; Hurley L. H.; Neidle S. Targeting G-quadruplexes in gene promoters: a novel anticancer strategy? *Nat. Rev. Drug Discovery*. **2011**; *10* (4): 261-275.
21. Bugaut A.; Balasubramanian S. 5'-UTR RNA G-quadruplexes: translation regulation and targeting. *Nucleic Acids Res*. **2012**; *40* (11): 4727-4741.
22. Azzalin C. M.; Reichenbach P.; Khoriauli L.; Giulotto E.; Lingner J. Telomeric repeat containing RNA and RNA surveillance factors at mammalian chromosome ends. *Science*. **2007**; *318* (5851): 798-801.
23. Huppert J. L.; Bugaut A.; Kumari S.; Balasubramanian S. G-quadruplexes: the beginning and end of UTRs. *Nucleic Acids Res*. **2008**; *36* (19): 6260-6268.

24. Yan Y.; Tan J.; Ou T.; Huang Z.; Gu L. DNA G-quadruplex binders: a patent review. *Expert Opin. Ther. Pat.* **2013**; *23* (11): 1495-1509.
25. Biffi G.; Tannahill D., McCafferty J.; Balasubramanian S. Quantitative visualization of DNA G-quadruplex structures in human cells. *Nat. Chem*. **2013**; *5* (3): 182-186.
26. Biffi G.; Di Antonio M.; Tannahill D.; Balasubramanian S. Visualization and selective chemical targeting of RNA G-quadruplex structures in the cytoplasm of human cells. *Nat. Chem*. **2014**; *6* (1): 75-80.
27. Henderson A.; Wu Y. L.; Huang Y. C.; Chavez E. A.; Platt J.; Johnson F.B. *et al*. Detection of G-quadruplex DNA in mammalian cells. *Nucleic Acids Res*. **2014**; *42* (2): 860-869.
28. Gomez D.; Wenner T.; Brassart B.; Douarre C.; O'Donohue M. F.; El Khoury V. *et al*. Telomestatin-induced telomere uncapping is modulated by POT1 through G-overhang extension in HT1080 human tumor cells. *J. Biol. Chem*. **2006**; *281* (50): 38721-38729.
29. Sun D. Y.; Thompson B.; Cathers B. E.; Salazar M.; Kerwin S. M.; Trent J. O. *et al*. Inhibition of human telomerase by a G-quadruplex-interactive compound. *J. Med. Chem.* **1997**; *40* (14): 2113-2116.
30. Ilyinsky N. S.; Varizhuk A. M.; Beniaminov A. D.; Puzanov M. A.; Shchyolkina A. K.; Kaluzhny D. N. G-quadruplex ligands: Mechanisms of anticancer action and target binding. *Molecular Biology*. **2014**; *48* (6): 778-794.
31. Phatak P.; Cookson J. C.; Dai F.; Smith V.; Gartenhaus R. B.; Stevens M. F. *et al*. Telomere uncapping by the G-quadruplex ligand RHPS4 inhibits clonogenic tumour cell growth in vitro and in vivo consistent with a cancer stem cell targeting mechanism. *Br. J. Cancer*. **2007**; *96* (8): 1223-1233.
32. Siddiqui-Jain A.; Grand C. L.; Bearss D. J.; Hurley L. H. Direct evidence for a G-quadruplex in a promoter region and its targeting with a small molecule to repress *c-MYC* transcription. *Proc. Natl. Acad. Sci. U. S. A*. **2002**; *99* (18): 11593-11598.
33. Drygin D.; Siddiqui-Jain A.; O'Brien S.; Schwaebe M.; Lin A.; Bliesath J. *et al*. Anticancer Activity of CX-3543: A Direct Inhibitor of rRNA Biogenesis. *Cancer Res*. **2009**; *69* (19): 7653-7661.
34. Bochman M. L.; Paeschke K.; Zakian V. A. DNA secondary structures: stability and function of G-quadruplex structures. *Nat. Rev. Genet*. **2012**; *13* (11): 770-780.
35. Li Q.; Xiang J. F.; Yang Q. F.; Sun H. X.; Guan A. J.; Tang Y. L. G4LDB: a database for discovering and studying G-quadruplex ligands. *Nucleic Acids Res*. **2012**; *41*(D1):D1115-D1123.
36. Shin-ya K.; Wierzba K.; Matsuo K.; Ohtani T.; Yamada Y.; Furihata K. *et al*. Telomestatin, a novel telomerase inhibitor from Streptomyces anulatus. *J. Am. Chem. Soc.* **2001**; *123* (6): 1262-1263.
37. De Cian A.; Guittat L.; Shin-ya K.; Riou J. F.; Mergny J. L. Affinity and selectivity of G4 ligands measured by FRET. *Nucleic Acids Symp. Ser*. **2005**; 49: 235-236.
38. Monchaud D.; Granzhan A.; Saettel N.; Guédin A.; Mergny J-L.; Teulade-Fichou M-P. "One Ring to Bind Them All"—Part I: The Efficiency of the Macrocyclic Scaffold for G-Quadruplex DNA Recognition. *J. Nucleic Acids*. **2010**; *2010*: 525862.
39. Pilch D. S.; Barbieri C. M.; Rzuczek S. G.; Lavoie E. J.; Rice J. E. Targeting human telomeric G-quadruplex DNA with oxazole-containing macrocyclic compounds. *Biochimie*. **2008**; *90* (8): 1233-1249.
40. Iida K.; Nagasawa K. Macrocyclic polyoxazoles as G-quadruplex ligands. *Chem. Rec*. **2013**; *13* (6): 539-548.
41. Minhas G. S. ; Pilch D. S.; Kerrigan J. E.; LaVoie E. J.; Rice J. E. Synthesis and G-quadruplex stabilizing properties of a series of oxazole-containing macrocycles. *Bioorg. Med. Chem. Lett.* **2006**; *16* (15): 3891-3895.
42. Rzuczek S. G.; Pilch D. S.; LaVoie E. J.; Rice J. E. Lysinyl macrocyclic hexaoxazoles: synthesis and selective G-quadruplex stabilizing properties. *Bioorg. Med. Chem. Lett*. **2008**; *18* (3): 913-917.

43. Satyanarayana M.; Rzuczek S. G.; Lavoie E. J.; Pilch D. S.; Liu A.; Liu L. F. *et al*. Ring-closing metathesis for the synthesis of a highly G-quadruplex selective macrocyclic hexaoxazole having enhanced cytotoxic potency. *Bioorg. Med. Chem. Lett*. **2008**; *18* (13): 3802-3804.
44. Satyanarayana M.; Kim Y. A.; Rzuczek S. G.; Pilch D. S.; Liu A. A.; Liu L. F. *et al*. Macrocyclic hexaoxazoles: Influence of aminoalkyl substituents on RNA and DNA G-quadruplex stabilization and cytotoxicity. *Bioorg. Med. Chem. Lett*. **2010**; *20* (10): 3150-3154.
45. An Q.; Li G. T.; Tao C. G.; Li Y.; Wu Y. G.; Zhang W. X. A general and efficient method to form self-assembled cucurbit[n]uril monolayers on gold surfacest. *Chem. Commun*. **2008**; 17: 1989-1991.
46. Sakuma M.; Ma Y.; Tsushima Y.; Iida K.; Hirokawa T.; Nagasawa K. Design and synthesis of unsymmetric macrocyclic hexaoxazole compounds with an ability to induce distinct G-quadruplex topologies in telomeric DNA. *Org. Biomol. Chem.* **2016**; *14* (22): 5109-5116.
47. Nagasawa K.; Ma Y.; Iida K.; Nakamura T.; Seimiya H.; Ohtake T. Design, Synthesis and Evaluation of an L-Dopa-Derived Macrocyclic Hexaoxazole (6otd) as a G-Quadruplex-Selective Ligand. *Heterocycles*. **2016**; *92* (2): 305-315.
48. Blankson G. A.; Pilch D. S.; Liu A. A.; Liu L. F.; Rice J. E; LaVoie E. J. Macrocyclic biphenyl tetraoxazoles: Synthesis, evaluation as G-quadruplex stabilizers and cytotoxic activity. *Bioorg. Med. Chem.* **2013**; *21* (15): 4511-4520.
49. Rzuczek S. G.; Pilch D. S.; Liu A.; Liu L.; LaVoie E. J.; Rice J. E. Macrocyclic Pyridyl Polyoxazoles: Selective RNA and DNA G-Quadruplex Ligands as Antitumor Agents. *J. Med. Chem.* **2010**; *53* (9): 3632-3644.
50. Blankson G.; Rzuczek S.; Bishop C.; Pilch D.; Liu A.; Liu L. et al. Macrocyclic Pyridyl Polyoxazoles: Structure-Activity Studies of the Aminoalkyl Side-Chain on G-Quadruplex Stabilization and Cytotoxic Activity. *Molecules.* **2013**; *18* (10):11938-11963.
51. Jantos K.; Rodriguez R.; Ladame S.; Shirude P. S.; Balasubramanian S. Oxazole-based peptide macrocycles: a new class of G-quadruplex binding ligands. *J. Am. Chem. Soc*. **2006**; *128* (42): 13662-13663.
52. Bugaut A.; Jantos K.; Wietor J-L.; Rodriguez R.; Sanders J. K. M.; Balasubramanian S. Exploring the Differential Recognition of DNA G-Quadruplex Targets by Small Molecules Using Dynamic Combinatorial Chemistry. *Angew. Chem., Int. Ed.* **2008**; *47* (14): 2677-2680.
53. Masoud S. S.; Tsushima Y.; Iida K.; Nagasawa K. Synthesis of Macrocyclic Penta- and Tetraoxazoles as G-Quadruplexes Ligands. *Heterocycles*. **2015**; *90* (2): 866-873.
54. Tera M.; Iida K.; Ikebukuro K.; Seimiya H.; Shin-Ya K.; Nagasawa K. Visualization of G-quadruplexes by using a BODIPY-labeled macrocyclic heptaoxazole. *Org. Biomol. Chem.* **2010**; *8* (12): 2749-2755.
55. Tera M.; Iida K.; Ishizuka H.; Takagi M.; Suganuma M.; Doi T. *et al*. Synthesis of a potent G-quadruplex-binding macrocyclic heptaoxazole. *ChemBioChem*. **2009**; *10* (3): 431-435.
56. Agarwal T.; Roy S.; Chakraborty T. K.; Maiti S. Selective targeting of G-quadruplex using furan-based cyclic homooligopeptides: effect on *c-MYC* expression. *Biochemistry*. **2010**; *49* (38): 8388-8397.
57. Chakraborty T. K.; Arora A.; Roy S.; Kumar N.; Maiti S. Furan based cyclic oligopeptides selectively target G-quadruplex. *J. Med. Chem.* **2007**; *50* (23): 5539-5542.
58. Iida K.; Tera M.; Hirokawa T.; Shin-ya K.; Nagasawa K. Synthesis of Macrocyclic Hexaoxazole (6OTD) Dimers, Containing Guanidine and Amine Functionalized Side Chains, and an Evaluation of Their Telomeric G4 Stabilizing Properties. *J. Nucleic Acids*. **2010**; *2010*: 217627.
59. Iida K.; Tera M.; Hirokawa T.; Shin-ya K.; Nagasawa K. G-quadruplex recognition by macrocyclic hexaoxazole (6OTD) dimer: greater selectivity than monomer. *Chem. Commun*. **2009**; *42*: 6481-6483.
60. Shirude P. S.; Gillies E. R.; Ladame S.; Godde F.; Shin-Ya K.; Huc I. *et al*. Macrocyclic and helical oligoamides as a new class of G-quadruplex ligands. *J. Am. Chem. Soc.* **2007**; *129* (39): 11890-11891.

61. Jena P. V.; Shirude P. S.; Okumus B.; Laxmi-Reddy K.; Godde F.; Huc I. *et al*. G-quadruplex DNA bound by a synthetic ligand is highly dynamic. *J. Am. Chem. Soc.* **2009**; *131* (35): 12522-12523.
62. Monchaud D.; Allain C.; Teulade-Fichou M. P. Development of a fluorescent intercalator displacement assay (G4-FID) for establishing quadruplex-DNA affinity and selectivity of putative ligands. *Bioorg. Med. Chem. Lett.* **2006**; *16* (18): 4842-4845.
63. Ren J.; Chaires J. B. Sequence and structural selectivity of nucleic acid binding ligands. *Biochemistry*. **1999**; *38* (49): 16067-16075.
64. Wei C.; Wang L.; Jia G.; Zhou J.; Han G.; Li C. The binding mode of porphyrins with cation side arms to (TG4T)4 G-quadruplex: Spectroscopic evidence. *Biophys. Chem*. **2009**; *143* (1–2): 79-84.
65. Wang P.; Ren L.; He H.; Liang F.; Zhou X.; Tan Z. A phenol quaternary ammonium porphyrin as a potent telomerase inhibitor by selective interaction with quadruplex DNA. *ChemBioChem*. **2006**; *7* (8): 1155-1159.
66. Wang S. R.; Zhang D.; Luo F. L.; Liu L.; Weng X. C.; Huang J. *et al*. Some cationic porphyrins: synthesis, stabilization of G-quadruplexes, and down-regulation of *c-MYC* in Hep G2 cells. *J. Porphyrins Phthalocyanines*. **2009**; *13* (08n09): 865-875.
67. Murashima T.; Sakiyama D.; Miyoshi D.; Kuriyama M.; Yamada T.; Miyazawa T. *et al*. Cationic Porphyrin Induced a Telomeric DNA to G-Quadruplex Form in Water. *Bioinorg. Chem. Appl.* **2008**; *2008*: 294756.
68. Huang X.-X.; Zhu L.-N.; Wu B.; Huo Y.-F.; Duan N.-N.; Kong D.-M. Two cationic porphyrin isomers showing different multimeric G-quadruplex recognition specificity against monomeric G-quadruplexes. *Nucleic Acids Res*. **2014**; *42* (13): 8719-8731.
69. Kang C.-C.; Chen C.-T.; Cho C.-C.; Lin Y.-C.; Chang C.-C.; Chang T.-C. A Dual Selective Antitumor Agent and Fluorescence Probe: the Binary BMVC–Porphyrin Photosensitizer. *ChemMedChem*. **2008**; *3* (5): 725-728.
70. Mion G.; Gianferrara T.; Bergamo A.; Gasser G.; Pierroz V.; Rubbiani R. *et al*. Phototoxic Activity and DNA Interactions of Water-Soluble Porphyrins and Their Rhenium(I) Conjugates. *ChemMedChem*. **2015**; *10* (11): 1901-1914.
71. Ikawa Y.; Touden S.; Furuta H. N-fused porphyrin with pyridinium side-arms: a new class of aromatic ligand with DNA-binding ability. *Org. Biomol. Chem*. **2011**; *9* (23): 8068-8078.
72. Fu B.; Huang J.; Ren L.; Weng X.; Zhou Y.; Du Y. *et al*. Cationic corrole derivatives: a new family of G-quadruplex inducing and stabilizing ligands. *Chem. Commun*. **2007**; *31*: 3264-3266.
73. Baker E. S.; Lee J. T.; Sessler J. L.; Bowers M. T. Cyclo[*n*]pyrroles: Size and Site Specific Binding to G-Quadruplexes. *J. Am. Chem. Soc*. **2006**; *128* (8): 2641-2648.
74. Zhang L.; Huang J.; Ren L.; Bai M.; Wu L.; Zhai B. *et al*. Synthesis and evaluation of cationic phthalocyanine derivatives as potential inhibitors of telomerase. *Bioorg. Med. Chem.* **2008**; *16* (1): 303-312.
75. Rodriguez R.; Pantoş G. D.; Gonçalves D. P. N.; Sanders J. K. M.; Balasubramanian S. Ligand-Driven G-Quadruplex Conformational Switching By Using an Unusual Mode of Interaction. *Angew. Chem., Int. Ed*. **2007**; *46* (28): 5405-5407.
76. Goncalves D. P.; Rodriguez R.; Balasubramanian S.; Sanders J. K. Tetramethylpyridiniumporphyrazines – a new class of G-quadruplex inducing and stabilising ligands. *Chem. Commun*. **2006**; 45: 4685-4687.
77. Rezler E. M.; Seenisamy J.; Bashyam S.; Kim M. Y.; White E.; Wilson W. D. *et al*. Telomestatin and diseleno sapphyrin bind selectively to two different forms of the human telomeric G-quadruplex structure. *J. Am. Chem. Soc.* **2005**; *127* (26): 9439-9447.
78. Seenisamy J.; Bashyam S.; Gokhale V.; Vankayalapati H.; Sun D.; Siddiqui-Jain A. *et al*. Design and synthesis of an expanded porphyrin that has selectivity for the *c-MYC* G-quadruplex structure. *J. Am. Chem. Soc.* **2005**; *127* (9): 2944-2959.

79. Ragazzon P.; Chaires J. B. Use of competition dialysis in the discovery of G-quadruplex selective ligands. *Methods*. **2007**; *43* (4): 313-323.
80. Nicoludis J. M.; Barrett S. P.; Mergny J. L.; Yatsunyk L. A. Interaction of human telomeric DNA with *N*-methyl mesoporphyrin IX. *Nucleic Acids Res*. **2012**; *40* (12): 5432-5447.
81. Fu B.; Zhang D. ; Weng X.; Zhang M.; Ma H.; Ma Y. *et al*. Cationic Metal-Corrole Complexes: Design, Synthesis, and Properties of Guanine-Quadruplex Stabilizers. *Chem. - Eur. J.* **2008**; *14* (30): 9431-9441.
82. Keating L. R.; Szalai V. A. Parallel-stranded guanine quadruplex interactions with a copper cationic porphyrin. *Biochemistry*. **2004**; *43* (50): 15891-15900.
83. Evans S. E.; Mendez M. A.; Turner K. B.; Keating L. R.; Grimes R. T.; Melchoir S. *et al*. End-stacking of copper cationic porphyrins on parallel-stranded guanine quadruplexes. *JBIC, J. Biol. Inorg. Chem*. **2007**; *12* (8): 1235-1249.
84. Gaier A. J., McMillin D. R. Binding Studies of G-Quadruplex DNA and Porphyrins: Cu(T4) vs Sterically Friendly Cu(*t*D4). *Inorg. Chem*. **2015**; *54* (9): 4504-4511.
85. Sabater L.; Fang P.-J. ; Chang C.-F.; De Rache A.; Prado E.; Dejeu J. *et al*. Cobalt(III)porphyrin to target G-quadruplex DNA. *Dalton Trans*. **2015**; *44* (8): 3701-3707.
86. Rubio-Magnieto J.; Di Meo F.; Lo M.; Delcourt C.; Clement S.; Norman P. *et al*. Binding modes of a core-extended metalloporphyrin to human telomeric DNA G-quadruplexes. *Org. Biomol. Chem.* **2015**; *13* (8): 2453-2463.
87. Maraval A.; Franco S.; Vialas C.; Pratviel G.; Blasco M. A.; Meunier B. Porphyrin-aminoquinoline conjugates as telomerase inhibitors. *Org. Biomol. Chem*. **2003**; *1* (6): 921-927.
88. Dixon I. M.; Lopez F.; Estève J.-P., Tejera A. M.; Blasco M. A.; Pratviel G. *et al*. Porphyrin Derivatives for Telomere Binding and Telomerase Inhibition. ChemBioChem. **2005**; *6* (1): 123-132.
89. Sabater L.; Nicolau-Travers M.-L.; De Rache A.; Prado E.; Dejeu J.; Bombarde O. *et al*. The nickel(II) complex of guanidinium phenyl porphyrin, a specific G-quadruplex ligand, targets telomeres and leads to POT1 mislocalization in culture cells. *JBIC, J. Biol. Inorg. Chem.* **2015**; *20* (4): 729-738.
90. Sabharwal N. C.; Mendoza O.; Nicoludis J. M.; Ruan T.; Mergny J.-L., Yatsunyk L. A. Investigation of the interactions between Pt(II) and Pd(II) derivatives of 5,10,15,20-tetrakis (*N*-methyl-4-pyridyl)porphyrin and G-quadruplex DNA. *JBIC, J. Biol. Inorg. Chem.* **2016**; *21* (2): 227-239.
91. Alzeer J.; Vummidi B. R.; Roth P. J. C.; Luedtke N. W. Guanidinium-Modified Phthalocyanines as High-Affinity G-Quadruplex Fluorescent Probes and Transcriptional Regulators. *Angew. Chem., Int. Ed*. **2009**; *48* (49): 9362-9365.
92. Manet I.; Manoli F.; Donzello M. P.; Viola E.; Andreano G.; Masi A. et al. A cationic Zn^{II} porphyrazine induces a stable parallel G-quadruplex conformation in human telomeric DNA. *Org. Biomol. Chem.* **2011**; *9* (3): 684-688.
93. Membrino A.; Paramasivam M.; Cogoi S.; Alzeer J.; Luedtke N. W.; Xodo L. E. Cellular uptake and binding of guanidine-modified phthalocyanines to KRAS/HRAS G-quadruplexes. *Chem. Commun.* **2010**; *46* (4): 625-627.
94. Ren L.; Zhang A.; Huang J.; Wang P.; Weng X.; Zhang L. *et al*. Quaternary Ammonium Zinc Phthalocyanine: Inhibiting Telomerase by Stabilizing G quadruplexes and Inducing G-Quadruplex Structure Transition and Formation. ChemBioChem. **2007**; *8* (7): 775-80.
95. Pan J.; Zhang S. Interaction between cationic zinc porphyrin and lead ion induced telomeric guanine quadruplexes: evidence for end-stacking. *JBIC, J. Biol. Inorg. Chem*. **2008**; *14* (3): 401-407.
96. Dixon I. M.; Lopez F.; Tejera A. M.; Estève J.-P.; Blasco M. A.; Pratviel G. *et al*. A G-Quadruplex Ligand with 10000-Fold Selectivity over Duplex DNA. *J. Am. Chem. Soc*. **2007**; 129 (6): 1502-1503.

97. Zheng X.-H.; Cao Q.; Ding Y.-L.; Zhong Y.-F.; Mu G.; Qin P. Z. *et al*. Platinum(II) clovers targeting G-quadruplexes and their anticancer activities. *Dalton Trans*. **2015**; *44* (1): 50-53.
98. Granzhan A.; Monchaud D.; Saettel N.; Guédin A.; Mergny J.-L.; Teulade-Fichou M.-P. "One Ring to Bind Them All" - Part II: Identification of Promising G-Quadruplex Ligands by Screening of Cyclophane-Type Macrocycles. *J. Nucleic Acids*. **2010**; *2010*: 460561.
99. Marchetti C.; Minarini A.; Tumiatti V.; Moraca F.; Parrotta L.; Alcaro S. *et al*. Macrocyclic naphthalene diimides as G-quadruplex binders. *Bioorg. Med. Chem*. **2015**; *23* (13): 3819-3830.
100. Islam M.; Fujii S.; Sato S.; Okauchi T.; Takenaka S. A Selective G-Quadruplex DNA-Stabilizing Ligand Based on a Cyclic Naphthalene Diimide Derivative. *Molecules*. **2015**; *20* (6): 10963-10979.
101. Teulade-Fichou M.-P.; Carrasco C.; Guittat L.; Bailly C.; Alberti P.; Mergny J.-L. *et al*. Selective Recognition of G-Quadruplex Telomeric DNA by a Bis(quinacridine) Macrocycle. *J. Am. Chem. Soc*. **2003**; *125* (16): 4732-4740.
102. Alberti P.; Ren J.; Teulade-Fichou M. P. ; Guittat L.; Riou J. F.; Chaires J. *et al*. Interaction of an acridine dimer with DNA quadruplex structures. *J. Biomol. Struct. Dyn*. **2001**; *19* (3): 505-513.
103. Esaki Y.; Islam M. M.; Fujii S.; Sato S.; Takenaka S. Design of tetraplex specific ligands: cyclic naphthalene diimide. *Chem. Commun*. **2014**; *50* (45): 5967-5969.
104. Bazzicalupi C.; Chioccioli M.; Sissi C.; Porcù E.; Bonaccini C.; Pivetta C. *et al*. Modeling and Biological Investigations of an Unusual Behavior of Novel Synthesized Acridine-Based Polyamine Ligands in the Binding of Double Helix and G-Quadruplex DNA. *ChemMedChem*. **2010**; *5* (12): 1995-2005.
105. Kaiser M.; De Cian A.; Sainlos M.; Renner C.; Mergny J.-L.; Teulade-Fichou M.-P. Neomycin-capped aromatic platforms: quadruplex DNA recognition and telomerase inhibition. *Org. Biomol. Chem*. **2006**; *4* (6): 1049-1057.
106. De Cian A.; Grellier P.; Mouray E.; Depoix D.; Bertrand H.; Monchaud D. *et al*. Plasmodium Telomeric Sequences: Structure, Stability and Quadruplex Targeting by Small Compounds. *ChemBioChem*. **2008**; *9* (16): 2730-2739.
107. Harrison R. J.; Gowan S. M.; Kelland L. R., Neidle S. Human telomerase inhibition by substituted acridine derivatives. *Bioorg. Med. Chem. Lett*. **1999**; *9* (17): 2463-2468.
108. Sparapani S.; Haider S. M.; Doria F.; Gunaratnam M.; Neidle S. Rational design of acridine-based ligands with selectivity for human telomeric quadruplexes. *J. Am. Chem. Soc.* **2010**; *132* (35): 12263-12272.
109. Campbell N. H.; Smith D. L.; Reszka A. P.; Neidle S.; O'Hagan D. Fluorine in medicinal chemistry: β-fluorination of peripheral pyrrolidines attached to acridine ligands affects their interactions with G-quadruplex DNA. *Org. Biomol. Chem*. **2011**; *9* (5): 1328-1331.
110. Li J.-L.; Harrison R. J.; Reszka A. P.; Brosh R. M.; Bohr V. A.; Neidle S. *et al*. Inhibition of the Bloom's and Werner's Syndrome Helicases by G-Quadruplex Interacting Ligands. *Biochemistry*. **2001**; *40* (50): 15194-15202.
111. Moore M. J. B.; Schultes C. M.; Cuesta J.; Cuenca F.; Gunaratnam M.; Tanious F. A. *et al*. Trisubstituted Acridines as G-quadruplex Telomere Targeting Agents. Effects of Extensions of the 3,6- and 9-Side Chains on Quadruplex Binding, Telomerase Activity, and Cell Proliferation. *J. Med. Chem*. **2006**; *49* (2): 582-599.
112. Howell L. A.; Bowater R. A.; O'Connell M. A.; Reszka A. P.; Neidle S.; Searcey M. Synthesis of Small Molecules Targeting Multiple DNA Structures using Click Chemistry. *ChemMedChem*. **2012**; 7 (5): 792-804.
113. Zhou G.; Liu X; Li Y.; Xu S.; Ma C.; Wu X.; Cheng Y.; Yu Z.; Zhao G.; Chen Y. Telomere targeting with a novel G-quadruplex-interactive ligand BRACO-19 induces T-loop disassembly and telomerase displacement in human glioblastoma cells. *Oncogenes*. **2016;** *7* (12): 14925–14939.

114. Burger A. M.; Dai F.; Schultes C. M.; Reszka A. P.; Moore M. J.; Double J. A. *et al*. The G-quadruplex-interactive molecule BRACO-19 inhibits tumor growth, consistent with telomere targeting and interference with telomerase function. *Cancer Res*. **2005**; *65* (4): 1489-1496.
115. Fu Y.-T.; Keppler B. R.; Soares J.; Jarstfer M. B. BRACO19 analog dimers with improved inhibition of telomerase and hPot 1. *Bioorg. Med. Chem*. **2009**; *17* (5): 2030-2037.
116. Stanslas J.; Hagan D. J.; Ellis M. J.; Turner C.; Carmichael J.; Ward W. *et al*. Antitumor Polycyclic Acridines. 7. Synthesis and Biological Properties of DNA Affinic Tetra- and Pentacyclic Acridines. *J. Med. Chem*. **2000**; *43* (8): 1563-1572.
117. Liao S.-R.; Zhou C.-X.; Wu W.-B.; Ou T.-M.; Tan J.-H.; Li D. *et al*. 12-*N*-Methylated 5,6-dihydrobenzo[*c*]acridine derivatives: A new class of highly selective ligands for *c-MYC* G-quadruplex DNA. *Eur. J. Med. Chem*. **2012**; *53*: 52-63.
118. Cheng M.-K.; Modi C.; Cookson J. C.; Hutchinson I.; Heald R. A.; McCarroll A. J. *et al*. Antitumor Polycyclic Acridines. 20. Search for DNA Quadruplex Binding Selectivity in a Series of 8,13-Dimethylquino[4,3,2-*kl*]acridinium Salts: Telomere- Targeted Agents. *J. Med. Chem*. **2008**; *51* (4): 963-975.
119. Heald R.A.; Stevens M. F. Antitumour polycyclic acridines. Palladium(0) mediated syntheses of quino[4,3,2-*kl*]acridines bearing peripheral substituents as potential telomere maintenance inhibitors. *Org. Biomol. Chem*. **2003**; *1* (19): 3377-3389.
120. Hounsou C.; Guittat L.; Monchaud D.; Jourdan M.; Saettel N.; Mergny J. L. *et al*. G-quadruplex recognition by quinacridines: a SAR, NMR, and biological study. *ChemMedChem*. **2007**; *2* (5): 655-666.
121. Mergny J.-L.; Lacroix L.; Teulade-Fichou M.-P.; Hounsou C.; Guittat L.; Hoarau M. *et al*. Telomerase inhibitors based on quadruplex ligands selected by a fluorescence assay. *Proc. Natl. Acad. Sci. U. S. A*. **2001**; *98* (6): 3062-3067.
122. Lagah S.; Tan I. L.; Radhakrishnan P.; Hirst R. A.; Ward J. H.; O'Callaghan C. *et al*. RHPS4 G-Quadruplex Ligand Induces Anti-Proliferative Effects in Brain Tumor Cells. *Plos One*. **2014**; *9* (1): e86187.
123. Harrison R. J.; Reszka A. P.; Haider S. M.; Romagnoli B.; Morrell J.; Read M. A. *et al*. Evaluation of by disubstituted acridone derivatives as telomerase inhibitors: the importance of G-quadruplex binding. *Bioorg. Med. Chem. Lett*. **2004**; *14* (23): 5845-5849.
124. Cuenca F.; Moore M. J. B.; Johnson K.; Guyen B.; De Cian A.; Neidle S. Design, synthesis and evaluation of 4,5-di-substituted acridone ligands with high G-quadruplex affinity and selectivity, together with low toxicity to normal cells. *Bioorg. Med. Chem. Lett*. **2009**; *19* (17): 5109-5113.
125. Laronze-Cochard M.; Kim Y. M.; Brassart B.; Riou J. F.; Laronze J. Y.; Sapi J. Synthesis and biological evaluation of novel 4,5-bis(dialkylaminoalkyl)-substituted acridines as potent telomeric G-quadruplex ligands. *Eur. J. Med. Chem*. **2009**; *44* (10): 3880-3888.
126. Altieri A.; Alvino A.; Ohnmacht S.; Ortaggi G.; Neidle S.; Nocioni D. *et al*. Xanthene and xanthone derivatives as G-quadruplex stabilizing ligands. *Molecules*. **2013**; *18* (11): 13446-13470.
127. Franceschin M.; Nocioni D.; Biroccio A.; Micheli E.; Cacchione S.; Cingolani C. *et al*. Design and synthesis of a new dimeric xanthone derivative: enhancement of G-quadruplex selectivity and telomere damage. *Org. Biomol. Chem*. **2014**; *12* (47): 9572-9582.
128. Manet I.; Manoli F.; Zambelli B.; Andreano G.; Masi A.; Cellai L. *et al*. Affinity of the anthracycline antitumor drugs Doxorubicin and Sabarubicin for human telomeric G-quadruplex structures. *Phys. Chem. Chem. Phys*. **2011**; *13* (2): 540-551.
129. Pradeep T. P.; Barthwal R. NMR structure of dual site binding of mitoxantrone dimer to opposite grooves of parallel stranded G-quadruplex [d-(TTGGGGT)]$_4$. *Biochimie*. **2016**; *128-129*: 59-69.

130. Perry P. J.; Gowan S. M.; Reszka A. P.; Polucci P.; Jenkins T. C.; Kelland L. R. *et al*. 1,4- and 2,6-disubstituted amidoanthracene-9,10-dione derivatives as inhibitors of human telomerase. *J. Med. Chem*. **1998**; *41* (17): 3253-3260.
131. Perry P. J.; Reszka A. P.; Wood A. A.; Read M. A.; Gowan S. M.; Dosanjh H. S. *et al*. Human telomerase inhibition by regioisomeric disubstituted amidoanthracene-9,10-diones. *J. Med. Chem*. **1998**; *41* (24): 4873-4884.
132. Zagotto G.; Sissi C.; Lucatello L.; Pivetta C.; Cadamuro S. A.; Fox K. R. *et al*. Aminoacyl−Anthraquinone Conjugates as Telomerase Inhibitors: Synthesis, Biophysical and Biological Evaluation. *J. Med. Chem*. **2008**; *51* (18): 5566-5574.
133. Zorzan E.; Ros S. D.; Musetti C.; Shahidian L. Z.; Coelho N. F.; Bonsembiante F. *et al*. Screening of candidate G-quadruplex ligands for the human *c-KIT* promotorial region and their effects in multiple *in-vitro* models. *Oncotarget*. **2016**; *7* (16): 21658-21675.
134. Zagotto G.; Ricci A.; Vasquez E.; Sandoli A.; Benedetti S.; Palumbo M. *et al*. Tuning G-Quadruplex vs Double-Stranded DNA Recognition in Regioisomeric Lysyl-Peptidyl-Anthraquinone Conjugates. *Bioconjugate Chem*. **2011**; *22* (10): 2126-2135.
135. Ranjan N.; Davis E.; Xue L.; Arya D. P. Dual recognition of the human telomeric G-quadruplex by a neomycin-anthraquinone conjugate. *Chem. Commun*. **2013**; *49* (51): 5796-5798.
136. Percivalle C.; Sissi C.; Greco M. L.; Musetti C.; Mariani A.; Artese A. *et al*. Aryl ethynyl anthraquinones: a useful platform for targeting telomeric G-quadruplex structures. *Org. Biomol. Chem*. **2014**; *12* (22): 3744-3754.
137. Huang H.-S.; Chen T.-C.; Chen R.-H.; Huang K.-F.; Huang F.-C.; Jhan J.-R. *et al*. Synthesis, cytotoxicity and human telomerase inhibition activities of a series of 1,2-heteroannelated anthraquinones and anthra[1,2-*d*]imidazole-6,11-dione homologues. *Bioorg. Med. Chem*. **2009**; *17* (21): 7418-7428.
138. Ilyinsky N. S.; Shchyolkina A. K.; Borisova O. F.; Mamaeva O. K.; Zvereva M. I.; Azhibek D. M. *et al*. Novel multi-targeting anthra[2,3-*b*]thiophene-5,10-diones with guanidine-containing side chains: Interaction with telomeric G-quadruplex, inhibition of telomerase and topoisomerase I and cytotoxic properties. Eur. J. Med. Chem. **2014**; *85*: 605-614.
139. Chang L.-C.; Chen T.-C.; Chen S.-J.; Chen C.-L.; Lee C.-C.; Wu S.-H. *et al*. Identification of a new class of *WNT1* inhibitor: Cancer cells migration, G-quadruplex stabilization and target validation. *Oncotarget*. **2016**; *7* (42): 67986-8001.
140. Perry P. J.; Read M. A.; Davies R. T.; Gowan S. M.; Reszka A. P.; Wood A. A. *et al*. 2,7-Disubstituted amidofluorenone derivatives as inhibitors of human telomerase. *J. Med. Chem*. **1999**; *42* (14): 2679-2684.
141. Alcaro S.; Artese A.; Iley J. N.; Missailidis S.; Ortuso F.; Parrotta L. *et al*. Rational Design, Synthesis, Biophysical and Antiproliferative Evaluation of Fluorenone Derivatives with DNA G-Quadruplex Binding Properties. ChemMedChem. **2010**; *5* (4): 575-583.
142. Alcaro S.; Artese A.; Iley J. N.; Maccari R.; Missailidis S.; Ortuso F. *et al*. Tetraplex DNA specific ligands based on the fluorenone-carboxamide scaffold. *Bioorg. Med. Chem. Lett*. **2007**; *17* (9): 2509-2514.
143. Folini M.; Pivetta C.; Zagotto G.; De Marco C.; Palumbo M.; Zaffaroni N. *et al*. Remarkable interference with telomeric function by a G-quadruplex selective bisantrene regioisomer. *Biochem. Pharmacol*. **2010**; *79* (12): 1781-1790.
144. Ribaudo G.; Scalabrin M.; Pavan V.; Fabris D.; Zagotto G. Constrained bisantrene derivatives as G-quadruplex binders. *Arkivoc*. **2016**; *2016* (3): 145-160.
145. De Cian A.; Delemos E.; Mergny J. L.; Teulade-Fichou M. P.; Monchaud D. Highly efficient G-quadruplex recognition by bisquinolinium compounds. *J. Am. Chem. Soc*. **2007**; *129* (7): 1856-1857.
146. Nielsen M. C.; Larsen A. F.; Abdikadir F. H.; Ulven T. Phenanthroline-2,9-bistriazoles as selective G-quadruplex ligands. *Eur. J. Med. Chem*. **2014**; *72*: 119-126.

147. Wang L.; Wen Y.; Liu J.; Zhou J.; Li C.; Wei C. Promoting the formation and stabilization of human telomeric G-quadruplex DNA, inhibition of telomerase and cytotoxicity by phenanthroline derivatives. *Org. Biomol. Chem*. **2011**; *9* (8): 2648-2653.
148. Musetti C.; Lucatello L.; Bianco S.; Krapcho A. P.; Cadamuro S. A.; Palumbo M. *et al*. Metal ion-mediated assembly of effective phenanthroline-based G-quadruplex ligands. *Dalton Trans*. **2009**; 19: 3657-3660.
149. Talib J.; Green C.; Davis K. J.; Urathamakul T.; Beck J. L.; Aldrich-Wright J. R. *et al.* A comparison of the binding of metal complexes to duplex and quadruplex DNA. *Dalton Trans*. **2008**; *8*:1018-1026.
150. Wang J.; Lu K.; Xuan S.; Toh Z.; Zhang D.; Shao F. A Pt(II)-Dip complex stabilizes parallel *c-MYC* G-quadruplex. *Chem. Commun*. **2013**; *49* (42): 4758-4760.
151. Reed J. E.; White A. J.; Neidle S.; Vilar R. Effect of metal coordination on the interaction of substituted phenanthroline and pyridine ligands with quadruplex DNA. *Dalton Trans*. **2009**; *14*: 2558-2568.
152. Reed J. E.; Neidle S.; Vilar R. Stabilisation of human telomeric quadruplex DNA and inhibition of telomerase by a platinum-phenanthroline complex. *Chem. Commun.* **2007**; *42*: 4366-4368.
153. Nielsen M. C.; Borch J.; Ulven T. Design, synthesis and evaluation of 4,7-diamino-1,10-phenanthroline G-quadruplex ligands. *Bioorg. Med. Chem*. **2009**; *17* (24): 8241-8246.
154. Duskova K.; Sierra S.; Arias-Pérez M.-S.; Gude L. Human telomeric G-quadruplex DNA interactions of *N*-phenanthroline glycosylamine copper(II) complexes. *Bioorg. Med. Chem*. **2016**; *24* (1): 33-41.
155. Larsen A. F.; Nielsen M. C.; Ulven T. Tetrasubstituted phenanthrolines as highly potent, water-soluble, and selective G-quadruplex ligands. *Chem. - Eur. J*. **2012**; *18* (35): 10892-10902.
156. Bianco S.; Musetti C.; Waldeck A.; Sparapani S.; Seitz J.D.; Krapcho A.P. *et al*. Bis-phenanthroline derivatives as suitable scaffolds for effective G-quadruplex recognition. *Dalton Trans*. **2010**; *39* (25): 5833-5841.
157. Wei C.-Y.; Wang J.-H.; Wen Y.; Liu J.; Wang L.-H. 4-(1*H*-Imidazo[4,5-*f*]-1,10-phenanthrolin-2-yl)phenol-based G-quadruplex DNA binding agents: Telomerase inhibition, cytotoxicity and DNA-binding studies. *Bioorg. Med. Chem*. **2013**; *21* (11):3379-3387.
158. Liu J.; Chen M.; Wang Y.; Zhao X.; Wang S.; Wu Y. *et al*. Synthesis and the interaction of 2-(1*H*-pyrazol-4-yl)-1H-imidazo[4,5-*f*][1,10]phenanthrolines with telomeric DNA as lung cancer inhibitors. *Eur. J. Med. Chem*. **2017**;*133*:36-49.
159. Kieltyka R.; Fakhoury J.; Moitessier N.; Sleiman HF. Platinum Phenanthroimidazole Complexes as G-Quadruplex DNA Selective Binders. *Chem. - Eur. J*. **2008**; 14 (4): 1145-1154.
160. Sun D.; Zhang R.; Yuan F.; Liu D.; Zhou Y.; Liu J. Studies on characterization, telomerase inhibitory properties and G-quadruplex binding of η^6-arene ruthenium complexes with 1,10-phenanthroline-derived ligands. *Dalton Trans*. **2012**; *41* (6): 1734-1741.
161. Li Q.; Zhang J.; Yang L.; Yu Q.; Chen Q.; Qin X. *et al*. Stabilization of G-quadruplex DNA and inhibition of telomerase activity studies of ruthenium(II) complexes. *J. Inorg. Biochem*. **2014**; *130*: 122-129.
162. Zhang J.; Yu Q.; Li Q.; Yang L.; Chen L.; Zhou Y. *et al*. A ruthenium(II) complex capable of inducing and stabilizing bcl-2 G-quadruplex formation as a potential cancer inhibitor. *J. Inorg. Biochem*. **2014**; *134*: 1-11.
163. Zhang Z.; Wu Q.; Wu X.-H.; Sun F.-Y.; Chen L.-M.; Chen J.-C. *et al*. Ruthenium(II) complexes as apoptosis inducers by stabilizing *c-myc* G-quadruplex DNA. *Eur. J. Med. Chem*. **2014**; *80*: 316-324.
164. Wu Q.; Zheng K.; Liao S.; Ding Y.; Li Y.; Mei W. Arene Ruthenium(II) Complexes as Low-Toxicity Inhibitor against the Proliferation, Migration, and Invasion of MDA-MB-231 Cells through Binding and Stabilizing *c-myc* G-Quadruplex DNA. *Organometallics*. **2016**; *35* (3): 317-326.

165. Wei C.; Wen Y.; Wang J. Novel platinum complexes as efficient G-quadruplex DNA binders and telomerase inhibitors. *Int. J. Biol. Macromol*. **2013**; *55*: 185-92.
166. Mancini J.; Rousseau P.; Castor K. J.; Sleiman H. F.; Autexier C. Platinum(II) phenanthroimidazole G-quadruplex ligand induces selective telomere shortening in A549 cancer cells. *Biochimie*. **2016**; *121*: 287-297.
167. Castor K. J.; Metera K. L.; Tefashe U. M.; Serpell C. J.; Mauzeroll J.; Sleiman H. F. Cyclometalated Iridium(III) Imidazole Phenanthroline Complexes as Luminescent and Electrochemiluminescent G-Quadruplex DNA Binders. *Inorg. Chem*. **2015**; *54* (14): 6958-6967.
168. Głuszyńska A. Biological potential of carbazole derivatives. *Eur. J. Med. Chem*. **2015**; *94*: 405-426.
169. Chu J.-F.; Wang Z.-F.; Tseng T.-Y.; Chang T.-C. A Novel Method for Screening G-quadruplex Stabilizers to Human Telomeres. *J. Chinese Chemical Society*. **2011**; *58* (3): 296-300.
170. Maji B.; Kumar K.; Kaulage M.; Muniyappa K.; Bhattacharya S. Design and Synthesis of New Benzimidazole–Carbazole Conjugates for the Stabilization of Human Telomeric DNA, Telomerase Inhibition, and Their Selective Action on Cancer Cells. *J. Med. Chem*. **2014**; *57* (16): 6973-6988.
171. Maji B.; Kumar K.; Muniyappa K.; Bhattacharya S. New dimeric carbazole-benzimidazole mixed ligands for the stabilization of human telomeric G-quadruplex DNA and as telomerase inhibitors. A remarkable influence of the spacer. *Org. Biomol. Chem*. **2015**; *13* (30): 8335-8348.
172. Dumat B.; Bordeau G.; Faurel-Paul E.; Mahuteau-Betzer F.; Saettel N.; Bombled M. *et al*. *N*-phenyl-carbazole-based two-photon fluorescent probes: Strong sequence dependence of the duplex vs quadruplex selectivity. *Biochimie*. **2011**; *93* (8): 1209-1218.
173. Alberti P.; Schmitt P.; Nguyen C.-H.; Rivalle C.; Hoarau M.; Grierson D. S. *et al*. Benzoindoloquinolines interact with DNA tetraplexes and inhibit telomerase. *Bioorg. Med. Chem. Lett.* **2002**; *12* (7): 1071-1074.
174. Guyen B.; Schultes C. M.; Hazel P.; Mann J.; Neidle S. Synthesis and evaluation of analogues of 10*H*-indolo[3,2-*b*]quinoline as G-quadruplex stabilising ligands and potential inhibitors of the enzyme telomerase. *Org. Biomol. Chem*. **2004**; *2* (7): 981-988.
175. Le Sann C.; Huddleston J.; Mann J. Synthesis and preliminary evaluation of novel analogues of quindolines as potential stabilisers of telomeric G-quadruplex DNA. *Tetrahedron*. **2007**; *63* (52): 12903-12911.
176. Caprio V.; Guyen B.; Opoku-Boahen Y.; Mann J.; Gowan S. M.; Kelland L. M. *et al*. A novel inhibitor of human telomerase derived from 10*H*-indolo[3,2-*b*]quinoline. *Bioorg. Med. Chem. Lett*. **2000**; *10* (18): 2063-2066.
177. Boddupally P. V.; Hahn S.; Beman C.; De B.; Brooks T. A.; Gokhale V. *et al*. Anticancer activity and cellular repression of *c-MYC* by the G-quadruplex-stabilizing 11-piperazinylquindoline is not dependent on direct targeting of the G-quadruplex in the *c-MYC* promoter. *J. Med. Chem*. **2012**; *55* (13): 6076-6086.
178. Zhou J. L.; Lu Y. J.; Ou T. M.; Zhou J. M.; Huang Z. S.; Zhu X. F. *et al*. Synthesis and evaluation of quindoline derivatives as G-quadruplex inducing and stabilizing ligands and potential inhibitors of telomerase. *J. Med. Chem*. **2005**; *48* (23): 7315-7321.
179. Zhou J. M.; Zhu X. F.; Lu Y. J.; Deng R.; Huang Z. S.; Mei Y. P. *et al*. Senescence and telomere shortening induced by novel potent G-quadruplex interactive agents, quindoline derivatives, in human cancer cell lines. *Oncogene*. **2006**; *25* (4): 503-511.
180. Funke A.; Dickerhoff J.; Weisz K. Towards the Development of Structure-Selective G-Quadruplex-Binding Indolo[3,2-*b*]quinolines. *Chem. - Eur. J*. **2016**; *22* (9): 3170-3181.
181. Ou T.-M.; Lin J.; Lu Y.-J.; Hou J.-Q.; Tan J.-H.; Chen S.-H. *et al*. Inhibition of Cell Proliferation by Quindoline Derivative (SYUIQ-05) through its Preferential Interaction with *c-myc* Promoter G-Quadruplex. *J. Med. Chem*. **2011**; *54* (16): 5671-5679.

182. Lu Y.-J.; Ou T.-M.; Tan J.-H.; Hou J.-Q.; Shao W.-Y.; Peng D. *et al*. 5-*N*-Methylated Quindoline Derivatives as Telomeric G-Quadruplex Stabilizing Ligands: Effects of 5-*N* Positive Charge on Quadruplex Binding Affinity and Cell Proliferation. *J. Med. Chem*. **2008**; *51* (20): 6381-6392.
183. Lavrado J.; Reszka A. P.; Moreira R.; Neidle S.; Paulo A. C-11 diamino cryptolepine derivatives NSC748392, NSC748393, and NSC748394: anticancer profile and G-quadruplex stabilization. *Bioorg. Med. Chem. Lett*. **2010**; *20* (23): 7042-7045.
184. Lavrado J.; Borralho P. M.; Ohnmacht S. A.; Castro R. E.; Rodrigues C. M.; Moreira R. *et al*. Synthesis, G-quadruplex stabilisation, docking studies, and effect on cancer cells of indolo[3,2-*b*]quinolines with one, two, or three basic side chains. *ChemMedChem*. **2013**; *8* (10): 1648-1661.
185. Brito H.; Martins A. C.; Lavrado J.; Mendes E.; Francisco A. P.; Santos S. A. *et al*. Targeting KRAS Oncogene in Colon Cancer Cells with 7-Carboxylate Indolo[3,2-*b*]quinoline Tri-Alkylamine Derivatives. *Plos One*. **2015**; *10* (5): e0126891.
186. Lavrado J.; Ohnmacht S. A.; Correia I.; Leitão C.; Pisco S.; Gunaratnam M. *et al*. Indolo[3,2-*c*]quinoline G-Quadruplex Stabilizers: a Structural Analysis of Binding to the Human Telomeric G-Quadruplex. *ChemMedChem*. **2015**; *10* (5): 836-849.
187. Lavrado J.; Brito H.; Borralho P. M.; Ohnmacht S. A.; Kim N.-S.; Leitão C. *et al*. KRAS oncogene repression in colon cancer cell lines by G-quadruplex binding indolo[3,2-*c*]quinolines. *Sci. Rep*. **2015**; 5: 9696.
188. Guittat L.; Alberti P.; Rosu F.; Van Miert S.; Thetiot E.; Pieters L. *et al*. Interactions of cryptolepine and neocryptolepine with unusual DNA structures. *Biochimie*. **2003**; *85* (5): 535-547.
189. Long Y.; Li Z.; Tan J.-H.; Ou T.-M.; Li D.; Gu L.-Q. *et al*. Benzofuroquinoline Derivatives Had Remarkable Improvement of their Selectivity for Telomeric G-Quadruplex DNA over Duplex DNA upon Introduction of Peptidyl Group. *Bioconjugate Chem*. **2012**; *23* (9): 1821-1831.
190. Zhong Y.-n.; Zhang Y.; Gu Y.-q.; Wu S.-y.; Shen W.-y.; Tan M.-x. Novel Fe^{II} and Co^{II} Complexes of Natural Product Tryptanthrin: Synthesis and Binding with G-Quadruplex DNA. *Bioinorg. Chem. Appl.* **2016**; *2016*: 5075847.
191. Yu H.-j.; Yu L.; Hao Z.-f.; Zhao Y. Interactions of ruthenium complexes containing indoloquinoline moiety with human telomeric G-quadruplex DNA. *Spectrochim. Acta, Part A*. **2014**; *124*: 187-193.
192. Yu H.-j.; Zhao Y.; Mo W.-j.; Hao Z.-f.; Yu L. Ru-indoloquinoline complex as a selective and effective human telomeric G-quadruplex binder. *Spectrochim. Acta, Part A*. **2014**; *132*: 84-90.
193. Ghosh S.; Dasgupta D. Quadruplex forming promoter region of *c-myc* oncogene as a potential target for a telomerase inhibitory plant alkaloid, chelerythrine. *Biochem. Bioph. Res. Commun*. **2015**; *459* (1): 75-80.
194. Bhat J.; Chatterjee S. Skeleton selectivity in complexation of chelerythrine and chelerythrine-like natural plant alkaloids with the G-quadruplex formed at the promoter of *c-MYC* oncogene: *in silico* exploration. *RSC Adv*. **2016**; *6* (43): 36667-36680.
195. Padmapriya K.; Barthwal R. NMR based structural studies decipher stacking of the alkaloid coralyne to terminal guanines at two different sites in parallel G-quadruplex DNA, $[d(TTGGGGT)]_4$ and $[d(TTAGGGT)]_4$. *Biochim. Biophys. Acta*. **2017**; *1861* (2): 37-48.
196. Bhadra K.; Kumar G. S. Interaction of berberine, palmatine, coralyne, and sanguinarine to quadruplex DNA: a comparative spectroscopic and calorimetric study. *Biochim. Biophys. Acta*. **2011**; *1810* (4): 485-496.
197. Bazzicalupi C.; Ferraroni M.; Bilia A. R.; Scheggi F.; Gratteri P. The crystal structure of human telomeric DNA complexed with berberine: an interesting case of stacked ligand to G-tetrad ratio higher than 1:1. *Nucleic Acids Res*. **2013**; *41* (1): 632-638.
198. Xiong Y. X.; Su H. F.; Lv P.; Ma Y.; Wang S. K.; Miao H. *et al*. A newly identified berberine derivative induces cancer cell senescence by stabilizing endogenous G-quadruplexes and

sparking a DNA damage response at the telomere region. *Oncotarget*. **2015**; *6* (34): 35625-35635.

199. Ma Y.; Ou T.-M.; Hou J.-Q.; Lu Y.-J.; Tan J.-H.; Gu L.-Q. *et al*. 9-*N*-Substituted berberine derivatives: Stabilization of G-quadruplex DNA and down-regulation of oncogene *c-myc*. *Bioorg. Med. Chem*. **2008**; *16* (16): 7582-7591.
200. Ma Y.; Ou T.-M.; Tan J.-H.; Hou J.-Q.; Huang S.-L.; Gu L.-Q. *et al*. Synthesis and evaluation of 9-*O*-substituted berberine derivatives containing aza-aromatic terminal group as highly selective telomeric G-quadruplex stabilizing ligands. *Bioorg. Med. Chem. Lett*. **2009**; *19* (13): 3414-3417.
201. Ferraroni M.; Bazzicalupi C.; Papi F.; Fiorillo G.; Guamán-Ortiz L. M.; Nocentini A. *et al*. Solution and Solid-State Analysis of Binding of 13-Substituted Berberine Analogues to Human Telomeric G-quadruplexes. *Chem. - Asian J*. **2016**; *11* (7): 1107-1115.
202. Franceschin M.; Rossetti L.; D'Ambrosio A.; Schirripa S.; Bianco A.; Ortaggi G. *et al*. Natural and synthetic G-quadruplex interactive berberine derivatives. *Bioorg. Med. Chem. Lett*. **2006**; *16* (6): 1707-1711.
203. Tera M.; Hirokawa T.; Okabe S.; Sugahara K.; Seimiya H.; Shimamoto K. Design and Synthesis of a Berberine Dimer: A Fluorescent Ligand with High Affinity towards G-Quadruplexes. *Chem. - Eur. J*. **2015**; *21* (41): 14519-14528.
204. Zhou C.-Q.; Yang J.-W.; Dong C.; Wang Y.-M.; Sun B.; Chen J.-X. *et al*. Highly selective, sensitive and fluorescent sensing of dimeric G-quadruplexes by a dimeric berberine. *Org. Biomol. Chem.* **2016**; *14* (1): 191-197.
205. Ma Y.; Ou T.-M.; Tan J.-H.; Hou J.-Q.; Huang S.-L.; Gu L.-Q. *et al*. Quinolino-benzo-[5,6]-dihydroisoquindolium compounds derived from berberine: A new class of highly selective ligands for G-quadruplex DNA in *c-myc* oncogene. *Eur. J. Med. Chem*. **2011**; *46* (5): 1906-1913.
206. Maji B.; Bhattacharya S. Advances in the molecular design of potential anticancer agents *via* targeting of human telomeric DNA. *Chem. Commun*. **2014**; *50* (49): 6422-6438.
207. Franceschin M.; Alvino A.; Ortaggi G.; Bianco A. New hydrosoluble perylene and coronene derivatives. *Tetrahedron Lett*. **2004**; *45* (49): 9015-9020.
208. Sissi C.; Lucatello L.; Krapcho A. P.; Maloney D. J.; Boxer M. B.; Camarasa M.V. *et al*. Tri-, tetra- and heptacyclic perylene analogues as new potential antineoplastic agents based on DNA telomerase inhibition. *Bioorg. Med. Chem*. **2007**; *15* (1): 555-562.
209. Micheli E.; Lombardo C. M.; D'Ambrosio D.; Franceschin M.; Neidle S.; Savino M. Selective G-quadruplex ligands: the significant role of side chain charge density in a series of perylene derivatives. *Bioorg. Med. Chem. Lett*. **2009**; *19* (14): 3903-3908.
210. Casagrande V.; Salvati E.; Alvino A.; Bianco A.; Ciammaichella A.; D'Angelo C. *et al*. *N*-Cyclic Bay-Substituted Perylene G-Quadruplex Ligands Have Selective Antiproliferative Effects on Cancer Cells and Induce Telomere Damage. *J. Med. Chem*. **2011**; *54* (5):1140-1156.
211. Hu Y.; Han D.; Zhang Q.; Wu T.; Li F.; Niu L. Perylene ligand wrapping G-quadruplex DNA for label-free fluorescence potassium recognition. *Biosens. Bioelectron*. **2012**; *38* (1): 396-401.
212. Franceschin M.; Alvino A.; Casagrande V.; Mauriello C.; Pascucci E.; Savino M. *et al*. Specific interactions with intra- and intermolecular G-quadruplex DNA structures by hydrosoluble coronene derivatives: a new class of telomerase inhibitors. *Bioorg. Med. Chem*. **2007**; *15* (4): 1848-1858.
213. Peduto A.; Pagano B.; Petronzi C.; Massa A.; Esposito V.; Virgilio A. *et al*. Design, synthesis, biophysical and biological studies of trisubstituted naphthalimides as G-quadruplex ligands. *Bioorg. Med. Chem*. **2011**; *19* (21): 6419-6429.
214. Cuenca F.; Greciano O.; Gunaratnam M.; Haider S.; Munnur D.; Nanjunda R. *et al*. Tri- and tetra-substituted naphthalene diimides as potent G-quadruplex ligands. *Bioorg. Med. Chem. Lett.* **2008**; *18* (5): 1668-1673.

215. Milelli A.; Tumiatti V.; Micco M.; Rosini M.; Zuccari G.; Raffaghello L. *et al*. Structure-activity relationships of novel substituted naphthalene diimides as anticancer agents. *Eur. J. Med. Chem.* **2012**; *57*: 417-428.
216. Collie G. W.; Promontorio R.; Hampel S. M.; Micco M.; Neidle S.; Parkinson G. N. Structural basis for telomeric G-quadruplex targeting by naphthalene diimide ligands. *J. Am. Chem. Soc.* **2012**; *134* (5): 2723-2731.
217. Micco M.; Collie G. W.; Dale A. G.; Ohnmacht S. A.; Pazitna I.; Gunaratnam M. *et al*. Structure-Based Design and Evaluation of Naphthalene Diimide G-Quadruplex Ligands As Telomere Targeting Agents in Pancreatic Cancer Cells. *J. Med. Chem*. **2013**; *56* (7): 2959-2974.
218. Mitchell T.; Ramos-Montoya A.; Di Antonio M.; Murat P.; Ohnmacht S.; Micco M. *et al*. Downregulation of Androgen Receptor Transcription by Promoter G-Quadruplex Stabilization as a Potential Alternative Treatment for Castrate-Resistant Prostate Cancer. *Biochemistry*. **2013**; *52* (8): 1429-1436.
219. Mpima S.; Ohnmacht S. A.; Barletta M; Husby J.; Pett L. C.; Gunaratnam M. *et al*. The influence of positional isomerism on G-quadruplex binding and anti-proliferative activity of tetra-substituted naphthalene diimide compounds. *Bioorg. Med. Chem*. **2013**; *21* (20): 6162-6170.
220. Hampel S. M.; Sidibe A.; Gunaratnam M.; Riou J. F.; Neidle S. Tetrasubstituted naphthalene diimide ligands with selectivity for telomeric G-quadruplexes and cancer cells. *Bioorg. Med. Chem. Lett*. **2010**; *20* (22): 6459-6463.
221. Czerwinska I.; Sato S.; Juskowiak B.; Takenaka S. Interactions of cyclic and non-cyclic naphthalene diimide derivatives with different nucleic acids. *Bioorg. Med. Chem.* **2014**; *22* (9): 2593-2601.
222. Ohnmacht S. A.; Neidle S. Small-molecule quadruplex-targeted drug discovery. *Bioorg. Med. Chem. Lett*. **2014**; *24* (12): 2602-2612.
223. Gunaratnam M.; de la Fuente M.; Hampel S. M.; Todd A. K.; Reszka A. P.; Schatzlein A. *et al*. Targeting pancreatic cancer with a G-quadruplex ligand. *Bioorg. Med. Chem*. **2011**; *19* (23): 7151-7157.
224. Czerwinska I.; Sato S.; Takenaka S. Improving the affinity of naphthalene diimide ligand to telomeric DNA by incorporating Zn^{2+} ions into its dipicolylamine groups. *Bioorg. Med. Chem*. **2012**; *20* (21): 6416-6422.
225. Sato S.; Takenaka S. Ferrocenyl naphthalene diimides as tetraplex DNA binders. *J. Inorg. Biochem.* **2017**; *167*: 21-26.
226. Doria F.; Nadai M.; Sattin G.; Pasotti L.; Richter S. N.; Freccero M. Water soluble extended naphthalene diimides as pH fluorescent sensors and G-quadruplex ligands. *Org. Biomol. Chem.* **2012**; *10* (19): 3830-3840.
227. Nadai M.; Doria F.; Di Antonio M.; Sattin G.; Germani L.; Percivalle C. *et al*. Naphthalene diimide scaffolds with dual reversible and covalent interaction properties towards G-quadruplex. *Biochimie*. **2011**; *93* (8): 1328-1340.
228. Arévalo-Ruiz M.; Doria F.; Belmonte-Reche E.; De Rache A.; Campos-Salinas J.; Lucas R. *et al*. Synthesis, Binding Properties, and Differences in Cell Uptake of G-Quadruplex Ligands Based on Carbohydrate Naphthalene Diimide Conjugates. *Chem. - Eur. J*. **2017**; *23* (9): 2157-2164.
229. Lombardo C. M.; Martínez I. S.; Haider S.; Gabelica V.; De Pauw E.; Moses J. E. *et al*. Structure-based design of selective high-affinity telomeric quadruplex-binding ligands. *Chem. Commun*. **2010**; *46* (48): 9116-9118.
230. Largy E.; Hamon F.; Rosu F.; Gabelica V.; De Pauw E.; Guedin A. *et al*. Tridentate *N*-Donor Palladium(II) Complexes as Efficient Coordinating Quadruplex DNA Binders. *Chem-Eur J*. **2011**; *17* (47): 13274-13283.

231. Bertrand H.; Bombard S.; Monchaud D.; Talbot E.; Guedin A.; Mergny J. L. *et al*. Exclusive platination of loop adenines in the human telomeric G-quadruplex. *Org. Biomol. Chem.* **2009**; *7* (14): 2864-2871.
232. Pennarun G.; Granotier C.; Gauthier L. R.; Gomez D.; Hoffschir F.; Mandine E. *et al*. Apoptosis related to telomere instability and cell cycle alterations in human glioma cells treated by new highly selective G-quadruplex ligands. *Oncogene*. **2005**; *24* (18): 2917-2928.
233. Monchaud D.; Yang P.; Lacroix L.; Teulade-Fichou M. P.; Mergny J. L. A metal-mediated conformational switch controls G-quadruplex binding affinity. *Angew. Chem., Int. Ed*. **2008**; *47* (26): 4858-4861.
234. Muller S.; Sanders D. A.; Di Antonio M.; Matsis S.; Riou J. F.; Rodriguez R. *et al*. Pyridostatin analogues promote telomere dysfunction and long-term growth inhibition in human cancer cells. *Org. Biomol. Chem*. **2012**; *10* (32): 6537-6546.
235. Rodriguez R.; Muller S.; Yeoman J. A.; Trentesaux C.; Riou J. F.; Balasubramanian S. A Novel Small Molecule That Alters Shelterin Integrity and Triggers a DNA-Damage Response at Telomeres. *J. Am. Chem. Soc*. **2008**; *130* (47): 15758-15759.
236. Riou J. F.; Guittat L.; Mailliet P.; Laoui A.; Renou E.; Petitgenet O. *et al.* Cell senescence and telomere shortening induced by a new series of specific G-quadruplex DNA ligands. *Proc. Natl. Acad. Sci. U. S. A.* **2002**; *99* (5): 2672-2677.
237. Gomez D.; Lemarteleur T.; Lacroix L.; Mailliet P.; Mergny J. L.; Riou J. F. Telomerase downregulation induced by the G-quadruplex ligand 12459 in A549 cells is mediated by hTERT RNA alternative splicing. *Nucleic Acids Res*. **2004**; *32* (1): 371-379.
238. De Cian A.; DeLemos E.; Mergny J. L.; Teulade-Fichou M. P.; Monchaud D. Highly efficient G-quadruplex recognition by bisquinolinium compounds. *J. Am. Chem. Soc*. **2007**; *129* (7): 1856-1857.
239. Liu Z. Q.; Zhuo S. T.; Tan J. H.; Ou T. M.; Li D.; Gu L. Q. *et al*. Facile syntheses of disubstituted bis(vinylquinolinium)benzene derivatives as G-quadruplex DNA binders. *Tetrahedron*. **2013**; *69* (24): 4922-4932.
240. Dhamodharan V.; Harikrishna S.; Jagadeeswaran C.; Halder K.; Pradeepkumar P. I. Selective G-quadruplex DNA Stabilizing Agents Based on Bisquinolinium and Bispyridinium Derivatives of 1,8-Naphthyridine. *J. Org. Chem*. **2012**; *77* (1): 229-242.
241. Muller S.; Kumari S.; Rodriguez R.; Balasubramanian S. Small-molecule-mediated G-quadruplex isolation from human cells. *Nat. Chem*. **2010**; *2* (12): 1095-1098.
242. Di Antonio M.; Biffi G.; Mariani A.; Raiber E. A.; Rodriguez R.; Balasubramanian S. Selective RNA Versus DNA G-Quadruplex Targeting by *In Situ* Click Chemistry. *Angew. Chem., Int. Ed*. **2012**; *51* (44): 11073-11078.
243. Betzer J.-F.; Nuter F.; Chtchigrovsky M.; Hamon F.; Kellermann G.; Ali S. *et al*. Linking of Antitumor *trans* NHC-Pt(II) Complexes to G-Quadruplex DNA Ligand for Telomeric Targeting. *Bioconjugate Chem*. **2016**; *27* (6): 1456-1470.
244. Rahman K. M.; Tizkova K.; Reszka A. P.; Neidle S.; Thurston D. E. Identification of novel telomeric G-quadruplex-targeting chemical scaffolds through screening of three NCI libraries. *Bioorg. Med. Chem. Lett*. **2012**; *22* (8): 3006-3010.
245. Jain A. K.; Paul A.; Maji B.; Muniyappa K.; Bhattacharya S. Dimeric 1,3-Phenylene-bis(piperazinyl benzimidazole)s: Synthesis and Structure-Activity Investigations on their Binding with Human Telomeric G-Quadruplex DNA and Telomerase Inhibition Properties. *J. Med. Chem*. **2012**; *55* (7): 2981-2993.
246. Peng D.; Tan J. H.; Chen S. B.; Ou T. M.; Gu L. Q.; Huang Z. S. Bisaryldiketene derivatives: A new class of selective ligands for *c-myc* G-quadruplex DNA. *Bioorg. Med. Chem*. **2010**; *18* (23): 8235-8242.
247. Shirude P. S.; Gillies E. R.; Ladame S.; Godde F.; Shin-Ya K.; Huc I. *et al*. Macrocyclic and helical oligoamides as a new class of G-quadruplex ligands. *J. Am. Chem. Soc.* **2007**; *129* (39): 11890-11891.

248. Moorhouse A. D.; Santos A. M.; Gunaratnam M.; Moore M.; Neidle S.; Moses J. E. Stabilization of G-quadruplex DNA by highly selective ligands *via* click chemistry. *J. Am. Chem. Soc*. **2006**; *128* (50): 15972-15973.
249. Moorhouse A. D.; Haider S.; Gunaratnam M.; Munnur D.; Neidle S.; Moses J. E. Targeting telomerase and telomeres: a click chemistry approach towards highly selective G-quadruplex ligands. *Mol. Biosyst*. **2008**; *4* (6): 629-642.
250. Lombardo C. M.; Welsh S. J.; Strauss S. J.; Dale A. G.; Todd A. K.; Nanjunda R. *et al*. A novel series of G-quadruplex ligands with selectivity for HIF-expressing osteosarcoma and renal cancer cell lines. *Bioorg. Med. Chem. Lett*. **2012**; *22* (18): 5984-5988.
251. Ohnmacht S. A.; Ciancimino C.; Vignaroli G.; Gunaratnam M.; Neidle S. Optimization of anti-proliferative activity using a screening approach with a series of bis-heterocyclic G-quadruplex ligands. *Bioorg. Med. Chem. Lett.* **2013**; *23* (19): 5351-5355.
252. Moses J. E.; Ritson D. J.; Zhang F. Z.; Lombardo C. M.; Haider S.; Oldham N. *et al*. A click chemistry approach to C_3 symmetric, G-quadruplex stabilising ligands. *Org. Biomol. Chem*. **2010**; *8* (13): 2926-2930.
253. Dash J.; Shirude P. S.; Balasubramanian S. G-quadruplex recognition by bis-indole carboxamides. *Chem. Commun*. **2008**; *26*:3055-3057.
254. Dash J.; Das R. N.; Hegde N.; Pantos G. D.; Shirude P. S.; Balasubramanian S. Synthesis of Bis-indole Carboxamides as G-Quadruplex Stabilizing and Inducing Ligands. *Chem-Eur J.* **2012**; *18* (2): 554-564.
255. Chen Z.; Zheng K. W.; Hao Y. H.; Tan Z. Reduced or Diminished Stabilization of the Telomere G-Quadruplex and Inhibition of Telomerase by Small Chemical Ligands under Molecular Crowding Condition. *J. Am. Chem. Soc*. **2009**; *131* (30): 10430-10438.
256. Ranjan N.; Arya D. Targeting *C-myc* G-Quadruplex: Dual Recognition by Aminosugar-Bisbenzimidazoles with Varying Linker Lengths. *Molecules*. **2013**; *18* (11): 14228-14240.
257. Dhamodharan V.; Harikrishna S.; Bhasikuttan A. C.; Pradeepkumar P. I. Topology Specific Stabilization of Promoter over Telomeric G-Quadruplex DNAs by Bisbenzimidazole Carboxamide Derivatives. *ACS Chem. Biol*. **2015**; *10* (3): 821-833.
258. Li G. R.; Huang J.; Zhang M.; Zhou Y. Y.; Zhang D.; Wu Z. G. *et al*. Bis(benzimidazole)pyridine derivative as a new class of G-quadruplex inducing and stabilizing ligand. *Chem. Commun*. **2008**; *38*: 4564-4566.
259. Bhattacharya S.; Chaudhuri P.; Jain A. K.; Paul A. Symmetrical Bisbenzimidazoles with Benzenediyl Spacer: The Role of the Shape of the Ligand on the Stabilization and Structural Alterations in Telomeric G-Quadruplex DNA and Telomerase Inhibition. *Bioconjugate Chem*. **2010**; *21* (7): 1148-1159.
260. Paul A.; Maji B.; Misra S. K.; Jain A. K.; Muniyappa K.; Bhattacharya S. Stabilization and Structural Alteration of the G-Quadruplex DNA Made from the Human Telomeric Repeat Mediated by Troger's Base Based Novel Benzimidazole Derivatives. *J. Med. Chem*. **2012**; *55* (17): 7460-7471.
261. Hamon F.; Largy E.; Guedin-Beaurepaire A.; Rouchon-Dagois M.; Sidibe A.; Monchaud D. *et al*. An Acyclic Oligoheteroaryle That Discriminates Strongly between Diverse G-Quadruplex Topologies. *Angew. Chem., Int. Ed*. **2011**; *50* (37): 8745-8749.
262. Ritson D. J.; Moses J. E. A fragment based click chemistry approach towards hybrid G-quadruplex ligands: design, synthesis and biophysical evaluation. *Tetrahedron*. **2012**; *68* (1): 197-203.
263. Drewe W. C.; Nanjunda R.; Gunaratnam M.; Beltran M.; Parkinson G. N.; Reszka A. P. *et al*. Rational Design of Substituted Diarylureas: A Scaffold for Binding to G-Quadruplex Motifs. *J. Med. Chem*. **2008**; *51* (24): 7751-7767.
264. Drewe W. C.; Neidle S. Click chemistry assembly of G-quadruplex ligands incorporating a diarylurea scaffold and triazole linkers. *Chem. Commun*. **2008**; 42:5295-5297.

265. Benz A.; Singh V.; Mayer T. U.; Hartig J. S. Identification of Novel Quadruplex Ligands from Small Molecule Libraries by FRET-Based High-Throughput Screening. *ChemBioChem*. **2011**; *12* (9): 1422-1426.
266. Dash J.; Shirude P. S.; Hsu S. T. D.; Balasubramanian S. Diarylethynyl Amides That Recognize the Parallel Conformation of Genomic Promoter DNA G-Quadruplexes. *J. Am. Chem. Soc*. **2008**; *130* (47): 15950-15956.
267. Dash J.; Waller Z. A. E.; Pantos G. D.; Balasubramanian S. Synthesis and Binding Studies of Novel Diethynyl-Pyridine Amides with Genomic Promoter DNA G-Quadruplexes. *Chem-Eur J*. **2011**; *17* (16): 4571-4581.
268. Waller Z. A. E.; Shirude P. S.; Rodriguez R.; Balasubramanian S. Triarylpyridines: a versatile small molecule scaffold for G-quadruplex recognition. *Chem. Commun*. **2008**; 12:1467-1469.
269. Wang J. T.; Li Y.; Tan J. H.; Ji L. N.; Mao Z. W. Platinum(II)-triarylpyridines complexes with electropositive pendants as efficient G-quadruplex binders. *Dalton Trans*. **2011**; *40* (3): 564-566.
270. Wei C. Y.; Ren L. J.; Gao N. Interactions of terpyridines and their Pt(II) complexes with G-quadruplex DNAs and telomerase inhibition. *Int. J. Biol. Macromol*. **2013**; *57*: 1-8.
271. Chu W. H.; Wang Y. C.; Liu S. Y.; Yang X. Y.; Wang S. X.; Li S. H. *et al*. Synthesis, cytotoxicity and DNA-binding properties of Pd(II), Cu(II) and Zn(II) complexes with 4 '-(4-(2-(piperidin-1-yl)ethoxy)phenyl)-2,2 ':6 ',2 ''-terpyridine. *Bioorg. Med. Chem. Lett*. **2013**; *23* (18): 5187-5191.
272. Bertrand H.; Monchaud D.; De Cian A.; Guillot R.; Mergny J.-L.; Teulade-Fichou M-P. The importance of metal geometry in the recognition of G-quadruplex-DNA by metal-terpyridine complexes. *Org. Biomol. Chem*. **2007**; *5* (16): 2555-2559.
273. Stafford V. S.; Suntharalingam K.; Shivalingam A.; White A. J. P.; Mann D. J.; Vilar R. Syntheses of polypyridyl metal complexes and studies of their interaction with quadruplex DNA. *Dalton Trans*. **2015**; *44* (8): 3686-3700.
274. Wei C.; Gao N. Cytotoxicities, telomerase and topoisomerases I inhibitory activities and interactions of terpyridine derivatives with DNAs. *Chem. Res. Chin. Univ*. **2015**; *31* (6): 970-975.
275. Suntharalingam K.; White A. J. P.; Vilar R. Two Metals Are Better than One: Investigations on the Interactions between Dinuclear Metal Complexes and Quadruplex DNA. *Inorg. Chem*. **2010**; *49* (18): 8371-8380.
276. Smith N. M.; Labrunie G.; Corry B.; Phong L. T. T.; Norret M.; Djavaheri-Mergny M. *et al*. Unraveling the relationship between structure and stabilization of triarylpyridines as G-quadruplex binding ligands. *Org. Biomol. Chem*. **2011**; *9* (17): 6154-6162.
277. Kerkour A.; Mergny J.-L.; Salgado G. F. NMR based model of human telomeric repeat G-quadruplex in complex with 2,4,6-triarylpyridine family ligand. *Biochim Biophys Acta*. **2017**; *1861* (5 Pt B): 1293-1302.
278. Moore M. J. B.; Cuenca F.; Searcey M.; Neidle S. Synthesis of distamycin A polyamides targeting G-quadruplex DNA. *Org. Biomol. Chem*. **2006**; *4* (18): 3479-3488.
279. Rahman K. M.; Reszka A. P.; Gunaratnam M.; Haider S. M.; Howard P. W.; Fox K. R. *et al.* Biaryl polyamides as a new class of DNA quadruplex-binding ligands. *Chem. Commun*. **2009**; *27*: 4097-4099.
280. Tan J. H.; Ou T. M.; Hou J. Q.; Lu Y. J.; Huang S. L.; Luo H. B. *et al*. Isaindigotone Derivatives: A New Class of Highly Selective Ligands for Telomeric G-Quadruplex DNA. *J. Med. Chem*. **2009**; *52* (9): 2825-2835.
281. Hou J. Q.; Tan J. H.; Wang X. X.; Chen S. B.; Huang S. Y.; Yan J. W. *et al*. Impact of planarity of unfused aromatic molecules on G-quadruplex binding: Learning from isaindigotone derivatives. *Org. Biomol. Chem*. **2011**; *9* (18): 6422-6436.
282. Yan J. W.; Ye W. J.; Chen S. B.; Wu W. B.; Hou J. Q.; Ou T. M. *et al*. Development of a Universal Colorimetric Indicator for G-Quadruplex Structures by the Fusion of Thiazole Orange and Isaindigotone Skeleton. *Anal. Chem*. **2012**; *84* (15): 6288-6292.

283. Li Z.; Tan J. H.; He J. H.; Long Y.; Ou T. M.; Li D. *et al*. Disubstituted quinazoline derivatives as a new type of highly selective ligands for telomeric G-quadruplex DNA. *Eur. J. Med. Chem*. **2012**; *47*: 299-311.
284. He J. H.; Liu H. Y.; Li Z.; Tan J. H.; Ou T. M.; Huang S. L. *et al*. New quinazoline derivatives for telomeric G-quadruplex DNA: Effects of an added phenyl group on quadruplex binding ability. *Eur J Med Chem*. **2013**; *63*: 1-13.
285. Wang X. X.; Zhou C. X.; Yan J. W.; Hou J. Q.; Chen S. B.; Ou T. M. *et al*. Synthesis and Evaluation of Quinazolone Derivatives as a New Class of *c-KIT* G-Quadruplex Binding Ligands. *ACS Med. Chem. Lett*. **2013**; *4* (10): 909-914.
286. Murat P.; Singh Y.; Defrancq E. Methods for investigating G-quadruplex DNA/ligand interactions. *Chem. Soc. Rev*. **2011**; *40* (11): 5293-5307.
287. Jaumot J.; Gargallo R. Experimental Methods for Studying the Interactions between G-Quadruplex Structures and Ligands. *Curr. Pharm. Des*. **2012**; *18* (14): 1900-1916.
288. Watkins D.; Ranjan N.; Kumar S.; Gong C.; Arya D. P. An assay for human telomeric G-quadruplex DNA binding drugs. *Bioorg. Med. Chem. Lett*. **2013**; *23* (24): 6695-6699.
289. Huppert J. L. Four-stranded nucleic acids: structure, function and targeting of G-quadruplexes. *Chem. Soc. Rev*. **2008**; *37* (7): 1375-1384.
290. Collie G.; Reszka A. P.; Haider S. M.; Gabelica V.; Parkinson G. N.; Neidle S. Selectivity in small molecule binding to human telomeric RNA and DNA quadruplexes. *Chem. Commun*. **2009**; *48*: 7482-7484.
291. Zamecnik P. C.; Stephenson M. L. Inhibition of Rous sarcoma virus replication and cell transformation by a specific oligodeoxynucleotide. *Proc. Natl. Acad. Sci. U. S. A*. **1978**; *75* (1): 280-284.
292. Bell N. M.; Micklefield J. Chemical modification of oligonucleotides for therapeutic, bioanalytical and other applications. *ChemBioChem*. **2009**; *10* (17): 2691-2703.
293. Sharma V. K.; Rungta P.; Prasad A. K. Nucleic acid therapeutics: basic concepts and recent developments. *RSC Adv*. **2014**; *4* (32): 16618-16631.
294. Yamada T.; Okaniwa N.; Saneyoshi H.; Ohkubo A.; Seio K.; Nagata T. *et al*. Synthesis of 2'-O-[2-(*N*-methylcarbamoyl)ethyl]ribonucleosides using oxa-Michael reaction and chemical and biological properties of oligonucleotide derivatives incorporating these modified ribonucleosides. *J. Org. Chem*. **2011**; *76* (9): 3042-3053.
295. Buhr C. A.; Wagner R. W.; Grant D.; Froehler B. C. Oligodeoxynucleotides Containing C-7 Propyne Analogs of 7-Deaza-2'-Deoxyguanosine and 7-Deaza-2'-Deoxyadenosine. *Nucleic Acids Res*. **1996**; *24* (15): 2974-2980.
296. Flanagan W. M.; Kothavale A.; Wagner R. W. Effects of Oligonucleotide Length, Mismatches and mRNA Levels on C-5 Propyne-Modified Antisense Potency. *Nucleic Acids Res*. **1996**; *24* (15): 2936-2941.
297. Nielsen P. E.; Egholm M. An introduction to peptide nucleic acid. *Curr. Issues Mol. Biol*. **1999**; *1* (1-2): 89-104.
298. Egholm M.; Buchardt O.; Nielsen P. E.; Berg R. H. Peptide nucleic acids (PNA). Oligonucleotide analogs with an achiral peptide backbone. *J. Am. Chem. Soc*. **1992**; *114* (5): 1895-1897.
299. Nielsen P. E.; Egholm M.; Berg R. H.; Buchardt O. Sequence-selective recognition of DNA by strand displacement with a thymine-substituted polyamide. *Science*. **1991**; *254* (5037): 1497-1500.
300. Uhlmann E.; Peyman A.; Breipohl G.; Will D. W. PNA: Synthetic Polyamide Nucleic Acids with Unusual Binding Properties. *Angew. Chem., Int. Ed*. **1998**; *37* (20): 2796-2823.
301. Demidov V. V.; Potaman V. N.; Frank-Kamenetskil M. D.; Egholm M.; Buchard O.; Sönnichsen S. H. *et al*. Stability of peptide nucleic acids in human serum and cellular extracts. *Biochem. Pharmacol*. **1994**; *48* (6): 1310-1313.
302. Lundin K. E.; Good L.; Strömberg R.; Gräslund A.; Smith C. I. E. Biological Activity and Biotechnological Aspects of Peptide Nucleic Acid. *Adv. Genet*. **2006**; *56*: 1-51.

303. McMahon B. M.; Mays D.; Lipsky J.; Stewart J. A.; Fauq A.; Richelson E. Pharmacokinetics and Tissue Distribution of a Peptide Nucleic Acid After Intravenous Administration. *Antisense Nucleic Acid Drug Dev*. **2002**; *12* (2): 65-70.
304. Nielsen P. E.; Haaima G.; Lohse A.; Buchardt O. Peptide Nucleic Acids (PNAs) Containing Thymine Monomers Derived from Chiral Amino Acids: Hybridization and Solubility Properties of D-Lysine PNA. *Angew. Chem., Int. Ed. Engl*. **1996**; *35* (17): 1939-1942.
305. Joergensen M.; Agerholm-Larsen B.; Nielsen P. E.; Gehl J. Efficiency of Cellular Delivery of Antisense Peptide Nucleic Acid by Electroporation Depends on Charge and Electroporation Geometry. *Oligonucleotides*. **2011**; *21* (1): 29-37.
306. Karras J. G.; Maier M. A.; Lu T.; Watt A.; Manoharan M. Peptide Nucleic Acids Are Potent Modulators of Endogenous Pre-mRNA Splicing of the Murine Interleukin-5 Receptor-α Chain. *Biochemistry*. **2001**; *40* (26): 7853-7859.
307. Shammas M. A.; Simmons C. G.; Corey D. R.; Shmookler Reis R. J. Telomerase inhibition by peptide nucleic acids reverses 'immortality' of transformed human cells. *Oncogene*. **1999**; *18* (46): 6191-6200.
308. Fabani M. M.; Gait M. J. miR-122 targeting with LNA/2'-*O*-methyl oligonucleotide mixmers, peptide nucleic acids (PNA), and PNA-peptide conjugates. *RNA*. **2008**; *14* (2): 336-346.
309. Wang G.; Xu X.; Pace B.; Dean D. A.; Glazer P. M.; Chan P. *et al*. Peptide nucleic acid (PNA) binding-mediated induction of human γ-globin gene expression. *Nucleic Acids Res*. **1999**; *27* (13): 2806-2813.
310. Faruqi A. F.; Egholm M.; Glazer P. M. Peptide nucleic acid-targeted mutagenesis of a chromosomal gene in mouse cells. *Proc. Natl. Acad. Sci. U. S. A*. **1998**; *95* (4): 1398-1403.
311. Boffa L. C.; Morris P. L.; Carpaneto E. M.; Louissaint M.; Allfrey VG. Invasion of the CAG Triplet Repeats by a Complementary Peptide Nucleic Acid Inhibits Transcription of the Androgen Receptor and TATA-binding Protein Genes and Correlates with Refolding of an Active Nucleosome Containing a Unique AR Gene Sequence. *J. Biol. Chem*. **1996**; *271* (22): 13228-13233.
312. Norton J. C.; Piatyszek M. A.; Wright W. E.; Shay J. W.; Corey D. R. Inhibition of human telomerase activity by peptide nucleic acids. *Nat. Biotechnol.* **1996**; *14* (5): 615-619.
313. Sazani P.; Kang S.-H.; Maier M. A.; Wei C.; Dillman J.; Summerton J. *et al*. Nuclear antisense effects of neutral, anionic and cationic oligonucleotide analogs. *Nucleic Acids Res*. **2001**; *29* (19): 3965-3974.
314. Nielsen P. The many faces of PNA. *Int. J. Pept. Res. Ther*. **2003**; *10* (3-4): 135-147.
315. Borgatti M.; Breda L.; Cortesi R.; Nastruzzi C.; Romanelli A.; Saviano M. *et al*. Cationic liposomes as delivery systems for double-stranded PNA-DNA chimeras exhibiting decoy activity against NF-κB transcription factors. *Biochem. Pharmacol*. **2002**; *64* (4): 609-616.
316. Shiraishi T. Down-regulation of MDM2 and activation of p53 in human cancer cells by antisense 9-aminoacridine-PNA (peptide nucleic acid) conjugates. *Nucleic Acids Res*. **2004**; *32* (16): 4893-4902.
317. Kim H.; Lee K. H.; Kim K. B.; Park Y. S.; Kim K.-S.; Kim D.-E. Antiviral Efficacy of a Short PNA Targeting microRNA-122 Using Galactosylated Cationic Liposome as a Carrier for the Delivery of the PNA-DNA Hybrid to Hepatocytes. *Bull. Korean Chem. Soc*. **2013**; *34* (3): 735-742.
318. Mologni L.; Marchesi E.; Nielsen P. E.; Gambacorti-Passerini C. Inhibition of promyelocytic leukemia (PML)/retinoic acid receptor-α and PML expression in acute promyelocytic leukemia cells by anti-PML peptide nucleic acid. *Cancer Res*. **2001**; *61* (14): 5468-5473.
319. Antopolsky M.; Cordier C.; Boutimah F.; Bourdeloux M.; Dupuy F.; Met E. *et al*. Delivery of Antisense Peptide Nucleic Acids to Cells by Conjugation with Small Arginine-Rich Cell-Penetrating Peptide (R/W)9. *Plos One*. **2014**; *9* (8): e104999.
320. Oh S. Y.; Ju Y.; Park H. A Highly Effective and Long-Lasting Inhibition of miRNAs with PNA-Based Antisense Oligonucleotides. *Mol. Cells*. **2009**; *28* (4): 341-345.

321. Villa R.; Folini M.; Lualdi S.; Veronese S.; Daidone M. G.; Zaffaroni N. Inhibition of telomerase activity by a cell-penetrating peptide nucleic acid construct in human melanoma cells. *FEBS Lett*. **2000**; *473* (2): 241-248.
322. Lee S. H.; Moroz E.; Castagner B.; Leroux J.-C. Activatable Cell Penetrating Peptide–Peptide Nucleic Acid Conjugate via Reduction of Azobenzene PEG Chains. *J. Am. Chem. Soc.* **2014**; *136* (37): 12868-12871.
323. Boffa L. C.; Scarfi' S.; Mariani M. R.; Damonte G.; Allfrey V. G.; Benatti U. *et al*. Dihydrotestosterone as a Selective Cellular/Nuclear Localization Vector for Anti-Gene Peptide Nucleic Acid in Prostatic Carcinoma Cells. *Cancer Res*. **2000**; *60* (8): 2258-2262.
324. Cutrona G.; Carpaneto E. M.; Ulivi M.; Roncella S.; Landt O.; Ferrarini M. *et al*. Effects in live cells of a *c-myc* anti-gene PNA linked to a nuclear localization signal. *Nat. Biotechnol*. **2000**; *18* (3): 300-303.
325. Shiraishi T.; Nielsen P. E. Peptide nucleic acid (PNA) cell penetrating peptide (CPP) conjugates as carriers for cellular delivery of antisense oligomers. *Artif. DNA PNA XNA*. **2011**; *2* (3): 90-99.
326. Pardridge W. M.; Boado R. J.; Kang Y. S. Vector-mediated delivery of a polyamide ("peptide") nucleic acid analogue through the blood-brain barrier *in vivo*. *Proc. Natl. Acad. Sci. U. S. A*. **1995**; *92* (12): 5592-5596.
327. Basu S.; Wickstrom E. Synthesis and Characterization of a Peptide Nucleic Acid Conjugated to a D-Peptide Analog of Insulin-like Growth Factor 1 for Increased Cellular Uptake. *Bioconjugate Chem*. **1997**; *8* (4): 481-488.
328. Ishihara T.; Kano A.; Obara K.; Saito M.; Chen X.; Park T. G. *et al*. Nuclear localization and antisense effect of PNA internalized by ASGP-R-mediated endocytosis with protein/DNA conjugates. *J. Controlled Release*. **2011**; *155* (1): 34-39.
329. Svahn M. G.; Salih G.; Simonson E. O.; Smith C. I. E.; Brandén L. J. Protease-induced release of functional peptides from bioplexes. *J. Controlled Release*. **2004**; *98* (1): 169-177.
330. Bøe S. L.; Hovig E. Enhancing nucleic acid delivery by photochemical internalization. *Ther. Delivery*. **2013**; *4* (9): 1125-1140.
331. Meerovich I.; Muthukrishnan N.; Johnson G. A.; Erazo-Oliveras A.; Pellois J-P. Photodamage of lipid bilayers by irradiation of a fluorescently labeled cell-penetrating peptide. *Biochim Biophys Acta*. **2014**; *1840* (1): 507-515.
332. Egholm M.; Buchardt O.; Christensen L.; Behrens C.; Freier S. M.; Driver D. A. *et al*. PNA hybridizes to complementary oligonucleotides obeying the Watson–Crick hydrogen-bonding rules. *Nature*. **1993**; *365* (6446): 566-568.
333. Wittung P.; Nielsen P. E.; Buchardt O.; Egholm M.; Norden B. DNA-like double helix formed by peptide nucleic acid. *Nature*. **1994**; *368* (6471): 561-563.
334. Shah V. J.; Cerpa R.; Kuntz J. I. D.; Kenyon GL. Solid-Phase Synthesis of Peptide-Derived Enantiospecific Nucleic Acid Analogs. *Bioorg. Chem*. **1996**; *24* (2): 201-206.
335. Kim J.-H.; Kim K.-H.; Møllegaard N. E.; Nielsen P. E.; Koo H.-S. Helical periodicity of $(PNA)_2$ (DNA) triplexes in strand displacement complexes. *Nucleic Acids Res*. **1999**; *27* (14): 2842-2847.
336. Larsen H. J.; Nielsen P. E. Transcription-mediated binding of peptide nucleic acid (PNA) to double-stranded DNA: Sequence-specific suicide transcription. *Nucleic Acids Res*. **1996**; *24* (3): 458-463.
337. Bentin T.; Nielsen P. E. Enhanced peptide nucleic acid binding to supercoiled DNA: Possible implications for DNA ''breathing'' dynamics. *Biochemistry*. **1996**; *35* (27): 8863-8869.
338. Kurakin A.; Larsen H. J.; Nielsen P. E. Cooperative strand displacement by peptide nucleic acid (PNA). *Chem. Biol*. **1998**; *5* (2): 81-89.
339. Pellestor F.; Paulasova P. The peptide nucleic acids (PNAs), powerful tools for molecular genetics and cytogenetics. *Eur. J. Hum. Genet*. **2004**; *12* (9): 694-700.

340. Izvolsky K. I.; Demidov V. V.; Nielsen P. E.; Frank-Kamenetskii M. D. Sequence-Specific Protection of Duplex DNA against Restriction and Methylation Enzymes by Pseudocomplementary PNAs. *Biochemistry*. **2000**; *39* (35): 10908-10913.
341. Dueholm K. L.; Petersen K. H.; Jensen D. K.; Egholm M.; Nielsen P. E.; Buchardt O. Peptide nucleic acid (PNA) with a chiral backbone based on alanine. *Bioorg. Med. Chem. Lett*. **1994**; *4* (8): 1077-1080.
342. Sforza S.; Haaima G.; Marchelli R.; Nielsen P. E. Chiral Peptide Nucleic Acids (PNAs): Helix Handedness and DNA Recognition. *Eur. J. Org. Chem*. **1999**; *1999* (1): 197-204.
343. Calabretta A.; Tedeschi T.; Corradini R.; Marchelli R.; Sforza S. DNA and RNA binding properties of an arginine-based 'Extended Chiral Box' Peptide Nucleic Acid. *Tetrahedron Lett*. **2011**; *52* (2): 300-304.
344. Hyrup B.; Egholm M.; Rolland M.; Nielsen P. E.; Berg R. H.; Buchardt O. Modification of the binding affinity of peptide nucleic acids (PNA). PNA with extended backbones consisting of 2-aminoethyl-β-alanine or 3-aminopropylglycine units. *J. Chem. Soc., Chem. Commun*. **1993**; *6*: 518-519.
345. Hyrup B.; Egholm M.; Buchardt O.; Nielsen P. E. A flexible and positively charged PNA analogue with an ethylene-linker to the nucleobase: Synthesis and hybridization properties. *Bioorg. Med. Chem. Lett*. **1996**; *6* (10): 1083-1088.
346. Zhou P.; Wang M.; Du L.; Fisher G. W.; Waggoner A.; Ly D. H. Novel Binding and Efficient Cellular Uptake of Guanidine-Based Peptide Nucleic Acids (GPNA). *J. Am. Chem. Soc*. **2003**; *125* (23): 6878-6879.
347. Zengeya T.; Gindin A.; Rozners E. Improvement of sequence selectivity in triple helical recognition of RNA by phenylalanine-derived PNA. *Artif. DNA PNA XNA*. **2013**; *4* (3): 69-76.
348. Govindaraju T.; Madhuri V.; Kumar V. A.; Ganesh K. N. Cyclohexanyl Peptide Nucleic Acids (chPNAs) for Preferential RNA Binding: Effective Tuning of Dihedral Angle β in PNAs for DNA/RNA Discrimination. *J. Org. Chem*. **2006**; *71* (1): 14-21.
349. Tatyana V. A.; Vladimir N. S. Synthesis and properties of carbohydrate–phosphate backbone-modified oligonucleotide analogues and nucleic acid mimetics. *Russ. Chem. Rev*. **2011**; *80* (5): 429.
350. Falkiewicz B. Peptide nucleic acids and their structural modifications. *Acta Biochim. Pol*. **1999**; *46* (3): 509-529.
351. Nollet A. J.; Pandit U. K. Unconventional nucleotide analogues. II. Synthesis of the adenyl analogue of Willardiine. *Tetrahedron*. **1969**; *25* (24): 5983-5987.
352. Doel M. T.; Jones A. S.; Taylor N. An approach to the synthesis of peptide analogues of oligonucleotides (nucleopeptides). *Tetrahedron Lett*. **1969**; *10* (27): 2285-2288.
353. Nollet A. J.; Huting C. M.; Pandit U. K. Unconventional nucleotide analogues. I. N9-purinyl alpha-amino acids. *Tetrahedron*. **1969**; *25* (24): 5971-5981.
354. Nollet A. J.; Pandit U. K. Unconventional nucleotide analogues. 3. 4-(N1-pyrimidyl)-2-aminobutyric acids. *Tetrahedron*. **1969**; *25* (24): 5989-5994.
355. Korshunova G. A.; Ilicheva I. A.; Sumbatyan N. V.; Hyun K. Design and synthesis of new types of oligonucleopeptides. *Int. J. Pept. Res. Ther*. **1997**; *4* (4-6): 473-476.
356. Doel M. T.; Jones A. S.; Walker R. T. Synthesis of Peptides Containing Purine and Pyrimidine-Derivatives of DL-Alanine. *Tetrahedron*. **1974**; *30* (16): 2755-2759.
357. Lewis I. Peptide analogues of DNA incorporating nucleobase-Ala-Pro subunits. *Tetrahedron Lett*. **1993**; *34* (36): 5697-5700.
358. Roviello G.; Benedetti E.; Pedone C.; Bucci E. Nucleobase-containing peptides: an overview of their characteristic features and applications. *Amino Acids*. **2010**; *39* (1): 45-57.
359. Huang P. C.; Hsu G. J.; Zhuang B. R.; Sung K. Novel synthesis of α-PNA monomers by U-4CR. *Amino Acids*. **2008**; *34* (3): 449-453.
360. Geotti-Bianchini P.; Moretto A.; Peggion C.; Beyrath J.; Bianco A.; Formaggio F. Replacement of Ala by Aib improves structuration and biological stability in thymine-based α-nucleopeptides. *Org. Biomol. Chem*. **2010**; *8* (6): 1315-1321.

361. Geotti-Bianchini P.; Beyrath J.; Chaloin O.; Formaggio F.; Bianco A. Design and synthesis of intrinsically cell-penetrating nucleopeptides. *Org. Biomol. Chem*. **2008**; *6* (20): 3661-3663.
362. Diederichsen U.; Weicherding D.; Diezemann N. Side chain homologation of alanyl peptide nucleic acids: pairing selectivity and stacking. *Org. Biomol. Chem*. **2005**; *3* (6): 1058-1066.
363. Roviello G. N.; Gröschel S.; Pedone C.; Diederichsen U. Synthesis of novel MMT/acyl-protected nucleo alanine monomers for the preparation of DNA/alanyl-PNA chimeras. *Amino Acids*. **2010**; *38* (5): 1301-1309.
364. Talukder P.; Dedkova L. M.; Ellington A. D.; Yakovchuk P.; Lim J.; Anslyn E. V. *et al*. Synthesis of alanyl nucleobase amino acids and their incorporation into proteins. *Bioorg. Med. Chem*. **2016**; *24* (18): 4177-4187.
365. Lenzi A.; Reginato G.; Taddai M. Synthesis of *N*-Boc-α-amino acids with nucleobase residues as building blocks for the preparation of chiral PNA (peptidic nucleic acids). *Tetrahedron Lett*. **1995**; *36* (10): 1713-1716.
366. Shah V. J.; Kuntz J. I. D.; Kenyon G. L. Synthesis of Amino-Acid-Derived Nucleo(side/tide) Analogs for Peptide-Derived Enantiospecific Nucleic Acid Analogs. *Bioorg. Chem*. **1996**; *24* (2): 194-200.
367. Howarth N. M.; Wakelin L. P. G. α-PNA: A Novel Peptide Nucleic Acid Analogue of DNA. *J. Org. Chem.* **1997**; *62* (16): 5441-5450.
368. Lenzi A.; Reginato G.; Taddei M.; Trifilieff E. Solid phase synthesis of a self complementary (antiparallel) chiral peptidic nucleic acid strand. *Tetrahedron Lett*. **1995**; *36* (10): 1717-1718.
369. Yamazaki T.; Komatsu K.; Umemiya H.; Hashimoto Y.; Shudo K.; Kagechika H. Dinucleotide-analogous tetrapeptides. Specific triplex formation with complementary polynucleotides. *Tetrahedron Lett*. **1997**; *38* (48): 8363-8366.
370. Brasun J.; Oldziej S.; Taddei M.; Kozlowski H. Impact of Cu(II) and Ni(II) on a structure of chiral peptide nucleic acids having four, six and eight thymines in a peptide side chain. *J. Inorg. Biochem*. **2001**; *85* (2-3): 79-87.
371. Brasuń J.; Ciapetti P.; Kozłowski H.; Ołdziej S.; Taddei M.; Valensin D. *et al*. Chiral peptide nucleic acids having thymine and adenine in their side chain as specific ligands for Ni^{II} and Cu^{II}. *J. Chem. Soc., Dalton Trans*. **2000**; *15*: 2639-2644.
372. Matsumura S.; Ueno A.; Mihara H. Peptides with nucleobase moieties as a stabilizing factor for a two-stranded alpha-helix. *Chem. Commun*. **2000**; *17*:1615-1616.
373. Matsumura S.; Takahashi T.; Ueno A.; Mihara H. Complementary nucleobase interaction enhances peptide - Peptide recognition and self-replicating catalysis. *Chem-Eur J*. **2003**; *9* (19): 4829-4837.
374. Diederichsen U.; Schmitt H. W. Self-pairing PNA with alternating alanyl/homoalanyl backbone. *Tetrahedron Lett*. **1996**; *37* (4): 475-478.
375. Garner P.; Yoo J. U. Peptide-based nucleic acid surrogates incorporating ser[CH_2B]-gly subunits. *Tetrahedron Lett*. **1993**; *34* (8): 1275-1278.
376. Garner P.; Dey S.; Huang Y.; Zhang X. Modular Nucleic Acid Surrogates. Solid Phase Synthesis of α-Helical Peptide Nucleic Acids (αPNAs). *Org. Lett*. **1999**; *1* (3): 403-406.
377. Huang Y.; Dey S.; Zhang X.; Sönnichsen F.; Garner P. The α-Helical Peptide Nucleic Acid Concept: Merger of Peptide Secondary Structure and Codified Nucleic Acid Recognition. *J. Am. Chem. Soc*. **2004**; *126* (14): 4626-4640.
378. Garner P.; Dey S.; Huang Y. α-Helical Peptide Nucleic Acids (αPNAs): A New Paradigm for DNA-Binding Molecules. *J. Am. Chem. Soc*. **2000**; *122* (10): 2405-2406.
379. Roviello G. N.; Musumeci D.; Bucci E. M.; Pedone C. Evidences for supramolecular organization of nucleopeptides: synthesis, spectroscopic and biological studies of a novel dithymine L-serine tetrapeptide. *Mol. Biosyst*. **2011**; *7* (4): 1073-1080.
380. Roviello G. N.; Musumeci D.; Bucci E. M.; Pedone C. Synthesis and characterization of a novel ester-based nucleoamino acid for the assembly of aromatic nucleopeptides for biomedical applications. *Int. J. Pharm*. **2011**; *415* (1-2): 206-210.

381. Roviello G. N.; Musumeci D.; D'Alessandro C.; Pedone C. Synthesis of a thymine-functionalized nucleoamino acid for the solid phase assembly of cationic nucleopeptides. *Amino Acids*. **2013**; *45* (4): 779-784.
382. Roviello G. N.; Musumeci D.; D'Alessandro C.; Pedone C. Binding ability of a thymine-functionalized oligolysine towards nucleic acids. *Bioorg. Med. Chem*. **2014**; *22* (3): 997-1002.
383. Lowe G.; Vilaivan T.; Westwell M. S. Hybridization Studies with Chiral Peptide Nucleic Acids. *Bioorg. Chem*. **1997**; *25* (5–6): 321-329.
384. Jordan S.; Schwemler C.; Kosch W.; Kretschmer A.; Schwenner E.; Stropp U. *et al*. Synthesis of new building blocks for peptide nucleic acids containing monomers with variations in the backbone. *Bioorg. Med. Chem. Lett*. **1997**; *7* (6): 681-686.
385. Merrifield R. B. Solid Phase Peptide Synthesis. I. The Synthesis of a Tetrapeptide. *J. Am. Chem. Soc.* **1963**; *85* (14): 2149-2154.
386. Thomson S. A.; Josey J. A.; Cadilla R.; Gaul M. D.; Hassman C. F.; Luzzio M. J. *et al*. Fmoc mediated synthesis of Peptide Nucleic Acids. *Tetrahedron*. **1995**; *51* (22): 6179-6194.
387. Lönnberg H. Solid-Phase Synthesis of Oligonucleotide Conjugates Useful for Delivery and Targeting of Potential Nucleic Acid Therapeutics. *Bioconjugate Chem*. **2009**; *20* (6): 1065-1094.
388. Svensen N.; Díaz-Mochón J. J.; Bradley M. Microwave-assisted orthogonal synthesis of PNA–peptide conjugates. *Tetrahedron Lett*. **2008**; *49* (46): 6498-6500.
389. Kofoed T.; Hansen H. F.; Ørum H.; Koch T. PNA synthesis using a novel Boc/acyl protecting group strategy. *J. Pept. Sci*. **2001**; *7* (8): 402-412.
390. Kovacs G.; Timar Z.; Kupihar Z.; Kele Z.; Kovacs L. Synthesis and analysis of peptide nucleic acid oligomers using Fmoc/acyl-protected monomers. *J. Chem. Soc., Perkin Trans. 1*. **2002**; *10*: 1266-1270.
391. Liu Z.-C.; Shin D.-S.; Lee K.-T.; Jun B.-H.; Kim Y.-K.; Lee Y-S. Synthesis of photolabile *o*-nitroveratryloxycarbonyl (NVOC) protected peptide nucleic acid monomers. *Tetrahedron*. **2005**; *61* (33): 7967-7973.
392. Breipohl G.; Will D. W.; Peyman A.; Uhlmann E. Novel synthetic routes to PNA monomers and PNA-DNA linker molecules. *Tetrahedron*. **1997**; *53* (43): 14671-14686.
393. Pothukanuri S.; Pianowski Z.; Winssinger N. Expanding the scope and orthogonality of PNA synthesis. *Eur. J. Org. Chem*. **2008**; *18*:3141-3148.
394. Wojciechowski F.; Hudson R. H. E. A Convenient Route to *N*-[2-(Fmoc)aminoethyl]glycine Esters and PNA Oligomerization Using a Bis-*N*-Boc Nucleobase Protecting Group Strategy. *J. Org. Chem.* **2008**; *73* (10): 3807-3816.
395. Debaene F.; Winssinger N. Azidopeptide Nucleic Acid. An Alternative Strategy for Solid-Phase Peptide Nucleic Acid (PNA) Synthesis. *Org. Lett*. **2003**; *5* (23): 4445-4447.
396. Bialy L.; Díaz-Mochón J. J.; Specker E.; Keinicke L.; Bradley M. Dde-protected PNA monomers, orthogonal to Fmoc, for the synthesis of PNA–peptide conjugates. *Tetrahedron*. **2005**; *61* (34): 8295-8305.
397. Breipohl G.; Knolle J.; Langner D.; O'Malley G.; Uhlmann E. Synthesis of polyamide nucleic acids (PNAs) using a novel Fmoc/Mmt protecting-group combination. *Bioorg. Med. Chem. Lett.* **1996**; *6* (6): 665-670.
398. Aiyar S. E.; Helmann J. D.; deHaseth P. L. A mismatch bubble in double-stranded DNA suffices to direct precise transcription initiation by Escherichia coli RNA polymerase. *J. Biol. Chem*. **1994**; *269* (18): 13179-13184.
399. Møllegaard N. E.; Buchardt O.; Egholm M.; Nielsen P. E. Peptide nucleic acid. DNA strand displacement loops as artificial transcription promoters. *Proc. Natl. Acad. Sci. U. S. A*. **1994**; *91* (9): 3892-3895.
400. Wang G.; Jing K.; Balczon R.; Xu X. Defining the peptide nucleic acids (PNA) length requirement for PNA binding-induced transcription and gene expression. *J. Mol. Biol*. **2001**; *313* (5): 933-940.

401. Hanvey J.; Peffer N.; Bisi J.; Thomson S.; Cadilla R.; Josey J. *et al*. Antisense and antigene properties of peptide nucleic acids. *Science*. **1992**; *258* (5087): 1481-1485.
402. Lohse J.; Dahl O.; Nielsen P. E. Double duplex invasion by peptide nucleic acid: A general principle for sequence-specific targeting of double-stranded DNA. *Proc. Natl. Acad. Sci. U. S. A.* **1999**; *96* (21): 11804-11808.
403. Peffer N. J.; Hanvey J. C.; Bisi J. E.; Thomson S. A.; Hassman C. F.; Noble S. A. *et al*. Strand-invasion of duplex DNA by peptide nucleic acid oligomers. *Proc. Natl. Acad. Sci. U. S. A*. **1993**; *90* (22): 10648-10652.
404. Pesce C. D.; Bolacchi F.; Bongiovanni B.; Cisotta F.; Capozzi M.; Diviacco S. *et al*. Anti-gene peptide nucleic acid targeted to proviral HIV-1 DNA inhibits *in vitro* HIV-1 replication. *Antiviral Res*. **2005**; *66* (1): 13-22.
405. Macadangdang B.; Zhang N.; Lund P. E.; Marple A. H.; Okabe M.; Gottesman M. M. *et al*. Inhibition of multidrug resistance by SV40 pseudovirion delivery of an antigene peptide nucleic acid (PNA) in cultured cells. *Plos One*. **2011**; *6* (3): e17981.
406. Tyler B. M.; Jansen K.; McCormick D. J.; Douglas C. L.; Boules M.; Stewart J. A. *et al*. Peptide nucleic acids targeted to the neurotensin receptor and administered i.p. cross the blood–brain barrier and specifically reduce gene expression. *Proc. Natl. Acad. Sci. U. S. A*. **1999**; *96* (12): 7053-7058.
407. McMahon B. M.; Stewart J. A.; Bitner M. D.; Fauq A.; McCormick D. J.; Richelson E. Peptide nucleic acids specifically cause antigene effects *in vivo* by systemic injection. *Life Sci*. **2002**; *71* (3): 325-337.
408. Hu J.; Corey D. R. Inhibiting Gene Expression with Peptide Nucleic Acid (PNA)−Peptide Conjugates That Target Chromosomal DNA. *Biochemistry*. **2007**; *46* (25):7581-7589.
409. Nielsen P. E. PNA Technology. *Methods Mol. Biol.* **2002**; *208*: 3-26.
410. Gambari R. Peptide nucleic acids: a review on recent patents and technology transfer. *Expert Opin. Ther. Pat*. **2014**; *24* (3): 267-294.
411. Gambari R.; Borgatti M.; Bezzerri V.; Nicolis E.; Lampronti I.; Dechecchi M. C. *et al*. Decoy oligodeoxyribonucleotides and peptide nucleic acids-DNA chimeras targeting nuclear factor kappa-B: Inhibition of IL-8 gene expression in cystic fibrosis cells infected with *Pseudomonas aeruginosa*. *Biochem. Pharmacol*. **2010**; *80* (12): 1887-1894.
412. Panyutin I. G.; Onyshchenko M. I.; Englund E. A.; Appella D. H.; Neumann R. D. Targeting DNA G-Quadruplex Structures with Peptide Nucleic Acids. *Curr. Pharm. Des*. **2012**; *18* (14): 1984-1991.
413. Dias N.; Stein C. A. Antisense oligonucleotides: basic concepts and mechanisms. *Mol. Cancer Ther.* **2002**; *1* (5): 347-355.
414. Knudsen H.; Nielsen P. E. Antisense properties of duplex- and triplex-forming PNAs. *Nucleic Acids Res.* **1996**; *24* (3): 494-500.
415. Malchere C.; Verheijen J.; van der Laan S.; Bastide L.; van Boom J.; Lebleu B. *et al*. A short phosphodiester window is sufficient to direct RNase H-dependent RNA cleavage by antisense peptide nucleic acid. *Antisense Nucleic Acid Drug Dev*. **2000**; *10* (6):463-468.
416. Siwkowski A. M.; Malik L.; Esau C. C.; Maier M. A.; Wancewicz E.V.; Albertshofer K. *et al*. Identification and functional validation of PNAs that inhibit murine CD40 expression by redirection of splicing. *Nucleic Acids Res*. **2004**; *32* (9): 2695-2706.
417. Shiraishi T.; Eysturskarð J.; Nielsen P. E. Modulation of mdm2 pre-mRNA splicing by 9-aminoacridine-PNA (peptide nucleic acid) conjugates targeting intron-exon junctions. *BMC Cancer*. **2010**; *10* (1): 342.
418. Yin H.; Betts C.; Saleh A. F.; Ivanova G. D.; Lee H.; Seow Y. *et al*. Optimization of Peptide Nucleic Acid Antisense Oligonucleotides for Local and Systemic Dystrophin Splice Correction in the *mdx* Mouse. *Mol. Ther*. **2010**; *18* (4): 819-827.
419. Doyle D. F.; Braasch D. A.; Simmons C. G.; Janowski B. A.; Corey D. R. Inhibition of gene expression inside cells by peptide nucleic acids: effect of mRNA target sequence, mismatched bases, and PNA length. *Biochemistry*. **2001**; *40* (1): 53-64.

420. Wang H.; He Y.; Xia Y.; Wang L.; Liang S. Inhibition of gene expression and growth of multidrug-resistant *Acinetobacter baumannii* by antisense peptide nucleic acids. *Mol. Biol. Rep*. **2014**; *41* (11): 7535-7541.
421. Soofi M. A.; Seleem M. N. Targeting Essential Genes in *Salmonella enterica* Serovar Typhimurium with Antisense Peptide Nucleic Acid. *Antimicrob. Agents Chemother*. **2012**; *56* (12): 6407-6409.
422. Montagner G.; Bezzerri V.; Cabrini G.; Fabbri E.; Borgatti M.; Lampronti I. *et al*. An antisense peptide nucleic acid against *Pseudomonas aeruginosa* inhibiting bacterial-induced inflammatory responses in the cystic fibrosis IB3-1 cellular model system. *Int. J. Biol. Macromol.* **2017**; *99*: 492-498.
423. Good L.; Sandberg R.; Larsson O.; Nielsen P. E.; Wahlestedt C. Antisense PNA effects in *Escherichia coli* are limited by the outer-membrane LPS layer. *Microbiology*. **2000**; *146* (Pt 10): 2665-2670.
424. Pandey V. N.; Upadhyay A.; Chaubey B. Prospects for antisense peptide nucleic acid (PNA) therapies for HIV. *Expert Opin. Biol. Ther*. **2009**; *9* (8): 975-989.
425. Chaubey B.; Tripathi S.; Ganguly S.; Harris D.; Casale R. A.; Pandey V. N. A PNA-transportan conjugate targeted to the TAR region of the HIV-1 genome exhibits both antiviral and virucidal properties. *Virology*. **2005**; *331* (2):418-428.
426. Trylska J.; Thoduka S. G.; Dąbrowska Z. Using Sequence-Specific Oligonucleotides To Inhibit Bacterial rRNA. *ACS Chem. Biol*. **2013**; *8* (6): 1101-1109.
427. Kulik M.; Markowska-Zagrajek A.; Wojciechowska M.; Grzela R.; Wituła T.; Trylska J. Helix 69 of *Escherichia coli* 23S ribosomal RNA as a peptide nucleic acid target. *Biochimie*. **2017**; *138*: 32-42.
428. Koppelhus U.; Zachar V.; Nielsen P. E.; Liu X.; Eugen-Olsen J.; Ebbesen P. Efficient *in vitro* inhibition of HIV-1 gag reverse transcription by peptide nucleic acid (PNA) at minimal ratios of PNA/RNA. *Nucleic Acids Res*. **1997**; *25* (11): 2167-2173.
429. Hamilton S. E.; Pitts A. E.; Katipally R. R.; Jia X.; Rutter J. P.; Davies B. A. *et al*. Identification of determinants for inhibitor binding within the RNA active site of human telomerase using PNA scanning. *Biochemistry*. **1997**; *36* (39): 11873-11880.
430. Lee R.; Kaushik N.; Modak M. J.; Vinayak R.; Pandey V. N. Polyamide nucleic acid targeted to the primer binding site of the HIV-1 RNA genome blocks *in vitro* HIV-1 reverse transcription. *Biochemistry*. **1998**; *37* (3): 900-910.
431. Fabbri E.; Manicardi A.; Tedeschi T.; Sforza S.; Bianchi N.; Brognara E. *et al*. Modulation of the biological activity of microRNA-210 with peptide nucleic acids (PNAs). *ChemMedChem*. **2011**; *6* (12): 2192-2202.
432. Torres A. G.; Fabani M. M.; Vigorito E.; Williams D.; Al-Obaidi N.; Wojciechowski F, *et al*. Chemical structure requirements and cellular targeting of microRNA-122 by peptide nucleic acids anti-miRs. *Nucleic Acids Res*. **2012**; *40* (5): 2152-2167.
433. Fabani M. M.; Abreu-Goodger C.; Williams D.; Lyons P. A.; Torres A. G.; Smith K. G. *et al*. Efficient inhibition of miR-155 function *in vivo* by peptide nucleic acids. *Nucleic Acids Res*. **2010**; *38* (13): 4466-4475.
434. Lee H. J.; Xu X.; Kim H.; Jin Y.; Sun P.; Kim J. E. *et al*. Comparison of Direct Sequencing, PNA Clamping-Real Time Polymerase Chain Reaction, and Pyrosequencing Methods for the Detection of *EGFR* Mutations in Non-small Cell Lung Carcinoma and the Correlation with Clinical Responses to EGFR Tyrosine Kinase Inhibitor Treatment. *Korean J. Pathol*. **2013**; *47* (1): 52-60.
435. Kang J. Y.; Park C. K.; Yeo C. D.; Lee H. Y.; Rhee C. K.; Kim S. J. *et al*. Comparison of PNA clamping and direct sequencing for detecting *KRAS* mutations in matched tumour tissue, cell block, pleural effusion and serum from patients with malignant pleural effusion. *Respirology*. **2015**; *20* (1): 138-146.
436. Juskowiak B. Nucleic acid-based fluorescent probes and their analytical potential. *Anal. Bioanal. Chem*. **2010**; *399* (9): 3157-3176.

437. Ortiz E.; Estrada G.; Lizardi P. M. PNA molecular beacons for rapid detection of PCR amplicons. *Mol. Cell. Probes*. **1998**; *12* (4): 219-226.
438. Seitz O. Solid-Phase Synthesis of Doubly Labeled Peptide Nucleic Acids as Probes for the Real-Time Detection of Hybridization. *Angew. Chem., Int. Ed.* **2000**; *39* (18): 3249-3252.
439. Singh R. P.; Oh B.-K.; Choi J.-W. Application of peptide nucleic acid towards development of nanobiosensor arrays. *Bioelectrochemistry*. **2010**; *79* (2): 153-161.
440. Yao D.; Kim J.; Yu F.; Nielsen P. E.; Sinner E.-K.; Knoll W. Surface Density Dependence of PCR Amplicon Hybridization on PNA/DNA Probe Layers. *Biophys. J*. **2005**; *88* (4): 2745-2751.
441. Kuhn H.; Demidov V. V.; Gildea B. D.; Fiandaca M. J.; Coull J. C.; Frank-Kamenetskii M. D. PNA Beacons for Duplex DNA. *Antisense Nucleic Acid Drug Dev*. **2001**; *11* (4): 265-270.
442. Kummer S.; Knoll A.; Socher E.; Bethge L.; Herrmann A.; Seitz O. PNA FIT-Probes for the Dual Color Imaging of Two Viral mRNA Targets in Influenza H1N1 Infected Live Cells. *Bioconjugate Chem*. **2012**; *23* (10): 2051-2060.
443. Kummer S.; Knoll A.; Socher E.; Bethge L.; Herrmann A.; Seitz O. Fluorescence Imaging of Influenza H1N1 mRNA in Living Infected Cells Using Single-Chromophore FIT-PNA. *Angew. Chem., Int. Ed.* **2011**; *50* (8): 1931-1934.
444. Kam Y.; Rubinstein A.; Nissan A.; Halle D.; Yavin E. Detection of endogenous *K-ras* mRNA in living cells at a single base resolution by a PNA molecular beacon. *Mol. Pharm*. **2012**; *9* (3): 685-693.
445. Kam Y.; Rubinstein A.; Naik S.; Djavsarov I.; Halle D.; Ariel I. *et al*. Detection of a long non-coding RNA (CCAT1) in living cells and human adenocarcinoma of colon tissues using FIT–PNA molecular beacons. *Cancer Lett*. **2014**; *352* (1): 90-96.
446. Wang Z.; Zhang K.; Shen Y.; Smith J.; Bloch S.; Achilefu S. *et al*. Imaging mRNA expression levels in living cells with PNA·DNA binary FRET probes delivered by cationic shell-crosslinked nanoparticles. *Org. Biomol. Chem*. **2013**; *11* (19): 3159-3167.
447. Blanco A. M.; Artero R. A practical approach to FRET-based PNA fluorescence *in situ* hybridization. *Methods*. **2010**; *52* (4): 343-351.
448. Fontenete S.; Barros J.; Madureira P.; Figueiredo C.; Wengel J.; Azevedo N. F. Mismatch discrimination in fluorescent *in situ* hybridization using different types of nucleic acids. *Appl. Microbiol. Biotechnol*. **2015**; *99* (9): 3961-3969.
449. Genet M. D.; Cartwright I. M.; Kato T. A. Direct DNA and PNA probe binding to telomeric regions without classical *in situ* hybridization. *Mol. Cytogenet*. **2013**; *6* (1): 42.
450. Bracco E.; Rosso V.; Serra A.; Carnuccio F.; Gaidano V.; Nicoli P. *et al*. Design and application of a novel PNA probe for the detection at single cell level of $JAK2^{V617F}$ mutation in Myeloproliferative Neoplasms. *BMC Cancer*. **2013**; *13*: 348.
451. Bonvicini F.; Filippone C.; Manaresi E.; Gentilomi G. A.; Zerbini M.; Musiani M. *et al*. Peptide nucleic acid-based *in situ* hybridization assay for detection of parvovirus B19 nucleic acids. *Clin. Chem*. **2006**; *52* (6): 973-978.
452. Kim H. J.; Brehm-Stecher B. F. Design and Evaluation of Peptide Nucleic Acid Probes for Specific Identification of *Candida albicans*. *J. Clin. Microbiol*. **2015**; *53* (2):511-521.
453. Stone N. R. H.; Gorton R. L.; Barker K.; Ramnarain P.; Kibbler C. C. Evaluation of PNA-FISH Yeast Traffic Light for Rapid Identification of Yeast Directly from Positive Blood Cultures and Assessment of Clinical Impact. *J. Clin. Microbiol*. **2013**; *51* (4): 1301-1302.
454. Ferreira A. M.; Cruz-Moreira D.; Cerqueira L.; Miranda J. M.; Azevedo N. F. Yeasts identification in microfluidic devices using peptide nucleic acid fluorescence *in situ* hybridization (PNA-FISH). *Biomed. Microdevices*. **2017**; *19* (1): 11.
455. Almeida C.; Constante D.; Ferreira A.; Cerqueira L.; Vieira M. J.; Azevedo N. F. A new colorimetric peptide nucleic acid-based assay for the specific detection of bacteria. *Future Microbiol*. **2014**; *9* (10): 1131-1142.
456. Jensen H. E.; Jensen L. K.; Barington K.; Pors S. E.; Bjarnsholt T.; Boye M. Fluorescence *in situ* hybridization for the tissue detection of bacterial pathogens associated with porcine infections. *Methods Mol. Biol*. **2015**; *1247*: 219-234.

457. Santos R. S.; Guimarães N.; Madureira P.; Azevedo N. F. Optimization of a peptide nucleic acid fluorescence in situ hybridization (PNA-FISH) method for the detection of bacteria and disclosure of a formamide effect. *J. Biotechnol*. **2014**; *187*: 16-24.
458. Zhang X. F.; Li K.; Wu S.; Shuai J. B.; Fang W. H. Peptide nucleic acid fluorescence *in-situ* hybridization for identification of *Vibrio* spp. in aquatic products and environments. *Int. J. Food Microbiol*. **2015**; *206*: 39-44.
459. Kim N.; Lee S. H.; Yi J.; Chang C. L. Evaluation of Dual-Color Fluorescence *In Situ* Hybridization With Peptide Nucleic Acid Probes for the Detection of *Mycobacterium tuberculosis* and Non-Tuberculous Mycobacteria in Clinical Specimens. *Ann. Lab. Med*. **2015**; *35* (5): 500-505.
460. Machado A.; Castro J.; Cereija T.; Almeida C.; Cerca N. Diagnosis of bacterial vaginosis by a new multiplex peptide nucleic acid fluorescence *in situ* hybridization method. *PeerJ*. **2015**; 3: e780.
461. Fazli M.; Bjarnsholt T.; Hoiby N.; Givskov M.; Tolker-Nielsen T. PNA-based fluorescence *in situ* hybridization for identification of bacteria in clinical samples. *Methods Mol. Biol*. **2014**; *1211*: 261-271.
462. Ring H. C.; Theut Riis P.; Bay L.; Kallenbach K.; Bjarnsholt T.; Jemec G. B. Hematoxylin and Eosin staining identifies medium to large bacterial aggregates with a reliable specificity: A comparative analysis of follicular bacterial aggregates in axillary biopsies using PNA-FISH and Hematoxylin and Eosin staining. *Exp. Dermatol*. **2017**; *26* (10): 943-945.
463. Tavares M. A.; Yi S.; Masangcay C. Y.; Ota M. M.; Herrmann P. C. Chromogenic *In Situ* Hybridization Using Peptide Nucleic Acid Probes: A Promising Adjunct to Immunohistochemistry for Identifying Light Chain Restriction in Multiple Myeloma Patients. *Lab Med*. **2010**; *41* (4): 237-241.
464. Sato Y.; Fujimoto K.; Kawaguchi H. Detection of a *K-ras* point mutation employing peptide nucleic acid at the surface of a SPR biosensor. *Colloids Surf., B*. **2003**; *27* (1): 23-31.
465. Corradini R.; Feriotto G.; Sforza S.; Marchelli R.; Gambari R. Enhanced recognition of cystic fibrosis W1282X DNA point mutation by chiral peptide nucleic acid probes by a surface plasmon resonance biosensor. *J. Mol. Recognit*. **2004**; *17* (1): 76-84.
466. D'Agata R.; Breveglieri G.;Zanoli L. M.; Borgatti M.; Spoto G.; Gambari R. Direct Detection of Point Mutations in Nonamplified Human Genomic DNA. *Anal. Chem*. **2011**; *83* (22): 8711-8717.
467. Joung H. A.; Lee N. R.; Lee S. K.; Ahn J.; Shin Y. B.; Choi H. S. *et al*. High sensitivity detection of 16s rRNA using peptide nucleic acid probes and a surface plasmon resonance biosensor. *Anal. Chim. Acta*. **2008**; *630* (2): 168-173.
468. D'Agata R.; Spoto G. Artificial DNA and surface plasmon resonance. *Artif. DNA PNA XNA*. **2012**; *3* (2): 45-52.
469. Kim Y.-T.; Kim J. W.; Kim S. K.; Joe G. H.; Hong I. S. Simultaneous Genotyping of Multiple Somatic Mutations by Using a Clamping PNA and PNA Detection Probes. *ChemBioChem*. **2015**; *16* (2): 209-213.
470. Lapitan Jr L. D. S.; Guo Y.; Zhou D. Nano-enabled bioanalytical approaches to ultrasensitive detection of low abundance single nucleotide polymorphisms. *Analyst*. **2015**; *140* (12): 3872-3887.
471. Demidov V.; Frank-Kamenetskii M. D.; Egholm M.; Buchardt O.; Nielsen P. E. Sequence selective double strand DNA cleavage by peptide nucleic acid (PNA) targeting using nuclease S1. *Nucleic Acids Res*. **1993**; *21* (9): 2103-2107.
472. Veselkov A. G.; Demidov V. V.; FrankKamenetskii M. D.; Nielsen P. E. PNA as a rare genome-cutter. *Nature*. **1996**; *379* (6562): 214.
473. Komiyama M. Cut-and-Paste of DNA Using an Artificial Restriction DNA Cutter. *Int. J. Mol. Sci.* **2013**; *14* (2): 3343-3357.
474. Nielsen P. E.; Egholm M.; Berg R. H.; Buchardt O. Sequence specific inhibition of DNA restriction enzyme cleavage by PNA. *Nucleic Acids Res*. **1993**; *21* (2): 197-200.

475. Perry-O'Keefe H.; Yao X.-W.; Coull J. M.; Fuchs M.; Egholm M. Peptide nucleic acid pre-gel hybridization: An alternative to Southern hybridization. *Proc. Natl. Acad. Sci. U. S. A*. **1996**; *93* (25): 14670-14675.
476. Kerman K.; Matsubara Y.; Morita Y.; Takamura Y.; Tamiya E. Peptide nucleic acid modified magnetic beads for intercalator based electrochemical detection of DNA hybridization. *Sci. Technol. Adv. Mater.* **2004**; *5* (3): 351-357.
477. Medeiros-Silva J.; Guédin A.; Salgado G. F.; Mergny J.-L.; Queiroz J. A.; Cabrita E. J. *et al*. Phenanthroline-bis-oxazole ligands for binding and stabilization of G-quadruplexes. *Biochim. Biophys. Acta*. **2017**; *1861* (5): 1281-1292.
478. Ohnmacht S. A.; Micco M.; Petrucci V.; Todd A. K.; Reszka A. P.; Gunaratnam M. *et al*. Sequences in the HSP90 promoter form G-quadruplex structures with selectivity for disubstituted phenyl bis-oxazole derivatives. *Bioorg. Med. Chem. Lett*. **2012**; *22* (18): 5930-5935.
479. Maluenda I.; Navarro O. Recent Developments in the Suzuki-Miyaura Reaction: 2010–2014. *Molecules*. **2015**; *20* (5): 7528-7557.
480. Cordovilla C.; Bartolomé C.; Martínez-Ilarduya J. M.; Espinet P. The Stille Reaction, 38 Years Later. *ACS Catal*. **2015**; *5* (5): 3040-3053.
481. Lowe A. B. Thiol-ene "click" reactions and recent applications in polymer and materials synthesis. *Polym. Chem*. **2010**; *1* (1): 17-36.
482. Simonetti S. O.; Larghi E. L.; Kaufman T. S. A facile and convenient sequential homobimetallic catalytic approach towards β-methylstyrenes. A one-pot Stille cross-coupling/isomerization strategy. *Org. Biomol. Chem*. **2014**; *12* (22): 3735-3743.
483. Sanjeeva Rao K.; Wu T.-S. Chan–Lam coupling reactions: synthesis of heterocycles. *Tetrahedron*. **2012**; *68* (38): 7735-7754.
484. Lee H.-W.; Kyung T.; Yoo J.; Kim T.; Chung C.; Ryu J. Y. *et al*. Real-time single-molecule co-immunoprecipitation analyses reveal cancer-specific Ras signalling dynamics. *Nat. Commun*. **2013**; *4*: 1505.
485. Yong J. W.; Yeo X.; Khan M. M.; Lee M. B.; Hande M. P. Stable expression of promyelocytic leukaemia (PML) protein in telomerase positive MCF7 cells results in alternative lengthening of telomeres phenotype. *Genome Integr*. **2012**; 3 (1): 5.
486. Zhang H.; Song J.; Ren H.; Xu Z.; Wang X.; Shan L. *et al*. Detection of Low-Abundance KRAS Mutations in Colorectal Cancer Using Microfluidic Capillary Electrophoresis-Based Restriction Fragment Length Polymorphism Method with Optimized Assay Conditions. *Plos One.* **2013**; *8* (1): e54510.
487. Blanco R.; Iwakawa R.; Tang M.; Kohno T.; Angulo B.; Pio R. *et al*. A Gene-Alteration Profile of Human Lung Cancer Cell Lines. *Hum. Mutat*. **2009**; *30* (8): 1199-1206.
488. An J.; Hu J.; Shang Y.; Zhong Y.; Zhang X.; Yu Z. The cytotoxicity of organophosphate flame retardants on HepG2, A549 and Caco-2 cells. *J. Environ. Sci. Health, Part A: Toxic/Hazard. Subst. Environ. Eng*. **2016**; *51* (11): 980-988.
489. Liu Q.; Chang J. W.; Wang J.; Kang S. A.; Thoreen C. C.; Markhard A. *et al*. Discovery of 1-(4-(4-propionylpiperazin-1-yl)-3-(trifluoromethyl)phenyl)-9-(quinolin-3-yl)benzo[*h*][1,6]naphthyridin-2(1*H*)-one as a highly potent, selective mammalian target of rapamycin (mTOR) inhibitor for the treatment of cancer. *J. Med. Chem*. **2010**; *53* (19): 7146-7155.
490. Liu Q.; Wang J.; Kang S. A.; Thoreen C. C.; Hur W.; Ahmed T. *et al*. Discovery of 9-(6-Aminopyridin-3-yl)-1-(3-(trifluoromethyl)phenyl)benzo[*h*][1,6]naphthyridin-2(1*H*)-one (Torin2) as a Potent, Selective, and Orally Available Mammalian Target of Rapamycin (mTOR) Inhibitor for Treatment of Cancer. *J. Med. Chem*. **2011**; *54* (5): 1473-1480.
491. Hanson K. K.; Ressurreição A. S.; Buchholz K.; Prudêncio M.; Herman-Ornelas J. D.; Rebelo M. *et al*. Torins are potent antimalarials that block replenishment of *Plasmodium* liver stage parasitophorous vacuole membrane proteins. *Proc. Natl. Acad. Sci. U. S. A*. **2013**; *110* (30): E2838-E2847.

492. Wang Z. Gould-Jacobs Reaction. *Comprehensive Organic Name Reactions and Reagents.* Hoboken, N.J.: John Wiley & Sons, Inc.; **2010**.
493. Bruice P. Y. *Organic chemistry*. Upper Saddle River, NJ: Pearson/Prentice Hall; **2004**. 4th edition.
494. Isidro-Llobet A.; Álvarez M.; Albericio F. Amino Acid-Protecting Groups. *Chem. Rev*. **2009**; *109* (6): 2455-2504.
495. Clayden J.; Greeves N.; Warren S. G. *Organic chemistry*. New York: Oxford University Press; **2012**. 2nd edition.
496. Zweifel G. S.; Nantz M. H. *Modern organic synthesis: an introduction*. New York: W.H. Freeman; **2007**.
497. Wang Z. *Comprehensive organic name reactions and reagents*. Hoboken, N.J.: John Wiley & Sons, Inc.; **2010**.
498. da Silva R. A.; Estevam I. H. S.; Bieber L. W. Reductive methylation of primary and secondary amines and amino acids by aqueous formaldehyde and zinc. *Tetrahedron Lett*. **2007**; *48* (43): 7680-7682.
499. Smith J. A.; Jones R. K.; Booker G. W.; Pyke S. M. Sequential and Selective Buchwald−Hartwig Amination Reactions for the Controlled Functionalization of 6-Bromo-2-chloroquinoline: Synthesis of Ligands for the Tec Src Homology 3 Domain. *J. Org. Chem*. **2008**; *73* (22): 8880-8892.
500. Sunesson Y.; Limé E.;, Nilsson Lill S. O.; Meadows R. E.; Norrby P.-O. Role of the Base in Buchwald–Hartwig Amination. *J. Org. Chem*. **2014**; *79* (24): 11961-11969.
501. Ragnarsson U.; Grehn L. Dual protection of amino functions involving Boc. *RSC Adv*. **2013**; *3* (41): 18691-18697.
502. Kholod I.; Vallat O.; Buciumas A.-M.; Neels A.; Neier R. Synthetic Strategies for the Synthesis and Transformation of Substituted Pyrrolinones as Advanced Intermediates for Rhazinilam Analogues. *Eur. J. Org. Chem*. **2014**; *2014* (35): 7865-7877.
503. Nicolaou K. C.; Montagnon T.; Baran P. S.; Zhong Y. L. Iodine(V) reagents in organic synthesis. Part 4. *o*-iodoxybenzoic acid as a chemospecific tool for single electron transfer-based oxidation processes. *J. Am. Chem. Soc*. **2002**; *124* (10): 2245-2258.
504. Frigerio M.; Santagostino M.; Sputore S.; Palmisano G. Oxidation of Alcohols with *o*-Iodoxybenzoic Acid in DMSO: A New Insight into an Old Hypervalent Iodine Reagent. *J. Org. Chem*. **1995**; *60* (22): 7272-7276.
505. Nicolaou K. C.; Mathison C. J. N.; Montagnon T. *o*-Iodoxybenzoic Acid (IBX) as a Viable Reagent in the Manipulation of Nitrogen- and Sulfur-Containing Substrates: Scope, Generality, and Mechanism of IBX-Mediated Amine Oxidations and Dithiane Deprotections. *J. Am. Chem. Soc*. **2004**; *126* (16): 5192-5201.
506. Ura Y.; Beierle J. M.; Leman L. J.; Orgel L. E.; Ghadiri M. R. Self-Assembling Sequence-Adaptive Peptide Nucleic Acids. *Science*. **2009**; *325* (5936): 73-77.
507. Khalafi-Nezhad A.; Rad M. N. S.; Moosavi-Movahedi A. A.; Kosari M. Synthesis of Acyclic Nucleosides with *N*-[(Benzyloxy)(aryl)methyl] Substituents as Potential HEPT, EBPU, and TNK-651 Analogues. *Helv. Chim. Acta*. **2007**; *90* (4):730-737.
508. Holý A.; Dvořáková H.; Jindřich; Masojídková M.; Buděšínský M.; Balzarini J. *et al*. Acyclic Nucleotide Analogs Derived from 8-Azapurines: Synthesis and Antiviral Activity. *J. Med. Chem*. **1996**; *39* (20): 4073-4088.
509. Choi J.-R.; Cho D.-G.; Roh K. Y.; Hwang J.-T.; Ahn S.; Jang H. S. *et al*. A Novel Class of Phosphonate Nucleosides. 9-[(1-Phosphonomethoxycyclopropyl)methyl]guanine as a Potent and Selective Anti-HBV Agent. *J. Med. Chem*. **2004**; *47* (11): 2864-2869.
510. Boesen T.; Madsen C.; Sejer Pedersen D.; Nielsen B. M.; Petersen A. B.; Petersen M. A. *et al*. Preparation and antiviral properties of new acyclic, achiral nucleoside analogues: 1- or 9-[3-hydroxy-2-(hydroxymethyl)prop-1-enyl]nucleobases and 1- or 9-[2,3-dihydroxy-2-(hydroxymethyl)propyl]nucleobases. *Org. Biomol. Chem*. **2004**; *2* (8): 1245-1254.

511. Khalafi-Nezhad A.; Zarea A.; Soltani Rad M. N.; Mokhtari B.; Parhami A. Microwave-Assisted Michael Addition of Some Pyrimidine and Purine Nucleobases with α,β-Unsaturated Esters: A Rapid Entry into Carboacyclic Nucleoside Synthesis. *Synthesis*. **2005**; *2005* (3): 419-424.
512. Ze-Qi X.; Joshi R. V.; Zemlicka J. Alkylation of adenine with functionalized *tert*-Propargyl carbonates. Synthesis of 3'-hydroxymethyladenallene — A new analogue of 2'-deoxyadenosine. *Tetrahedron*. **1995**; *51* (1): 67-76.
513. Amblard F.; Nolan S. P.; Schinazi R. F.; Agrofoglio L. A. Efficient synthesis of various acycloalkenyl derivatives of pyrimidine using cross-metathesis and Pd(0) methodologies. *Tetrahedron*. **2005**; *61* (3): 537-544.
514. Khalafi-Nezhad A.; Soltani Rad M.; Behrouz S.; Asrari Z.; Behrouz M.; Amini Z. One-Pot Synthesis of *N*-Alkyl Purine, Pyrimidine and Azole Derivatives from Alcohols using Ph_3P/CCl_4: A Rapid Route to Carboacyclic Nucleoside Synthesis. *Synthesis*. **2009**; *2009* (18): 3067-3076.
515. Fletcher S. The Mitsunobu reaction in the 21st century. *Org. Chem. Front*. **2015**; *2* (6):739-752.
516. Kazemi M.; Shiri L.; Kohzadi H. Recent Advances in Aryl Alkyl and Dialkyl Sulfide Synthesis. *Phosphorus, Sulfur Silicon Relat. Elem*. **2014**; *190* (7): 978-1003.
517. Conte M. L.; Carroll K. S. The Chemistry of Thiol Oxidation and Detection. In: Jakob U, Reichmann D, editors. *Oxidative Stress and Redox Regulation*. Dordrecht: Springer Netherlands. **2013**.
518. Rogers S. J. Composite pK's of cysteine. *J. Chem. Educ*. **1969**; *46* (4): 239-240.
519. Yang C. C.; Marlowe C. K.; Kania R. Efficient method for regioselective isoprenylation of cysteine thiols in unprotected peptides. *J. Am. Chem. Soc*. **1991**; *113* (8): 3177-3178.
520. Brown M. J.; Milano P. D.; Lever D. C.; Epstein W. W.; Poulter C. D. Prenylated proteins. A convenient synthesis of farnesyl cysteinyl thioethers. *J. Am. Chem. Soc*. **1991**; *113* (8): 3176-3177.
521. Lumbierres M.; Palomo J. M.; Kragol G.; Roehrs S.; Müller O.; Waldmann H. Solid-Phase Synthesis of Lipidated Peptides. *Chem. - Eur. J*. **2005**; *11* (24): 7405-7415.
522. Włostowski M.; Czarnocka S.; Maciejewski P. Efficient *S*-alkylation of cysteine in the presence of 1,1,3,3-tetramethylguanidine. *Tetrahedron Lett*. **2010**; *51* (46): 5977-5979.
523. Salvatore R. N.; Smith R. A.; Nischwitz A. K.; Gavin T. A mild and highly convenient chemoselective alkylation of thiols using Cs_2CO_3–TBAI. *Tetrahedron Lett*. **2005**; *46* (51): 8931-8935.
524. Triola G.; Brunsveld L.; Waldmann H. Racemization-Free Synthesis of *S*-Alkylated Cysteines *via* Thiol-ene Reaction. *J. Org. Chem*. **2008**; *73* (9): 3646-3649.
525. White J. D.; Lee C.-S.; Xu Q. Total synthesis of (+)-kalkitoxin. *Chem. Commun*. **2003**; *16*: 2012-2013.
526. Tang G.; Ji T.; Hu A.-F.; Zhao Y.-F. Novel *N*,*S*-Phenacyl Protecting Group and Its Application for Peptide Synthesis. *Synlett*. **2008**; *2008* (12): 1907-1909.
527. Marrone L.; Siemann S.; Beecroft M.; Viswanatha T. Specificity of Lysine: N^6-Hydroxylase: A Hypothesis for a Reactive Substrate Intermediate in the Catalytic Mechanism. *Bioorg. Chem.* **1996**; *24* (4): 401-416.
528. Perrey D. A.; Uckun F. M. An improved method for cysteine alkylation. *Tetrahedron Lett*. **2001**; *42* (10): 1859-1861.
529. Yang S.-H.; Harris P. W. R.; Williams G. M.; Brimble M. A. Lipidation of Cysteine or Cysteine-Containing Peptides Using the Thiol-Ene Reaction (CLipPA). *Eur. J. Org. Chem*. **2016**; *2016* (15): 2608-2616.
530. Pahimanolis N.; Kilpeläinen P.; Master E.; Ilvesniemi H.; Seppälä J. Novel thiol- amine- and amino acid functional xylan derivatives synthesized by thiol–ene reaction. *Carbohydr. Polym*. **2015**; *131*: 392-398.
531. Gunnoo S. B.; Madder A. Chemical Protein Modification through Cysteine. *ChemBioChem*. **2016**; *17* (7): 529-553.

532. Sacarescu L.; Atudosie I.; Simionescu M.; Sacarescu G.; Harabagiu V. Microwave-Assisted *N*-Allylation of Uracil and Thymine Pyrimidine Bases. *Chem. Heterocycl. Compd*. **2011**; *47* (5): 602-606.
533. Thibon J.; Latxague L.; Deleris G. Synthesis of silicon analogues of acyclonucleotides incorporable in oligonucleotide solid-phase synthesis. *J. Org. Chem*. **1997**; *62* (14): 4635-4642.
534. Paryzek Z.; Tabaczka B. The Preparation of 1-Allyluracil. *N*(1)-Alkylation of *N*(3)-Protected Uracil Derivatives. *Org. Prep. Proced. Int*. **2001**; *33* (4): 400-405.
535. Amblard F.; Nolan S. P.; Gillaizeau I.; Agrofoglio L. A. A new route to acyclic nucleosides via palladium-mediated allylic alkylation and cross-metathesis. *Tetrahedron Lett*. **2003**; *44* (51): 9177-9180.
536. Dunetz J. R.; Magano J.; Weisenburger G. A. Large-Scale Applications of Amide Coupling Reagents for the Synthesis of Pharmaceuticals. *Org. Process Res. Dev*. **2016**; *20* (2): 140-177.
537. Porcheddu A.; Giacomelli G.; Piredda I.; Carta M.; Nieddu G. A Practical and Efficient Approach to PNA Monomers Compatible with Fmoc-Mediated Solid-Phase Synthesis Protocols. *Eur. J. Org. Chem*. **2008**; *2008* (34): 5786-5797.
538. Dey S.; Garner P. Synthesis of *tert*-Butoxycarbonyl (Boc)-Protected Purines. *J. Org. Chem*. **2000**; *65* (22): 7697-7699.
539. Katritzky A. R.; Akutagawa K. Formaldehyde: a reagent for the simultaneous protection of nucleophilic centers and the activation and stabilization of alternative locations to electrophilic attack. I. A new synthetic method for the 2-substitution of *N*-unsubstituted benzimidazoles: formaldehyde as a versatile protecting agent for heterocyclic NH. *J. Org. Chem.* **1989**; *54* (12): 2949-2952.
540. Lang P.; Magnin G.; Mathis G.; Burger A.; Biellmann J.-F. Synthesis of 8-(ω-Hydroxyalkyl)-, 8-(ω-Hydroxyalk-1-enyl)-, and 8-(ω-Hydroxyalk-1-ynyl)adenines Using the *tert*-Butyldimethylsilyloxymethyl Group, a New and Versatile Protecting Group of Adenine. *J. Org. Chem*. **2000**; *65* (23): 7825-7832.
541. Wang Z. Finkelstein Reaction. *Comprehensive Organic Name Reactions and Reagents*. Hoboken, N.J.: John Wiley & Sons, Inc.; **2010**.
542. Breugst M.; Bautista F. C.; Mayr H. Nucleophilic Reactivities of the Anions of Nucleobases and Their Subunits. *Chem-Eur J*. **2012**; *18* (1):127-137.
543. Hernández J. N.; Ramírez M. A.; Martín V. S. A New Selective Cleavage of *N,N*-Dicarbamoyl-Protected Amines Using Lithium Bromide. *J. Org. Chem*. **2003**; *68* (3): 743-746.
544. Mohapatra D. K.; Durugkar K. A. Efficient and selective cleavage of the *tert*-butoxycarbonyl (Boc) group under basic condition. *Arkivoc*. **2005**; *2005* (14): 20-28.
545. Stafford J. A.; Brackeen M. F.; Karanewsky D. S.; Valvano N. L. A Highly Selective Protocol for the Deprotection of Boc-Protected Amides and Carbamates. *Tetrahedron Lett*. **1993**; *34* (49): 7873-7876.
546. Harnden M. R.; Jarvest R. L.; Bacon T. H.; Boyd M. R. Synthesis and Antiviral Activity of 9-[4-hydroxy-3-(hydroxymethyl)but-1-yl]purines. *J. Med. Chem*. **1987**; *30* (9): 1636-1642.
547. Abushanab E.; Sarma M. S. P. 1',2'-*seco*-Dideoxynucleosides as Potential Anti-HIV Agents. *J. Med. Chem*. **1989**; *32* (1): 76-79.
548. Ashwell M.; Bleasdale C.; Golding B. T.; O'Neill I. K. An improved route to guanines substituted at *N*-9. *J. Chem. Soc., Chem. Commun*. **1990**; *14*: 955-956.
549. Robins M. J.; Uznanski B. Nucleic-Acid Related-Compounds. 33. Conversions of Adenosine and Guanosine to 2,6-Dichloro, 2-Amino-6-Chloro, and Derived Purine Nucleosides. *Can. J. Chem*. **1981**; *59* (17): 2601-2607.
550. Linn J. A.; McLean E. W.; Kelley J. L. 1,4-Diazabicyclo[2.2.2]octane (DABCO)-catalysed hydrolysis and alcoholysis reactions of 2-amino-9-benzyl-6-chloro-9*H*-purine. *J. Chem. Soc., Chem. Commun*. **1994;** *8*: 913-914.
551. Dondoni A.; Massi A.; Nanni P.; Roda A. A New Ligation Strategy for Peptide and Protein Glycosylation: Photoinduced Thiol-Ene Coupling. *Chem. - Eur. J*. **2009**; *15* (43): 11444-11449.

552. Rapireddy S.; Nhon L.; Meehan R. E.; Franks J.; Stolz D. B.; Tran D. *et al*. RTD-1Mimic Containing γPNA Scaffold Exhibits Broad-Spectrum Antibacterial Activities. *J. Am. Chem. Soc*. **2012**; *134* (9): 4041-4044.
553. Frigoli M.; Moustrou C.; Samat A.; Guglielmetti R. Synthesis of New Thiophene-Substituted 3,3-Diphenyl-3*H*-naphtho[2,1-*b*]pyrans by Cross-Coupling Reactions, Precursors of Photomodulated Materials. *Eur. J. Org. Chem*. **2003**; *2003* (15): 2799-2812.
554. Matsubara R.; Gutierrez A. C.; Jamison T. F. Nickel-Catalyzed Heck-Type Reactions of Benzyl Chlorides and Simple Olefins. *J. Am. Chem. Soc*. **2011**; *133* (47): 19020-19023.
555. Takeuchi M.; Tuihiji T.; Nishimura J. [2.2]Naphthalenophanes from intermolecular [2+2] photocycloadditions of divinylnaphthalenes. *J. Org. Chem*. **1993**; *58* (26): 7388-7392.
556. Katz T. J.; Liu L.; Willmore N. D.; Fox J. M.; Rheingold A. L.; Shi S. *et al*. An Efficient Synthesis of Functionalized Helicenes. *J. Am. Chem. Soc*. **1997**; *119* (42): 10054-10063.
557. Malvacio I.; Moyano E. L.; Vera D. M. A. Gas-phase synthesis of 3-carboethoxy-quinolin-4-ones. A comprehensive computational mechanistic study to uncover the dark side of the Gould-Jacobs reaction. *RSC Adv*. **2016**; *6* (87): 83973-83981.
558. Bender S. L.; Bhumralkar D.; Collins M. R.; Cripps S. J.; Deal J. G.; Jia L. *et al*. Amide compounds and pharmaceutical compositions for inhibiting protein kinases, and methods for their use. Google Patents; **2003**.
559. Ma X.; Lv X.; Qiu N.; Yang B.; He Q.; Hu Y. Discovery of novel quinoline-based mTOR inhibitors *via* introducing intra-molecular hydrogen bonding scaffold (iMHBS): The design, synthesis and biological evaluation. *Bioorg. Med. Chem*. **2015**; *23* (24): 7585-7596.
560. Schwarz M. K.; Tumelty D.; Gallop M. A. Solid-Phase Synthesis of 3,5-Disubstituted 2,3-Dihydro-1,5-benzothiazepin-4(5*H*)-ones. *J. Org. Chem*. **1999**; *64* (7): 2219-2231.
561. Nowshuddin S.; Ram Reddy A. Synthesis of dipeptides from *N*-hydroxy-3-azaspiro[5,5]undecane-2,4-dione activated α-amino acids. *Tetrahedron: Asymmetry*. **2011**; *22* (1): 22-25.
562. Tateoka Y.; Kimura T.; Watanabe K..; Yamamoto I.; Ho I. K. Potentiating effects of N^1,N^3-diallyluracil, N^1,N^3-diallylthymine and N^1,N^3-diallyl-6-methyluracil on pentobarbital-induced sleep and diazepam-induced motor incoordination. *Chem. Pharm. Bull*. **1987**; *35* (12): 4928-4934.
563. Thomson S. A.; Noble S. A.; Ricca D. J. Peptide nucleic acids and their effect on genetic material. Google Patents; **1993**.